

INVESTIGATION OF CHEMOPREVENTIVE AND APOPTOTIC  
CHARACTERISTICS OF TURKISH MEDICINAL PLANT *RHEUM RIBES*

A THESIS SUBMITTED TO  
THE GRADUATE SCHOOL OF NATURAL AND APPLIED SCIENCES  
OF  
MIDDLE EAST TECHNICAL UNIVERSITY

BY

PEMBEGÜL UYAR

IN PARTIAL FULFILLMENT OF THE REQUIREMENTS  
FOR  
THE DEGREE OF DOCTOR OF PHILOSOPHY  
IN  
BIOTECHNOLOGY

MARCH 2011

Approval of the thesis:

**INVESTIGATION OF CHEMOPREVENTIVE AND APOPTOTIC  
CHARACTERISTICS OF TURKISH MEDICINAL PLANT RHEUM RIBES**

submitted by **PEMBEGUL UYAR** in partial fulfillment of the requirements for the  
degree of **Doctor of Philosophy in Biotechnology Department, Middle East  
Technical University** by,

Prof. Dr. Canan Özgen \_\_\_\_\_  
Dean, Graduate School of **Natural and Applied Sciences**

Prof. Dr. İnci Eroğlu \_\_\_\_\_  
Head of Department, **Biotechnology**

Prof. Dr. Mesude İşcan \_\_\_\_\_  
Supervisor, **Biological Sciences Dept., METU**

Assoc. Prof. Dr. Nursen Çoruh \_\_\_\_\_  
Co-Supervisor, **Chemistry Dept., METU**

**Examining Committee Members:**

Prof. Dr. Orhan Adalı \_\_\_\_\_  
Biological Sciences Dept., METU

Prof. Dr. Mesude İşcan \_\_\_\_\_  
Biological Sciences Dept., METU

Prof. Dr. İsmet Deliloğlu Gürhan \_\_\_\_\_  
Bioengineering Dept., EGE Uni.

Prof. Dr. Arif Ahmet Başaran \_\_\_\_\_  
Pharmacy, Hacettepe Uni.

Assist. Prof. Dr. Sreeparna Banerjee \_\_\_\_\_  
Biological Sciences Dept., METU

**Date: 14.03.2011**

**I hereby declare that all information in this document has been obtained and presented in accordance with academic rules and ethical conduct. I also declare that, as required by these rules and conduct, I have fully cited and referenced all material and results that are not original to the this work.**

Name, Last name : Pembegul UYAR

Signature:

## ABSTRACT

### INVESTIGATION OF CHEMOPREVENTIVE AND APOPTOTIC CHARACTERISTICS OF TURKISH MEDICINAL PLANT *RHEUM RIBES*

Uyar, Pembegül

Ph.D., Department of Biotechnology

Supervisor: Prof. Dr. Mesude İřcan

Co-Supervisor: Assoc. Prof. Dr. Nursen oruh

March 2011, 227 pages

*Rheum* species are medicinally important plants due to the presence of anthracene derivatives and in this study antioxidative, cytotoxic, apoptotic and chemopreventive characteristics of *R. ribes* extracts were evaluated.

*R. ribes* shoot and root dry powder samples were prepared and extracted with ethyl acetate, ethanol and water. The extracts were revealed to be a potential scavenger of DPPH radicals and the chemical composition of the extracts was quantified by colorimetric determination of total phenol (GAE) and flavonoid (CAE) contents.

HL-60 cells were cultured in the presence of various concentrations of extracts up to 72 hr. *R. ribes* inhibited the survival of HL-60 cells in a concentration- and time-dependent manner, shown by trypan blue and XTT.

*R. ribes* caused HL-60 cells apoptosis via formation of phosphatidylserine externalization, as evidenced by flow cytometry. Exposure of HL-60 cells to higher

concentrations of extracts for 72 h resulted in a shift of 87% of the cell population from normal to the early/late apoptotic stage.

The *R. ribes* induced apoptosis may be partially attributed to the activation of caspase-3 and up-regulation of caspase-3 expression was detected in western blot.

The significant release of cytochrome c from the mitochondria into the cytosol was observed. The mRNA expression ratio of Bax/Bcl-2 was increased. The apoptosis was also demonstrated by DNA ladder and TUNEL.

Chemopreventive effects of *R.ribes* were investigated at the gene level of CYP1B1 and CYP1A1, and GST enzyme activity against cDNB and concluded that *R.ribes* modulated activities of these enzymes generally at a time dependent level.

These findings suggest that *Rheum ribes* exhibits potential antioxidant and anticancer properties by inducing caspase-dependent cell death in HL-60 cells.

**Keywords:** *Rheum ribes*, Antioxidant, Apoptosis, Chemoprevention

## ÖZ

### TÜRK TIBBİ BİTKİSİ RHEUM RİBES'İN KEMOPREVENTİF VE APOPTOTİK ÖZELLİKLERİNİN İNCELENMESİ

Uyar, Pembegül

Doktora, Biyoteknoloji Bölümü

Tez Yöneticisi: Prof. Dr. Mesude İşcan

Ortak Tez Yöneticisi: Doç. Dr. Nursen Çoruh

Mart 2011, 227 sayfa

*Rheum* türleri anthracene içerdikleri için tıbbi yönden önemli bitkilerdir ve bu çalışmada *Rheum ribes* bitkisinden elde edilen özütlerin antioksidatif, sitotoksik apoptotik ve kemopreventif özellikleri incelenmiştir.

*R.ribes* bitkisinin gövde ve köklerinden kuru toz örnekleri hazırlandı ve etil asetat, etanol ve su ile özütlendi. Özütlerin DPPH radikalini süpürme potensiyali ortaya çıkarıldı ve kimyasal bileşimleri toplam fenol (GAE) ve flavonoid (CAE) içeriklerinin kolorimetrik tayini ile ölçüldü.

HL-60 hücreleri çeşitli ektre konsantrasyonlarında varlığında 72 saat kültüre edildi. Hücre canlılığı tripan mavisi ve XTT ile belirlendi. *R. ribes* HL-60 hücrelerinin büyümesini konsantrasyona ve zamana bağlı olarak engellemiştir.

*R.ribes*'in neden olduğu apoptosiz, fosfatidilserin eksternalizasyonunun akım sitometrisi ile belirlenmesi ile kanıtlanmıştır. Buna göre, yüksek dozda uygulanan özütlerin 72 saatte HL-60 hücrelerinin % 87'sinin normalden erken ya da geç apoptosoza geçmesiyle sonuçlandığı belirlenmiştir.

*R.ribes*'in neden olduğu apoptosizin kısmen kaspaz-3 aktivasyonu ve western blot ile saptanan kaspaz-3 ekspresyonunun upregulasyonu ile olabileceği ile belirlenmiştir.

Mitokondriden sitozol içine anlamlı miktarda sitokrom c salımı gözlemlenmiştir. mRNA ekspresyon analizinde Bax/Bcl-2 oranının arttığı görülmüştür. Ayrıca, apoptoz DNA merdiven ve TUNEL yöntemleri ile de belirlenmiştir.

*R.ribes*'in kemopreventif etkisi CYP1A1 ve CYP1B1 gen ifadelerindeki ve GST enzim aktivitesinin CDNB'ye karşı değişimle belirlenmiştir. Sonuç olarak *R.ribes*'in belirtilen enzimlerde konsantrasyona bağlı etkiler yaptığı belirlenmiştir.

Bu bulgular *Rheum ribes* bitkisinin HL-60 hücrelerinde kaspaza bağımlı hücre ölümü sergileyen potansiyel antioksidan ve antikanser özelliklerinin olduğunu düşündürmektedir.

**Anahtar Kelimeler:** *Rheum ribes*, Antioksidant, Apoptosiz, Kemoprevansiyon

To My Family

## ACKNOWLEDGMENTS

I would like to gratefully acknowledge my supervisor Prof. Dr. Mesude Iscan for her advice, endless support, suggestions and criticism at every stage of this work. I owe her a debt of gratitude for her lovely attitude, which is absolutely not restricted with scientific area.

I also would like to thank to my co-supervisor Prof. Dr. Nursen Çoruh for her valuable contributions, support and encouragement in this research.

I appreciate Prof. Dr. Orhan Adali and Prof. Dr. Ismet Delilolu Gurhan for contributions to the study, for their valuable suggestions and encouragements, throughout the research.

I would like to thank to our botanist Assist. Prof. Dr. Fevzi Özgökçe for collecting our plant samples and his collaboration.

I would like to thank to Doc. Dr. Craig Walsh for his collaboration and permitting the conductance of my research in his laboratory with his support, encouragements and guidance throughout the research.

I acknowledge examining committee members Prof. Dr. Arif Ahmet Basaran and Assist. Prof. Dr. Sreeparna Banerjee for evaluating my thesis and their contributions.

I would like to thank to Dr. Serap Topsoy Kolukisa for her collaboration and help in the beginning of the work.

I would like to thank to my lab mates Metin Konuř, Can Yılmaz, Nizamettin Özdogan, Elif Sakallı, Dr. Ebru Saatci and Dr.Gokhan Sadi and special project students for their helps and friendship making the lab work more enjoyable throughout my study.

I appreciate my colleagues in University of California, Irvine, Department of Molecular Biology and Biochemistry for their friendship and support.

I would like to express my great appreciation to my family members Münevver Terziler, Nermin- Reřat Yalınay, Aslıhan-Özge Yalınay for their physical and moral support and encouragement in my life.

I gratefully thank to my mother Ayře, my father Kaya and my brother Yusuf and his wife Aylin and my niece Ayça Uyar and nephew Ömer Uyar for their endless support, love and trust in me.

This study was supported by the Research Fund of METU ÖYP Grant No: BAP-08-11-DPT-2002K120510.

## TABLE OF CONTENTS

ABSTRACT .....	IV
ÖZ .....	VI
ACKNOWLEDGEMENTS.....	IX
TABLE OF CONTENTS .....	XI
LIST OF TABLES.....	XIV
LIST OF FIGURES .....	XVI
LIST OF SYMBOLS AND ABBREVIATIONS .....	XX
CHAPTERS	
1. INTRODUCTION .....	1
1.1 Rheum ribes .....	2
1.2 Botany.....	2
1.3 Ethnobotanical Use.....	3
1.4 Free Radicals .....	4
1.4.1 Mechanism of free radical propagation .....	6
1.4.2 Biological Disorders Induced by Free Radicals .....	6
1.4.3 Radical Scavengers in Cellular Organisms.....	7
1.5 Antioxidant Compounds in Plants .....	10
1.5.1 Phenolic Compounds .....	10
1.5.1.1 The Major Classes of Polyphenolic Compounds.....	10
1.5.2 The Phenolic Constituents of Rheum ribes .....	16
1.6 Antioxidant properties of Rheum ribes .....	16
1.7 Extraction of Phenolic Compounds .....	17
1.7.1 Liquid–liquid .....	17
1.7.2 Solid–liquid.....	18
1.8 Quantification of Polyphenols .....	19
1.8.1 Spectrophotometric Methods used in Quantification of Total Phenolics.....	19
1.9 2,2-Diphenyl-1-picrylhydrazyl (DPPH) Assay .....	20
1.10 Cancer .....	21
1.10.1 HL-60 Cell Line.....	23
1.11 Cytotoxicity of Rheum ribes.....	23
1.11.1 Cell Viability .....	24
1.12 Apoptosis and Necrosis .....	24
1.13 Glutathione S-Transferases.....	29
1.14 Scope of The Study.....	33
2. MATERIAL AND METHODS.....	35
2.1 Materials .....	35
2.1.1 HL-60 Cell Lines .....	35
2.1.2 Plant Material.....	35
2.1.3 Chemicals and Other Materials .....	35
2.1.4 Primers.....	37
2.1.5 Antibodies.....	38

2.2 METHODS .....	39
2.2.1 Preparation of Rheum ribes freeze-dried extracts .....	39
2.2.2 Fractionation of Rheum ribes Methanol Extracts .....	42
2.2.3 Determination of in vitro Antioxidant Activity .....	44
2.2.3.1 Free Radical Scavenging Activity of Freeze-dried Extracts by DPPH method .....	44
2.2.3.2 Determination of Total Phenolic Contents of Freeze-dried Extracts .....	46
2.2.3.3 Determination of Total Flavonoid Contents of Freeze-dried Extracts .....	48
2.2.4 Cell Line and Culture Conditions .....	49
2.2.4.1 Cell Thawing .....	50
2.2.4.2 Cell Counting with Trypan Blue Exclusion Method .....	50
2.2.4.3 Freezing The Cells .....	51
2.2.4.5 Growth Curve Construction .....	52
2.2.4.6 Cell Treatment with Extracts .....	53
2.2.4.7 Measuring Viability of HL-60 Cells Using XTT Assay .....	54
2.2.5 Flow cytometry .....	55
2.2.5.1 Determination of cell size and granularity .....	56
2.2.5.2 Detection of apoptosis by Annexin V-APC .....	56
2.2.6 Microscopic analysis of Rheum ribes-treated cells .....	58
2.2.6.1 Morphology of apoptotic cells .....	58
2.2.6.2 Microscopic Detection of DNA fragmentation in HL-60 cells by the Terminal deoxynucleotidyl Transferase (TdT)-mediated dUTP-biotin Nick End-labeling (TUNEL) Method .....	58
2.2.7 Detection of DNA Fragmentation .....	59
2.2.8 Gene Expression Analysis by RT-PCR .....	60
2.2.8.1 Isolation of Total RNA from HL-60 cells .....	60
2.2.8.2 Calculation of RNA Concentration with Spectrophotometry .....	61
2.2.8.3 Electrophoresis of RNA .....	61
2.2.8.4 Complementary DNA (cDNA) Preparation .....	62
2.2.8.5 Primer preparation .....	63
2.2.8.6 Polymerase Chain Reaction (PCR) .....	63
2.2.8.7 Agarose gel electrophoresis .....	64
2.2.8.8 Data Acquisition .....	65
2.2.8.9 Quantitative Real-Time Polymerase Chain Reaction .....	66
2.2.9 Protein expression analysis .....	67
2.2.9.1 Protein Determination of Cytosol by Micro-Lowry Assay .....	67
2.2.9.2 Western Blot Detection of Bax, Cytochrome <i>c</i> and Caspase-3 .....	68
2.2.9.2.1 Cell Fractionation to visualize the Cytochrome <i>c</i> Release and Caspase-3 Cleavage .....	68
2.2.9.2.2 SDS-Polyacrylamide Gel Electrophoresis .....	69
2.2.9.2.3 Electroblotting of the Gels from SDS-PAGE .....	72
2.2.9.2.4 Immunostaining of the PVDF Membranes .....	74
2.2.10 Determination of Fluorimetric Caspase-3 Activity .....	75
2.2.11 Determination of GST Enzyme Activity towards CDNB .....	77
2.2.12 Statistical Analysis .....	78
3. RESULTS AND DISCUSSION .....	79
3.1 Yield of Plant Extraction .....	79

3.2 Absorption Spectrum of Extracts and Fractions.....	81
3.3 Antioxidant Efficiency of Rheum ribes.....	86
3.3.1 Incubation Time Optimization of DPPH assay .....	86
3.3.2 The Effects of Incubation Time in Different Extract Concentrations on DPPH Assay .....	87
3.3.3 Determination of Antioxidant Capacities of Rheum ribes .....	89
3.4 Determination of Total Phenolic Contents of of Rheum ribes .....	96
3.5 Determination of Total Flavonoid Contents of of Rheum ribes .....	98
3.6 Viability of HL-60 Cells.....	101
3.7 Cytotoxicity of <i>Rheum ribes</i> Shoot and Root Extracts in HL-60 Cells.....	105
3.7.1 Light microscopic analysis of Cell Morphology .....	105
3.7.2 Viable Cell Counting with Trypan Blue .....	107
3.7.3 XTT Assay.....	113
3.8 <i>Rheum ribes</i> Shoot and Root Extracts Induces Apoptotic Cell Death .....	120
3.8.1 Changes in cell size and granularity .....	120
3.8.2 Detection of phosphatidylserine translocated to the cell surface.....	123
3.8.3 Dose and time kinetics for Rheum ribes induction of apoptosis .....	127
3.9 Terminal deoxynucleotidyl Transferase Biotin-dUTP Nick End Labeling....	140
3.10 DNA Fragmentation Induced By <i>Rheum ribes</i> .....	144
3.11 Modulation of the levels of Bcl-2 family members by Rheum ribes in HL-60 cells.....	145
3.11.1 Qualification of RNA by Agarose Gel Electrophoresis .....	145
3.11.2 Qualification of RNA by Bioanalyzer .....	146
3.11.3 Determination of RNA purity and concentration .....	150
3.11.4 Expression Analysis of Apoptosis Related Genes Bcl-2 and Bax.....	150
3.12 Western Blot Analysis of Apoptosis Related Protein <i>Bax</i> .....	155
3.13 Detection of cytochrome c release.....	157
3.14 The role of Caspase-3 Rheum ribes Induced Apoptotic Pathway .....	160
3.14.1 Rheum ribes induces activation of caspase-3 .....	160
3.14.2 Rheum ribes induces catalytic activity of caspase-3.....	164
3.14.3 Inhibition of the Caspase cascade Did not Suppress the Antiproliferative Effects of Rheum ribes .....	167
3.15 Effect of Rheum ribes on CYP1A1 and CYP 1B1 mRNA Expressions in HL- 60 cells.....	173
3.16 Effect of Rheum ribes on GST Enzyme Activity in HL-60 cells.....	176
4. CONCLUSION .....	180
REFERENCES .....	184
APPENDICES	
A DPPH Assay Plate Design .....	197
B Standard Curve for Total Phenol Quantification .....	198
C Standard Curve for Total Flavanol Quantification .....	199
D XTT Assay Plate Design.....	200
E Buffers and Solutions.....	201
F Standard Curve for Lowry Assay .....	206
G Flow Cytometry Analysis .....	228
H qRT-PCR Melting and Standard Curve .....	221
CURRICULUM VITAE.....	223

## LIST OF TABLES

<b>Table 1.1</b> The most important classes of total phenolic compounds in plants...	12
<b>Table 1.2</b> Organic solvents used for polyphenols extraction.....	18
<b>Table 2.1</b> Primers used in this study.....	37
<b>Table 2.2</b> Antibodies used in this study.....	38
<b>Table 2.3</b> Physical constants of solvents used in the study, listed in order of decreasing solvent polarity.....	41
<b>Table 2.4</b> Ingredients of reverse transcription reaction.....	63
<b>Table 2.5</b> Ingredients of PCR master mix.....	64
<b>Table 2.6</b> Markers detected by PCR: primer sequences, temperature profiles, sizes of amplified fragments.....	65
<b>Table 2.7</b> Real Time PCR Conditions.....	66
<b>Table 2.8</b> cDNA Standard Dilutions for qPCR Optimizations.....	67
<b>Table 2.9</b> The list of used molecular weight standards.....	69
<b>Table 2.10</b> Formulations for SDS-PAGE separating and stacking gels.....	71
<b>Table 2.11</b> Constituents of cytosolic GST enzyme assay medium.....	77
<b>Table 3.1</b> Maximum extraction efficiency as expressed by percent yield (w/w) of <i>Rheum ribes</i> shoot and root dry powder with ethyl acetate (EtOAc), methanol (MetOH), ethanol (EtOH) and ddH <sub>2</sub> O solvent systems.....	80
<b>Table 3.2</b> Antioxidant activity (EC <sub>50</sub> µg/ml± SD <sup>o</sup> ) and % Radical Scavenging Activity (%RSA± SD <sup>o</sup> ) in the different extracts of <i>Rheum ribes</i> .....	92
<b>Table 3.3</b> Total phenol contents in different extracts of <i>Rheum ribes</i> as expressed in gallic acid equivalents (GAE) .....	97
<b>Table 3.4</b> Total flavonoid content in different extracts of <i>Rheum ribes</i> as expressed in Catechin Equivalents (CAE) .....	99
<b>Table 3.5</b> Summary of antioxidant activity, contents of Total phenol and flavonoid in the different extracts of <i>Rheum ribes</i> .....	100
<b>Table 3.6</b> The viability of HL-60 cells incubated for 144 hours: Number of alive and dead cells was shown.....	103
<b>Table 3.7</b> IC <sub>50</sub> values and % Viability in HL-60 cells obtained by counting with trypan blue after treatment of <i>Rheum ribes</i> for 24, 48 and 72 h.....	111
<b>Table 3.8</b> IC <sub>50</sub> values and % Viability in HL-60 cells obtained with XTT Assay after treatment of <i>Rheum ribes</i> extracts for 24, 48 and 72 h.....	118
<b>Table 3.9</b> Comparison of IC <sub>50</sub> values in HL-60 cells obtained by TBE and XTT Assay after treatment of <i>Rheum ribes</i> for 24, 48 and 72 h.....	119

<b>Table 3.10</b> Percents of Typical Quadrant Analysis of Annexin V-apc/7AAD Flow Cytometry of HL-60 Cells Treated with ASE for 24, 48 and 72 h.....	128
<b>Table 3.11</b> Percents of Typical Quadrant Analysis of Annexin V-apc/7AAD Flow Cytometry of HL-60 Cells Treated with ARE for 24, 48 and 72 h.....	130
<b>Table 3.12</b> Percents of Typical Quadrant Analysis of Annexin V-apc/7AAD Flow Cytometry of HL-60 Cells Treated with ESE for 24, 48 and 72 h.....	133
<b>Table 3.13</b> Percents of Typical Quadrant Analysis of Annexin V-apc/7AAD Flow Cytometry of HL-60 Cells Treated with ERE for 24, 48 and 72 h.....	135
<b>Table 3.14</b> Percents of Typical Quadrant Analysis of Annexin V-apc/7AAD Flow Cytometry of HL-60 Cells Treated with WSE for 72 h.....	137
<b>Table 3.15</b> Percents of Typical Quadrant Analysis of Annexin V-apc/7AAD Flow Cytometry of HL-60 Cells Treated with WRE for 72 h.....	138
<b>Table 3.16</b> Spectrophotometric determination of total RNA concentration ( <i>mg/ml</i> ) and OD <sub>260</sub> /OD <sub>280</sub> ratios of all samples.....	150
<b>Table 3.17</b> Effects of 100 µg/ml of ESE and ERE treatment on Bax/Bcl-2 ratio in HL-60 cells for 24 hours .....	151
<b>Table 3.18</b> Effects of 100 µg/ml of WSE and WRE treatment on Bax/Bcl-2 ratio in HL-60 cells for 24 hours .....	154
<b>Table 3.19</b> Percents of Typical Quadrant Analysis of Annexin V-apc/7AAD Flow Cytometry of HL-60 Cells Treated with ASE for 72 h in the presence of zvad and nec-1.....	168
<b>Table 3.20</b> Percents of Typical Quadrant Analysis of Annexin V-apc/7AAD Flow Cytometry of HL-60 Cells Treated with ESE for 72 h in the presence of zvad and nec.....	169
<b>Table 3.21</b> Percents of Typical Quadrant Analysis of Annexin V-apc/7AAD Flow Cytometry of HL-60 Cells Treated with ARE for 24, 48 and 72 h in the presence of zvad and nec-1.....	170
<b>Table 3.22</b> Percents of Typical Quadrant Analysis of Annexin V-apc/7AAD Flow Cytometry of HL-60 Cells Treated with ERE for 24, 48 and 72 h in the presence of zvad and nec-1 .....	171
<b>Table 3.23</b> Effects of 100 µg/ml of ESE and ERE treatment on CYP 1B1 gene expression in HL-60 cells for 24 hours.....	174
<b>Table 3.24</b> Effects of 100 µg/ml of ESE and ERE treatment on CYP 1A1 gene expression in HL-60 cells for 24 hours.....	175
<b>Table 3.25</b> Effects of ESE treatment on GST Enzyme Activity in HL-60 cells with the indicated concentrations for 24, 48 and 72 hours.....	176
<b>Table 3.26</b> Effects of ERE treatment on GST Enzyme Activity in HL-60 cells with the indicated concentrations for 24, 48 and 72 hours.....	178

## LIST OF FIGURES

<b>Figure 1.1</b> <i>Rheum ribes</i> L.....	2
<b>Figure 1.2</b> Phenolic compounds in foods.....	13
<b>Figure 1.3</b> The simplest of the monophenol .....	14
<b>Figure 1.4</b> The structure of flavonoids .....	14
<b>Figure 1.5</b> Representation of intrinsic and extrinsic apoptosis pathway.....	25
<b>Figure 1.6</b> Release of cytochrome c from the mitochondria can trigger a series of events leading to the activation of effector caspases .....	28
<b>Figure 1.7</b> Figure shows the death receptor pathway and its direct and indirect effects on the effector caspases.....	28
<b>Figure 1.8</b> Conjugation, reduction, thiolysis and isomerization reactions catalyzed by GST.....	31
<b>Figure 2.1</b> Freshly collected <i>Rheum ribes</i> shoots, May 2007.....	39
<b>Figure 2.2</b> Flow chart for the solvent fractionation of <i>Rheum ribes</i> .....	43
<b>Figure 2.3</b> Diagrammatic representation of chemical reaction of the reduction of DPPH in the presence of an electron donating antioxidant.....	44
<b>Figure 2.4</b> Dot plot analysis of cell populations by double staining.....	57
<b>Figure 2.5</b> NBT/BCIP reaction scheme.....	75
<b>Figure 3.1</b> Absorption spectra of A) Shoot and B) Root <i>Rheum ribes</i> freeze-dried extracts .....	83
<b>Figure 3.2</b> Concentration curve of <i>Rheum ribes</i> shoot extracts.....	84
<b>Figure 3.3</b> Absorption spectra of <i>Rheum ribes</i> root fractions.....	85
<b>Figure 3.4</b> Reaction Kinetics of DPPH Radical Scavenging Activity.....	87
<b>Figure 3.5</b> Time and concentration effects of ESE on DPPH radical scavenging activity.....	88
<b>Figure 3.6</b> 3D Bar Diagram of the effects incubation time effects of different ESE concentrations on DPPH radical scavenging activity	89
<b>Figure 3.7</b> 96-well microtiter plate prepared for use in the DPPH assay.....	90
<b>Figure 3.8</b> Percent DPPH scavenging activities (% RSA) of <i>Rheum ribes</i> shoot and root extracts prepared in ethyl acetate (EtOAc), methanol (MetOH), ethanol (EtOH) and water.....	91
<b>Figure 3.9</b> Comparison of percent DPPH scavenging capacities of <i>Rheum ribes</i> root extract and the reference materials.....	94
<b>Figure 3.10</b> Percent DPPH scavenging activities of <i>Rheum ribes</i> chloroform, n-butanol and aqueous shoot and root fractions.....	95
<b>Figure 3.11</b> a) the healthy HL-60 cells c) the alive and dead HL-60 cells were side by side at 400X magnification.....	102
<b>Figure 3.12</b> The Growth Curve of HL-60 Cells.....	104
<b>Figure 3.13</b> Light Microscopic Analysis of effects of <i>Rheum ribes</i> Extracts on morphological changes in HL-60 cells for 48 h.....	106
<b>Figure 3.14</b> Effects of <i>Rheum ribes</i> shoot (A) and root (B) ethyl acetate extract	108

<b>Figure 3.15</b> Effects of <i>Rheum ribes</i> shoot (A) and root (B) ethanol extract on cell survival in HL-60 cells by the TBE assay.....	109
<b>Figure 3.16</b> Effects of <i>Rheum ribes</i> shoot (A) and root (B) aqueous extract on cell survival in HL-60 cells by the TBE assay.....	110
<b>Figure 3.17</b> 96-well microtiter plate prepared for use in the XTT assay	114
<b>Figure 3.18</b> Effects of <i>Rheum ribes</i> shoot (A) and root (B) ethyl acetate extract on cell survival in HL-60 cells by the XTT assay.....	115
<b>Figure 3.19</b> Effects of <i>Rheum ribes</i> shoot (A) and root (B) ethanol extract on cell survival in HL-60 cells by the XTT assay.....	116
<b>Figure 3.20</b> Effects of <i>Rheum ribes</i> shoot (A) and root (B) aqueous extract on cell survival in HL-60 cells by the XTT assay.....	117
<b>Figure 3.21</b> Etoposide and Sodium azide stimulated HL-60 cells exhibit characteristic morphological apoptotic features.....	121
<b>Figure 3.22</b> Rheum ribes-treated HL-60 cells exhibit characteristic morphological apoptotic features for 72 h. ....	122
<b>Figure 3.23</b> Etoposide and Sodium azide induced translocation of phosphatidyl-serine to the outer cell membrane in HL-60 cells.....	124
<b>Figure 3.24</b> <i>Rheum ribes</i> induced translocation of phosphatidylserine to the outer cell membrane in HL-60 cells.....	126
<b>Figure 3.25</b> ASE induced apoptosis in a different time and dose fashion.....	129
<b>Figure 3.26</b> ARE induced apoptosis in a different time and dose fashion.....	131
<b>Figure 3.27</b> ESE induced apoptosis in a different time and dose fashion.....	134
<b>Figure 3.28</b> ERE induced apoptosis in a different time and dose fashion.....	136
<b>Figure 3.29</b> WSE induced apoptosis in a different time and dose fashion.....	137
<b>Figure 3.30</b> WSE induced apoptosis in a different time and dose fashion.....	139
<b>Figure 3.31</b> TUNEL image of 0.1 % DMSO treated HL-60 cells, control indicating unfragmented DNA.....	140
<b>Figure 3.32</b> TUNEL image of HL-60 cells treated with 100 µg/ml of ESE.....	141
<b>Figure 3.33</b> TUNEL image of HL-60 cells treated with 100 µg/ml of ERE.....	142
<b>Figure 3.34</b> <i>Rheum ribes</i> treated HL-60 cells show apoptosis specific DNA ladder.....	144
<b>Figure 3.35</b> Total RNA isolated from HL-60 cells which were 0.1 % DMSO treated and 100 µg/ml of ARE, ERE, WRE, ESE and WSE for 24 h.....	145
<b>Figure 3.36</b> Gel image of Bioanalyzer (Agilent) result of total RNA isolated from HL-60 cells.....	147
<b>Figure 3.37</b> Bioanalyzer (Agilent) result of total RNA isolated from HL-60 cells.....	148
<b>Figure 3.38</b> Bioanalyzer (Agilent) RIN result of total RNA isolated from HL-60 cells.....	149
<b>Figure 3.39</b> Expression of Bax and Bcl-2 genes in HL-60 cells upon treatment with 100 µg/ml of ESE and ERE for 24 hours.....	152
<b>Figure 3.40</b> The gel image of RT-PCR product of Bax and Bcl-2 genes in HL-60 cells upon treatment with 100 µg/ml of WSE and WRE for 24 hours.....	153
<b>Figure 3.41</b> Expression of Bax and Bcl-2 genes in HL-60 cells upon treatment with 100 µg/ml of WSE and WRE for 24 hours.....	154
<b>Figure 3.42</b> Expression of Bax protein in HL-60 cells upon treatment with 100	155

<b>Figure 3.43</b> Expression of Bax protein in HL-60 cells upon treatment with 100, 250 and 500 µg/ml of ESE and ERE for 72 hours. ....	156
<b>Figure 3.44</b> Expression of Bax protein in HL-60 cells upon treatment with 250, 500 and 1000 µg/ml of WSE and WRE for 72 hours.....	157
<b>Figure 3.45</b> Cytochrome c release from mitochondria into cytosol induced by 100 µg/ml of ASE and ARE for 24 hours.....	158
<b>Figure 3.46</b> Cytochrome c release from mitochondria into cytosol induced by 100 µg/ml of ESE and ERE for 24 hours.....	159
<b>Figure 3.47</b> Caspase-3 was cleaved with ASE and ARE. ....	161
<b>Figure 3.48</b> Caspase-3 was cleaved with ESE and ERE.....	162
<b>Figure 3.49</b> Caspase-3 was cleaved with WSE and WRE.....	163
<b>Figure 3.50</b> ASE and ARE induced the activation of caspase-3.....	164
<b>Figure 3.51</b> ESE and ERE induced the activation of caspase-3.....	165
<b>Figure 3.52</b> ARE and ERE induced the activation of caspase-3.....	166
<b>Figure 3.53</b> Expression of CYP1B1 genes in HL-60 cells upon treatment with 100 µg/ml of ESE and ERE for 24 and 48 hours.....	174
<b>Figure 3.54</b> Expression of CYP1A1 genes in HL-60 cells upon treatment with 100 µg/ml of ESE and ERE for 24 and 48 hours.....	175
<b>Figure 3.55</b> Effects of ESE treatment at the indicated concentrations for 24, 48 and 72 h on GST activity against CDNB in HL-60 cells.....	177
<b>Figure 3.56</b> Effects of ERE treatment at the indicated concentrations for 24, 48 and 72 h on GST activity against CDNB in HL-60 cells.....	179
<b>Figure A.1</b> Representative 96-well microtiter plate, indicating final concentrations of plant extracts .....	197
<b>Figure B.1</b> Gallic Acid Standart Curve obtained in Folin Ciocalteu Micro Method.....	198
<b>Figure C.1</b> Catechin Standart Curve obtained in Aluminium Micro Method....	199
<b>Figure D.1</b> Representative 96-well microtiter plate, indicating concentrations of plant extracts.....	200
<b>Figure F.1</b> Standard curve for the determination of protein amount by micro lowry.....	206
<b>Figure G.1</b> Cell apoptosis, percentage of HL-60 cells after treatment with ASE by flow cytometric analysis for 24 h.....	207
<b>Figure G.2</b> Cell apoptosis, percentage of HL-60 cells after treatment with ASE by flow cytometric analysis for 48 h.....	208
<b>Figure G.3</b> Cell apoptosis, percentage of HL-60 cells after treatment with ASE by flow cytometric analysis for 72 h.....	209
<b>Figure G.4</b> Cell apoptosis, percentage of HL-60 cells after treatment with ARE by flow cytometric analysis for 24 h.....	210
<b>Figure G.5</b> Cell apoptosis, percentage of HL-60 cells after treatment with ARE by flow cytometric analysis for 48 h.....	211
<b>Figure G.6</b> Cell apoptosis, percentage of HL-60 cells after treatment with ARE by flow cytometric analysis for 72 h.....	212
<b>Figure G.7</b> Cell apoptosis, percentage of HL-60 cells after treatment with ESE	213
<b>Figure G.8</b> Cell apoptosis, percentage of HL-60 cells after treatment with ESE	214

<b>Figure G.9</b> Cell apoptosis, percentage of HL-60 cells after treatment with ESE by flow cytometric analysis for 72 h.....	215
<b>Figure G.10</b> Cell apoptosis, percentage of HL-60 cells after treatment with ERE by flow cytometric analysis for 24 h.....	216
<b>Figure G.11</b> Cell apoptosis, percentage of HL-60 cells after treatment with ERE by flow cytometric analysis for 48 h.....	217
<b>Figure G.12</b> Cell apoptosis, percentage of HL-60 cells after treatment with ERE by flow cytometric analysis for 72 h.....	218
<b>Figure G.13</b> Cell apoptosis, percentage of HL-60 cells after treatment with WSE by flow cytometric analysis for 72 h.....	219
<b>Figure G.14</b> Cell apoptosis, percentage of HL-60 cells after treatment with WRE by flow cytometric analysis for 72 h. ....	220
<b>Figure H.1</b> Melting curve showing the fluorescence of SYBR Green I dye versus the temperature.....	221
<b>Figure H.2</b> Quantitation data for Cycling A.Green.....	222
<b>Figure H.3</b> qRT-PCR Standart Curve.....	222

## LIST OF SYMBOLS AND ABBREVIATIONS

- AP-1: Activator protein 1
- ARE: Antioxidant Response Element
- Bax: Bcl-2-associated X protein
- Bcl-2: B-cell lymphoma 2
- Caspase: Cysteine-dependent aspartate-directed proteases
- CDNB: 1-Chloro-2,4-dinitrobenzene
- DMSO: Dimethyl sulfoxide
- ER: Estrogen Receptor
- ERE: Estrogen Response Element
- GSH: Reduced glutathione
- GST: Glutathione S-transferases
- IC50: Inhibitory Concentration 50
- Lck: Lymphocyte-specific protein tyrosine kinase
- p53: Protein 53
- ROS: Reactive Oxygen Species
- MMP: Matrix metalloproteinase
- NFkB: Nuclear Factor-kappa B
- SDS Sodium Dodecyl Sulfate
- TEMED N, N, N', N'-Tetramethylethylenediamine
- PCR: Polymerase Chain Reaction
- RT-PCR: Reverse Transcriptase-Polymerase Chain Reaction
- qRT-PCR: Quantitative Reverse Transcription Polymerase Chain Reaction
- dNTP: Deoxy Nucleotide Triphosphate
- EtBr: Ethidium Bromide
- PBS: Phosphate Buffered Saline

GAPDH: Glyceraldehyde-3-Phosphate Dehydrogenase

TUNEL: Terminal deoxynucleotidyl Transferase Biotin-dUTP Nick End Labeling

XTT: 2,3-bis[2-methoxy-4-nitro-5-sulfo-phenyl]-2H-tetrazolium-5-carboxyanilide  
innersalt

# CHAPTER I

## 1. INTRODUCTION

The modern pharmacotherapy has its seeds in the application of natural drugs. Extracts of plants or animal products are used for medicinal treatment since thousands of years. The knowledge of natural drugs and their potential use in medicine continuously increased throughout the centuries. Advanced preparative and analytical methods in phytochemistry led to the isolation and structural characterisation of a huge number of natural compounds, usually defined as secondary metabolites. The screening with innovative biological assays allows the verification of their active principle. These improvements provided the basis for rational drug discovery and have fundamentally contributed to the development of important pharmaceuticals of natural origin.

Though significant development has been made in the combinatorial chemistry field, drugs derived from natural products still play an important role in the drug discovery process. Today, natural drugs obtained from plants still represent high percentage of the prescription drug market in the United States. Furthermore, according to the World Health Organization, 80% of the population in developing countries depends on traditional medicine for their primary health care, and 85% of traditional medicine is derived from plant extracts.

As Davis (1965-1985) stated that Turkey has one of the richest plant diversity in the world. Almost 10,500 plant species have been identified and among all 30% of these are endemic (Güner, 2000).

East Anatolia has variable climate and high number of ecological zones which allows a rich flora in that region and as a result of it a rich source of medicinal plants. (Özgökçe and Özçelik, 2004).

Turkish people living in rural areas use plants for nourishment and medical purposes. In recent years, the plants – used traditionally for curative purposes – have attracted attention of the researchers (Yeşilada, 1999)

## 1.1 Rheum ribes

*Rheum* species has anthracene derivatives found in the subterranean parts of the plant which makes them medicinally important. *Rheum ribes* L. (Polygonaceae) is used to obtain a component of a most important crude drugs in the Middle East (Kashiwada, 1988). *Rheum ribes* L. (Polygonaceae) is grown mostly in Iran, Lebanon and Eastern Turkey (Shokravi, 1997).



**Figure 1.1** *Rheum ribes* L.

## 1.2 Botany

*Medicinal species:* *Rheum ribes* L.

*Common names:* Revas, ışkın, uğgun or uçgun

*Botanical family:* Polygonaceae

*Rheum ribes* L. is cultivated in some temperate countries for its edible red leaf stalks and a hardy perennial. Polygonaceae family in Turkey, is represented by eight genera and seventy species. *Rheum ribes* is the only *Rheum* species growing in Turkey (Cullen, 1966).

### 1.3 Ethnobotanical Use

*R. ribes* (young shoots and petioles) is used against diarrhea and also stomachic and antiemetic as well as against hemorrhoids, measles, smallpox and cholagogue (Baytop, 1999). Fresh stems and petioles of *Rheum ribes* are consumed as vegetable, and used as digestive and appetizer in Eastern Turkey, while the roots are used to treat diabetes (Abu-Irmaileh, 2003; Tabata, 1994), hypertension, obesity (Abu-Irmaileh, 2003), ulcer (Tabata, 1994), diarrhea (Tabata, 1994) and as antihelmintic and expectorant (Tabata, 1994). *Rheum ribes* decoction root extracts showed significant blood sugar lowering activity in alloxan-induced diabetic mice, although this extract did not show hypoglycemic action in healthy mice (Özbek, 2004).

There are not so much chemical studies on *R. ribes* in Turkey; in one study, they isolated, from the roots collected from Erzincan, chrysophanol, physcion, rhein, aloemodin, physcion-8-O-glucoside, aloemodin-8-O-glucoside, sennoside A and rhaponticin (Meriçli, 1990; Tuzlacı, 1992). In another study, chrysophanol, physcion, emodin, quercetin, 5-desoxyquercetin, quercetin 3-O-rhamnoside, quercetin 3-O-galactoside and quercetin 3-O-rutinoside have been found from the aerial parts of the plants collected from Hakkari (Tosun, 2003).

Antimicrobial activity of *Rheum ribes* was investigated against gram negative pathogens such as *Escherichia coli*, *Klebsiella pneumoniae*, *Proteus spp.*, *Pseudomonas aeruginosa* and *Neisseria gonorrhoeae* and *Bordetella bronchiseptica*, *Micrococcus luteus*, *K. pneumoniae*, *Serratia marcescens* and three isolates of *Staphylococcus aureus* in Iran. *R. ribes* root extracts demonstrated an effective antibacterial activity on *M. luteus*, *K. pneumoniae* and *S. aureus* (Bonjar, 2004). Some studies on *Rheum* species rather than *R. ribes* were carried out; *Rheum tangiticum*, *Rheum palmatum*, *Rheum coreanum* and *Rheum undulatum* (Matsuda,

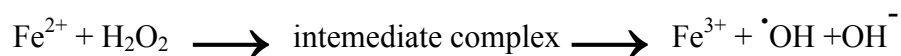
2001), *Rheum officinale* (Cai, Sun, Xing, 2004; Leonard, 2006), *Rheum emodi* (Krenn, 2003), *Rheum maximowiczii* (Kogure, 2004), have been studied for their antioxidant activity. From *R. undulatum*, four anthraquinone glucosides, a naphthalene glucoside and ten stilbenes were isolated, and their radical scavenging activities (DPPH and O-2) were investigated.

## 1.4 Free Radicals

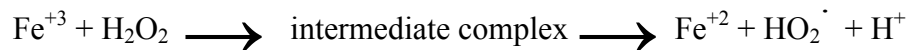
Electrons occupy regions called orbitals. These orbitals can hold two electrons, which spin in directions opposite to each other. A free radical is any species that can act independently with one or more unpaired electrons in their make-up (Halliwell, 1995). An unpaired electron is in an orbital and this causes the species to be attracted slightly to a magnetic field. This situation can be defined as paramagnetism and it sometimes gives a considerable degree of reactivity as the free radical (Halliwell, 1990).

Some examples of free radicals can be considered as hydrogen atom trichloromethyl, superoxide, peroxy, hydroxyl, alkoxy, and oxides of nitrogen. Hydrogen peroxide, lipid peroxide, singlet oxygen and hypochlorous acid which are also strong oxidizing agents (Punchard, 1996).

As to radical generating reaction, we can name a Fenton type reaction, which involves an iron (II) salt with hydrogen peroxide, which produces hydroxyl radicals as shown below.



Traces of  $\text{Fe}^{+3}$  can also react with  $\text{H}_2\text{O}_2$  as shown below, but this is a very slow reaction at physiological pH.



Naturally, The oxygen molecule has two unpaired electrons each located in degenerate  $\pi$ -antibonding orbital, if a single electron is added to the ground state  $\text{O}_2$  molecule, it must enter to one of the  $\pi$ -antibonding orbitals, forming a superoxide radical  $\text{O}_2^-$ .

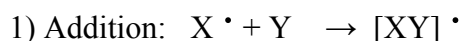
#### 1.4.1 Generation of Free Radicals in Biological Systems

Biological system have factors that causes free radical formation in themselves, but they face other factors which come from the surroundings in which they are exposed to, such as chemicals and irradiation. Factors that cause to form reactive species constantly within a biological system can have strong effects on the system.

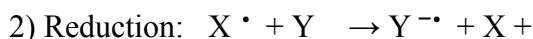
Most of the oxygen radicals are produced within the electron transport system. Save the basal anti-oxidation cytochrome P450 and cyclooxygenases as well as certain lipoxygenases and dehydrogenases and peroxidases generate free radical intermediates (Punchard, 1996).

Oxygen is the terminal electron receptor during the production of ATP in the electron transport chain. And nearly 1-5% of all oxygen used in metabolism escapes as free radical intermediates. The biggest sources of  $\text{O}^{2-}$  *in vivo* in most aerobic cells are probably the electron transport chains of mitochondria and endoplasmic reticulum.

### ***1.4.1 Mechanism of free radical propagation***



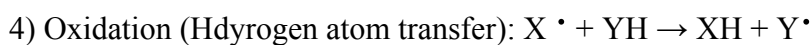
For example: Addition of OH· to guanine in DNA



For example: Reduction of O<sub>2</sub> to O<sub>2</sub><sup>·-</sup> by paraquat radical



For example: Oxidation of ascorbic acid



For example: Reaction of alpha-tocopherol with lipid peroxy radical

Most of the molecules in the biological systems are non-radicals, however, in the presence of even one free radical in the system may cause to initiate new radicals from the non-radicals and usually proceeds to radical chain reactions.

### ***1.4.2 Biological Disorders Induced by Free Radicals***

Biological molecules have three-dimensional structures and their functionalities also depend on their structures. The composition of intracellular medium is highly different than the surrounding tissues and this difference is maintained by the cell membrane structures is great importance of the homeostasis. However, peroxidation of lipids, can lead to severe damage to lipid membranes and as a result to the cell's inner composition. There are at least two well-known mechanisms, which bring about such damages through an unreparable damage in the anatomical integrity of membranes and the other is through the production of toxic compounds, which can diffuse through membranes. The most important substances of this type are aldehydes that are produced in large amounts from peroxidizing lipids and are secreted from their site of production (Basaga, 1997). Studies suggest that high concentrations of aldehydes may accumulate in certain areas and then block an essential sulphhydryl group in an enzyme molecule. These toxic compounds are

metabolized and detoxified through some mechanism within the cells. Anaerobic removal of aldehydes is catalyzed by aldehyde dehydrogenases. Enzymes such as aldehyde reductase, alcohol dehydrogenase and glutathione transferase play important roles with some other compounds containing sulphhydryl in this removal.

The production of radicals increased proportionally with the abundance of iron. Iron is a redox-capable catalyst and this causes an increase in the number of radicals produced. If iron is not strictly compartmentalized and bound to chelators it causes, more reactive and damaging species to be created.

Studies suggest that free radicals are highly responsible for aging and tumor production. A theory asserts that free radical reactions in the cell can lead to the cross-linking of major macromolecules such as nucleic acids and proteins, causing functional damage (Penzes, 1984).

Some other approaches tried to explain the aging process on the basis of leakage, which occurs during the operation of mitochondrial respiratory chain. Excessive leakage of  $O_2$  is believed to have a possible cumulative effect on mitochondrial functions because the efficiency of protective systems decrease with age. When the amount of reducing agents transported to the mitochondrial respiratory chain is reduced, less oxygen is needed, leading to decreased basal metabolism (Harman, 1995). The fact that small animals with high respiratory rates live shorter than larger animals with lower respiratory rates, is very reasonable in this sense. There has also been some other experimental evidence recently, which indicates of some sort of relation between aging, carcinogenesis and mutagenesis.

### ***1.4.3 Radical Scavengers in Cellular Organisms***

In order to protect tissues against the deleterious effects of reactive oxygen species (ROS), all cells possess numerous defence mechanisms that include enzymes such as SOD (superoxide dismutase), catalase, glutathione reductase and glutathione peroxidase. Radical scavengers in cells may be classified into five groups (Rossel, 1990) as follows:

### 1) Primary Antioxidants

They are also referred to as chain-breaking antioxidants. They have ability to react with lipid radicals to convert them to more stable products. They are mainly phenolic substances. More specifically, a molecule will be able to act as a primary antioxidant if it is able to donate a hydrogen atom rapidly to a lipid radical ( $\text{ROO}^\cdot$ ) and if the radical derived from the antioxidant is more stable than the lipid radical, or is converted to more stable products (Maidt, 1996). Natural and synthetic tocopherols, alkyl gallates, butylated hydroxyanisole (BHA), butylated hydroxytoluene (BHT), tertiary butyl hydroquinone (TBHQ) etc. belong to this group and function as electron donating agents. However, BHA and BHT are synthetic compounds, which are used as food preservatives, and their usage have been restricted in the United States since 1995, because they have been found suspicious structures of carcinogenesis (Barlow, 1990).

### 2) Oxygen Scavengers

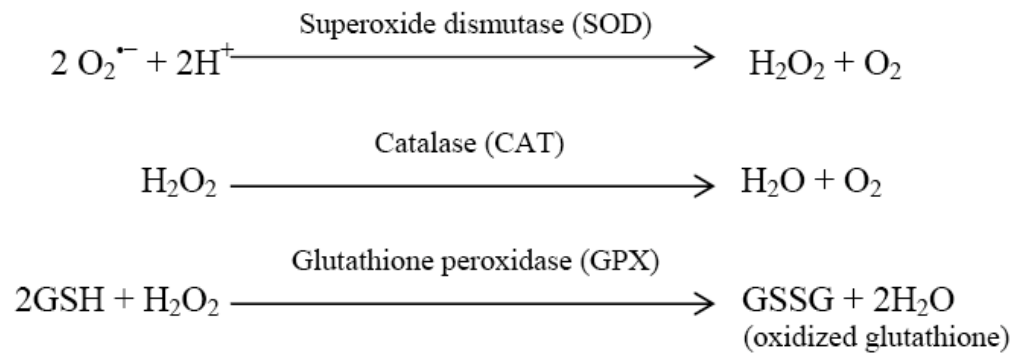
Ascorbic acid (Vitamin C), ascorbyl palmitate, erythorbic acid (d-isomer of ascorbic acid) and its sodium salt etc. belong to this group of antioxidants. They can react with oxygen and can thus remove it in a closed system.

### 3) Secondary Antioxidants

They are also known as preventive antioxidants and they reduce the rate of chain initiation by a variety of mechanisms including compounds that bind metal ions, scavenge oxygen, decompose hydroperoxides to non-radical species, absorb UV radiation or deactivate singlet oxygen. Dilauryl thiopropionate and thiodipropionic acid, which function by decomposing the lipid hydroperoxides into stable end products, examples of this category.

### 4) Enzymic Antioxidants

This group of antioxidants function as either by removing dissolved/ headspace oxygen or by removing highly oxidative species from food systems. Glucose oxidase, superoxide dismutase, catalase, glutathione peroxidase, etc. belong to this group of antioxidant.



The enzyme superoxide dismutase decomposes superoxide radicals by converting them to hydrogen peroxide plus oxygen. Catalase and glutathione (GSH) peroxidase are enzymes that decompose peroxides, particularly hydrogen peroxide. There are two forms of superoxide dismutase: a mitochondrial enzyme, which contains manganese, and a cytosolic enzyme, which contains copper and zinc. Catalase contains iron, while glutathione peroxidase contains selenium. These metal ions must come from the diet. At least some of the effects that selenium, copper, zinc, iron and glutathione have on immune function relate to their roles in antioxidant defence

#### 5) Chelating Agents

Amino acids, Citric acid, EDTA etc. chelate metallic ions such as iron and copper that promote lipid oxidation through a catalytic reaction. The chelates greatly increase the action of phenolic antioxidants and due to this referred to as synergists. Most of these synergists exhibit little or no activity when used alone, except amino acids, which can show antioxidant or pro-oxidant activity.

## **1.5 Antioxidant Compounds in Plants**

### ***1.5.1 Phenolic Compounds***

Phenolic compounds are synthesized by plants during their normal course of development (Harborne, 1982; Pridham, 1960), which are considered to be secondary metabolites synthesized in this development and in phenomena such as, response to stress conditions as in infections, wounding, and UV radiation among others (Beckman, 2000; 1992). These compounds are found in plants very frequently (Harborne and Turner 1984) and have a great range of variety and diversity as a group of phytochemicals, which are derived from phenylalanine and tyrosine (Shahidi, 2000).

As an example of diversity of these compounds, we can mention plant phenolics, which include simple phenols, coumarins, stilbenes, phenolic acids (both benzoic and cinnamic acid derivatives), flavonoids, hydrolyzable and condensed tannins, lignans, and lignins as shown in Figure 1.1. Phenolics contribute in various processes in plants as phytoalexins contributors to the plant pigmentation, protective agents UV light, antifeedants antioxidants, attraction for pollinators and so on. In foods, they also participate in the taste of bitterness, flavor, astringency, and color. Moreover, some plant phenolics have health-protecting capacities, and oxidative stability. These are advantageous for producers, processors, and consumers (Shahidi, 2004).

#### **1.5.1.1 The Major Classes of Polyphenolic Compounds**

Phenolic compounds have a polyphenol structure with one or several hydroxyl groups on aromatic rings. According to the number of phenol rings, they are divided into several classes and to the structural elements that bind these rings to one another. The main groups of polyphenols are: flavonoids, phenolic acids, tannins (hydrolyzable and condensed), stilbenes and lignans (D'Archivio, 2007).

The phenolic compounds which occur commonly in food material may be classified into three groups, namely, simple phenols and phenolic acids, hydroxycinnamic acid derivatives and flavonoids (Table 1.1 and Figure 1.2).

1) The simple phenols and phenolic acids include monophenols (Figure 1.3) such as gallic acid, a triphenol, is present in an esterified form in tea catechins.

2) The hydroxycinnamic acid derivatives are almost exclusively derived from p-coumaric, caffeic, and ferulic acid, whereas sinapic acid is comparatively rare.

3) The flavonoids (Figure 1.4) are the most important single group of phenolics in food. They consist mainly of catechins, proanthocyanins, anthocyanidins and flavons, flavonols and their glycosides.

**Table 1.1** The most important classes of total phenolic compounds in plants. (Wikipedia foundation, Inc., www, 2010)

Number of C-atoms	Basic skeleton	Class	Examples
6	$C_6$	simple phenols, benzoquinones	Catechol, Hydroquinone, 2,6-Dimethoxybenzoquinone
7	$C_6 - C_1$	phenolic acids	Gallic, salicylic acids
8	$C_6 - C_2$	acetophenone, phenylacetic acid	3-Acetyl-6-methoxybenzaldehyde, Tyrosol, p-Hydroxyphenylacetic acid
9	$C_6 - C_3$	hydroxycinnamic acid, polypropene, coumarin, isocoumarin	Caffeic, ferulic acids, Myristicin, Eugenol, Umbelliferone, aesculetin, Bergenon, Eugenin
10	$C_6 - C_4$	naphthoquinone	Juglone, Plumbagin
13	$C_6 - C_1 - C_6$	Xanthone	Mangiferin
14	$C_6 - C_2 - C_6$	stilbene, anthrachinone	Resveratrol, Emodin
15	$C_6 - C_3 - C_6$	flavonoids, isoflavonoids	Quercetin, cyanidin, Genistein
18	$(C_6 - C_3)_2$	lignans, neolignans	Pinoresinol, Eusiderin
30	$(C_6 - C_3 - C_3)_2$	biflavonoids	Amentoflavone
N	$(C_6 - C_3)_n$ $(C_6)_n (C_6 - C_3)_n$	lignins catecholmelanine (condensed tannins)	

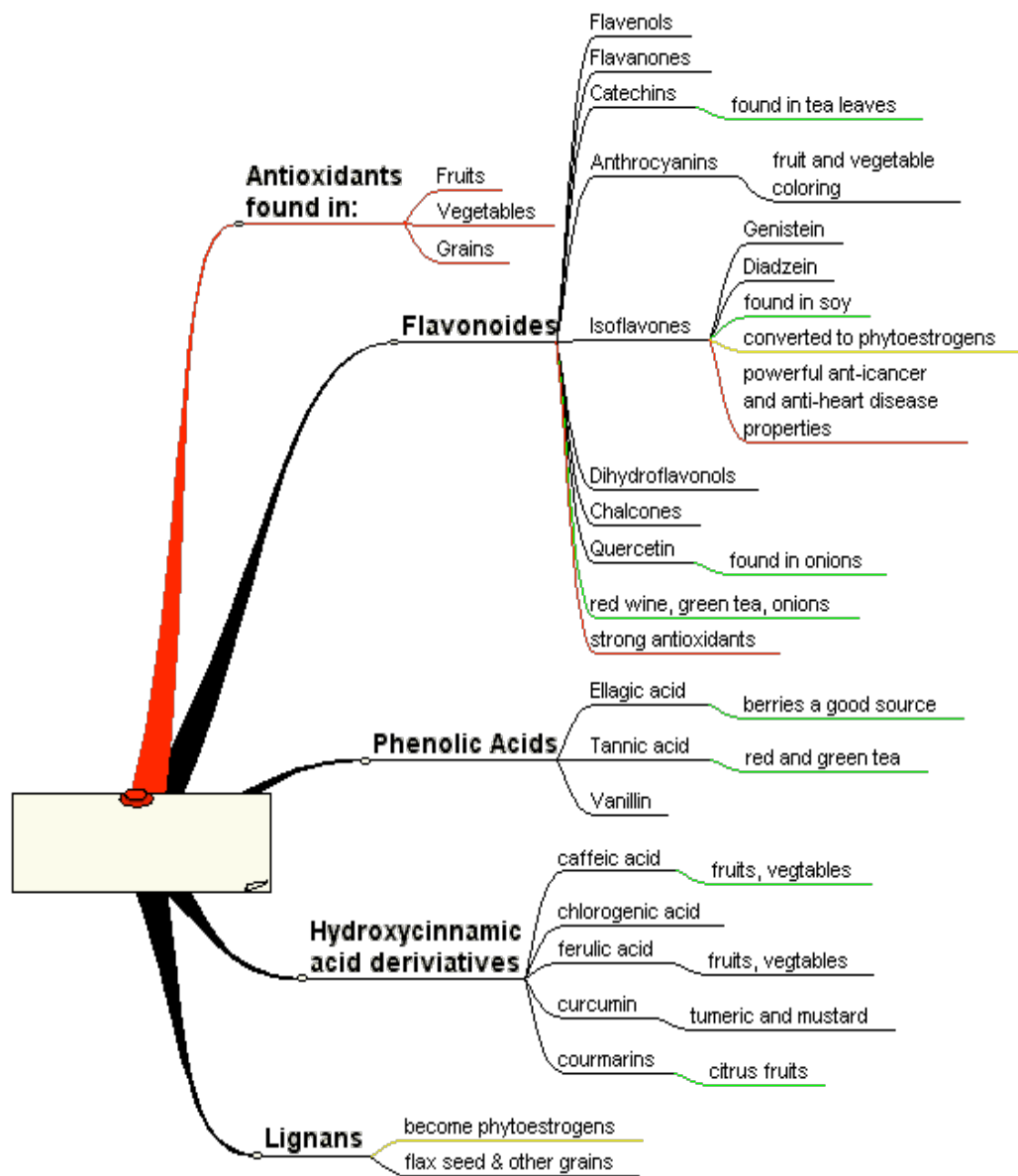


**Figure 1.2** Phenolic compounds in foods (Novus research, Inc., www, 2003)

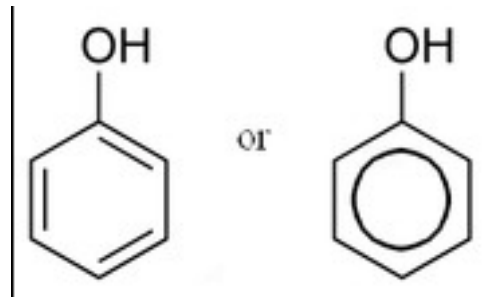


**Figure 1.3** The simplest of the monophenols (Wikipedia foundation, Inc., www, 2010).

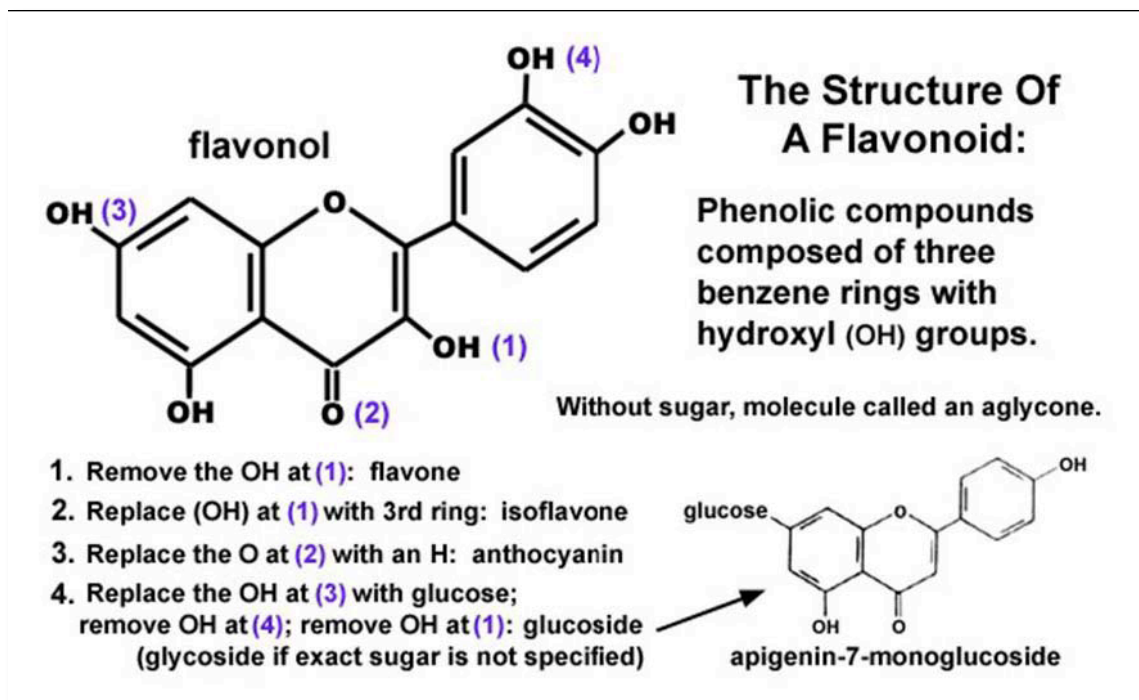


**Figure 1.4** The structure of flavonoids (Armstrong, www, 2007)

The recent explosion of interest in the bioactivity of the the flavonoids of higher plants is due, at least in part, to the potential health benefits of these polyphenolic components of major dietary constituents. (Rice, 1996). Flavonoids are plant pigments that are synthesised from phenylalanine, generally display marvelous colors known from flower petals, mostly emit brilliant fluorescence when they are excited by UV light, and are ubiquitous to green plant cells. They regulate plant growth by inhibition of the exocytosis of the auxin indolyl acetic acid, as well as by induction of gene expression, and they influence other biological cells in numerous ways.

Havsteen (2002) described that the flavonoids are very reactive compounds. They can enter into almost any type of reaction known to organic chemistry, e.g., oxidation-reduction reactions, carbonyl reaction, acid-base reactions, free-radical reaction, hydrophobic interactions, tautomerism, and isomerisations. The substituents may also exert their influence by electronic induction, hyperconjugation, resonance, steric hindrance, and complexation with heavy metal ions. The basis of the great variability of the flavonoids is: differences in the ring structure of the aglycone and in its state of oxidation/reduction; differences in the extent of hydroxylation of the aglycone and in the positions of the hydroxyl groups and differences in the derivatisation of the hydroxyl groups, e.g., with methyl groups, carbohydrates, or isoprenoids.

Williams (2004) reported that the cellular effects of flavonoids will ultimately depend on the extent to which they associate with cells, either by interactions at the membrane or by uptake into the cytosol. Information regarding uptake of flavonoids and their metabolites from the circulation into various cell types and whether they are modified further by cell interactions has become increasingly important as attention focuses on the new concept of flavonoids as potential modulators of intracellular signalling cascades vital to cellular function.

Flavonoids have the potential to bind to the ATP-binding sites of a large number of proteins (Conseil, 1998), including mitochondrial ATPase, calcium plasma membrane ATPase, protein kinase A, protein kinase C and topoisomerase (Williams, 2004). Some flavonoids inhibit tyrosine-specific protein kinases, topoisomerases I and II, as well as the cell division control protein kinases. The result is that growth metabolism, including cell division, is slowed. This effect supports the claim of the slow tumor ablating effect of flavonoids (Havsteen, 2002).

### ***1.5.2 The Phenolic Constituents of Rheum ribes***

Flavonoids, stilbenes and anthraquinones are the major phenolic constituents of *Rheum ribes* to provide a potential source of antioxidants. The major active chemical constituents of rhubarb include anthraquinones, oxalic acid, and tannins (Shang, 2002). The pharmaceutically relevant compounds in rhubarb are mainly anthraquinone derivatives, including emodin, rhein, aloe-emodin, physcion, chrysophanol and their glucosides. Among these anthraquinones, emodin has been under intensive investigations since last decade, and it has been shown that emodin possesses a number of biological activities.

## **1.6 Antioxidant properties of Rheum ribes**

It was found using the bleaching method of  $\beta$ -carotene that the chloroform extracts of the roots at concentrations of 50 and 100  $\mu\text{g/ml}$  ( $91.09 \pm 0.8\%$  and  $93.14 \pm 1.17\%$ , respectively) were more effective than the quercetin with same concentration ( $86.11 \pm 1.09\%$  and  $86.21 \pm 1.10\%$ , respectively). Furthermore, the DPPH assay showed that methanol extracts of both the stems and the roots exhibited higher activity than BHT at concentrations greater than 50  $\mu\text{g/ml}$ . The methanol extract of the stems showed the highest DPPH radical scavenging activity among all of the extracts tested ( $87.07 \pm 0.54\%$ ), followed by the methanol extract of the roots ( $60.60 \pm 0.86\%$ ) and the chloroform extract of the roots ( $50.87 \pm 0.3\%$ ) at a concentration of 100  $\mu\text{g/ml}$ .

In addition, the chloroform extract of the roots ( $48.66 \pm 1.23 \mu\text{g PE/mg extract}$ ) had a higher phenolic content than the other extracts, and the extract containing the lowest quantity of phenolics was the chloroform extract of the stems ( $22.68 \pm 1.10 \mu\text{g PE/mg extract}$ ). The most flavonoid-rich extract was found to be the chloroform extract of the roots ( $145.59 \pm 0.22 \mu\text{g QE/mg extract}$ ), while the methanol extract of the stems ( $13.66 \pm 0.75 \mu\text{g QE/mg extract}$ ) had the lowest flavonoid content (Ozturk , 2007).

## **1.7 Extraction of Phenolic Compounds**

Extraction of phenolic compounds occurring in natural products have attracted a special interest in the last several years (Pinelo, 2005). Extraction is a very important step in the isolation, identification and use of phenolic compounds and there is no single and standard extraction method. Solvent extraction (Baydar, 2004; Bucic-Kojic, 2007) and extraction with supercritical fluid (Bleve, 2008; Fredj, 1990; Nahar, 2005; Palma, 1999) are the most common techniques used for the isolation of phenolic compounds.

### ***1.7.1 Liquid–liquid***

Liquid–liquid extraction is a mass transfer operation in which a liquid solution (the feed) initially containing one or more solutes is thoroughly mixed with an immiscible or nearly immiscible liquid (solvent). The solvent exhibits preferential affinity or selectivity towards one or more of the components in the feed and has different density. Two streams result from this contact: the extract, which is the solvent rich solution containing the desired extracted solute, and the raffinate, the residual feed solution containing little solute. (Müller, 2008).

### 1.7.2 Solid–liquid

Solid–liquid extraction, or leaching can be defined as a mass transport phenomenon in which solids contained in a solid matrix migrate into a solvent brought into contact with the matrix (Corrales, 2009). It is a unit operation extensively used to recover many important food components: sucrose in cane or beets, lipids from oilseeds, phytochemicals from plants, functional hydrocolloids from algae and polyphenolic compounds from plants, fruits, vegetables, etc.

**Table 1.2** Organic solvents used for polyphenols extraction.

Polyphenolic compounds	Solvent	References
Phenolic acids, flavonols, antocyanins	Ethyl acetate	Pinelo et al. (2005); Russell et al. (2008)
Anthocyanins, Phenolic acids, catechins, flavanones, flavones, flavonols, procyanidins, ellagic acids, Rutin, chlorogenic acids	Methanol and different aqueous forms (50–90%, v/v)	Bleve et al. (2008); Caridi et al. (2007); Ross et al. (2009); Mattila and Kumpulainen (2002)
Anthocyanins, flavonols, free phenolic acids	Ethanol and different aqueous forms (10–90%, v/v)	Altiok et al. (in press); Balas and Popa (2007); Wang et al. (2009); Bleve et al. (2008); Bucić-Kojić et al. (2006); Corrales et al. (2009); Ross et al. (2009)
Flavonols, free phenolic acids	Chloroform	Shariffar, Deghn-Nudeh, and Mirtajaldini (2009)
Flavonols, phenolic acids	Diethyl ether	Ross et al. (2009)
Proantocyanidins, phenolic acids	Hot water 80–100°	Diouf, Stevanovic, and Cloutier (2009)
Tannins, bound phenolic acids	NaOH (2 N–10 N)	Nardini et al. (2002); Popa et al. (2008); Ross et al. (2009)
Phenolic compounds, phenolic acids	Petroleum ether	Zhang et al. (2009)
Flavonols, phenolic acids, hydroxycinnamic acids, coumarins, Flavonols xanthenes	Acetone/water 10–90% (v/v)	Altiok et al. (in press); Nacz & Shahidi (2006); Shariffar et al. (2008); Schieber et al. (2003)
Flavonols, phenolic acids, simple phenolics, anthocyanins	<i>n</i> -Hexane, isooctane, ethyl acetate	Alonso Garcia et al. (2004)
Polyphenols from olive leaves, oleuropein and rutin	Acetone, ethanol and their aqueous forms (10–90%, v/v)	Altiok et al. (in press)
Flavonols, quercetin 3,4'-diglucoside and quercetin 4'-monoglucoside.	Methanol/water 70% v/v	Caridi et al. (2007)

Extraction efficiency is known to be a function of process conditions. Several factors affect the concentration of the desired components in the extract: temperature, liquid–solid ratio, flow rate and particle size. For instance, the phenolic content of almond hull extracts was found to be three times higher when a batch liquid–solid extraction was performed at 50<sup>0</sup>C in comparison with that at 25<sup>0</sup>C. Time contact and liquid–solid ratio were also reported to be significant variables (Hayouni, 2007; Pinelo, 2004; Rubilar, 2003).

The most common solvents extraction methods are those using acidified methanol or ethanol as extractants (Amr, 2007; Awika, 2005; Caridi, 2007; Lapornik, 2005). From these methods, the extraction with methanol is the most efficient (Kapasakalidis, 2006); in fact, it has been found that in anthocyanin extractions from grape pulp, the extraction with methanol is 20% more effective than that with ethanol, and 73% more effective than water extraction (Castañeda, 2009) nevertheless, in food industry ethanol is preferred due to the methanol toxicity.

## **1.8 Quantification of Polyphenols**

There is an increasing demand for highly sensitive and selective analytical method for the determination of polyphenols (Liu, 2008). Despite a great number of investigations, the separation and quantification of different polyphenolics remain difficult, especially the simultaneous determination of polyphenolics of different groups (Tsao, 2003).

### ***1.8.1 Spectrophotometric Methods used in Quantification of Total Phenolics***

A number of spectrophotometric methods have been developed for the quantification of plant phenolics. These assays are based on different principles and are used to determine different structural groups present in phenolic compounds. The Folin–Ciocalteu assay (Tsao, 2003; Lapornik, 2005) is widely used for determining total phenolics, while the vanillin and proanthocyanidin assays have been used to estimate total proanthocyanidins (Naczki, 2006).

Spectrophotometric methods provide very useful qualitative and quantitative information; actually, spectroscopy is the main technique used for the quantification of different classes of polyphenols due to its simplicity and low cost. The major disadvantage of the spectrophotometric assays is that they only give an estimation of the total phenolic content. It does not separate nor does it give quantitative measurement of individual compounds.

Giusti (2003) published excellent reviews of the main methods used in the characterisation and quantification of anthocyanins by UV–Vis. On the other hand, the total flavonoids content can be determined using a colorimetric method based on the complexation of the phenolic compounds with Al (III) (Huang, 2009; Naczka, 2006).

### **1.9 2,2-Diphenyl-1-picrylhydrazyl (DPPH) Assay**

Recently, the DPPH assay has become quite popular in natural antioxidant studies. One of the reasons is that this method is simple and highly sensitive. This assay is based on the theory that a hydrogen donor is an antioxidant. Figure 5 shows the mechanism by which DPPH• accepts hydrogen from an antioxidant. DPPH• is one of the few stable and commercially available organic nitrogen radicals. The antioxidant effect is proportional to the disappearance of DPPH• in test samples. Various methods of monitoring the amount of DPPH• in the antioxidant test system have been reported: electron spin resonance spectroscopy (ESR)/plant powders, NMR/catechins, and UV spectrophotometry/polyphenols . However, monitoring DPPH• with a UV spectrometer has become the most widely and commonly used method recently because of its simplicity and accuracy. DPPH• shows a strong absorption maximum at 517 nm (purple). The color turns from purple to yellow followed by the formation of DPPH upon absorption of hydrogen from an antioxidant. This reaction is stoichiometric with respect to the number of hydrogen atoms absorbed. Therefore, the antioxidant effect can be easily evaluated by following the decrease of UV absorption at 517 nm.

To standardize the results from various studies, the Trolox equivalent (TE) unit has been used. Trolox is a commercial water-soluble vitamin E. The antioxidant activity of a sample is expressed in terms of micromoles of equivalents of Trolox per 100 g of sample (TE/100 g).

Results have also been reported as  $EC_{50}$ , which is the amount of antioxidant necessary to decrease the initial DPPH• concentration by 50%. This method was introduced as an easy and accurate method for use in fruit and vegetable juice extracts. Therefore, numerous studies on antioxidants present in plants have been conducted using the DPPH assay, including fruits and vegetables, medicinal plants, cereals and spices and herbs, and tea and leaves. Some unique studies on the antioxidant activities of algae and mushroom were also performed using this method.

## **1.10 Cancer**

Cancer is a group of many related diseases that originate in genome. Although there are many kinds of cancers, their common feature is loss of cell division control. Oncogenes and loss or mutation in tumor suppressor genes play major role in that abnormal cell growth. Oncogenes are normal regulatory genes whose activity increased as a consequence of genetic alteration. Only one allele of an oncogene needs to be change. The effect is dominant. Beside oncogenes the other players are suppressor genes that are coding for cell division inhibitory proteins whose function is lost in cancer. Oncogenes and repressors cooperate in carcinogenesis. As a consequence of extra cells a mass of tissue called tumor forms (King, 2000).

The life history of a cancer can be divided into stages. Carcinogenesis, the process of cancer development from normal cells, is divided into initiation and promotion stages. Progression describes the additional changes occurring after initial cancer cells have been formed. Risk factors associated with cancer are tobacco use, diet, ultraviolet radiation, alcohol, ionizing radiation, chemicals and hormone replacement therapy as well as life style.

According to the 2005 estimates of American Cancer Society, cancer is the second leading cause of death among the other diseases. Prostate cancers among men and breast cancer among women are the two primary cancers according to the incidence rate. Although leukemia ranks at the ninth position for incidence rate (%3) it raises up to sixth position when death rates are considered.

Leukemia is a cancer of blood-forming cells. It occurs when immature or mature cells multiply in an uncontrolled manner in the bone marrow. It is classified as lymphocytic or myeloid, according to the type of cell that is multiplying abnormally, and either acute, signifying rapidly progressing disease with a predominance of highly immature (blastic) cells, or chronic, which denotes slowly progressing disease with greater numbers of more mature cells (Cook, 1996).

When incidence of leukemia is considered they cover only 2-3% of all cancer types but the death rates increase to 4% according to 2005 estimates of American Cancer Society. That interesting data makes the people study on the factors causing leukemia and the treatment strategies for the disease. Although the causes of leukemia are not fully understood, certain factors are known to increase the risk of developing the disease. Among these are exposure to radiation, genetic and congenital factors, exposure to mutagenic chemicals and infection with certain viruses. However these factors change according to the type of leukemia (Lin, 1999).

Chronic leukemia is a cancer in which too many mature white blood cells are produced and build up in the body. Chronic leukemia develops slowly, often with no symptoms, and remains undetected for a long while. It is classified into two subgroups, according to the cell type that is affected, Chronic Lymphocytic and Chronic Myeloid Leukemia (Lin *et al.*, 1999).

Acute leukemias seem to arise when the normal process of cell maturation (also called differentiation) is interrupted at a very early (blast) stage of cell's life. The result is an accumulation of immature, nonfunctional, leukemic blast cells in the bone marrow and to a lesser extends in the blood. Acute leukemias are fatal if not treated. The distinction between the two subtypes acute lymphocytic leukemia (ALL) and acute myeloid leukemia (AML) is that blast cells associated with ALL are those that would mature into lymphoid cells, whereas blasts that would mature into myeloid cells are associated with AML.

### ***1.10.1 HL-60 Cell Line***

Cell lines that biologically resemble AML have been available since the 1980s and allowed careful study of the growth of leukemia cells under controlled conditions and of the effects of antileukemic agents (Devita, 2001).

One of the cell lines resembling AML is HL-60. The HL-60 cell line is a promyelocytic cell line derived from peripheral blood cells from a 36-year-old Caucasian female with acute promyelocytic leukemia. Because of its morphological and genetic characteristics it is classified as FAB-M3 (Gallagher, 1979). Typical characteristic of promyelocytic leukemia is owned by HL-60 cells, which is translocation between chromosomes 15 and 17 (t (15; 17)) (Dalton, 1988). The HL-60 cell line, derived from a single patient with acute promyelocytic leukemia, provides a unique in vitro model system for studying the cellular and molecular events involved in the proliferation and differentiation of normal and leukemic cells of the granulocyte/monocyte/macrophage lineage (Collins, 1987). HL-60 cells grow in suspension culture. The predominant cell population consists of neutrophilic promyelocytes.

## **1.11 Cytotoxicity of *Rheum ribes***

Cytotoxicity assays measure drug-induced alterations in metabolic pathways or structural integrity which may or may not be related directly to cell death, whereas survival assays measure the end result of such metabolic perturbations which may be either cell recovery or cell death. In order to follow cytotoxic effect of compounds on cell viability, there are many techniques are used such as MTT assay, dye exclusion technique etc.

3-(4, 5-Dimethylthiazol-2-yl)-2, 5-diphenyltetrazolium bromide (MTT) reduction is one of the most frequently used methods for measuring cell proliferation and neural cytotoxicity. It is widely assumed that MTT is reduced by active mitochondria in living cells. In addition, MTT is membrane impermeable and taken up by cells through endocytosis and that reduced MTT formazan accumulates

in the endosomal/lysosomal compartment and is then transported to the cell surface through exocytosis. The color development was measured at the ELIZA plate reader at 570 nm.

### ***1.11.1 Cell Viability***

Dye exclusion technique is the other type of test to follow cell viability. In this technique, Trypan blue is a specific dye used. The basis of trypan blue staining is the exclusion of dyes by living cells, so that under microscope only the dead cells appear as blue, whereas the living cells remain colourless because of their dye exclusion ability. In addition, cytotoxicity of any compound is also determined by apoptosis or/and necrosis, briefly cell death. The cytotoxic effect of most immuno and chemo therapeutic agents in vitro and in vivo depends on induction of apoptosis in susceptible tumor cells.

## **1.12 Apoptosis and Necrosis**

One of the most widely used principles in cancer treatment is causing the cancer cells die by apoptosis. Apoptosis (also called programmed cell death) is the term used to describe how cells die under a variety of physiological and pathological conditions. Apoptosis is defined as genetically programmed mechanism of the cell death resulting in the morphological changes, which are characterized by blebbing of the plasma membrane, shrinkage of the cell, condensation of the cytoplasm and nucleus, and cellular fragmentation into membrane apoptotic bodies. Also, cleavage of the DNA between histone octamers to generate the so-called nucleosomal ladder of fragments occurs during programmed cell death. A second mode of cell death, necrosis, is the classically defined form of cell death. Apoptosis and necrosis completely differ in many respects; apoptosis is a genetically regulated event whereas necrosis occurs when the cells were subjected to harsh conditions and when they are damaged.

Apoptosis is a programmed cell death and is needed for survival and proper development of cells. Many cells are produced excess during development and later undergo apoptosis to form the whole organism (Meier, 2000).

The formation of the fingers and toes of the fetus, the loss of frog tail, the neural development of the adult brain (Hutchins, 1998), development of reproductive organs are occurred by apoptosis (Meier, 2000). The balance between proliferation and death, regulation of the immune system, removal of the defective and harmful cells represents the importance of the apoptosis. Any defect in its mechanism may result in cancer and several other diseases (Fadell, 1999a). Less of survival signals like growth factor or having negative signals like x-ray, ultraviolet light, oxidative stress, chemicals that leads to DNA damage, defects in DNA repair mechanisms, ligation of cell surface receptors are all cause of apoptosis. (<http://users.rcn.com/jkimball.ma.ultranet/BiologyPages/A/Apoptosis.html>) There are two main pathways of apoptosis named as intrinsic and extrinsic pathways that are triggered by stimulus from inside and outside respectively. (Fig 1.5)

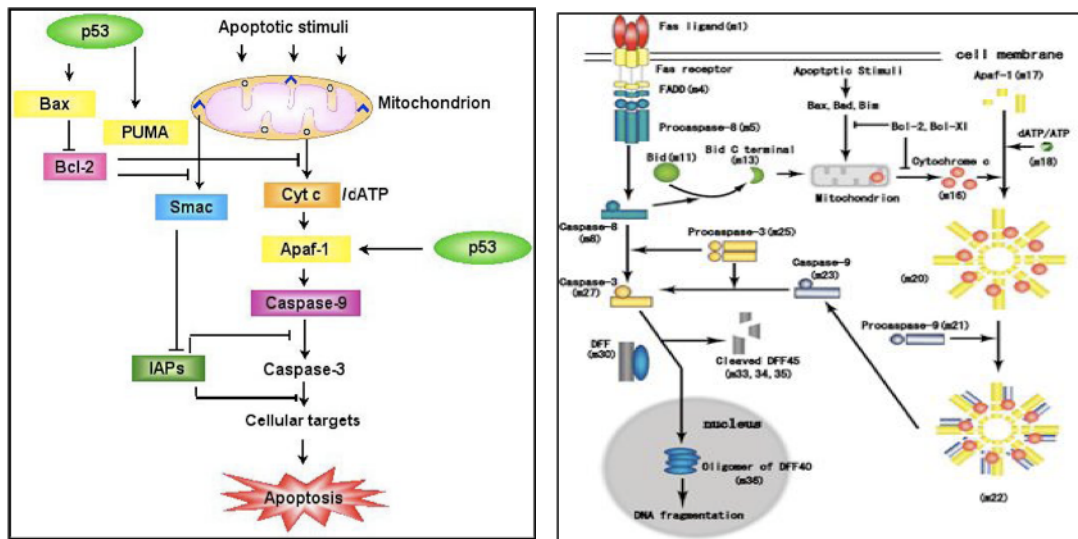


**Figure 1.5** Representation of intrinsic and extrinsic apoptosis pathways. ([http://www.weizmann.ac.il/home/ligivol/apoptosis\\_project/apoptotic\\_pathways.htm](http://www.weizmann.ac.il/home/ligivol/apoptosis_project/apoptotic_pathways.htm) l; <http://www.genomicobject.net/member3/GONET/apoptosis.html>)

The intrinsic pathway is triggered by tumor suppressor protein p53 which is activated as a transcription factor upon several factors like oncogene activation, DNA damage and these results in growth arrest or apoptosis. p53 stimulates the expression of apoptotic proteins like p21, Bax, Apaf-1, Puma, Noxa, Fas and DR5 cells.

(Vousden et al., 2002) and represses the expression of antiapoptotic proteins such as Bcl-2 and Bcl-XL (Hoffman et al., 2002; Wu et al., 2001). Bcl-2 family members regulates the mitochondrial integrity and control the release of apoptotic proteins to the cytoplasm (Cory and Adams, 2002). Bcl-2 is the first example of an oncogene found to inhibit cell death instead of proliferation (Vaux et al., 1988). Bcl-2 is located on the surface of the outer membrane of the mitochondria and suppresses the generation of ROS, stabilizes mitochondrial membrane potential and inhibits the release of cytochrome c (Reed, 1998). Bax together with other apoptotic members of the Bcl-2 family causes the cytochrome c release. In response to apoptotic stimulus Bax gains the ability to migrate from cytoplasm to outer membrane of mitochondria causes pore formation, permeability of transition and finally the release of cytochrome c to the cytoplasm (Borner, 2003).

Cytochrome c binds to the apoptotic protease activating factor-1 protein, Apaf-1, forming the complex named as apoptosome (Salvesen and Renatus, 2002b). Apoptosome binds procaspase-9 and activates it forming caspase-9 (Denault and Salvesen, 2002). Caspase-9 activates caspase-3. Caspase 3 activates caspase 6 and this activates caspase 7.

Apoptosis continues with digestion of structural proteins, DNA condensation, fragmentation. Caspase-3 activates DNA fragmentation factor, DFF, having DNase activity causes internucleosomal DNA fragmentation and final event is the phagocytosis of the cell (Earnshaw et al., 1999). The extrinsic pathway also named as death receptor pathway is triggered upon binding of specific ligands to cell surface receptors that belongs to the tumor necrosis factor receptor gene superfamily (Ashkenazi, 2002). Activated receptor complex activates caspase-8. There are two pathways for caspase-8 to activate caspase-3. In the first one, caspase-8 directly activates caspase-3 (Scaffidi et al., 1998). In the second pathway, the death signal coming from the activated receptor isn't enough for apoptosis to proceed and needs

to be amplified through mitochondrial apoptosis pathways. In this regard, caspase-8 cleaves Bcl-2 interacting protein, Bid, and its carboxy terminal migrates to mitochondria causing the release of cytochrome c. As in the case of intrinsic pathway cytochrome c binds to Apaf-1 and this complex activates caspase-9 and it activates caspase-3 (Luo et al., 1998). Apoptotic pathways were shown in Figure 1.7.

Suppression of the anti-apoptotic members or activation of the pro-apoptotic members of the Bcl-2 family leads to altered mitochondrial membrane permeability resulting in release of cytochrome c into the cytosol. In the cytosol, or on the surface of the mitochondria, cytochrome c is bound by the protein Apaf-1 (apoptotic protease activating factor), which also binds caspase-9 and dATP. Binding of cytochrome c triggers activation of caspase-9, which then accelerates apoptosis by activating other caspases. Release of cytochrome c from mitochondria has been established by determining the distribution of cytochrome c in subcellular fractions of cells treated or untreated to induce apoptosis (Kharbanda, 1997). Cytochrome c was primarily in the mitochondria-containing fractions obtained from healthy, non-apoptotic cells and in the cytosolic non-mitochondria-containing fractions obtained from apoptotic cells. Using mitochondria-enriched fractions from mouse liver, rat liver, or cultured cells it has been shown that release of cytochrome c from mitochondria is greatly accelerated by addition of Bax, (Li, 1998) fragments of BID, (Desagher, 1999) and by cell extracts (Kluck, 1997).

Mitochondria have crucial role in apoptosis. The mitochondrial pathway of apoptosis is triggered by either the internal signals such as DNA damage, cytoskeleton disruption and reactive oxygen species or by external signals such as death receptors. Release of cytochrome c from the mitochondria can trigger a series of events leading to the activation of effector caspases. For example, procaspase-9 is activated when complexed with dATP, APAF-1 and extramitochondrial cytochrome c. Following activation, caspase-9 can initiate apoptosis by cleaving additional caspases (Figure 1.6). Besides activating the mitochondrial pathway, death receptors may also trigger mitochondria independent pathway that involves the direct activation of initiator caspases through caspases 8 or caspase 10 (Figure 1.7).

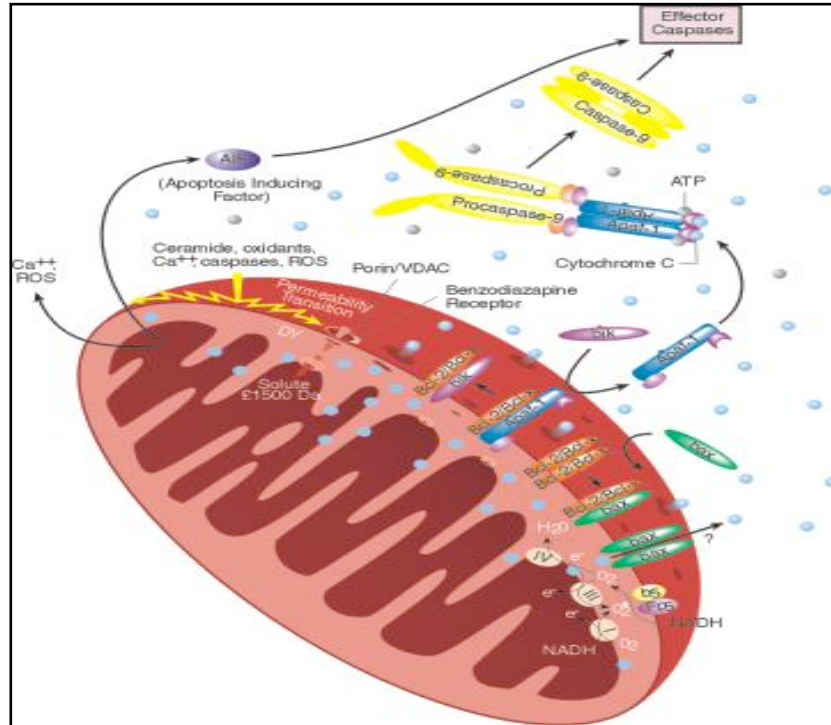


**Figure 1.6** Release of cytochrome c from the mitochondria can trigger a series of events leading to the activation of effector caspases.

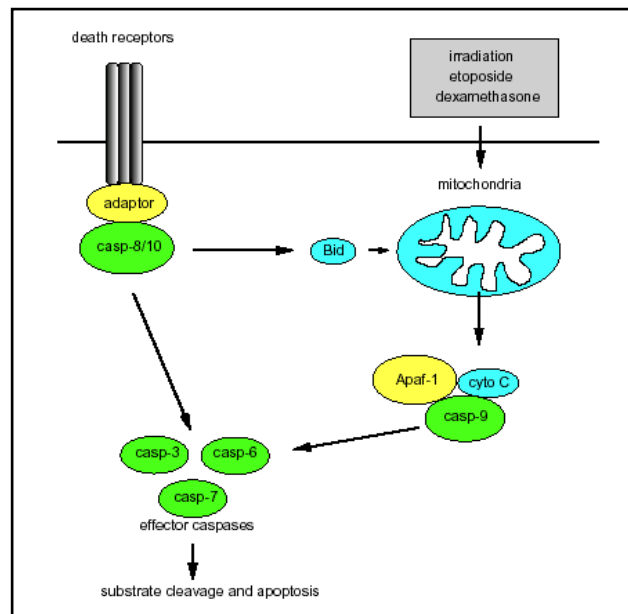


**Figure 1.7** Figure shows the death receptor pathway and its direct and indirect effects on the effector caspases.

The discovery of Bcl-2 family members and other apoptotic proteins goes back to the experiments in *C.elegans*. 131 cells of this organism undergo apoptosis during its development. Initially Ced-3, Ced-4 and Ced-9 genes were identified whose products have homology with a caspase, Apaf-1 and Bcl-2 protein respectively. Due to the experiments, it was understood that, Ced-3 and Ced-4 products were causing apoptosis while Ced-9 product was preventing apoptosis.

One of the mechanisms of the programmed mechanism of cell death results in the morphological changes. The process is extensive during development and a way of its regulation with many others ways is the growth factors for example neurons and haematopoietic cells apoptose with the growth factor removal.

### **1.13 Glutathione S-Transferases**

The glutathione S-transferases (GSTs) are primary phase II detoxification enzymes that has also many other important functions in the cell (Wilce and Parker, 1994). Their major activity in the cell is to catalyze the attack of reduced glutathione to compounds that have electrophilic nitrogen, sulphur or carbon atom. They have a wide range of substrate specificities. These include nitrobenzenes, epoxides, heterocyclic amines, quinones, arene oxides,  $\alpha,\beta$ -unsaturated carbonyls (Hayes and McLellan, 1999; Sheehan et al., 2001). GST enzymes are evolved from thioredoxin enzymes that are antioxidants and are found in many organisms ranging from bacteria to mammals and share structural and sequence similarities with other stress related proteins that are found in a wide range of organisms and it is suggested that a common stress related ancestor that is formed before thioredoxin is responsible for this relationship. (Martin, 1995; Rossjohn et al., 1996). These multiple enzyme families from one ancestor might have been formed from gene amplification, duplication, independently folding domains and inherited in proteins during evolution (Armstrong, 1998; Hansson et al., 1999).

There are three major families of glutathione transferases. Cytosolic and mitochondrial GST are soluble enzymes whereas the third class microsomal GST is membrane associated, named as, membrane associated proteins in eicosanoid and glutathione (MAPEG) metabolism. All three members of GST enzyme family catalyze the conjugation of reduced glutathione (GSH) with 1-chloro-2,4-dinitrobenzene (CDNB) a reaction involving a nucleophilic attack of a thiolate anion (GS<sup>-</sup>) on CDNB's aromatic ring with displacement with Cl and show glutathione peroxidase activity toward cumene hydroperoxide (CuOOH) as it was shown in Figure 1.9. The MAPEG and cytosolic GST enzymes catalyzes isomerization reaction and are involved in the formation of leukotrienes and prostaglandins (Hayes et al., 2005).

The largest family represents cytosolic GST enzymes and have lots of activities as shown in Figure 1.10. They have thiolysis, reduction, isomerization activities (Hayes, 2005). Beside having these activities, cytosolic GST enzymes can bind covalently and noncovalently to nonsubstrate ligands and have roles in intracellular transport and disposition of xenobiotics. These nonsubstrate hydrophobic ligands are some steroids, bilirubin, heme, lipophilic anticancer drugs and this binding has often roles with the inhibition of the GST enzyme activity (Hayes and Pulford, 1995). Cytosolic GSTs are found in humans in several classes having 60% amino acid homology; Alpha, Mu, Pi, Sigma, Theta, Omega, Zeta. Classification depends on the primary, tertiary structure similarities; immunological, kinetic properties. (Sheehan, 2001). The structural differences especially depends on the active site, general structure is similar and it is like the ancestor enzyme thioredoxin. The conserved part of the structure is the N terminal and this includes an important part of the active side; tyrosine, serine or cysteine residue that interact with the thiol group of GSH and lowers the pKa from 9 to 6-7. This is the catalytic activity of the GST enzyme (Atkins, 1993).

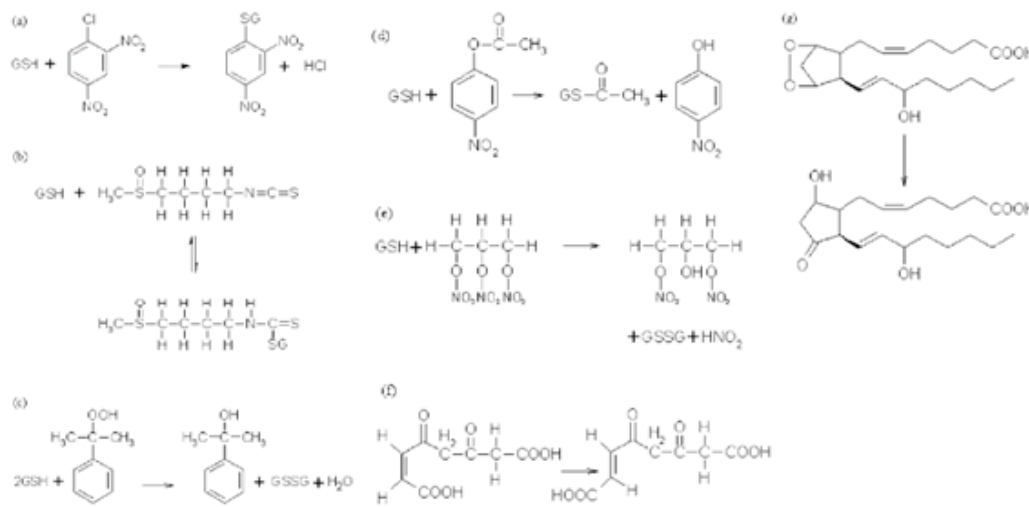


**Figure 1.8** Conjugation, reduction, thiolysis and isomerization reactions catalyzed by GST. Substrates are as the following; (a) CDNB (b) sulforaphane (c) CuOOH (d) 4-nitrophenyl acetate (e) trinitrolycerin (f) maleylacetoacetate (g) PGH<sub>2</sub> conversion to PGD<sub>2</sub> (Hayes, 2005).

Glutathione transferases have exogenous and endogenous substrates. They metabolize drugs, herbicides, insecticides, chemotherapeutic agents, carcinogens, environmental pollutants. Overexpression of GST enzymes in tumor tissues causes resistance to anticancer drugs and in these cases the goal of the treatment is to lower GSH and GST using some inhibitors. (Lewis, 1988). Also GST enzymes may activate xenobiotics for some instances. In this cases, if they transform prodrugs to active forms, the overexpression of these enzyme becomes an advantage (Findlay et al., 2004). Reactive oxygen species; superoxide anion O<sub>2</sub><sup>-</sup>, hydrogen peroxide H<sub>2</sub>O<sub>2</sub>, hydroxyl radical HO• produced during aerobic respiration, are endogenous substrates of GST enzymes. Superoxide dismutase, catalase, GST, glutathione peroxidase, aldehyde dehydrogenase, alcohol dehydrogenase, aldo-keto reductase are enzyme systems that protect the cell against products of oxidative stress. GSH, bilirubin, ascorbic acid, α-tocopherol are the compounds that help this process nonenzymatically (Hayes, 2005).

Reactive oxygen species causes the peroxidation of polyunsaturated fatty acids in membranes. This event causes destruction of the membranes. The GST enzymes reduce the end products of lipid peroxidation, as a result, protect the membranes. Base propanals are formed by oxidation of nucleotides and these are detoxified by GST. Oxidation of catecholamines causes the formation of quinone containing compounds, these can produce oxygen radical by redox cycling. GST causes the conjugation of GSH with these compounds and prevents radical formation (Hayes, 2005; Dagnino-Subiabre, 2000).

GST enzymes have roles in the catabolism of tyrosine and phenylalanine amino acids (Hayes, 2005). Also they have roles in the synthesis of steroid hormones; testosterone and progesterone (Johansson and Mannervik, 2001). GST enzymes catalyze the synthesis and inactivation of eicosanoids, this role has many biological consequences in the cell. GST enzymes has the ability to effect formation and degradation of eicosanoid 15-Deoxy- $\Delta$  12,14-prostaglandin J2 (15d-PGJ2) as shown in Figure 1.8. Overexpression of GST effect PPAR $\gamma$ , Nrf-2 and NF-kB dependent gene expressions (Paumi, 2004; Itoh, 2004; Rossi, 2000).

Beside GSTs, GSH has also effects on gene expressions, it conjugate with an endogenous lipid peroxidation product, 4-hydroxynonenal (4-HNE). Being an  $\alpha,\beta$ -unsaturated carbonyl, 4-HNE is an intracellular signalling molecule. 4-HNE has the ability to activate several cell surface receptors, stimulates expressions of JNK, PKC, p53 and promote apoptosis; also effect several transcription factors like NF-kB, c-Jun, Nrf2. As a result the reaction with GSH has many biological consequences (Echtay, 2003; Awasthi, 2003; Tjalkens, 1999). GST expression increases during carcinogenesis. Under oxidative stress, Nrf2, transcription factor that is normally located in the cytoplasm, is carried to the nucleus and reaches to ARE (Antioxidant Response Element) sequences, the genes that have ARE sequences are induced as a result. It is seen that ARE sequences are mostly overexpressed during tumorigenesis and the increase of GST enzymes during carcinogenesis might be because of this (Hayes, 2005). GST  $\pi$  gene is especially emphasized in this regard. Also GST  $\mu$  gene is important in carcinogenesis especially in lung cancer because 50% of human population lacks this gene, so it is highly polymorphic, person who lacks this enzyme is more susceptible to carcinogens (Seidegard, 1988; Seidegard, 1990).

## 1.14 Scope of The Study

Natural products are of great importance in the drug discovery process, particularly in the areas of cancer. The screening with innovative biological assays allows the verification of their active principle. These improvements provided the basis for rational drug discovery and have fundamentally contributed to the development of important pharmaceuticals of natural origin.

*Rheum* species are medicinally important plants due to the presence of anthracene derivatives occurring in the subterranean parts of the plant. *Rheum ribes* L. (Polygonaceae) is the source of one of the most important crude drugs in the Middle East.

*R. ribes* is the only *Rheum* species growing in Turkey. There are a few chemical studies on *R. ribes* in Turkey. Considering the phenolic constituent profile of *R. ribes*, particularly their flavonoids, stilbenes and anthraquinones, they appeared to provide a potential source of antioxidants, which have well known pharmacological actions such as free radical scavenging, chemoprevention and tumor suppression.

The aim of the present study was to investigate the bioactivities of the solvent extracts of *Rheum ribes*. This study was designed in order to evaluate antioxidative, cytotoxic and apoptotic characteristics of *R. ribes* extracts.

Prepared extracts were studied for free radical scavenging activities by DPPH method. The chemical composition of the extracts was quantified by colorimetric reaction in terms of total phenol and flavonoid contents.

The solvent extracts of *R. ribes* were examined for their inhibitory and cytotoxic effects on the human acute promyeloblastic leukemia HL-60 cells by using trypan blue dye exclusion test and XTT assay for different extract concentrations at different time points.

*R. ribes* caused HL-60 cells apoptosis via formation of phosphatidylserine externalization, as evidenced by flow cytometry analysis. The apoptosis caused by *R. ribes* were also demonstrated by DNA ladder formation and TUNEL. The study was designed to analyze the expression of pro-apoptotic and anti-apoptotic genes in transcriptional level. To see the role of mitochondria in *Rheum ribes* induced

apoptosis in HL-60 cells, cytochrome c release to the cytosol was also detected by western blot analysis.

The activation of caspase-3 was also evaluated by western blot and fluorometric enzyme activity assay against substrates Ac-DEVD-AFC.

Beside these investigations, experiments were conducted to demonstrate whether *Rheum ribes* extracts affect phase I and phase II enzyme systems in HL-60 cells (CYP1A1, CYP1B1 and GST) and to investigate the susceptibility of the relation between apoptosis and phase I and II enzyme families.

The study was designed to investigate the cellular and molecular changes induced by *Rheum ribes* extracts leading to the induction of apoptosis in HL-60 cells for the first time in literature. Our investigations for the pursuit of these interactions may not result in hundred percent prevention or in total cure of cancer, but this was a rational way forward, to catch on to the cutting-edge technologies.

## CHAPTER II

### 2. MATERIAL AND METHODS

#### 2.1 Materials

##### 2.1.1 *HL-60 Cell Lines*

HL-60 (human promyeloblastic leukemia cell line) was purchased from Foot-and-Mouth Disease Institute of Ministry of Agriculture & Rural Affairs of Turkey, Turkey (ATCC Grade, HÜKÜK no-96041201).

##### 2.1.2 *Plant Material*

*Rheum ribes* young shoots and roots were collected in May 2007 by Dr. Fevzi Özgökçe from Van, Turkey (Location: B9 Bitlis: Tatvan, Alacabük (Pelli) Mountain, northwest slopes, Zerzemin Pass, step, 28.v.2004, 2700m, 38° 23' 543" N ve 42° 41' 405" E and deposited in the herbarium of University of Yüzüncü Yıl , Van, Turkey (VANF) with number F 12100.

##### 2.1.3 *Chemicals and Other Materials*

Ethyl acetate, methanol and ethanol used in the preparation of extracts were purchased from Merck (Merck Company, Darmstadt, Germany). Water (ddH<sub>2</sub>O) that was distilled twice was purified using a Milli – Q system (Millipore, Bedford, MA, USA). 2, 2-diphenyl-1-picrylhydrazyl (DPPH) was purchased from Sigma (Sigma Chemical Company, Saint Louis, Missouri, USA)).

Dimethyl sulphoxide (DMSO), proteinase K was purchased from AppliChem GmbH (Darmstadt, Germany). Roswell Park Memorial Institute medium (RPMI 1640) 4-(2-hydroxyethyl)-1-piperazineethanesulfonic acid (HEPES) modified, Fetal-Calf Serum (Heat-inactivated) were purchased from Biochrom Ltd. (Cambridge, UK). Gentamicine, steril phosphate buffered saline (sPBS), and 0.5 % (w/v) trypan blue were purchased from Biological Industries (Haemek, Israel).

25-cm<sup>2</sup> (T25) and 75-cm<sup>2</sup> (T75) tissue culture flasks and 6-well, 24-well and 96 well microplates (flat and round bottom) were obtained from Greiner Bio-One, Germany. All were for suspension culture and were not modified and thus retained the natural hydrophobic properties of polystyrene.

Folin-Ciacceltau Phenol Reagent, 1-chloro-2,4-dinitrobenzene (CDNB), reduced glutathione (GSH), bovine serum albumin (BSA), ethylenediaminetetraacetic acid (EDTA), sodium dodecyl sulphate (SDS), ammonium persulphate (APS), bromophenol blue, coomassie brilliant blue R-250, N,N'-methylenebisacrylamide (Bis), hydroxymethyl aminomethane (Tris base), N,N,N',N'-tetramethylethylenediamine (TEMED), acrylamide, glycine, glycerol, sodium carbonate, sodium thiosulfate, Tween-20, 5-bromo-4-chloro-3-indolyl phosphate (BCIP), agarose were purchased from Sigma Chemical Company, St. Louis, MO, U.S.A.

SDS-polyacrylamide gel electrophoresis (PAGE) molecular weight markers, M-MuLV-reverse transcriptase (RevertAid<sup>TM</sup>), dNTP mix, Taq DNA polymerase, ribonuclease inhibitor and DNA ladder (GeneRuler<sup>TM</sup> 100 bp DNA Ladder Plus) were from MBI Fermentas, USA.

BD ApoAlert<sup>TM</sup> DNA Fragmentation and Cell Fractionation Kit, containing washing buffer, fractionation buffer, DTT, Protease Cocktail, monoclonal antibodies against Cytochrome c were purchased from Clontech Laboratories, U.S.A. Amplified alkaline phosphatase goat anti-rabbit immune-blot assay kit and sequi-blot polyvinylidene difluoride membrane (PVDF) were purchased from Bio-Rad Laboratories, Richmond, CA, U.S.A.

RNeasy RNA isolation kit was obtained from Qiagen, Hilden, Germany.

Cryovials (sterile, non-pyrogenic, DNase and RNase free) were purchased from Greiner Bio-One, Germany.

Annexin V-Apc and 7AAD were purchased from Caltag, Bensenville, IL, USA and Invitrogen, Carlsbad, CA, USA, respectively. Ac-DEVD-AFC was supplied from Axxora (San Diego, CA, USA).

All other chemicals were of analytical grade and obtained from commercial sources at the highest grade of purity available.

#### **2.1.4 Primers**

Bcl-2, Bax, CYP1A1, CYP 1B1, GAPDH and  $\beta$ - actin gene primers were obtained from Iontek, İstanbul, Turkey.

**Table 2.1** Primers used in this study

<b>Primer set</b>	<b>Sequence</b>	<b>Amplicon size (bp)</b>
Bcl-2 forward	5' GGATTGTGGCCTTCTTTGAG 3'	219
Bcl-2 reverse	5' TCTTCAGAGACAGCCAGGAGA 3'	
Bax forward	5' TCTGACGGCAACTTCAACTG 3'	188
Bax reverse	5'TTGAGGAGTCTCACCCAACC 3'	
$\beta$ -actin forward	5'CAGAGCAAGAGAGGCATCCT3'	201
$\beta$ -actin reverse	5'TTGAAGGTCTCAAACATGAT3'	
CYP 1A1 forward	5'TAGACACTGATCTGGCTGC3'	146
CYP 1A1 reverse	5'GGGAAGGCCCATCAGCATC3'	
CYP 1B1 forward	5'AACGTCATGAGTGCCGTGTGT3'	360
CYP 1B1 reverse	5'GGCCGGTACGTTCTCCAAATC3'	
GAPDH forward	5' TCTCTCTTTCTGGCCTGGAG 3'	122
GAPDH reverse	5'GGATGGATGAAACCCAGACA3'	

### 2.1.5 Antibodies

**Table 2.2** Antibodies used in this study

<b>Antibody</b>	<b>Isotypes</b>	<b>Dilution</b>	<b>Company</b>
<b>Cytochrome c</b>	Rabbit	1:100, 5% Non Fat Dry Milk	Clontech (USA)
<b>GAPDH</b>	Mouse	1:2000, 5% Non Fat Dry Milk	Abcam (UK)
<b>Caspase 3</b>	Rabbit	1:1000, 5% Non Fat Dry Milk	Cell Signaling (USA)
<b>Bax</b>	Rabbit	1:1000 5% BSA	Cell Signaling (USA)
<b><math>\alpha</math>-tubulin</b>	Mouse	1:100, 5% BSA	Abcam (UK)

## 2.2 METHODS

### 2.2.1 Preparation of *Rheum ribes* freeze-dried extracts

*Rheum ribes* shoot (Fig 2.1) and root were placed on filter papers separately and air-dried at shade for two weeks at room temperature (RT). Dry plants were powdered by Waring (model 32BL80) commercial blender at a high speed for at least 2 minutes and stored in dry, dark and tempered conditions (RT) until use.



**Figure 2.1** Freshly collected *Rheum ribes* shoots, May 2007

*Rheum ribes* shoot and root dry powdered samples (30 g) were separately suspended in absolute ethyl acetate (EtOAc), methanol (MeOH), ethanol (EtOH) and ddH<sub>2</sub>O at a ratio of 1:12 (w/v) in dark bottles. Solvent selection was based on increasing polarity shown as in the Table 2.3. The samples were extracted by sonicating at room temperature for 1 h in a bath sonicator (Bandelin Sonorex Model RK 100H, Berlin, Germany) followed by incubation at 50°C on a rotational incubator at 150 rpm for 24 h (Kim, 2003). Then extracts were filtered through a double-layered cheesecloth or a coarse filter paper on a Büchner funnel and were concentrated up to 5 ml at around 40°C under reduced pressure (ethyl acetate extract at: 240 mbar; methanolic extract at: 337 mbar; ethanolic extract at: 175 mbar; aqueous extract at: 72 mbar) with BÜCHI Rotavapor R-20 (Labortechnik AG, Flawil,

Switzerland) and finally lyophilized with *Maxi Dry Lyo* lyophilizator (*Heto-Holten, Allerod, Denmark*). The weight of freeze-dried extracts was recorded and the percent yield of extraction (w/w) was calculated by dividing them to the weight of the dry powdered samples. The freeze-dried extracts were kept at -20°C in the dark to provide consistency between tests.

Freeze-dried extracts were named and names were abbreviated as follow; ethyl acetate shoot extract (ASE), ethyl acetate root extract (ARE), methanol shoot extract (MSE), methanol root extract (MRE), ethanol shoot extract (ESE), ethanol root extract (ERE), aqueous shoot extract (WSE) and aqueous root extract (WRE).

**Table 2.3** Physical constants of solvents used in the study, listed in order of decreasing solvent polarity

<b>Name</b>	<b>Formula</b>	<b>Formula weight</b>	<b>Density</b>	<b>Boiling point</b>	<b>Polarity Index</b>
Water	H <sub>2</sub> O	18.02	1	100	9
Ethanol	C <sub>2</sub> H <sub>5</sub> OH	46.07	0.789	78.4	5.2
Methanol	CH <sub>3</sub> OH	32.04	0.7913	64.7	5.1
Chloroform	CHCl <sub>3</sub>	88.11	1.484	61.7	4.1
Ethyl acetate	CH <sub>3</sub> COOC <sub>2</sub> H <sub>5</sub>	119.39	0.9006	77.1	4.4
1-Butanol	C <sub>4</sub> H <sub>9</sub> OH	74.12	0.8097	117.7	3.9*

\* 1-Butanol was saturated with water at a ratio of 1:1 before use.

### ***2.2.2 Fractionation of Rheum ribes Methanol Extracts***

*Rheum ribes* shoot and root dry powdered samples (30 g) were separately suspended in 70% methanol (v/v) at a ratio of 1:12 (w/v) in dark bottles. The samples were extracted by sonicating at room temperature for 1 h in a bath sonicator followed by incubation at 50°C on a rotational incubator at 150 rpm for 24 h (Kim et al., 2003). Then extracts were filtered through a double-layered cheesecloth or a coarse filter paper on a Büchner funnel and were concentrated up to 200 ml at around 40°C under reduced pressure (at: 337 mbar) with BÜCHI Rotavapor R-20 and were fractionated by partitioning into solvents of increasing polarity (Table 2.2). They were successively exhausted first with chloroform and then with water-saturated n-butanol at a ratio of 1:1. Remaining residue was the aqueous soluble fraction. Chloroform fractions were obtained by evaporating at around 40°C under reduced pressure (at: 474 mbar) with BÜCHI Rotavapor R-20. n-butanol and aqueous fractions were lyophilized with *Maxi Dry Lyo* lyophilizator. The flowchart (Figure 2.2) illustrates the fractionation process of *Rheum ribes*. Each fraction was subjected to the DPPH assay, total phenol and total flavonoid determination assay.

Dry powdered fractions of *Rheum ribes* were named as fractions to differentiate them from previously mentioned extracts and names were abbreviated as follow; chloroform shoot fraction (CSF), chloroform root fraction (CRF), Butanol shoot fraction (BSF), Butanol root fraction (BRF), aqueous shoot fraction (WSF) and aqueous root fraction (WRF).

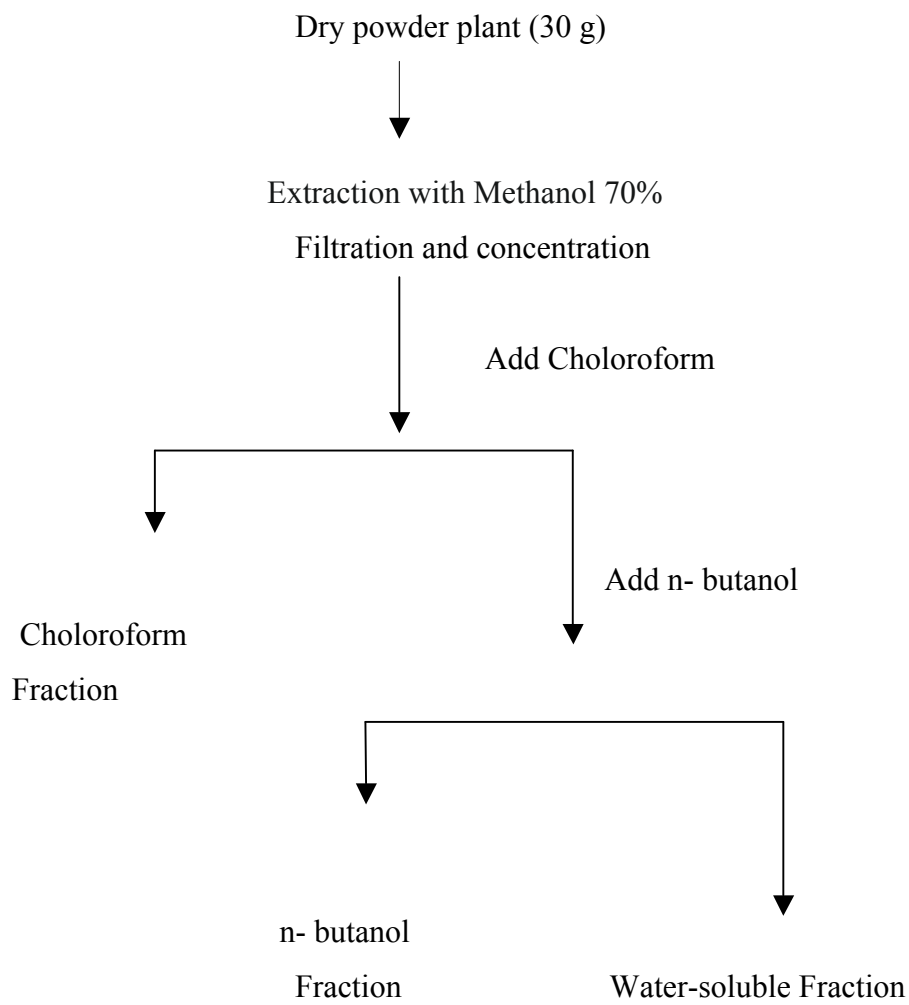


**Figure 2.2** Flow chart for the solvent fractination of *Rheum ribes*

### 2.2.3 Determination of *in vitro* Antioxidant Activity

All assays were scaled down to 96 well plate formats to be used for high-throughput screening of antioxidant activity, determination of total phenol and total flavonoid content. Flat bottom 96-well plates (Greiner, Frickenhausen, Germany) were used in order to accommodate a maximum volume of 350 µl without spillage.

#### 2.2.3.1 Free Radical Scavenging Activity of Freeze-dried Extracts by DPPH method

DPPH (2,2-Diphenyl-1-picrylhydrazyl) method was applied as proposed by Blois (1958) for determining the free radical scavenging activities of each of the freeze-dried extracts and adapted for microplate reader measurements. DPPH is the purple-colored stable free radical that is reduced into the yellow colored diphenylpicryl hydrazine compound by subtracting hydrogen from the phenolic compounds found in extracts. (Figure 2.3)



**Figure 2.3** Diagrammatic representation of chemical reaction of the reduction of DPPH in the presence of an electron donating antioxidant (*Rheum ribes*) (<http://www.naturalsolution.co.kr/tech21e.html>)

Flat bottom 96-well microtiter plates were used to generate the quantitative measure of the radical scavenging activity of *Rheum ribes* freeze-dried extracts prepared in different solvent systems, prepared as serial dilutions at different concentrations, ranging from 2.60 to 1333.33 µg/ml as final concentrations in wells. The assay was conducted in quadruplicates. Aliquots of 20 µl of freeze-dried extracts prepared in HPLC grade methanol or ddH<sub>2</sub>O (only for WSE and WRE) were plated out, to which 280 µl of DPPH ( $1.5 \times 10^{-4}$  M), prepared in HPLC grade methanol was added. A typical 96-well plate design for DPPH assay was shown in Appendix A. In the DPPH control wells 300 µl of DPPH and in methanol control wells 20 µl of methanol and 280 µl of DPPH was added. In order to eliminate the interference of extracted pigments with the DPPH reaction, the absorbance of the freeze-dried extracts (20 µl) was measured in 280 µl of methanol in the absence of DPPH. The positive controls were prepared using catechin, quercetin and emodin, to which 280 µl of DPPH was added. Plates were then tightly covered with lid and wrapped in aluminum foil to prevent evaporation and shaken for 1 min, after which it was stored in the dark for 30 min at room temperature. The decolourisation was measured spectrophotometrically at 517 nm using the SPECTRAMax 340PC microtiter plate reader, linked to a computer equipped with SoftMax Pro. Percent DPPH free radical scavenging activity (%RSA) was calculated for each of the test sample using Equation 2.1.

The antioxidant activity of plant extract was expressed as 50 % effective concentration (EC<sub>50</sub>), which is defined as the concentration (in µg/ml) of freeze-dried extract required scavenging 50% of DPPH in reaction mixture. %RSA was plotted against the concentration of the sample and the EC<sub>50</sub> values were determined using GraphPad Prism version 5 for Mac OS X (GraphPad Software, San Diego, California, USA, [www.graphpad.com](http://www.graphpad.com)).

### Equation 2.1

$$DPPH\ Scavenging\ Effect\ (\%RSA) = \frac{Av_c - (Av_{s(DPPH)} - Av_{s(MetOH)})}{Av_c} \times 100$$

Where:

$Av_c$  = Average absorbance of all methanol control wells

$Av_{s(DPPH)}$  = Average absorbance of sample wells with DPPH

$Av_{s(MetOH)}$  = Average absorbance of sample wells with methanol

$Abs$  = Absorbance at 517 nm

#### 2.2.3.2 Determination of Total Phenolic Contents of Freeze-dried Extracts

Total phenolic constituents of the freeze-dried extracts were analysed by Folin–Ciocalteu method using gallic acid as standard as described by Singleton, (1999) with some modifications. In this method the freeze-dried extracts were oxidized with Folin-Ciocalteu reagent, and sodium carbonate neutralized the reaction. The resulting blue colored product was quantified by measuring the absorbance spectrophotometrically at 765 nm after 120 min.

For the preparation of gallic acid stock solution, 50 mg of dry gallic acid was dissolved in 1ml of ethanol and diluted to 10 ml with ddH<sub>2</sub>O. Then the gallic acid stock solution was diluted with ddH<sub>2</sub>O at different concentrations, prepared as serial dilutions, ranging from 50 to 500µg/ml.

The extracts (3.5 µl) from a 10 mg/ml shoot and 1 mg/ml root freeze-dried extracts/fractions stock solution ( in methanol or ddH<sub>2</sub>O) or standard solutions gallic acid (3.5 µl) or ddH<sub>2</sub>O and methanol as blank were added to separate

wells and mixed thoroughly with 276.5 µl ddH<sub>2</sub>O and 17.5 µl of Folin-Ciocalteu reagent (1N). After 8 min 52.5 µl of 7% Na<sub>2</sub>CO<sub>3</sub> (0.66 M) solution was added, and mixed thoroughly by pipetting. The final concentration of the extracts in each well was 100 µg/ml for shoot and 10 µg/ml for root extracts/fractions. The plate was incubated in the dark for 2 hours at room temperature and the absorbance was read at 765 nm using the SPECTRAMax 340PC microtiter plate reader, linked to a computer equipped with SoftMax Pro. In order to get rid of the interference of pigments in extracts at 765 nm, blanks containing only extracts in ddH<sub>2</sub>O were prepared without addition of reagents. The total phenol content of the extracts was calculated by using the slope obtained from standard curve (Appendix B) of gallic acid according to Equation 2.2 and expressed as mg gallic acid equivalents (GAE) /g of dried extracts.

#### Equation 2.2

$$mg\ CAE/g\ of\ dried\ extracts = \frac{(Abs_s - Abs_{s(blank)}) - Abs_{blank} \times DF}{Slope}$$

Where;

$Abs_s$  = Average absorbance of sample wells with reactants

$Abs_{s(blank)}$  = Average absorbance of sample wells without reactants (only ddH<sub>2</sub>O)

$Abs_{blank}$  = Average absorbance of wells with ddH<sub>2</sub>O

$Slope$  = obtained from the standart curve in Appendix B

$Abs$  = Absorbance at 765 nm

### 2.2.3.3 Determination of Total Flavonoid Contents of Freeze-dried Extracts

The total flavonoid content in the extracts was determined by aluminium colorimetric assay (Zhishen, 1999) with some modifications. The principle of aluminum chloride colorimetric method is that aluminum chloride forms acid stable complexes with the C-4 keto group and either the C-3 or C-5 hydroxyl group of flavones and flavonols. In addition, aluminum chloride forms acid labile complexes with the orthodihydroxyl groups in the A- or B-ring of flavonoids. (Chia-Chi Chang, 2002)

A standard solution of (+) catechin at different concentrations from 25 to 500  $\mu\text{g}/\text{ml}$  was prepared by dissolving (+) catechin in ethanol. The shoot and root freeze-dried extracts/fractions (35  $\mu\text{l}$ ) from a 10  $\text{mg}/\text{ml}$  stock solution (in methanol or  $\text{ddH}_2\text{O}$ ) or standard (+) catechin solutions (35 $\mu\text{l}$ ) or solvents (as blank) were mixed thoroughly by pipetting with 140  $\mu\text{l}$   $\text{ddH}_2\text{O}$  in a 96 well plate. Then 10.5  $\mu\text{l}$  5% sodium nitrite ( $\text{NaNO}_2$ ) was added. The final concentration of the extracts in each well was 1000  $\mu\text{g}/\text{ml}$  for both shoot and root extracts/fractions. The mixture was incubated for 5 min at room temperature and 10.5  $\mu\text{l}$  of 10% aluminium chloride ( $\text{AlCl}_3$ ) was added to and then 6 min later, 70  $\mu\text{l}$  1 M  $\text{NaOH}$  was added to the wells. The total volume was made up to 350  $\mu\text{l}$  by adding  $\text{ddH}_2\text{O}$ . The absorbance was read at 490 nm using the SPECTRAMax 340PC microtiter plate reader, linked to a computer equipped with SoftMax Pro. Additionally, ethanol, methanol and  $\text{ddH}_2\text{O}$  only were processed in the same manner to account for any background due to solvents. In order to eliminate the interference of extracted pigments at 765 nm, the extracts in 315  $\mu\text{l}$  of  $\text{ddH}_2\text{O}$  were measured without adding reagents. The total flavonoid content of extracts was calculated by using the slope obtained from standard curve (Appendix C) of (+) catechin according to Equation 2.3 and expressed as  $\text{mg}$  of (+)catechin equivalents (CE)/g of dried extracts.

### Equation 2.3

$$mg\ CAE / g\ of\ dried\ extracts = \frac{(Abs_s - Abs_{s(blank)}) - Abs_{blank} \times DF}{Slope}$$

$Abs_s$  = Average absorbance of sample wells with reactants

$Abs_{s(blank)}$  = Average absorbance of sample wells without reactants (only ddH<sub>2</sub>O)

$Abs_{blank}$  = Average absorbance of wells with ddH<sub>2</sub>O

$Slope$  = obtained from the standart curve in Appendix C

$Abs$  = Absorbance at 490 nm

#### 2.2.4 Cell Line and Culture Conditions

HL-60 cells, a human promyeloblastic leukemia cell line, were grown in RPMI-1640 supplemented with 10% heat-inactivated fetal bovine serum (FBS), 2mM L- glutamine and 0.2 % (50mg/ml) gentamicine in the vessels appropriate for the designed experiment. The cells were incubated at 37<sup>0</sup>C with 95% air and 5% CO<sub>2</sub> in a Hepa filtered Heraeus Hera Cell 150 incubator. They were manipulated in a HERAsafe Class II Biological Safety (laminar flow) cabinet by using appropriate cell culture techniques in cell culture room. The medium was collected and refreshed every 2-3 days simulating usual cell culture conditions to maintain a constant cell to growth medium ratio.

#### **2.2.4.1 Cell Thawing**

The cryovial in which HL-60 cells found frozen was carefully taken out of the liquid nitrogen and immediately thawed in a water-bath (37°C). Cells were transferred to a tissue culture flask (T25) containing 10 ml prewarmed culture medium (37°C) and left in CO<sub>2</sub> incubator for 24 h. Next day, if no contamination and/or cell destruction was detected, media were removed by centrifuging (100 g, RT, 5 min) and the cells were washed with 5 ml sPBS by centrifuging twice (100 g, RT, 5 min) to remove cell debris, leaked toxic cell content and the DMSO, derived from the freezing medium. Cell pellet were redissolved in fresh complete medium in T75 flasks.

#### **2.2.4.2 Cell Counting with Trypan Blue Exclusion Method**

Trypan Blue is a dye used for distinguishing viable from non-viable cells. The basic principle of the method is that trypan blue only interacts with the cells if the membrane is damaged. Therefore, trypan blue only stains non-viable cells while viable cells exclude dye. Prior to use, stock trypan blue solution, 0.5 % (w/v), was diluted to 0.25 % (w/v) with sPBS.

In a 1.5 ml tube, 20 µl of 0.25 % (w/v) trypan blue solution added on 20 µl of cell suspension that were previously gently mixed to get homogenous mixture. The cell suspension in trypan blue solution was further pipetted up and down gently several times and 10 µl of the mixture was loaded in each of the two counting chambers of a Neubauer hemacytometer (Bright-line, Hausser Scientific, Horseam, PA, USA) by placing the pipette at the edge of the coverslip and allowing the suspension to fill the space by capillary action. The two 1x1mm-counting areas of the hemacytometer were then observed under a light microscope and the number of cells (total and viable) per counting area was determined. Additionally, a common rule was applied; cells that touch the middle lines (of the triple lines) to the left and top of the square were counted, cells similarly on the right or bottom of the square

were not counted to avoid double-counting. If the cells were on the top or right line they were counted in the square, otherwise not counted in that square. Non-viable cells appeared as blue, viable cells were clear in a bluish background.

Each square of the hemacytometer (with cover slip in place) represents a total volume of 0.1 mm<sup>3</sup> or 10<sup>-4</sup> cm<sup>3</sup>. Since 1 cm<sup>3</sup> is equivalent to 1 mL, the subsequent cell concentration per mL (and the total number of cells) will be determined using the following equations (shown with an example):

$$\text{Cells per mL} = \text{the average count per square} \times \text{the dilution factor} \times 10^4.$$

Total cell number = cells per mL  $\times$  the original volume of fluid from which cell sample was removed.

(Shown with an example):

#### Equation 2.4

Total (or viable) cells counted in 25 mm <sup>2</sup>	x dilution factor	=cells/10 <sup>-4</sup>	x 10 <sup>4</sup> = cells/ml	x total volume of cell suspension (10 ml)= Total (or viable) cells recovered
49(45)	2	98 (90)	9.8(9.0) x10 <sup>5</sup> cells/ml	10 ml x 9.8(9.0) x10 <sup>5</sup> cells/ml =9.8(9.0) x10 <sup>6</sup>

#### 2.2.4.3 Freezing The Cells

Microbial contamination or genotypic changes may appear in long-term cell cultures, leading to the loss of well-characterized cell lines. To prevent cell loss, cells can be frozen and stored almost indefinitely at a very low temperature in liquid nitrogen (196 °C). For this purpose high numbers of cells were require. For cryoprotection, 600µL of dimethylsulfoxide (DMSO) was added to 5.4 mL of FBS to obtain 90% FBS: 10% DMSO in freezing medium.

$5 \times 10^6$  cells were cultured in 75-cm<sup>2</sup> tissue culture flasks in 20 mL of complete media for 24 h. Next day, at least  $1 \times 10^7$  cells were poured in to 50 mL Falcon tube and pelleted by centrifugation (200xg, 10 min, 4 °C). The supernatant was discarded, and the pellet was resuspended in ice-cold freezing medium. It is important that cells should be exposed to freezing medium for as little time as possible prior to freezing. The cell suspension in the freezing medium equally transferred to cryovials (1.5 ml) and placed in a Mr. Frosty container is at room temperature and that has sufficient isopropanol to ensure gradual decrease in temperature for gentle freezing. The cryovials in Mr. Frosty container were then placed in the -86°C freezer overnight. Next day the cryovials were transferred to a liquid nitrogen container for long-term storage.

#### **2.2.4.5 Growth Curve Construction**

HL-60 cells require simple maintenance in vitro and grow as single-cell suspension. Doubling times are around 24 h in an actively growing culture. In order to determine doubling time of our culture, the cell number was adjusted to  $1.0 \times 10^5$  cells in 1mL growth media, distributed to 24 well plates and plates were placed into CO<sub>2</sub> incubator. Every corresponding day counts were made in triplicates from three different wells. Cells were stained with 0.25 % (w/v) trypan blue (Biological Industries, Israel) and counted in a Neubauer counting chamber under light microscopy. The cells were counted for 144 hours. During this period the medium was not refreshed. Percent cell viability of the cells was calculated according to Equation 2.5. Growth curve was constructed as number of cells ( $\times 10^4$ )/ ml versus time (hour).

### Equation 2.5

$$\% \text{ Cell Viability} = \frac{\text{Cell Number}_{\text{Trypan}^-}}{\text{Cell Number}_{\text{Trypan}^-} + \text{Cell Number}_{\text{Trypan}^+}} \times 100$$

Where;

$\text{Cell Number}_{\text{Trypan}^-}$  = Number of Viable cells

$\text{Cell Number}_{\text{Trypan}^+}$  = Number of Dead cells

#### 2.2.4.6 Cell Treatment with Extracts

HL-60 cells were plated in their growth medium at a density of  $1 \times 10^5$  cells/ml into 24 or 96 well plates for cytotoxicity studies and incubated at  $37^\circ \text{C}$  in  $\text{CO}_2$  incubator. After overnight growth, cells were treated with a concentration range of *Rheum ribes* (0-300  $\mu\text{g/ml}$ ) shoot and root freeze-dried extracts for 24, 48 and 72 hours. Ethyl acetate and ethanol extracts were first dissolved in DMSO and then diluted with complete RPMI 1640 medium. Aqueous extracts were dissolved directly in RPMI 1640 because aqueous extracts can only be dissolved in water and at the end DMSO was added to the wells to make the cell membrane more permeable to the extracts. DMSO was kept at a final concentration of 0.1% in each well. Control cultures were grown in complete medium only. DMSO was added at 0.1 % final concentration to the vehicle control cultures.

As the cells were grown for 72 hours, the effects of different extract concentrations at different time points (24, 48 and 72 h) on the cell growth and on the cell viability were detected by trypan blue-dye exclusion technique or XTT assay.

#### 2.2.4.7 Measuring Viability of HL-60 Cells Using XTT Assay

The effects of the *Rheum ribes* shoot and root ethyl acetate, ethanolic and aqueous extracts on the proliferation of HL-60 cell line were evaluated by means of the Cell Proliferation Kit (Biological Industries, Israel) in 96 well flat bottomed microtiter plates.

Briefly, aliquots of 50  $\mu\text{l}$  of the  $2 \times 10^4$  cells/ml cell suspension in complete medium were seeded into the 96-well microtiter plate, as detailed in Appendix D. The plates were then incubated at 37°C in 5% CO<sub>2</sub> overnight to achieve the cell maintenance. No cells were seeded into the blank wells (instead, 100  $\mu\text{l}$  of complete RPMI media was added). Plant extracts (50  $\mu\text{l}$ ) were added in triplicate to the wells already containing 50  $\mu\text{l}$  of cell suspension. The controls comprised of: (i) DMSO in complete RPMI media, <0.1 % (negative control), (ii) freeze-dried extracts with complete RPMI media in the absence of HL-60 cells (color control), (iii) complete RPMI media in absence of both plant extract and HL-60 cells (blank control), and (iv) quercetin (positive control). Control wells aided in the determination of any background extract absorbance, especially in the event of colour interferences or interaction of the extract with the XTT solution. At the end of the incubation time, 100  $\mu\text{L}$  of phenazine metho-sulfate is added to 5 mL of XTT reagent, and 50  $\mu\text{L}$  of this XTT solution was added to each well. After incubation at 37 °C for 5 h, the dissolution of formazan crystals that were produced by mitochondrial enzymes of the living cells occurred, the optical density of chromogenic product was measured at 415 nm with Bio-tek ELISA reader (Elx808-Bio-tek, GERMANY) linked to a computer equipped with KC Junior. The results were expressed in terms of percentage cellular viability, calculated using equation 2.6, taking the relevant controls into account. Statistical analysis of three independent experiments performed in quadruplicate and calculation of IC<sub>50</sub> from a dose response curve were performed using GraphPad Prism version 5 for Mac OS X.

### Equation 2.6

$$\% \text{ Cell Viability} = \frac{Abs_{s(\text{with cell})} - Abs_{s(\text{cell free})}}{Abs_{c(\text{with cell})} - Abs_{c(\text{cell free})}} \times 100$$

Where;

$Abs_{s(\text{with cell})}$  = Average absorbance of cells treated with extracts

$Abs_{s(\text{cell free})}$  = Average absorbance of extracts in cell free medium

$Abs_{c(\text{with cell})}$  = Average absorbance of untreated cells, control

$Abs_{c(\text{cell free})}$  = Average absorbance of cell free medium

$Abs$  = Absorbance at 415 nm

### 2.2.5 Flow cytometry

The two modes of cell death, apoptosis and accidental cell death (necrosis), differ fundamentally in their morphology, biochemistry and biological relevance (Majno, 1995). In this part, to characterize and differentiate between two different mechanisms of cell death, apoptosis and necrosis flow cytometry was used.

All measurements were performed on a FACScalibur (BD Biosciences, Palo Alto, CA, USA), equipped with a 488 nm argon-ion laser, using CellQuest™ software. Analysis was investigated using FlowJo software (Treestar, Ashland, OR, USA).

### 2.2.5.1 Determination of cell size and granularity

$2.5 \times 10^5$  cells/ml (1 ml/well) were seeded in a 24-well tissue culture plate. Cells were either left untreated or treated with a concentration range of *Rheum ribes* freeze-dried extracts for 24, 48 and 72 h. Cells were harvested in 5 ml polypropylene tubes by centrifugation (500xg, 10 min, 4°C), washed with cold sPBS and resuspended in a volume of 500 µl of cold PBS for flow cytometric analysis. All measurements were performed on a FACScalibur, equipped with a 488 nm argon-ion laser, using CellQuest™ software. Adjustments of the cytometer settings such as Forward Scatter (FSC) and Side Scatter (SSC) were carried out with untreated control cells. Cell size and granularity was analyzed using FlowJo software (Treestar, Ashland, OR, USA).

### 2.2.5.2 Detection of apoptosis by Annexin V-APC

Detection of apoptosis using Annexin V after *Rheum ribes* treatment was performed using an APC- labeled Recombinant Human Annexin V and 7AAD antibody. Annexin V-Apc ( $\lambda_{ex}$ : 633,  $\lambda_{em}$ : 660 nm) is detected in FL4 on dual laser instruments and 7AAD ( $\lambda_{ex}$ : 488,  $\lambda_{em}$ : 647 nm) is detected in FL3 channel on most instruments.

HL-60 cells ( $2.5 \times 10^5$  cells/ml; 1 ml; 24-well plate) were either left untreated or treated with a concentration range of *Rheum ribes* freeze-dried extracts for 24, 48 and 72 h. Etoposide (68 µg/ml) and sodium azide (0.02% w/v) were used as positive controls to stimulate apoptosis and necrosis, respectively. Zvad -fmk (50 µM) and necrostatin-1 (10 µM) were used as positive controls to inhibit caspase dependent and non-apoptotic cell death, respectively.

Cells were harvested by centrifugation (500xg, 5 min, RT), washed with cold PBS, resuspended in a volume of 500 µl cold PBS and incubated with 1X Annexin V-apc (50x) solution and 1X 7AAD (100x) solution for 15 min at room temperature in dark room. After centrifugation (500xg, 5 min, RT) the cells was washed twice with 1000 µl sPBS and then obtained cell pellet was resuspended with 500 µl sPBS.

The samples were immediately analysed by flow cytometry.

The following controls were used to set up compensation and quadrants on flow cytometer; (i) Unstained cells, (ii) *Rheum ribes*-treated cells stained with Annexin V-apc alone (no 7-AAD) and (iii) *Rheum ribes*-treated cells stained with 7-AAD alone (no Annexin V-apc).

It was important to have separate and distinctive populations. In these populations; (i) cells that stained positive for Annexin V-apc and negative for 7-AAD were undergoing apoptosis, (ii) cells that stain positive for both Annexin V-apc and 7-AAD were either in the end stage of apoptosis which were undergoing necrosis, or were already dead, (iii) cells that stain negative for both Annexin V-apc and 7-AAD were alive and not undergoing measurable apoptosis. (Fig 2.4)

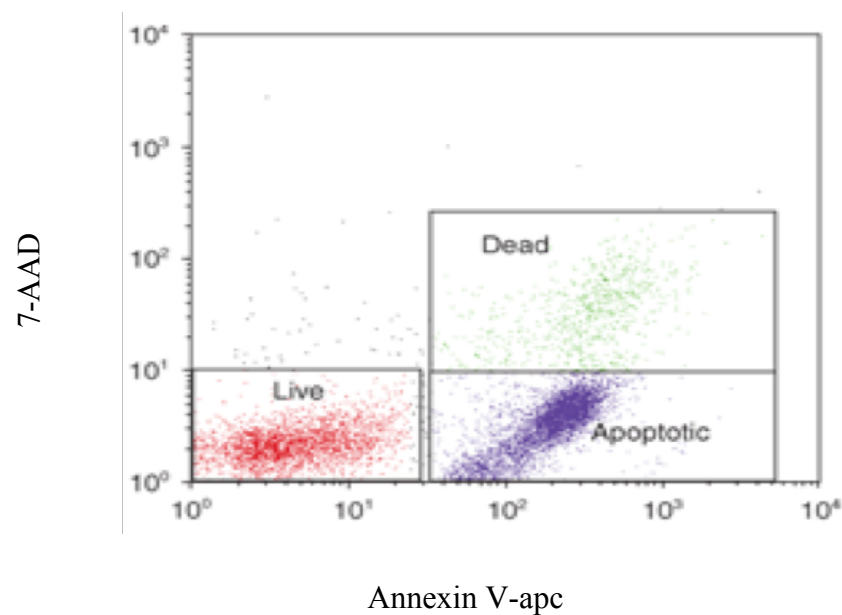


**Figure 2.4** Dot plot analysis of cell populations by double staining

## ***2.2.6 Microscopic analysis of Rheum ribes-treated cells***

### **2.2.6.1 Morphology of apoptotic cells**

Cell shrinkage, membrane blebbing and the formation of apoptotic bodies are characteristic events during apoptosis, which can be easily detected by light microscopy. HL-60 cells ( $2 \times 10^5$  cells/ml; 1 ml/well; 24-well plate) were either left untreated or stimulated with 100  $\mu$ g/ml ASE, ARE, ESE, ERE, WSE and WRE for different periods of time. Cells were viewed at a 400-fold magnification with an inverted microscope. (Olympus CKX 41).

### **2.2.6.2 Microscopic Detection of DNA fragmentation in HL-60 cells by the Terminal deoxynucleotidyl Transferase (TdT)-mediated dUTP-biotin Nick End-labeling (TUNEL) Method**

Apoptosis was also evaluated by DNA fragmentation according to Terminal deoxynucleotidyl transferase dUTP nick end labeling (TUNEL) assay using a ApoAlert® DNA Fragmentation Assay Kit (Clontech, [www.clontech.com](http://www.clontech.com)) in accordance with the manufacturer's protocol.

HL-60 cells were treated with 100  $\mu$ g/ml ESE and ERE for 16 h in the 6-well plates as described in cytotoxicity studies section. DMSO treated cells were used as vehicle control. At the end of the incubation time, cells were collected by centrifugation and washed with sPBS. Then, they were plated on poly-l-lysine-coated slides in 6-well plate and air-dried in a tissue culture hood for 1 h. Subsequently, the cells were rinsed twice with PBS and fixed with 4% (w/v) paraformaldehyde in PBS for 25 min at room temperature and rinsed twice with PBS. Then, the cells were immersed in 0.2% (v/v) Triton X-100 solution for 5 min and rinsed with PBS. The cells were equilibrated with equilibration buffer at room temperature for 5 min. Subsequently, TdT enzyme reaction mixture and biotinylated nucleotide mixture were added to the cells; then, the cells were covered with coverslips and incubated for 1 h at 37<sup>0</sup>C in CO<sub>2</sub> incubator.

Immersing the slides in  $2\times$  SSC for 15 min terminated the reaction. The slides were washed with PBS. The slides were then incubated in a final concentration of 10  $\mu\text{g/ml}$  PI solution in PBS for 30 min and rinsed with PBS with twice. TUNEL positive apoptotic cells were identified by their yellow nuclei seen under a fluorescence microscope (Olympus CKX 41) equipped with PI and fluorescein isothiocyanate filters.

### ***2.2.7 Detection of DNA Fragmentation***

The presence of internucleosomal DNA cleavage in HL-60 cells was investigated with DNA gel electrophoresis as described by Yang et al. (2000) with slight modifications.

HL-60 cells ( $2.5 \times 10^5$  cells/ml; 1 ml/well; 24-well plate) were treated with *Rheum ribes* freeze-dried extracts at concentrations of 100, 250 and 500  $\mu\text{g/ml}$  for 48 hours. DMSO was used as vehicle control.

The number of the treated and untreated (vehicle control) cells was adjusted to 10.000cells/ $\mu\text{l}$  with PBS. Then, 300  $\mu\text{l}$  of the cell suspension containing approximately  $3 \times 10^6$  cells was pipetted into the bottom of a sterile 1.5 ml microcentrifuge tube. Then, 30  $\mu\text{l}$  of Proteinase K was added on the cells and vortexed very well for a few seconds. Afterwards, 50  $\mu\text{l}$  Triton X-100 DNA Lysis Buffer (Appendix E) was added to the sample, mixed by vortexing for 15 seconds. In order to ensure efficient lysis, it's essential that the sample and DNA Lysis Buffer were mixed thoroughly to yield a homogenous solution. The microcentrifuge tubes are incubated for 10 minutes on ice and then, centrifuged (12.000 g,  $4^{\circ}\text{C}$ , 30 min). Next, supernatants were transferred to a clean 1.5 ml microcentrifuge tubes and then extracted with 1:1 mixture of phenol:chloroform. Aqueous (upper) layer was precipitated in two equivalents of cold ethanol (96-100 %) and one-tenth (0.1) volume equivalence of 3M Sodium Acetate was added to the sample and mixed again by vortexing for 15 seconds. After spinning down (12.000 xg,  $4^{\circ}\text{C}$ , 1 min), pellets were resuspended in 50  $\mu\text{l}$  TE Buffer (Appendix E). DNA concentration was estimated by measuring the absorbance at 260nm ( $A_{260}$ ).

8 µg of total DNA (10 µl) and supplemented with 1% (w/v) low melting agarose, was loaded onto a 2 % agarose gel at 80 Volts for 1-1.5 hours. The 100 bp-ladders with fragments ranging from 100 bp to just above 1000 bp were used as mass ladders.

## ***2.2.8 Gene Expression Analysis by RT-PCR***

### **2.2.8.1 Isolation of Total RNA from HL-60 cells**

RNeasy Kit (Qiagen) was used for the total RNA isolation from HL-60 cells to check the expression level analysis of target genes. Isolation was performed as described by the manufacturer.

In order to decrease the possibility of RNA degradation during the procedure, all glassware and plastics were treated by 0.1% DEPC (Diethyl Pyrocarbonate) solution overnight and then autoclaved and dried in oven, which converts DEPC into CO<sub>2</sub> and ethanol. Furthermore, all solutions were DEPC treated or prepared by 0.1% DEPC treated water (Appendix E).

All steps of the protocol, including centrifugation, were performed at room temperature.

5x 10<sup>6-7</sup> HL-60 cells (2 ml/well; 6-well) from treated and control (DMSO only) wells were centrifuged for 5 min at 300 g in a 15 ml sterile falcon tube. The supernatant discarded. Buffer RLT (lysis) (350 µL) including 10-µL β-mercaptoethanol per 1 mL of Buffer RLT was added onto the pellet and homogenized well by pipetting at least 10 times. One volume of 70% ethanol (350 µL) was added to the homogenized lysate and mixed well again by pipetting. The sample was then applied to an RNeasy Column in a 2 mL collection tube. The tube was closed gently, and centrifuged for 15 s at 8,000 g. The flow-through was discarded and 700 µL Buffer RW1 was added to the RNeasy Column. The tube was closed gently, and centrifuged for 15 s at 8,000 g. The flow-through and the collection tube were discarded. Another 500 µL Buffer RW1 (wash) was added into the RNeasy Column and centrifuged for 2 min at 8,000 g. The flow through was

discarded. The spin column was transferred to a new 1.5 mL collection tube. RNase-free water (40  $\mu$ L) was directly added onto the center of the silica-gel membrane in order to elute RNA bound on the column. The tube was centrifuged for 1 min at 8,000 g. RNA was collected and quality and quantity were estimated by measuring the absorbance at 260nm ( $A_{260}$ ) versus 280nm ( $A_{280}$ ) and 230 nm ( $A_{230}$ ).

The resulting RNA yield was either stored at  $-80^{\circ}$  in small aliquats or used directly reverse transcriptase-PCR to prepare cDNAs.

#### **2.2.8.2 Calculation of RNA Concentration with Spectrophotometry**

Seven microliters of total RNA isolate will be diluted with 693  $\mu$ l of Tris-EDTA (TE) buffer (pH 8.0) (Appendix E) in a quartz cuvette. Then, the absorbance of the solution was measured at 260 and 280 nm using TE buffer as blank. The purity of the isolated RNA will be determined by taking the ratio of  $A_{260}$  and  $A_{280}$  readings. The optimal value of  $A_{260} / A_{280}$  is accepted to be in between 1.9-2.2. The RNA concentration in the sample was calculated as shown in the equation 2.7, considering that 40 $\mu$ g/ml solution of single stranded RNA gives absorbance of 1.000 at wavelength of 260.

#### **Equation 2.7**

$$\text{RNA concentration } (\mu\text{g/ml}) = (\text{OD}_{260}) \times (\text{dilution factor}) \times (40 \mu\text{g RNA}/\mu\text{l})$$

#### **2.2.8.3 Electrophoresis of RNA**

##### *Cleaning of Electrophoresis Instrument:*

As in all RNA manipulation, it is important to minimize RNase activity when running agarose gels. Electrophoresis apparatus should never be directly exposed to DEPC because acrylic is not resistant to DEPC. Therefore in order to sterilize electrophoresis apparatus, they must be first cleaned with detergent solution, then rinsed with distilled water and dried with ethanol. After that, gel apparatus will be

filled with 3% hydrogen peroxide and soaked for 10 min. Then, they will be rinsed thoroughly with DEPC-treated water.

One percent of agarose gel was prepared in 1X Tris/Borate/EDTA (TBE) buffer (pH 7.0) (Appendix E) Ten microliters of total RNA was mixed with 1  $\mu$ l of loading solution (Appendix E) and loaded onto the gel. Electrophoresis was carried out at a maximum of 5V per 1 cm of distance between electrodes until bromophenol blue has traveled at least 80% of the way through the gel. Completing the electrophoresis, the gel was stained in 0.5  $\mu$ g/ml EtBr solution containing 0.1 M ammonium acetate at least for an hour. The RNA bands were visualized under UV transilluminator and photographed.

#### **2.2.8.4 Complementary DNA (cDNA) Preparation**

After isolation, RNAs were reverse transcribed with Moloney Murine Leukemia Virus Reverse Transcriptase (M-MuLV-RT) to produce complete cDNAs of mRNAs having polyA tails, because oligo-dT was used as a primer for reverse transcription. A typical reaction mixture for cDNA synthesis was given in Table 2.4 for 0.6 ml Eppendorf PCR tube, 2  $\mu$ g of total RNA (at least 1  $\mu$ l at most 10  $\mu$ l), 2  $\mu$ l of oligo-dT (0.5  $\mu$ g/ml) was added and the total volume was completed up to 12  $\mu$ l with nuclease free sterile water. Tubes were incubated at 70°C for 5 min and chilled on ice. Then, 4  $\mu$ l of 5X M-MuLV-reverse transcriptase buffer (final concentration 1X), 2  $\mu$ l of 10 mM dNTP mix (final concentration 1.0 mM), and 1  $\mu$ l of RNase inhibitor (20 U/ $\mu$ l) was added in the indicated order. After incubating at 37°C for 5 min, 1  $\mu$ l M-MuLV-reverse transcriptase (200 U/ $\mu$ l) were added and reverse transcription were carried out at 42°C for 60 min in thermal cycler. Finally, the tube was heated up to 70°C for 10 min to stop the reverse transcription by denaturing M-MuLV-RT and chilled on ice. Reverse transcribed samples were stored at -20°C for further use.

**Table 2.4**Ingredients of reverse transcription reaction

<b>Ingredients</b>	<b>Amount (<math>\mu</math>l)</b>	<b>Final Concentration</b>
Total RNA (2 $\mu$ g)	8 (varies)	2 $\mu$ g
oligo-dT (0.5 $\mu$ g/ml)	2	0.05 $\mu$ g/ml
5X Buffer	4	1
dNTP (10 mM)	2	1 mM
RNase inhibitor (20 U/ $\mu$ l)	1	1 U/ $\mu$ l
M-MuLV-RT (200 U/ $\mu$ l)	1	10 U/ $\mu$ l
Rnase Free Water	2 (varies)	-
<b>Total</b>	<b>20</b>	-

#### **2.2.8.5 Primer preparation**

All primers were obtained in powder form Iontek, Turkey. Upon delivery, primers were dissolved in commercially specified volume of RNase free water to get 100  $\mu$ M concentration. Primers were then diluted with RNase free water to a concentration of 5 pmol/ $\mu$ L, aliquoted and stored at -20° C.

#### **2.2.8.6 Polymerase Chain Reaction (PCR)**

PCR reaction was performed by simply adding the following items in Table 2.5 in the indicated order into a 1.5 ml Eppendorf tube to prepare a master mix solution.

**Table 2.5** Ingredients of PCR master mix

<b>Ingredients</b>	<b>Stock Solution</b>	<b>Final Concentration</b>
Pyrogen free sterile H <sub>2</sub> O	-	up to 50 µl
Reaction buffer	10X	1X
MgCl <sub>2</sub>	25 mM	1.5 mM
dNTP mix	10 mM (each)	0.1 mM (each)
forward / reverse primer	100 mM (each)	1.0 mM (each)

A 47.5 µl aliquots of freshly prepared master mix were placed into 0.6 ml PCR tubes. Then, 2 µl from the cDNA reaction mixture and 0.5 µl Taq DNA polymerase (final concentration 2.5 U/ml) was added making a final volume of 50 µl. The thermal cycler was programmed according to optimized results but started with initial denaturation at 94°C for 3 min. Temperature profile for PCR reactions that were performed in this study was given Table 2.5. Final extension was carried out at 72°C for 5 min and then finally reaction was kept at 4°C indefinitely. PCR products were either visualized directly by agarose gel electrophoresis or stored at +4°C.

#### **2.2.8.7 Agarose gel electrophoresis**

Agarose gels were prepared by mixing TBE solution with agarose powder at a concentration of 1.5%. The solution was heated in a microwave oven for 3 minutes and ethidium bromide was added at a concentration of 5% v/v and poured into a PCR chamber, a PCR gel comb was placed and gels were left to harden at room temperature. Gels were then immersed in TBE and 5 µL of each PCR product mixed with 1 µL of gel loading dye (Orange G buffer) were loaded in each well. Gels were run at a voltage of 90- V for 60 min. Gels were visualized under a UV illuminator and images were captured.

### 2.2.8.8 Data Acquisition

In order to quantify the PCR products on agarose gels, densitometric measurements were done. For densitometry, scanned gel images were analysed with the ImageJ picture-processing program. The intensities of the bands will be converted into peaks by the software. Gene expressions were calculated from the area under these peaks.

**Table 2.6** Markers detected by PCR: primer sequences, temperature profiles, sizes of amplified fragments.

Detected marker	Primer sequences	Temp. profile for PCR	Amplified fragment size
Bcl-2	Bcl-2 forward: 5' GGATTGTGGCCTTCTTTGAG 3'	30'' 94°C 30'' 53°C	219
	Bcl-2 reverse 5' TCTTCAGAGACAGCCAGGAGA 3'	30'' 72°C 30 cycles	
Bax	Bax forward: 5' TCTGACGGCAACTTCAACTG 3'	30'' 94°C 30'' 53°C	188
	Bax reverse 5'TTGAGGAGTCTCACCCAACC 3'	30'' 72°C 28 cycles	
β-actin	β-actin forward 5'CAGAGCAAGAGAGGCATCCT3'	30'' 94°C 45'' 50°C	201
	β-actin reverse 5'TTGAAGGTCTCAAACATGAT3'	60'' 72°C 30-35 cycles	
CYP 1A1	CYP 1A1 forward: 5'TAGACACTGATCTGGCTGC3'	20'' 94°C 20'' 50°C	146
	CYP 1A1 reverse: 5'GGGAAGGCCCATCAGCATC3'	40'' 72°C 35 cycles	
CYP 1B1	CYP 1B1 forward: 5'AACGTCATGAGTGCCGTGTGT3'	20'' 94°C 20'' 58°C	360
	CYP 1B1 reverse: 5'GGCCGGTACGTTCTCCAAATC3'	40'' 72°C 30 cycles	

### 2.2.8.9 Quantitative Real-Time Polymerase Chain Reaction

RT-PCR is a semiquantitative detection system for gene expression levels, whereas Real-time PCR (qRT-PCR) is an absolute quantitative technique. cDNA was used as template for the Realtime PCR reaction. FastStart Universal SYBR Green Master (Rox) Master ready to use hot start reaction mix (Basel, Switzerland) was used for amplification. 0.5- $\mu$ M primer (Table 2.5), 1X master mix, 7  $\mu$ L cDNA were the components of the 10  $\mu$ L reaction. For optimization of the runs, standard amplification curves (Appendix H) were constructed by using known dilutions of control cells cDNA as template. Finally the reaction was performed with five standard cDNAs, one non-template control (all the reaction components except cDNA) and the unknowns. Conditions for qPCR are summarized in Table 2.6. The total RNA concentrations of five standarts are presented in Table 2.7.

**Table 2.7** Real Time PCR Conditions

Analysis Mode	Cycles	Segment	Temperature $^{\circ}$ C	Time
		<b>Preincubation</b>		
	1		95	5 min
		<b>Amplification</b>		
<b>Quantification</b>	40	Denaturation	94	30 sec
		Annealing	53	30 sec
		Extention	72	30 sec
		<b>Cooling</b>		
	1		40	30 sec

**Table 2.8** cDNA Standard Dilutions for qPCR Optimizations.

<b>Standard (STD)</b>	<b>Dilution (Copy Number)</b>	<b>Preparation (<math>\mu</math>L cDNA)</b>
1	$10^4$	$7 \times 10^0$
2	$10^3$	$7 \times 10^{-1}$
3	$10^2$	$7 \times 10^{-2}$
4	$10^1$	$7 \times 10^{-3}$
5	$10^0$	$7 \times 10^{-4}$

The results were supplied automatically as fluorescent values that were obtained from unknown samples. The expression levels were quantified by converting fluorescent values to RNA amounts. The standard deviations of the values were also supplied automatically. The significant RNA level variations between treatments were demonstrated graphically.

Relative transcript quantities were calculated by the  $\Delta\Delta C_t$  method. Normalized samples were expressed relative to the average  $\Delta C_t$  value for untreated controls to obtain relative fold-change in expression levels. Fold change in mRNA expression was expressed as  $2^{\Delta\Delta C_t}$ .  $\Delta C_t$  is the difference in threshold cycles for the treated cells mRNAs and standart mRNAs.  $\Delta\Delta C_t$  is the difference between  $\Delta C_t$  non-treated control cells and  $\Delta C_t$  treated cells.

## ***2.2.9 Protein expression analysis***

### **2.2.9.1 Protein Determination of Cytosol by Micro-Lowry Assay**

The protein amount in the HL-60 cells were determined by the Lowry Method (1951) adjusted to the measurement by ELISA Plate Reader with crystalline bovine serum albumin (BSA) as the standard. Samples were diluted in water as 1/20 and 1/40 and 40  $\mu$ l applied to the 96 well plate as triplicates. Then, 200  $\mu$ l of Lowry ACR (including 2% copper sulfate ( $\text{CuSO}_4 \cdot 5\text{H}_2\text{O}$ ), 2% sodium-potassium tartarate,

2% (sodium carbonate in 0.1 M sodium hydroxide) in the ratio of 1:1:100 was added and mixed. After 10 min of incubation at room temperature, 1 N Folin Ciocalteu Phenol Solution was added as 20  $\mu$ l with immediate mixing. At the end of a 45 min. incubation, plate was read at 650 nm with Bio-tek ELISA reader (Elx808-Bio-tek, GERMANY) linked to a computer equipped with KC Junior. Protein concentration in each well calculated by the software after providing necessary dilution factors. Standard curve was prepared by using BSA solutions diluted as 1, 2.5, 5, 10  $\mu$ g/well.

### **2.2.9.2 Western Blot Detection of Bax, Cytochrome *c* and Caspase-3**

#### ***2.2.9.2.1 Cell Fractionation to visualize the Cytochrome *c* Release and Caspase-3 Cleavage***

Mitochondrial and cytological suspensions were prepared by ApoAlert Cell Fractination Kit and then, Immunostaining was carried out according to the instruction manual provided with the Amplified Alkaline Phosphatase (AP) Western Blotting Kit (Bio-Rad) that was used in the immunostaining of the electroblotted PVDF membranes.

After growing the cells in T25 as described in cytotoxicity studies for at 72 hours, the cells were centrifuged (600 g, 5 min, 4°C). The supernatant was discarded and then, the pellet was re-suspended in 1 mL of ice-cold wash Buffer (ApoAlert Cell Fractination Kit). After resuspending the pellet completely, the cells were centrifuged at (600 g, 5 min, 4°C). The supernatant was discarded; the pellet was re-suspended in 0.8 mL of ice-cold Fractionation Buffer Mix. The tubes were incubated on ice for 10 minutes. The cells were homogenized by ultrasonication with 40 mA for 5 secs. The homogenate was centrifuged at (700 g, 5 min, 4 °C). The supernatant was transferred to a fresh 1.5 mL microcentrifuge tube and the tubes were centrifuged (10, 000 g, 25 min, 4 °C). The supernatant (cytosolic fraction) was collected and the pellet is re-suspended in 0.1 mL of ice-cold Fractionation Buffer Mix (the mitochondrial fraction).

After the protein concentration determination by the method of Lowry et al. (1951), 20  $\mu$ g of each cytosolic and mitochondrial protein isolated from induced (apoptotic) and uninduced (nonapoptotic) cells were loaded on a 12 % SDS-PAGE. Then, any standard Western blot procedure was performed using cytochrome c antibody (1:100).

The resulting cytosolic fraction was also used to check the cleavage of caspase 3 using Anti-Caspase 3 (1:100) Antibody.

Anti-GAPDH and anti-tubulin antibodies were used as internal protein expression control.

#### **2.2.9.2.2 SDS-Polyacrylamide Gel Electrophoresis**

Polyacrylamide slab gel electrophoresis, in the presence of the anionic detergent sodium dodecyl sulfate (SDS), was performed on 4 % stacking gel and 12 % in a discontinuous buffer system as described by Laemmli (1970). The seven proteins given below were used as molecular weight standards.

**Table 2.9** The list of used molecular weight standards

- Bovine Albumin	(M <sub>r</sub> 66000)
- Egg Albumin	(M <sub>r</sub> 45000)
- Glyceraldehyde-3-Phosphate Dehydrogenase	(M <sub>r</sub> 36000)
- Carbonic Anhydrase	(M <sub>r</sub> 29000)
- Trypsinogen	(M <sub>r</sub> 24000)
- Trypsin Inhibitor	(M <sub>r</sub> 20100)
- $\alpha$ -Lactalbumin	(M <sub>r</sub> 14200)

Vertical slab gel electrophoresis was carried out using the EC120 Mini Vertical Gel System (E-C Apparatus Corp., NY, U.S.A) that could be used to run two gels simultaneously. The assembly of the glass plate cassettes (8.3 X 7.4 cm) and the process of gel casting were done according to instruction manual provided with the apparatus. Once the cassettes were properly assembled and mounted, the preparation of the separating and stacking gels was started.

The 12 % separating gel and 4 % stacking gel-polymerizing solutions were prepared just before use by mixing the given volumes of stock solutions in the written order in Table 2.9. First, the separating gel solution was prepared with the TEMED added just before casting the gel into the glass assembly from the edge of one of the spacers until the desired height of the solution (about 5 cm) was obtained. Then, the liquid gel was overlaid with distilled water (about 0.5 ml), without disturbing the gel surface, to obtain an even interface between the separating gel and the stacking gel. The gel was then allowed to polymerize at room temperature for a minimum of 30 minutes. After polymerization, the layer of water was removed completely using filter paper without hurting the gel surface. The stacking gel was then poured on the top of the resolving gel and the comb was inserted into the layer of the stacking gel without trapping air bubbles under the teeth of the comb. The gel was then allowed to polymerize for a minimum of 30 minutes.

After the gel was polymerized, the comb was removed carefully and the wells were washed with distilled water and filled with electrode buffer. At this point, the gel cassettes were removed from the casting stand, mounted and clamped onto the running frame with the notched glass plate of each cassette facing inside. When running only one gel, the blank plastic plate, provided with the system, was mounted in the place of the second cassette in the casting stand and in the running frame.

Aliquots from the protein samples to be analyzed and from the standards mixture were diluted 3:1 with the 4X sample buffer (3 parts sample and 1 part sample buffer), to have the samples in 62.5 mM Tris-HCl buffer, pH 6.8, 2 % SDS,

5 % 2-mercaptoethanol, 10 % glycerol and 0.001 % bromophenol blue. Then the samples were placed in a boiling water bath for 5 minutes. Afterwards, protein samples (20 µg) and standards were loaded into different wells.

After loading the samples, the running buffer (135 ml) (Appendix E) was added to the compartment formed by the running frame and the cassettes (the upper buffer compartment) and the system was checked for leakage. The running buffer (250ml) was then also added to the electrophoresis tank. Thereafter, the safety cover was replaced and the leads are plugged into the EC250-90 electrophoresis power supply. The power supply was adjusted to give a constant current of 15 mA when the samples were in the stacking gel and 30 mA when the samples passed to the separating gel. Under these conditions the voltage is about 250 V that took a total of about 1.5 hours.

**Table 2.10** Formulations for SDS-PAGE separating and stacking gels

	Separating Gel		Stacking Gel
Monomer Concentration	12 %	15 %	4 %
Acrylamide/bis	12.0 ml	15.0 ml	1.3 ml
distilled water	10.0 ml	7.0 ml	6.1 ml
1.5 M Tris-HCl, pH 8.8	7.5 ml	7.5 ml	----
0.5 M Tris-HCl, pH 6.8	----	----	2.5 ml
10% (w/v) SDS	300 µl	300 µl	100 µl
10 % APS	185 µl	185 µl	50 µl
TEMED	15 µl	15 µl	10 µl
Total monomer	30 ml	30 ml	10 ml

The power supply was switched off, when the dye front was just 0.5 cm from the lower end of the glass plates, the running frame was taken out and the buffer was removed from the upper buffer compartment. Afterwards, the clamps were detached

and the cassettes were removed from the running frame. To gain access to the gels in the cassette, the glass plates were pried apart using a spatula taking care not to chip the edges of the glass plates. The left-top corner of each gel was cut to indicate the order of wells.

The gels, usually adhered to one of the glass plates, were taken carefully using gloves and placed in the previously prepared appropriate solutions to stain the samples which have been resolved on the gels, or to prepare the gels for subsequent blotting.

### ***2.2.9.2.3 Electroblotting of the Gels from SDS-PAGE***

Electroblotting was carried out using EC140 Mini Blot Module of the EC120 Mini Vertical Gel System (E-C Apparatus Corp., NY, U.S.A.), and Polyvinylidene difluoride (PVDF) was used as a blotting membrane.

Prior to electroblotting, the gels taken from SDS-PAGE are placed for 30 min, with shaking, in the Towbin transfer buffer (25 mM Tris, 192 mM glycine and 20 % methanol) with shaking (Towbin *et al.*, 1979).

While the gels were incubated in the transfer buffer, the other system components and the transfer membrane were prepared. All of the electroblotting procedure was carried out wearing gloves. The PVDF transfer membrane, with the dimensions of the gel to be transferred, was soaked in 100 % methanol for 30 seconds with shaking, to overcome the hydrophobicity of the membrane. Then, the wet membrane was washed several times with distilled water and then with transfer buffer until it was equilibrated (submerged into the solution and not floating any more), the point at which the membrane was ready to bind the proteins in any blotting application. The membrane should not be allowed to dry, otherwise proteins would not bind to it, and so if it was dried during the procedure, the wetting procedure should be repeated again. Afterwards, two pieces of filter paper, the Scotch Brite sponge pads, and the transfer membrane were soaked in the transfer buffer for 30 min with continuous shaking.

The blotting stack was assembled on the top of stainless steel grid cathode located in the trough of the frame stand of the Mini Blot Module, to which a small amount of transfer buffer was added. The configuration of the assembly was as follows:

Top	Cover with Palladium Wire <u>Anode</u>
	Sponge Pad
	Sponge Pad
	Filter Paper
	PVDF Transfer Membrane
	Gel
	Filter Paper
	Sponge Pad
Bottom	Frame stand with Stainless steel Grid <u>Cathode</u>

After the above assembly was prepared, the cover of the electroblotting module was pressed onto the blotting stack and fixed with the clamps after turning assembled blotting module upright and then filled with the transfer buffer (about 100 ml). Thereafter, the fully assembled module was inserted into the outer tank and the safety cover with leads was replaced. The red lead was connected to the anode (+) and the black lead to the cathode (-), where the proteins would be transferred as anions to the direction of anode. The transfer process was performed at room temperature for 50 minutes using a constant voltage (20 V). When the blotting was finished, the PVDF membrane was immediately removed and placed in the blocking solution (5% non-fat dry milk in TTBS), previously prepared for overnight.

#### ***2.2.9.2.4 Immunostaining of the PVDF Membranes***

Immunostaining of the electroblotted PVDF membranes was carried out according to the instruction manual provided with the Amplified Alkaline Phosphatase (AP) Western Blotting Kit (Bio-Rad). All of the incubations were performed in a minimum of 5 ml of solutions in each step with continuous shaking at room temperature.

The electroblotted PVDF membrane was incubated in the blocking solution (5 % non-fat dry milk in TTBS buffer for overnight. PVDF membrane which was blocked in 5 % non-fat dry milk (in TTBS buffer) was incubated with the primary antibodies diluted in the blocking solution for 1 hour, where the monoclonal anti-cytochrome c (1/100 diluted) or the monoclonal anti-COX Subunit IV (1/500 diluted) were used. At the end of 1 h, primary antibody solution was removed and stored at -20 °C. The membrane was then washed five times, each for 5 min with TTBS and incubated with the secondary antibody (biotinylated goat anti-rabbit 1/7,500 diluted in TTBS) for 1 to 2 hours.

During the secondary antibody incubation period, the streptavidin - biotinylated AP complex is prepared by the addition of streptavidin to biotinylated AP (both 1/7,500 diluted in TTBS) and allowed to stand at least 1 hour and not more than 3 hours at room temperature. After the incubation with secondary antibody, the membrane was washed again with TTBS (five times, each 5 min) and then incubated for 1-2 hours in the previously prepared streptavidin - biotinylated AP complex.

Afterwards, the membrane was washed again with TTBS (five times, each 5 min) and the AP color developing solution (BCIP/NBT) is added. BCIP is hydrolyzed by alkaline phosphatase to form an intermediate that undergoes dimerization to produce an indigo dye as shown in Figure 2.5. The NBT is reduced to the NBT-formazan by the two reducing equivalents generated by the dimerization. The specific protein bands started to appear after 10-30 min. Finally, the membranes are carefully dried and the images are obtained using a scanner connected to the computer.

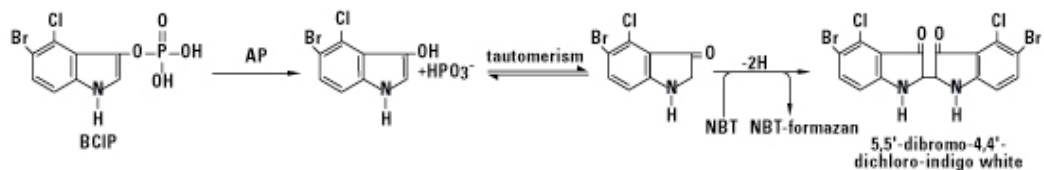


**Figure 2.5** NBT/BCIP reaction scheme

### 2.2.10 Determination of Fluorimetric Caspase-3 Activity

Cells were seeded at  $5 \times 10^5$  / ml in a 24-well plate and treated with a concentration range (50 to 500  $\mu\text{g/ml}$ ) of *Rheum ribes* shoot (ASE, ESE, WSE) and root (ARE, ERE, WRE) freeze-dried extracts for different periods of time. For some experiments, a preincubation with 50- $\mu\text{M}$  zvad-fmk preceded stimulation to inhibit caspase-3. Cells were harvested by centrifugation (370 x g, 4° C, 10 min) then counted with trypan blue dye exclusion method. Cells were washed twice with ice-cold PBS cells and were frozen at -80° C until next day. After defrosting, cell pellets were resuspended in 50  $\mu\text{l}$  prechilled lysis/reaction buffer, supplemented with protease inhibitors (Appendix E) per  $10^6$  cells. After incubating on ice for 20

min, cell lysates were collected by centrifugation (14,000 x g, 4° C, 10 min). 50  $\mu\text{l}$  of each supernatant (triplicates) were transferred to 96-well flat bottom plates for caspase 3-activity assay.

For caspase activity assay, 50  $\mu\text{l}$  of lysis/ reaction buffer and 10  $\mu\text{l}$  of the 0.1 mM Caspase-3 Substrate (DEVD-AFC; 10 mM final) were added to each well. Standard curve was constructed using a serial dilution of 4, 2, 1, 0.5  $\mu\text{M}$  prepared from stock 4 mM of AFC solution in lysis/reaction buffer. Then the plates were wrapped in foil and incubate on a rotator at room temperature for 1 h.

The plate was read on a fluorescent microplate reader (Molecular Devices, Sunnyvale, CA, USA) at  $\lambda_{\text{ex}}$ : 400 nm,  $\lambda_{\text{em}}$ : 535 nm, linked to a computer equipped with SoftMax Pro. Reaction buffer was used for background calibration. Substrate cleavage was quantitated using a standard calibration curves established with the free AFC fluorescent molecules.

A standard calibration curve (Appendix G) was plotted with AFC concentration (mM) versus fluorescence units (FU). Then, the slope ( $\Delta\text{FU}/\Delta\text{mM}$  AFC) of the curve was used to calculate caspase activity using the following formula:

### **Equation 2.8**

$$\text{Caspase 3 activity (pmol of AFC liberated per hour)} = \frac{(\Delta\text{FU/hr})}{\text{Curve slope}}$$

$\Delta\text{FU/hr}$ = the difference in FU between an untreated control and a treated sample.

### **2.2.11 Determination of GST Enzyme Activity towards CDNB**

GST enzyme activity was determined spectrophotometrically by monitoring the thio-ether formation at 340 nm using CDNB as substrate according to the method of Habig et al (1974) as modified previously for Elisa Plate Reader (Yılmaz 2006).

The enzyme source for this investigation was the resulting cytosolic fraction in the protein expression assay.

As shown in Table 2.10, each reaction mixture contained 100 mM potassium phosphate buffer, pH:7.4, 1.0 mM GSH, 1.0 mM CDNB and 3.5-6 mg/ml cytosolic protein in a final volume of 250  $\mu$ l in 96 well plate.

The reactions were started by the addition of enzyme into each well. The plate placed into Elisa Plate Reader adjusted at 25°C. After machine mixing, reading is started automatically at every 20 seconds for 10 minutes. The blank wells contained all the constituents except enzyme source. Phosphate buffer was added instead of enzyme source to complete the volume to 250  $\mu$ l.

**Table 2.11** Constituents of cytosolic GST enzyme assay medium

Component	Stock Solutions	Volume to be taken ( $\mu$ l)	Final Concentrations in reaction mixture
Potassium Phosphate Buffer (pH 7.4) GSH CDNB Sample (cytosolic fraction)	500 mM	50	100 mM
	25 mM	10	1 mM
	20 mM	12.5	1 mM
		15	8.8-1.5 $\mu$ g/well
Distilled water		162.5	
Volume		250	

Slopes of the reaction best lines drawn for each well separately by the software of the instrument were used as the rate of reaction (dA/dt) and the further calculations were completed. Reaction rates were calculated by subtracting the slopes of blanks from that reactions.

### Equation 2.9

$$\frac{dA / dt}{\epsilon \text{ (mM}^{-1}\text{)}} \times \frac{0,250 \text{ ml}}{1000 \text{ ml}} \times \frac{1000}{15} \times DF \times \frac{1}{\text{mg prot. / ml}}$$

The reaction rate at 340 nm was determined using the CDNB extinction coefficient of 0.00629  $\mu\text{M}^{-1}\text{cm}^{-1}$ . The actual extinction coefficient for CDNB at 340 nm is 0.0096  $\mu\text{M}^{-1}\text{cm}^{-1}$ . The value has been adjusted for the path length of the solution in the well (0.621 cm) for Elisa Plate Reader.

(<http://www.biovision.com/gst-colorimetric-assay-kit-2821.html>)

The GST activities were expressed as unit/mg protein where one unit of an enzyme is defined as the amount of enzyme producing 1 nmole of product in one minute under defined reaction conditions.

### 2.2.12 Statistical Analysis

All experiments were performed in triplicate unless otherwise noted; results are expressed as mean  $\pm$  standard deviation. Data analysis and graphing was performed using the GraphPad Prism version 5 (GraphPad Software, San Diego, California, USA). For all the measurements, oneway ANOVA followed by Tukey's Multiple Comparison Test was used to assess the statistical significance of difference between control and *Rheum ribes* extract-treated groups in in vitro. A statistically significant difference was considered to be at  $P < 0.05$ .

## CHAPTER III

### 3. RESULTS AND DISCUSSION

*Rheum ribes* has been used for treating various ailments in the eastern part of Turkey, however, the mechanism regarding the healing effects of this plant is still not clearly understood. *Rheum ribes* shoot and root dry powder samples were prepared and extracted with four different solvents namely ethyl acetate, methanol, ethanol and water. Additionally, 70% methanol extracts were fractionated with chloroform and n-butanol in order to gather all the biologically active compounds from the plant by polarity differentiation. The obtained *Rheum ribes* freeze-dried extracts and fractions were characterized by their antioxidant capacity and total polyphenol and flavonoid contents. Different biological activities of the extracts were determined by their cytotoxic and apoptotic properties on HL-60 cells with its mechanism of action in this study.

#### 3.1 Yield of Plant Extraction

*Rheum ribes* shoot and root dry powder samples (30 g) were extracted with ethyl acetate (EtOAc), methanol (MeOH), ethanol (EtOH) and ddH<sub>2</sub>O at 50°C for 24 h and extracts were concentrated and dried as described in the “Materials and Methods” part. The weight of dried extracts was recorded, and the percent yield of extraction was calculated as % (w/w) for each solvent system individually.

Solvent extractions are the most commonly used procedures to prepare extracts from plant materials due to their ease of use, efficiency, and wide applicability. It was concluded that the yield of chemical extraction depends on the type of solvents with varying polarities, pH, extraction time and temperature,

sample-to-solvent ratio as well as on the chemical compositions of the sample (Pinelo, 2004). Under the same conditions of time and temperature, the solvent and the chemical properties of the sample are two most important factors.

Solvents, such as methanol, ethanol, acetone, ethyl acetate, and their combinations have been used for the extraction of phenolics from plant materials, often with different proportions of water. Right solvent selection affects the amount of polyphenols extracted, and rate of extraction. Especially, in the extraction of lower molecular weight polyphenols it is more efficient to use methanol while aqueous acetone is better for the extraction of the higher molecular weight flavanols (Jin Dai, 2010). Ethanol is another good solvent for polyphenol extraction and is safe for human consumption.

The percent yields of the extraction obtained with the different solvents are given in Table 3.1. Maximum extraction yields were recorded in the range of 1.2-25.3 % for *Rheum ribes* shoot and 1.7-19.8 % for *Rheum ribes* root with selected solvents.

**Table 3.1** Maximum extraction efficiency as expressed by percent yield (w/w) of *Rheum ribes* shoot and root dry powder with ethyl acetate (EtOAc), methanol (MetOH), ethanol (EtOH) and ddH<sub>2</sub>O solvent systems

Extracts prepared with:	Part of plant	Abbreviation	% yield
Ethyl acetate	shoot	ASE	1.2
	root	ARE	1.7
Methanol	shoot	MSE	4.6
	root	MRE	7.4
Ethanol	shoot	ESE	4.5
	root	ERE	8.0
Water	shoot	WSE	25.3
	root	WRE	19.8

Ethyl acetate extraction of both shoot and root dry powder samples exhibited a lower yield than that of other solvents. This might be due to the presence of nonpolar compounds in the low quantity in *Rheum ribes*, as ethyl acetate is a nonpolar solvent with polarity index of 4.4.

The yield obtained from methanol and ethanol extractions were similar. This result was not unexpected, since the polarity index of two solvents were very close to each other (ethanol 5.2 and methanol 5.1), they might have extracted the same compounds from plants.

Aqueous extraction of both shoot and root dry powder samples exhibited a higher yield than that of other solvents. This might be due to the presence of polar compounds in the high quantity in *Rheum ribes*, as water is a polar solvent with polarity index of 9.

The polar solvents achieved the highest yield for extractable substances. The order of the yields from high to low was: Water > Ethanol  $\geq$  Methanol > Ethyl acetate.

Solvents such as aqueous methanol (1:1 v/v) and chloroform were used for the extraction of phenolics from *Rheum ribes* at 25 °C (Öztürk, 2006) and their yields were between 4 to 6 %. As compared to result of the present study, they observed lower yields in methanol extract of *Rheum ribes* roots.

### **3.2 Absorption Spectrum of Extracts and Fractions**

The absorption spectra of (4 mg/ml) *Rheum ribes* shoot and root freeze-dried extracts of ethyl acetate and ethanol solvent systems were recorded against ethanol. 4 mg/ml aqueous extracts, which was more soluble in water were taken in ddH<sub>2</sub>O against ddH<sub>2</sub>O. The absorption spectra of freeze-dried extracts were taken between 200 nm to 600 nm at room temperature and they were presented in Fig. 3.1.

Some differences in the absorption curves could be observed in the UV region between 250 and 290 nm when we compared different solvent systems. The peaks around 240 nm, 270 nm and 400 nm are the characteristic peaks for phenolicanthraquinones (Rajendran, 2007).

ASE exhibited different spectrum than ARE. Although their peak numbers were same as 10, their positions were not identical.

ERE had 10 peaks, which was more than 8 peaks that ESE had.

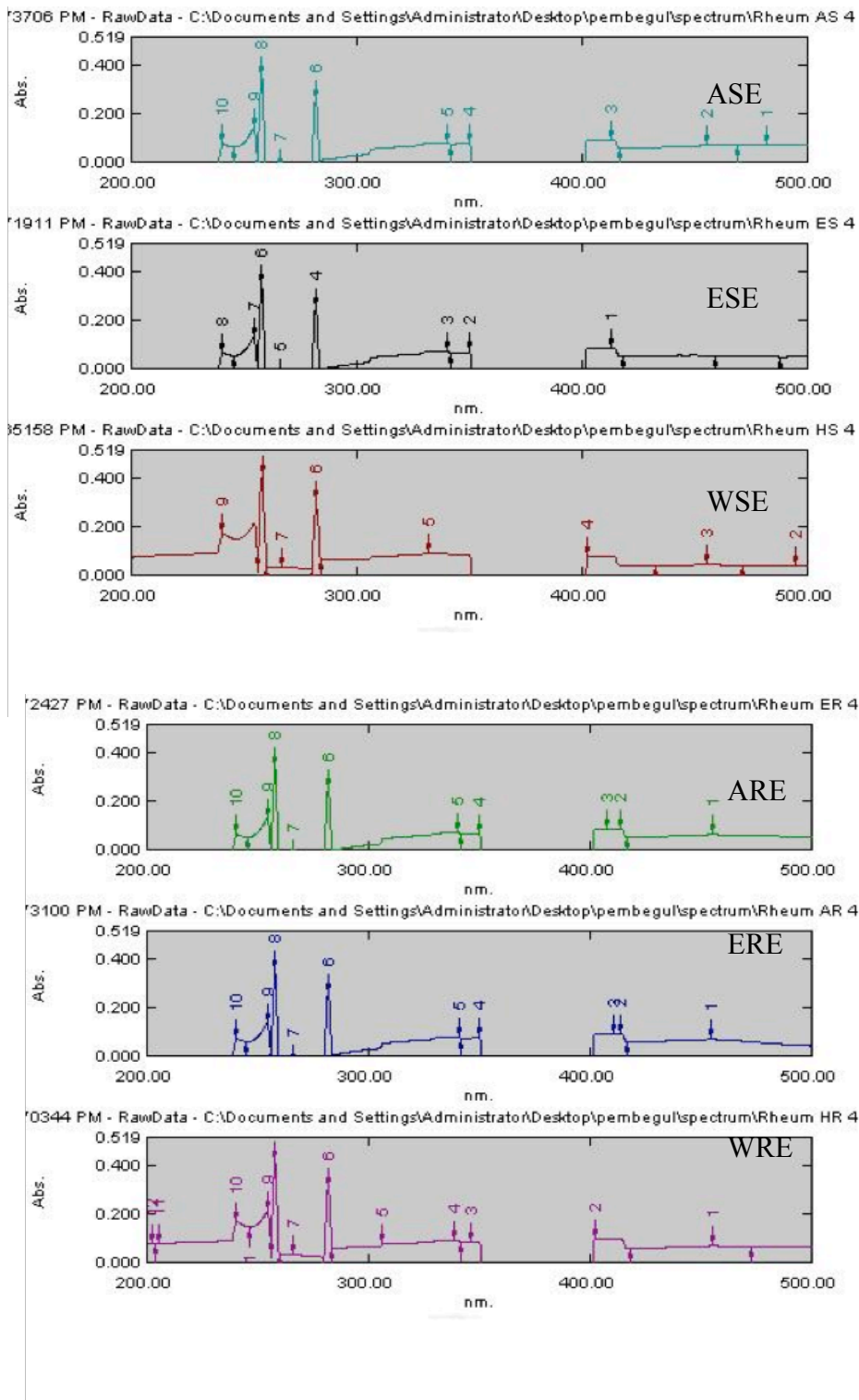
ARE and ERE exhibited similar absorption spectra with same number of peaks and their positions were almost identical.

WRE had 11 peaks, which was more than 9 peaks that WSE had and also the positions of the peaks were not identical.

WRE had more peaks than ARE and ERE. These results were not unexpected because the yield obtained in the extraction was higher in WRE due to having high polarity index than others.

It is already reported that the major bioactive constituents of *Rheum ribes* are anthraquinone derivative (Öztürk, 2006). All of the extracts had absorption maxima characteristic of hydroxyanthraquinones and their derivatives and flavonoids.

These absorption spectra of *Rheum ribes* shoot and root freeze-dried extracts were taken after all extraction. They were used in drawing a concentration curve for all extracts to develop technical standards for the extraction process as shown in Figure 3.2



A

B

**Figure 3.1** Absorption spectra of A) Shoot and B) Root *Rheum ribes* freeze-dried extracts (4 mg/ml) were taken in ethanol for ethanol and ethyl acetate extracts and in ddH<sub>2</sub>O for aqueous extract between 200 to 500 nm at room temperature against ethanol and ddH<sub>2</sub>O, respectively.

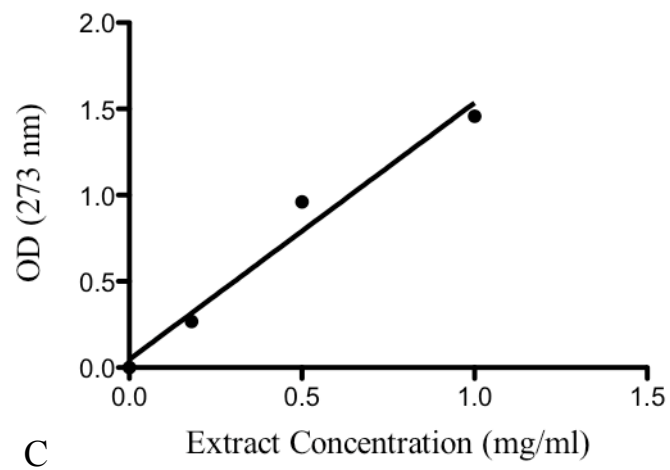
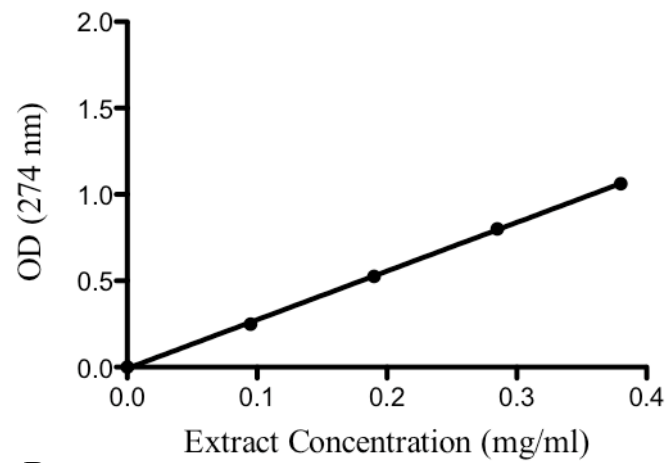
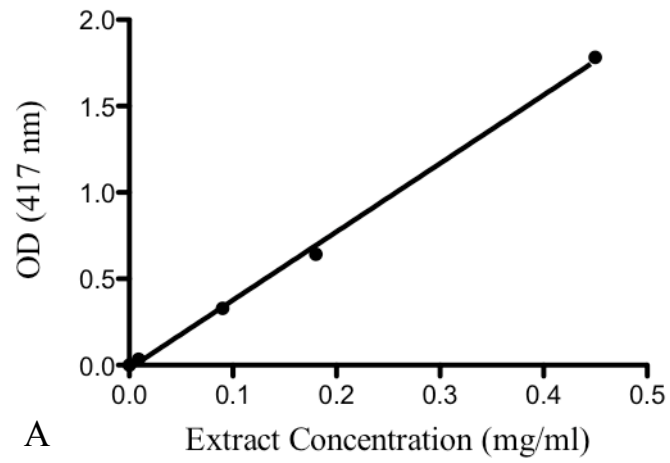


**Figure 3.2** Concentration curve of *Rheum ribes* shoot extracts of A) ethyl acetate B) ethanol and C) water at indicated nm against ethanol.

The absorption spectra of 50  $\mu\text{g/ml}$  *Rheum ribes* root methanol extract, chloroform and n-butanol fractions were taken in methanol and 50  $\mu\text{g/ml}$  water-soluble fractions, which were more soluble in water, were taken in ddH<sub>2</sub>O against ddH<sub>2</sub>O. The absorption spectra of 150  $\mu\text{g/ml}$  water-soluble *Rheum ribes* shoot fractions, which were more soluble in water, were taken in ddH<sub>2</sub>O against ddH<sub>2</sub>O. The absorption spectra of *Rheum ribes* were taken between 200 nm to 600 nm at room temperature and they were presented in Figure 3.3.

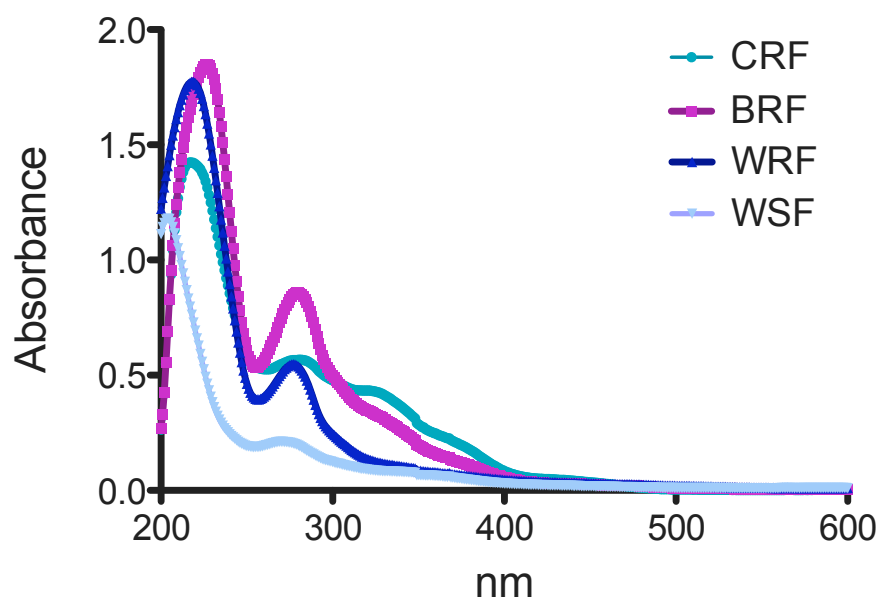


**Figure 3.3** Absorption spectra of *Rheum ribes* root fractions (50  $\mu\text{g/ml}$ ) and *Rheum ribes* aqueous shoot fractions (150  $\mu\text{g/ml}$ ) were taken in methanol for CRF and BRF and in ddH<sub>2</sub>O for WSF and WRF between 200 to 600 nm at room temperature against methanol and ddH<sub>2</sub>O, respectively.

All root fractions constituted similar absorption spectra, which were different from the peaks obtained from, shoot fractions.

All of the fractions had absorption maxima characteristic of hydroxyanthraquinones and their derivatives and flavonoids.

### 3.3 Antioxidant Efficiency of *Rheum ribes*

Relatively stable radicals such as DPPH• are often preferred in the assessment of radical scavenging activity. This radical has been widely used in various studies of plant extracts and foods (Koleva 2002; Lee, 2003). The popularity of using the DPPH free radical method for estimating free radical scavenging activity may be due to its simple, rapid and economic properties.

In the recent publications, it was shown that various research groups have used widely different protocols which differ in the concentration of DPPH (22.5–250 µM), incubation time (5 min–1 h), reaction solvent and pH of the reaction mixture. In the reaction mixture, using high concentrations of DPPH give absorbance beyond the accuracy of spectrophotometric measurements (Ayres, 1949; Sloane, 1977).

In our study, method by Blois (1958) was modified to evaluate DPPH radical scavenging activity of *Rheum ribes* freeze-dried extracts/fractions. The Radical Scavenging Activity (RSA) of each extract was calculated and used for determination of EC<sub>50</sub> values, which indicated the amount of the extract scavenging 50 % of DPPH radical.

#### 3.3.1 Incubation Time Optimization of DPPH assay

In order to optimize the DPPH Radical Scavenging activity with respect to time, decrease in the absorbance was recorded once per 1.5 min for 30 min for 100 µg/ml ESE. As shown in Figure 3.4 there was a rapid decrease of DPPH concentration at the early reaction phase (0–10 min) was followed by a slow reduction of the DPPH concentration later (10–30 min). The slow reaction rate suggests a complex reaction mechanism to reach a steady state (Bondet, 1997). In this investigation, any time point between 10 and 30 min could be arbitrarily selected as the steady state.

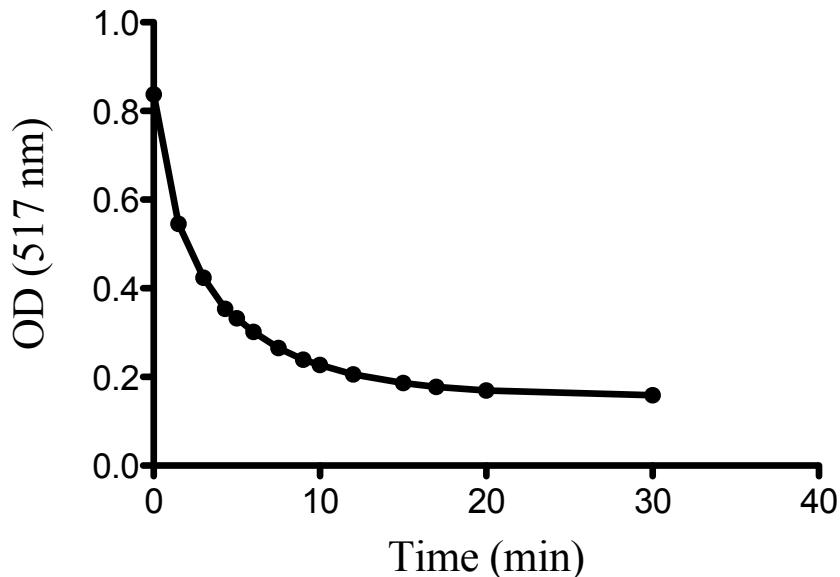


**Figure 3.4** Reaction Kinetics of DPPH Radical Scavenging Activity. Decrease in the absorbance was recorded once per 1.5 min for 30 min at room temperature. The initial concentration was  $1.5 \times 10^4$  M for DPPH radicals in the reaction. The final concentration of ESE was 100  $\mu$ g ESE per mL of the reaction mixture. The total reaction volume was 300  $\mu$ L for the reaction. The absorbance was measured at 517 nm. The calculation was conducted according to eq 2.1. Each experiment was repeated 4 times (n=4)

### ***3.3.2 The Effects of Incubation Time in Different Extract Concentrations on DPPH Assay***

The high-throughput DPPH assay in 96 well plates was carried out using a SPECTRAmax 340PC plate reader. Each reaction mixture contained 20  $\mu$ L of antioxidant sample at different concentrations. 10 different concentrations prepared in methanol were used for each antioxidant extract in the study. The absorption at 517 nm was determined, and each plate was read once per 5 min in 30 min.

In the original method a reaction time of 30 minutes was recommended, and this has been followed in more recent work (Kim, 2002). Shorter times have also been used, such as 5 minutes (Lebeau, 2000), or 10 minutes (Schwarz, 2001). Therefore, we followed the reaction until it has gone to completion in different

extracts at different concentrations by taking measurements at every 5 min in 30 min in view of the fact that the rate of reaction varies widely among different solvent system.

In our study, the classified kinetic behavior of *Rheum ribes* both shoot and root extracts is between 5 to 30 min. In Fig 3.5 and 3.6 it was only shown just for ESE. In this case, there is a linear relationship between the time at the steady state and the concentration of antioxidants.

Thought out this study, 30 min incubation was used in the procedure to estimate the EC<sub>50</sub> for all the samples as recommended in the original article (Blois, 1958).

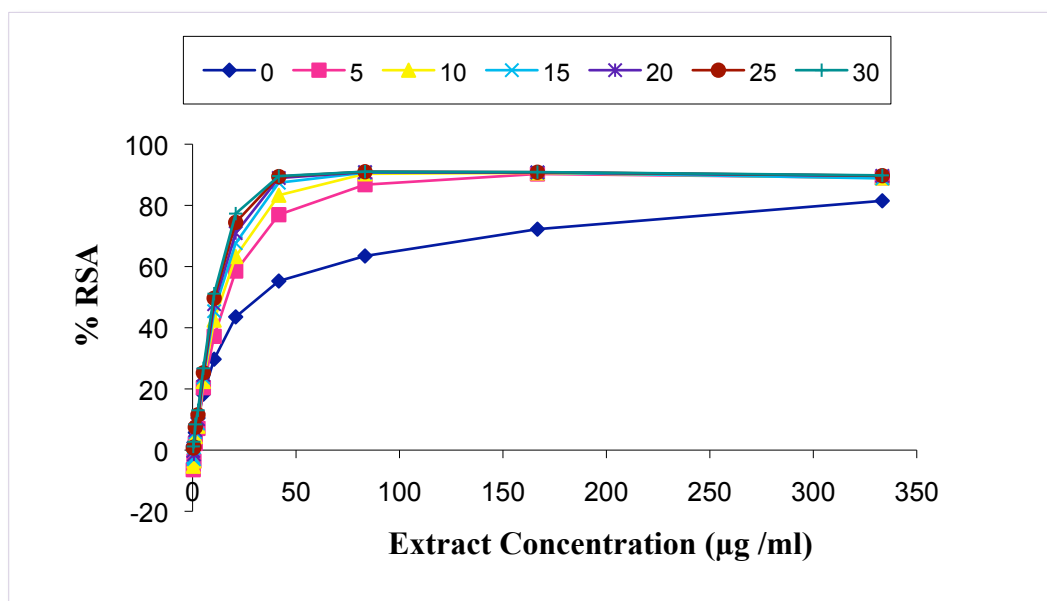


**Figure 3.5** Time and concentration effects of ESE on DPPH radical scavenging activity, read once per 5 min for 30 min. The initial concentration was  $1.5 \times 10^4$  M for DPPH radicals in all reactions. The initial concentrations were 0.33–333.0 µg ESE shoot extract per mL of the reaction mixture. The total reaction volume was 300 µL for all reactions. The absorbance was measured at 517 nm. The calculation was conducted according to eq 2.1. Each experiment was repeated 4 times (n=4).

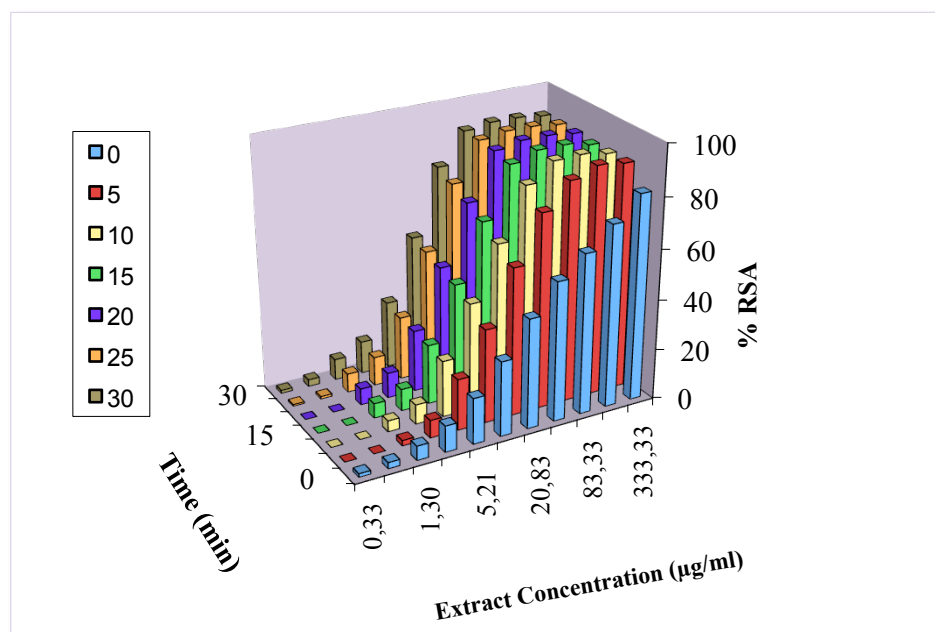


**Figure 3.6** 3D Bar Diagram of the effects incubation time effects of different ESE concentrations on DPPH radical scavenging activity, read once per 5 min for 30 min.

### 3.3.3 Determination of Antioxidant Capacities of *Rheum ribes*

Antioxidant activities of *Rheum ribes* shoot and root freeze-dried extracts/fractions were investigated by measuring their DPPH radical scavenging activity.

DPPH radical scavenging activity of extracts prepared by ethyl acetate, methanol, ethanol and water extraction were monitored at 517 nm for 30 minutes.

Measurements of percent DPPH radical scavenging activities were carried out for different final concentrations ranging between the values 0.0026–1.33 mg of plant crude extracts/ml, and the results for DPPH percent radical scavenging activity (% RSA) versus extract concentrations in µg/mL as shown in Figure 3.8 were given in Table 3.2, displayed EC<sub>50</sub> values of *Rheum ribes* ethyl acetate, methanol, ethanol and aqueous shoot and root extracts respectively.

Quercetin, emodin and catechin were used as reference materials for the DPPH assay. In the Figure 3.7 96-well microtiter plate prepared for use in the DPPH assay was shown at the end of 30 minutes incubation time.

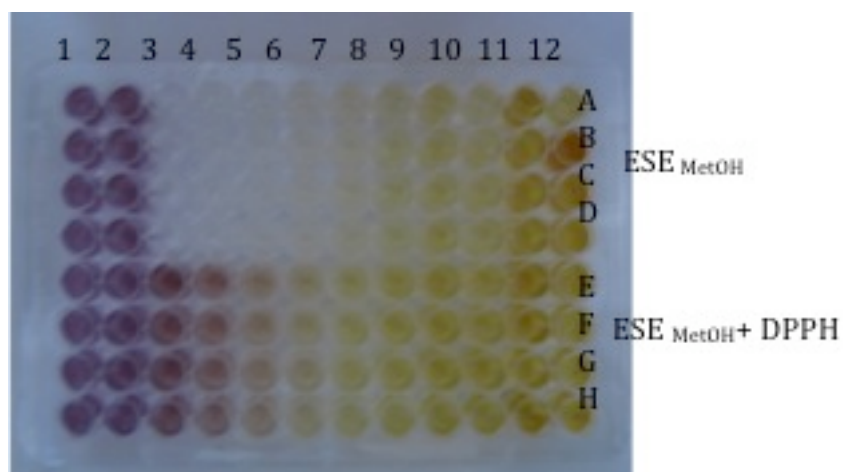


**Figure 3.7** 96-well microtiter plate prepared for use in the DPPH assay. Purple wells indicate the absence of an antioxidant effect; yellow wells are indicative of the presence of extracts with anti-oxidant activity. Plate design was as explained in Appendix A.

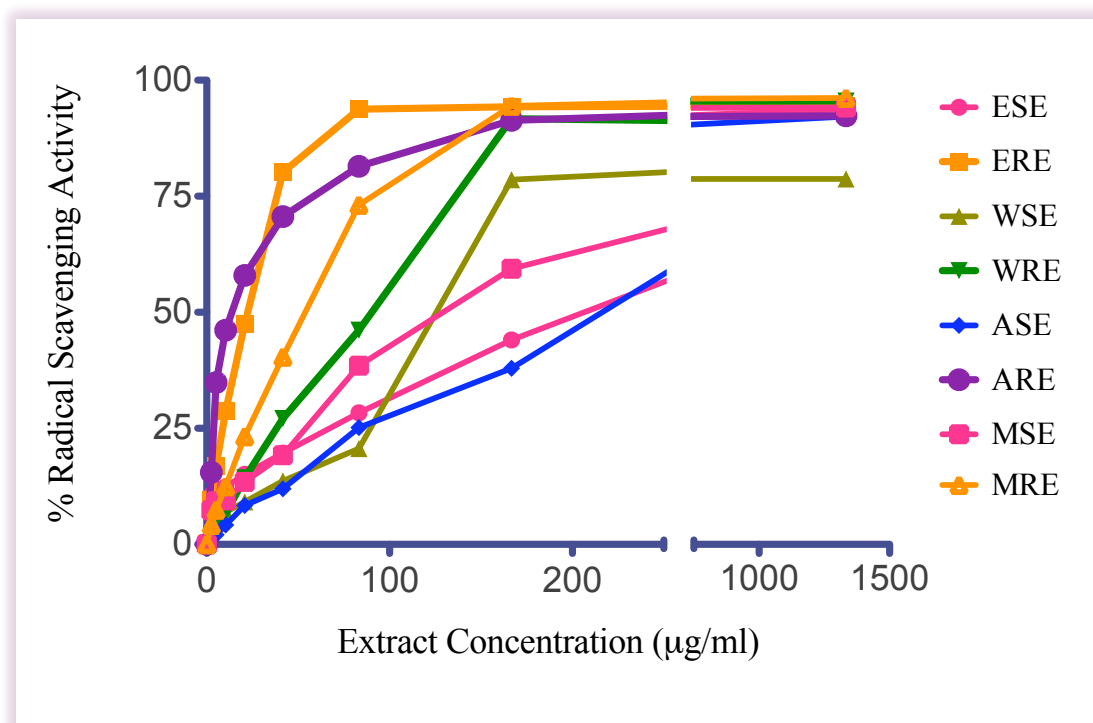


**Figure 3.8** Percent DPPH scavenging activities (% RSA) of *Rheum ribes* shoot and root extracts prepared in ethyl acetate (EtOAc), methanol (MetOH), ethanol (EtOH) and water. Each point is the mean of quadruple measurements from three different sets of experiments (n=3) (\*  $p < 0.05$  compared to and analyzed by one way ANOVA).

In Table 3.2, maximum DPPH radical scavenging achieved by the extracts and standards at the concentration range used in the experiments were also listed. As shown in Table 3.2 and Figure 3.8 the antioxidant capacities (%RSA) in all samples increased in a concentration dependent manner up to a certain extract concentration, and then reached a plateau.

**Table 3.2** Antioxidant activity ( $EC_{50}$   $\mu\text{g/ml} \pm SD^{\text{p}}$ ) and % Radical Scavenging Activity (%RSA  $\pm SD^{\text{p}}$ ) in the different extracts of *Rheum ribes*

<b>Samples</b>	<b>Antioxidant Activity (<math>EC_{50}</math> <math>\mu\text{g/ml} \pm SD^{\text{p}}</math>)</b>	<b>Maximum % Radical Scavenging Activity (%RSA <math>\pm SD^{\text{p}}</math>)</b>
<b>ASE</b>	206.28 $\pm$ 10.21	80.34 $\pm$ 0.98
<b>ARE</b>	10.92 $\pm$ 0.21	96.67 $\pm$ 0.98
<b>MSE</b>	192.36 $\pm$ 12.45	93.81 $\pm$ 2.36
<b>MRE</b>	24.67 $\pm$ 1.26	96.16 $\pm$ 0.85
<b>ESE</b>	177.48 $\pm$ 21.04	95.95 $\pm$ 1.99
<b>ERE</b>	16.31 $\pm$ 2.41	96.23 $\pm$ 1.56
<b>WSE</b>	110.37 $\pm$ 10.21	93.16 $\pm$ 1.72
<b>WRE</b>	87.95 $\pm$ 11.45	94.46 $\pm$ 1.11
<b>CSF</b>	58.73 $\pm$ 7.25	96.58 $\pm$ 2.83
<b>CRF</b>	35.68 $\pm$ 21.04	95.71 $\pm$ 1.54
<b>BSF</b>	ND	ND
<b>BRF</b>	5.21 $\pm$ 2.21	98.38 $\pm$ 1.32
<b>WSF</b>	116.19 $\pm$ 9.45	95.14 $\pm$ 2.13
<b>WRF</b>	11.95 $\pm$ 11.45	94.85 $\pm$ 2.31
<b>Emodin</b>	164.30 $\pm$ 23.13	85.98 $\pm$ 1.47
<b>Quercetin</b>	4.49 $\pm$ 2.54	95.39 $\pm$ 1.96
<b>Catechin</b>	108.71 $\pm$ 9.12	92.49 $\pm$ 1.99

<sup>p</sup>SD was derived from three independent experiments.

The highest DPPH radical scavenging capacity which was expressed as  $EC_{50}$  was obtained in ARE with 10.92 $\pm$ 0.21  $\mu\text{g/ml}$  and 96.67 $\pm$ 0.98, on the other hand the lowest radical scavenging activity was in ASE with 206.28 $\pm$ 10.21  $\mu\text{g/ml}$   $EC_{50}$  value, which was also exhibited maximum % 80.34 $\pm$ 0.98, scavenging potential as shown in the Figure 3.8 and Table 3.2. This difference obtained between the shoot and root residue with ethyl acetate extraction could be due to presence of less phenolic constitutes in the ASE than ARE.

EC<sub>50</sub> value from DPPH analysis for methanol and ethanol shoot extracts were 192.36±12.45 µg/ml and 177.48±21.04 µg/ml, respectively and were not significantly different from each other statistically ( $p>0.05$ ). Efficient DPPH activities were obtained in root extracts for both methanol and ethanol and had values of 24.67±1.26 µg/ml and 16.31±2.41 µg/ml, respectively. They were not significantly different from each other statistically ( $p>0.05$ ). This difference obtained between the shoot and root residue with ethanol extraction could be due to presence of less phenolic constitutes in the ESE than ERE, which was also observed in ethyl acetate extraction.

Aqueous extraction of both shoot and root dry powder samples exhibited similar antioxidant activity as WSE with EC<sub>50</sub> value of 110.37±10.21 µg/ml and WRE with EC<sub>50</sub> value of 87.95±11.45 µg/ml.

All of the extracts reached over 90 % RSA except ASE at extract concentrations of 0.0026–1.33 mg/ml in 30 min.

As compared to result of the present study, Ozturk et al., 2006 observed higher antioxidant activity with methanol extract of *Rheum ribes* shoots, however they obtained lower antioxidant activity with methanol root, chloroform shoot and root extracts. This could be due to the difference at applied time and temperature during extraction (Ozturk, 2006).

The values of % of antioxidant activity were found to be inversely proportional to EC<sub>50</sub> values. The smaller the EC<sub>50</sub> value the greater the RSA and reducing ability of *Rheum ribes*.

The order of % RSA of *Rheum ribes* was ASE<WSE<MSE<WRE<ESE<MRE<ERE<ARE. The order of EC<sub>50</sub> ARE<ERE<MRE<WRE<WSE<ESE<MSE<ASE.

DPPH radical scavenging capacities of reference materials such as quercetin, emodin and catechin were also determined since they were quite often used in the literature as phenolic standards, and displayed in the Figure 3.9 and compared with the ethanolic root extract of *Rheum ribes*, ERE that showed higher antioxidant activity among all tested extracts. Besides, emodin was one of the anthraquinones found in *Rheum ribes* (Tosun, 2003).

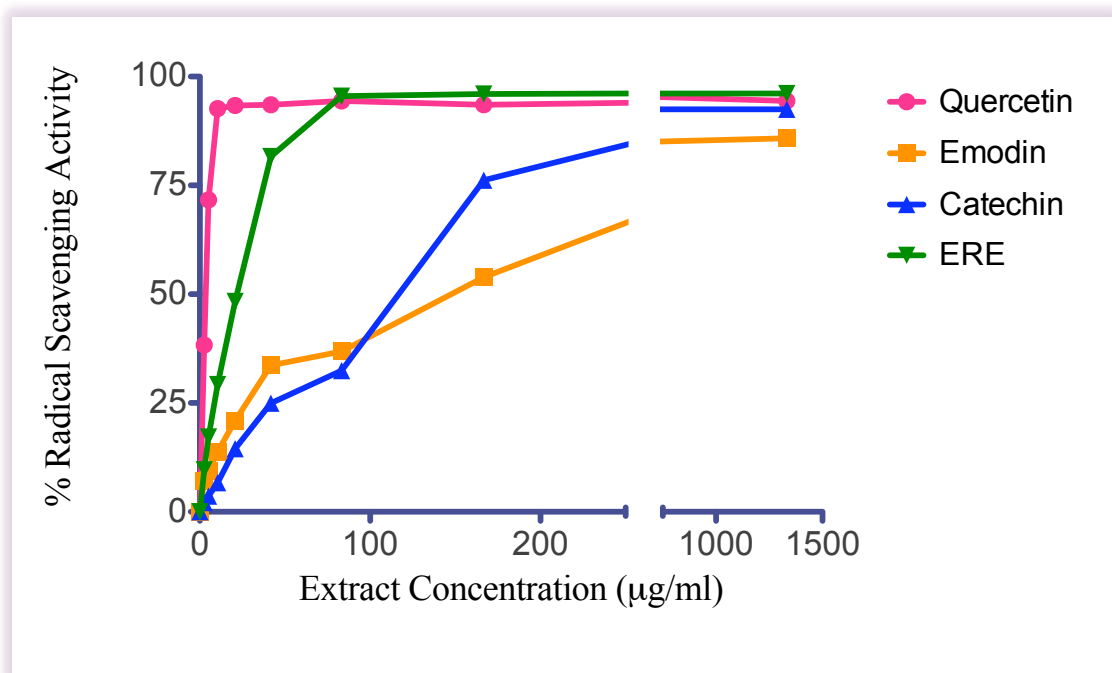


**Figure 3.9** Comparison of percent DPPH scavenging capacities of *Rheum ribes* root extract and the reference materials

All root extracts showed greater antioxidant activity than emodin and catechin, however only ARE showed almost the same activity to that of quercetin. Only WSE showed greater antioxidant activity than emodin, and almost the same activity to that of catechin among shoot extracts. In the literature, emodin showed  $EC_{50}$  value higher than 100  $\mu\text{g/ml}$  (Hsin-Tang Lin, 2010).

In this study, obtained  $EC_{50}$  values of emodin, catechin and quercetin were  $164.30 \pm 23.13$ ,  $108.71 \pm 9.12$  and  $4.49 \pm 2.54$   $\mu\text{g/ml}$ , respectively. % RSA of the standards were also inversely proportional to  $EC_{50}$  values as  $85.98 \pm 1.47$ ,  $92.49 \pm 1.99$  and  $95.39 \pm 1.96$ .

The highest DPPH radical scavenging capacity obtained among fractions was BRF with  $5.21 \pm 2.21$   $\mu\text{g/ml}$  of  $EC_{50}$  value and almost the same activity to that of quercetin. This was an expected result because during fractionation ethyl acetate was not used as a separation solvent.

As it was mentioned before, the highest DPPH radical scavenging capacity was obtained in ARE with  $EC_{50}$  value of  $10.92 \pm 0.21 \mu\text{g/ml}$ . However, BRF still showed higher DPPH scavenging activity than ARE. On the other hand the lowest capacity was in WSF with  $116.19 \pm 9.45 \mu\text{g/ml}$  of  $EC_{50}$  value, as shown in the Figure 3.10 and Table 3.2.

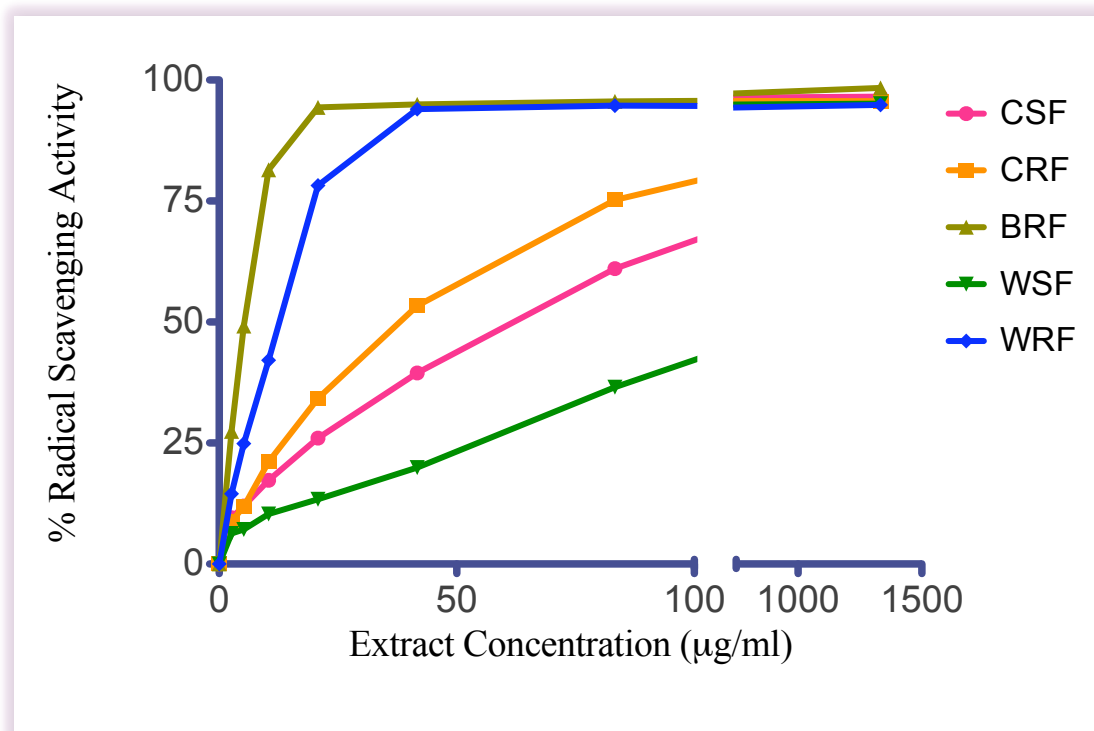


**Figure 3.10** Percent DPPH scavenging activities of *Rheum ribes* chloroform, n-butanol and aqueous shoot and root fractions. Each point was the mean of quadruple measurements from three different sets of experiments ( $n=3$ ) (\*  $p < 0.05$  compared to and analyzed by one way ANOVA).

$EC_{50}$  value from DPPH analysis for shoot and root chloroform fractions were  $58.73 \pm 7.25 \mu\text{g/ml}$  and  $35.68 \pm 21.04 \mu\text{g/ml}$ , respectively. It was similar to other solvent systems that root extracts showed greater antioxidant activity than shoot extracts in this investigation.

Aqueous fractions of *Rheum ribes* roots exhibited higher antioxidant activity than shoots with EC<sub>50</sub> value of 116.19±9.45 µg/ml and 11.95±11.45 µg/ml, respectively. This was the biggest difference, almost ten times, between shoot and root of *Rheum ribes* extracts. WSE and WSF were not significantly different from each other statistically ( $p>0.05$ ). However, WRE and WRF were significantly different ( $p<0.05$ ) and difference was due to fractionation procedure.

All of the extracts and fractions reached over 90 % RSA except ASE at extract concentrations of 0.0026–1.33 mg/ml in 30 min.

### **3.4 Determination of Total Phenolic Contents of of Rheum ribes**

Total phenolic contents of *Rheum ribes* extracts/fractions were determined by the method of Singleton and Rossi (1965), the Folin-Ciocalteu reagent assay. The Folin-Ciocalteu reagent (FC) assay is routinely used, as it is simple, sensitive and precise. The results were presented as mg phenolic equivalents of gallic acid (GAE) in g of extract given as in the Table 3.3.

Total phenolic compounds of the shoot and root extracts of *Rheum ribes* prepared in ethyl acetate, methanol, ethanol and water were determined as mg equivalents of gallic acid per g of freeze dry extracts.

Methanol extraction of root presented the highest total phenolic content, among the others, it was significantly different than the ethyl acetate, ethanol and water. However the phenolic content of water extract of root was statistically lower than all.

Methanol extraction of shoot presented the highest total phenolic content; among the other shoot extracts, although it was still not significantly different than the ethyl acetate, ethanol and water.

**Table 3.3** Total phenol contents in different extracts of *Rheum ribes* as expressed in gallic acid equivalents (GAE)

<b>Samples</b>	<b>Total Phenol (mg GAE/g dried extract<sup>±</sup> SD<sup>Ⓞ</sup>)</b>
<b>ASE</b>	21.11±1.11
<b>ARE</b>	207.22±6.96.72
<b>MSE</b>	27.04±2.43
<b>MRE</b>	308.91±24.45
<b>ESE</b>	26.16±3.06
<b>ERE</b>	226.61±10.65
<b>WSE</b>	26.24±2.25
<b>WRE</b>	46.92±4.56
<b>CSF</b>	162.53±3.26
<b>CRF</b>	204.12±15.04
<b>BSF</b>	ND
<b>BRF</b>	84.15±14.21
<b>WSF</b>	69.02±4.45
<b>WRF</b>	53.55±6.62

TP GAE : Total phenolic contents mg equivalents of gallic acid/g of plant extract

ND: not detectable

<sup>Ⓞ</sup>SD : was derived from three independent experiments.

Total phenolic content of shoot extracts significantly increased after fractionation, however it was not same for root fractions. FC assay gives a crude estimate of the total phenolic compounds present in an extract/fraction. It is not specific to polyphenols, but many interfering compounds may react with the reagent, giving elevated apparent phenolic concentrations (Prior, 2005). Moreover, various phenolic compounds respond differently in this assay, depending on the number of phenolic groups they have and total phenolics content does not incorporate necessarily all the antioxidants that may be present in an extract or fraction (Tawaha, 2007).

### **3.5 Determination of Total Flavonoid Contents of of *Rheum ribes***

Total flavonoid contents of *Rheum ribes* extracts/fractions were determined by using by aluminium colorimetric assay. (Whiten, 1999). Total flavonoid compounds of the shoot and root extracts of *Rheum ribes* prepared in ethyl acetate, methanol, ethanol and water were determined as mg equivalents of catechin per g of crude extracts given in the Table 3.4.

Ethanol extraction of root presented the highest total flavonoid content, among the others, it was significantly different than the ethyl acetate, methanol and water. However the flavonoid content of water extracts of root was statistically lower than all.

Ethanol extraction of shoot presented the highest total phenolic content; among the other shoot extracts, it was significantly different than the ethyl acetate, methanol and water. However the flavonoid content of ethyl acetate extracts of shoot was statistically lower than all.

Total flavonoid content of both shoots and root extracts significantly increased after fractionation of methanol extract.

**Table 3.4** Total flavonoid content in different extracts of *Rheum ribes* as expressed in Catechin Equivalents (CAE)

<b>Samples</b>	<b>Total Flavonoid (mg CAE/g dried extract<sup>ϕ</sup>)</b>
<b>ASE</b>	2.29±1.04
<b>ARE</b>	50.49±2.03
<b>MSE</b>	6.48±4.05
<b>MRE</b>	58.19±8.95
<b>ESE</b>	13.59±3.02
<b>ERE</b>	70.89±6.84
<b>WSE</b>	4.85±1.43
<b>WRE</b>	19.23±2.75
<b>CSF</b>	59.08±1.53
<b>CRF</b>	74.20±2.69
<b>BSF</b>	ND
<b>BRF</b>	30.56±1.72
<b>WSF</b>	25.19±1.34
<b>WRF</b>	30.59±2.18

TP CAE : Total flavonoid contents mg equivalents of catechin/g of plant extract

ND: not detectable

<sup>ϕ</sup>SD : was derived from three independent experiments.

**Table 3.5** Summary of antioxidant activity, contents of Total phenol and flavonoid in the different extracts of *Rheum ribes* GAE: Gallic Acid Equivalents CAE: Catechin Equivalents.

<b>Samples</b>	<b>Antioxidant Activity (EC<sub>50</sub> µg/ml± SD<sup>ρ</sup>)</b>	<b>Maximum % Radical Scavenging Activity (%RSA± SD<sup>ρ</sup>)</b>	<b>Total Phenol (mg GAE/g dried extract± SD<sup>ρ</sup>)</b>	<b>Total Flavonoid (mg CAE/g dried extract± SD<sup>ρ</sup>)</b>
<b>ASE</b>	206.28±10.21	80.34±0.98	21.11±1.11	2.29±1.04
<b>ARE</b>	10.92±0.21	96.67±0.98	207.22±6.96.72	50.49±2.03
<b>MSE</b>	192.36±12.45	93.81±2.36	27.04±2.43	6.48±4.05
<b>MRE</b>	24.67±1.26	96.16±0.85	308.91±24.45	58.19±8.95
<b>ESE</b>	177.48±21.04	95.95±1.99	26.16±3.06	13.59±3.02
<b>ERE</b>	16.31±2.41	96.23±1.56	226.61±10.65	70.89±6.84
<b>WSE</b>	110.37±10.21	93.16±1.72	26.24±2.25	4.85±1.43
<b>WRE</b>	87.95±11.45	94.46±1.11	46.92±4.56	19.23±2.75
<b>CSF</b>	58.73±7.25	96.58±2.83	162.53±3.26	59.08±1.53
<b>CRF</b>	35.68±21.04	95.71±1.54	204.12±15.04	74.20±2.69
<b>BSF</b>	ND	ND	ND	ND
<b>BRF</b>	5.21±2.21	98.38±1.32	84.15±14.21	30.56±1.72
<b>WSF</b>	116.19±9.45	95.14±2.13	69.02±4.45	25.19±1.34
<b>WRF</b>	11.95±11.45	94.85±2.31	53.55±6.62	30.59±2.18
<b>Emodin</b>	164.30±23.13	85.98±1.47	NA	NA
<b>Quercetin</b>	4.49±2.54	95.39±1.96	NA	NA
<b>Catechin</b>	108.71±9.12	92.49±1.99	NA	NA

TP GAE : Total phenolic contents mg equivalents of gallic acid/g of plant extract

TF CAE : Total flavonid contents mg equivalents of catechin/g of plant extract

ND: not detected

NA: not applicable

<sup>ρ</sup>SD : was derived from three independent experiments.

### **3.6 Viability of HL-60 Cells**

HL-60 cells have been used extensively as a model system for the study of phytochemical effects on biological systems. In order to get reliable results when a cell line was used, the growth and inoculation conditions had to be optimized. The viability of cells should be determined in order to be sure about the suitability of medium composition and other environmental conditions. All cells are sensitive to their environmental physical and chemical conditions even cancer cell although they are immortal. Nutrient requirements with respect to division time of cells should be under control. In order to get maximum growth, nutrient requirement and physical conditions had to be supportive to obtain over 90% cell viability for cells under investigation. Although RPMI 1640 is well-established growth medium, L-glutamine and pyruvate had to be added into culture medium as energy sources. Fetal Calf Serum contains high level of protein and growth factors to support growth. The sterility of the cultures is the requirement of prime importance. In the medium, sterility is stabilized by addition of antibiotics such as gentamicin. Although antibiotics are beneficial to protect cells from contaminations, they are harmful at high concentrations. In order to decrease the usage amount, starting the cultures and all further manipulations has to be done under strict aseptic conditions, which is achieved by UV sterilization in laminar flow hood or biological cabinet, filter sterilization of all chemical solutions used, autoclaving all glass wares at 120°C for 20 minutes.

The change in pH could be observed by naked eye with the help of phenol red present as a pH indicator in RPMI medium. It is red at pH: 7.4, turning yellow at pH: 6.5, lemon yellow below pH: 6.5. Another indicator of overgrowth, followed by naked eye was the cloudy appearance in the medium. The healthiness of the cells was controlled at least every 24 hours under the inverted microscope.

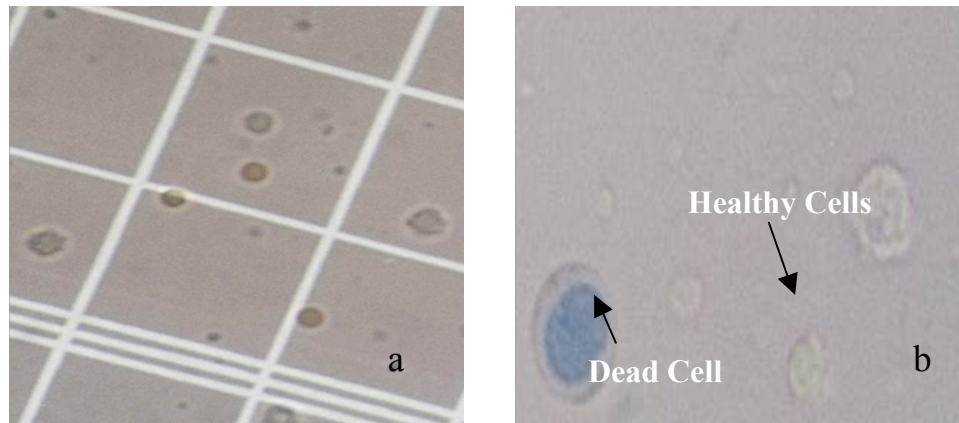


**Figure 3.11** a) the healthy HL-60 cells c) the alive and dead HL-60 cells were side by side at 400X magnification.

24-hour adaptation period had been conducted before getting the data in order to construct the growth curves and the time versus cell viability table. Then, the actual incubation study was established to get reliable data by eliminating physical and chemical environmental effects. This was carried out as follows; the HL-60 cells, which had been frozen at  $-180\text{ }^{\circ}\text{C}$  in the cryovial containing approximately at least  $2 \times 10^5$  HL-60 cells/ml, were thawed were inoculated into the 5 ml complete medium in  $25\text{ cm}^2$  sterile culture flasks. This incubation covered at least 24 hours and the aim is to understand the adaptation and survival of the cells in the new environmental conditions. After 24 hour period, the first cell count was taken as 0 time point and sampling was repeated at every 24-hour interval during 144 hours of incubation. The cell viability was determined by dye exclusion technique with the help of trypan blue and hemocytometer (Figure 3.11 (a)) in this study under light microscope by taking  $50\mu\text{l}$  cell suspension from the culture flasks under aseptic conditions. The healthy cells were observed round and shiny without trphan blue dye in their cytoplasm because they could pump out the dye by active transport system of their alive cell membranes ((Figure 3.11 (b)) . However, the dead cells contained the dye in their cytoplasm because of failure active transport system of dead cells (Figure 3.11 (b)). After thawing the frozen HL-60 cells, few

dead cell was observed in the flasks under inverted microscope during the preliminary period. The reason of these cells' dead might be that some cells could not be adapted easily into the environment or not preserved efficiently although DMSO was used in order to preserve the cytoplasm of cells during freezing of HL-60 cells.

In order to obtain the maximum cell number and growth over %90-cell viability, the optimal physical and chemical conditions were established for HL-60 cells. The optimum incubation time with the well established culture medium used in this study, was determined as 96 hours to get maximum cell number and growth over %90 cell viability, based on the growth curves of HL-60 cells as shown in Table 3.6 and Figure 3.12. After 96 hours, the viability of HL-60 cells used in this study decreased because of not only the nutrient deficiency but also increasing toxic waste materials of the cells and related changes in the pH of the culture medium.

**Table 3.6** The viability of HL-60 cells incubated for 144 hours: Number of alive and dead cells was shown.

Time (h)	# of alive HL-60 cells ( $\times 10^4$ )/ml of culture medium $\pm$ SD <sup>Y</sup>	# of death HL-60 cells ( $\times 10^4$ )/ml of culture medium $\pm$ SD <sup>Y</sup>	% Viability $\pm$ SD <sup>Y</sup>
0	10.0 $\pm$ 0.0	0.0 $\pm$ 0.0	100 $\pm$ 0.0
24	18.0 $\pm$ 0.7	1.0 $\pm$ 0.6	95.0 $\pm$ 3.2
48	34.0 $\pm$ 0.6	3.5 $\pm$ 1.0	93.0 $\pm$ 1.3
72	65.0 $\pm$ 0.5	4.5 $\pm$ 1.0	92.0 $\pm$ 1.0
96	139.0 $\pm$ 0.4	14.0 $\pm$ 1.6	90.8 $\pm$ 0.5
120	179.0 $\pm$ 0.6	31.0 $\pm$ 0.2	85.2 $\pm$ 0.7
144	187.0 $\pm$ 1.6	38.5 $\pm$ 1.7	82.9 $\pm$ 0.4

<sup>Y</sup>SD was derived from three independent experiments.

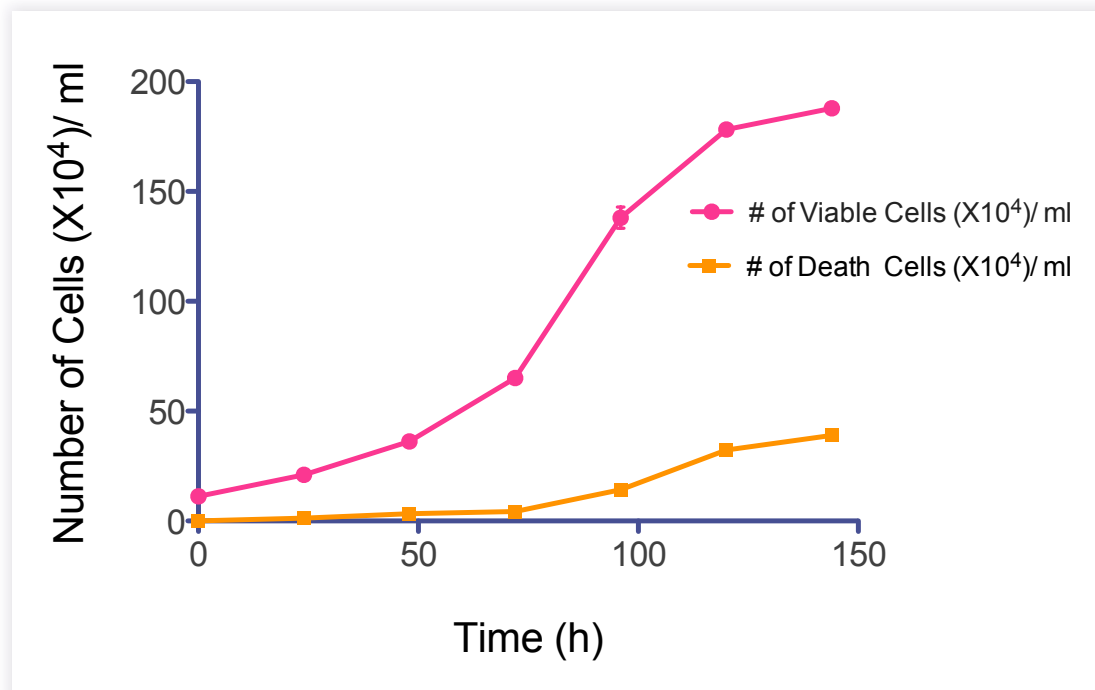


**Figure 3.12** The Growth Curve of HL-60 Cells; —●— # of Viable Cells, —■— # of Death Cells in 144 hours by trypan blue counting

As represented at time 0 in the Table 3.6 of the incubation time versus the number of alive and death cells and in the growth curve diagram (Fig. 3.8),  $1 \times 10^5$  healthy cells/ml were inoculated into the 10 ml complete medium in 25 cm<sup>2</sup> sterile culture flask at the beginning of the actual study following the adaptation period. Until 96<sup>th</sup> hour, the percent viability of cells was stabilized over 90 % in the complete medium. However at 120<sup>th</sup> and 144<sup>th</sup> hour, the percent viability became under %90. It is because of the nutrient depletion of the complete medium and the medium pH changes due to increase in cell number and deposition of excreted materials.

In this study, the table of cell viability for HL-60 cells showed that the cells had to be sub-cultured within no more than every 3 days to provide the maintenance of their robustness. Otherwise, some occurred changes on their membrane could be observed under inverted microscope and related to changes in their shapes they could die. The growth curves show that the curves become steady state after 120 hours.

### **3.7 Cytotoxicity of *Rheum ribes* Shoot and Root Extracts in HL-60 Cells**

#### ***3.7.1 Light microscopic analysis of Cell Morphology***

For the investigation of cytotoxic effects of *Rheum ribes* extracts, morphological criteria were combined with commonly accepted biochemical methods.

The effects of *Rheum ribes* on morphological changes and viability in HL-60 cells treated for 48h were analyzed under light inverted microscope (magnification, 400X) as shown in Figure 3.13. HL-60 cells ( $2 \times 10^5$  cells/ml; 1 ml/well; 24-well plate) were either left untreated or treated with 100 µg/ml ASE, ARE, ESE, ERE, WSE and WRE for 48 h.

The HL-60 cells grow in single cell suspension without any tendency to clump or to adhere to plastic or glass (Fig 3.13 a) with a round or ovoid shape, and occasional cells have blunt pseudo pods. The typical cell diameter is 13 µ, however, there is considerable variation in size, ranging from 9 µ to 25 µ in diameter. The larger cells are usually binucleated (R Gallagher, 1979).

HL-60 cells spontaneously differentiate and differentiation can be stimulated by butyrate, hypoxanthine, phorbol myristic acid (PMA, TPA), dimethylsulfoxide (DMSO, 1% to 1.5%), actinomycin D, and retinoic acid (Collins SJ, 1978). In this study DMSO was kept at a final concentration of 0.1% in each treatment.

After incubation with ASE, ARE, ESE and ERE, morphological alterations and cell growth inhibition in HL-60 cells were illustrated (Fig 3. 13 c, d, e, and f) comparing with control and DMSO treated cells (Fig 3.13 a and b). Control or DMSO treated cells were round in normal shape. Exposure of HL-60 cells to those ARE and ERE for 48 h led to the membrane blebbing and apoptotic body formation (Fig 3.9 d and f) which were observed by light inverted microscope (400X).

At 100 µg/ml concentration, decreased cell growth by ASE, ARE, ESE and ERE was observed significantly whereas there were no observed effects of WSE and WRE for 48 h in microscopic analysis.



**Figure 3.13** Light Microscopic Analysis of effects of *Rheum ribes* Extracts on morphological changes in HL-60 cells for 48 h. (a) Un-treated cell; (b) DMSO % 0.1, 100  $\mu\text{g}/\text{ml}$  of (c) ASE, (d) ARE, (e) ESE, (f) ERE, (g) WSE and (h) WRE; Arrows (d and f) indicate a typical apoptotic cell with apoptotic body. The cells were photographed under inverted light microscopy (magnification, 400X).

### ***3.7.2 Viable Cell Counting with Trypan Blue***

In order to get rid of the absorbance interference of *Rheum ribes* extract solutions on XTT assay, one of the principle cell culture methods, cell counting with trypan blue was also performed.

The effects of different extract concentrations at different time points (24, 48 and 72 h) on the cell growth and on the cell viability were detected by trypan blue exclusion and viable cell number. Averages of viable cell counts for different time points (0, 24, 48 and 72 h) versus 0 µg/ml, 10 µg/ml, 25 µg/ml, 50 µg/ml, 100 µg/ml, 250 µg/ml, 500 µg/ml *Rheum ribes* extracts concentrations vertical column bar graph were constructed (Figure 3.14,15,16).

Cell viability measurements obtained from cell count were converted to percent cell viability by setting control counts as 100% cell viable and cells that were grown in 0.1% DMSO containing medium are considered as controls and their counts were set as 100% cell viability. The IC<sub>50</sub> values were determined using GraphPad Prism version 5 for Mac OS X as shown in Table 3.8.

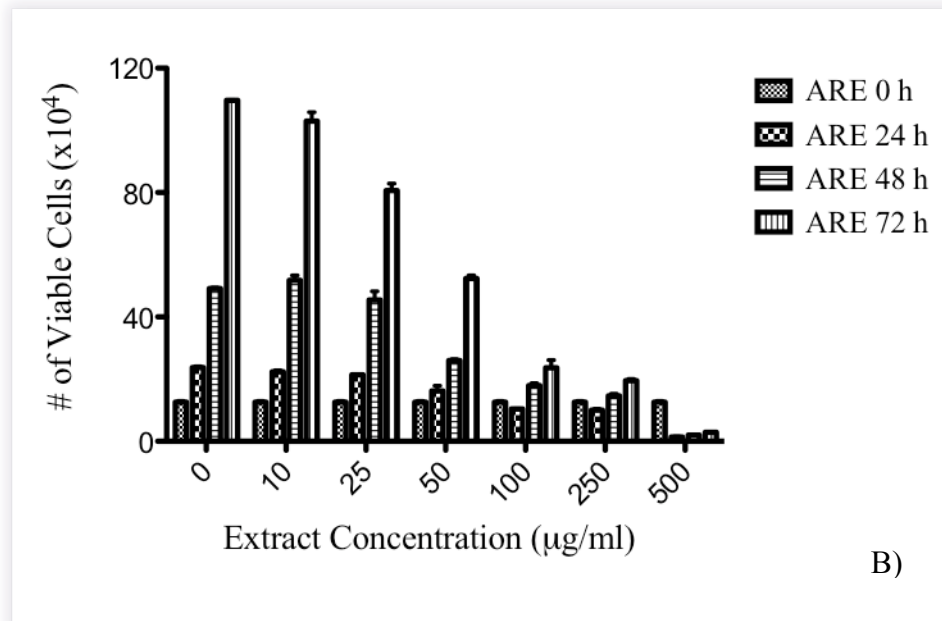
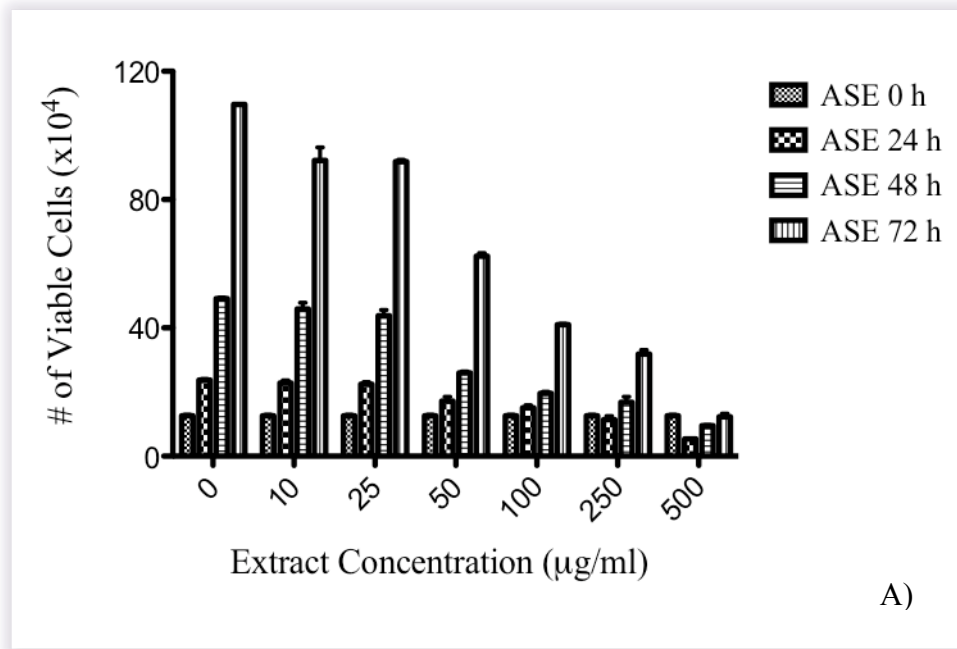


**Figure 3.14** Effects of *Rheum ribes* shoot (A) and root (B) ethyl acetate extract on cell survival in HL-60 cells by the TBE assay. HL-60 cells were precultured in 6-well microplates for overnight and then incubated with 0- 500 µg/ml of *Rheum ribes* shoot (A) and root (B) ethyl acetate extract for 24, 48 and 72 hr.

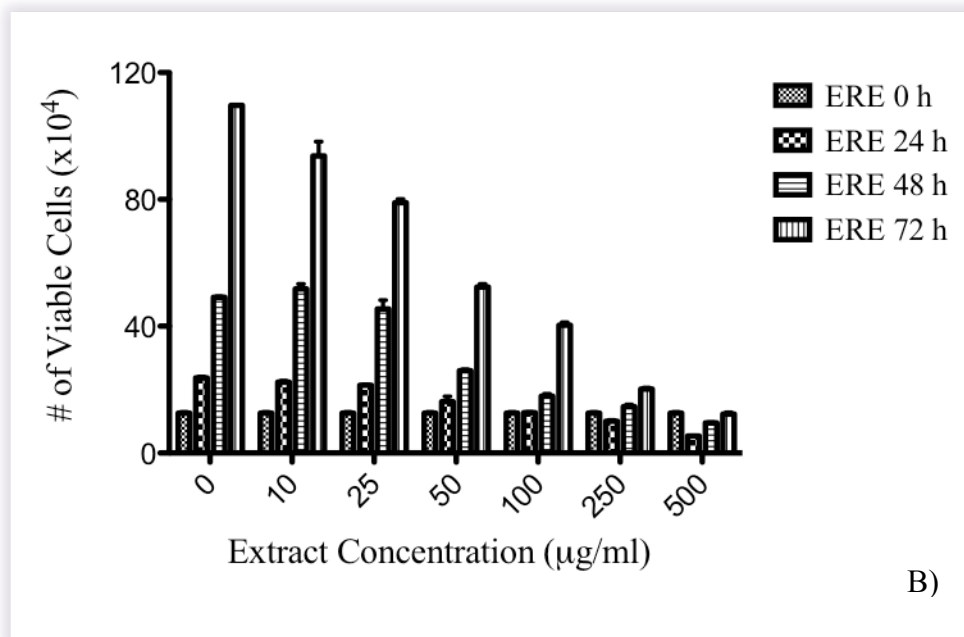
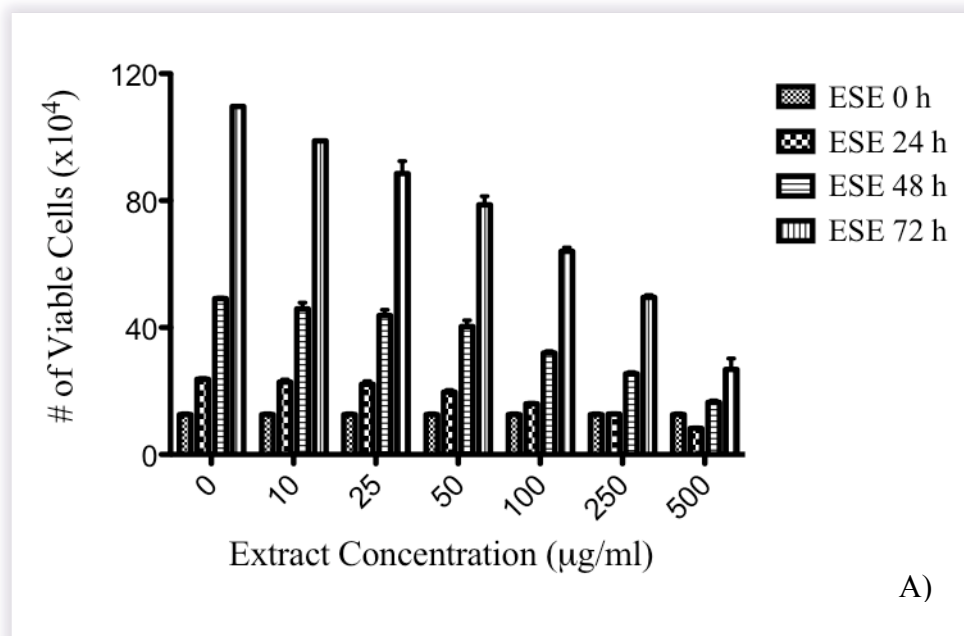


**Figure 3.15** Effects of *Rheum ribes* shoot (A) and root (B) ethanol extract extract on cell survival in HL-60 cells by the TBE assay. HL-60 cells were precultured in 6-well microplates for overnight and then incubated with 0- 500 µg/ml of *Rheum ribes* shoot (A) and root (B) ethanol extract for 24, 48 and 72 hr.

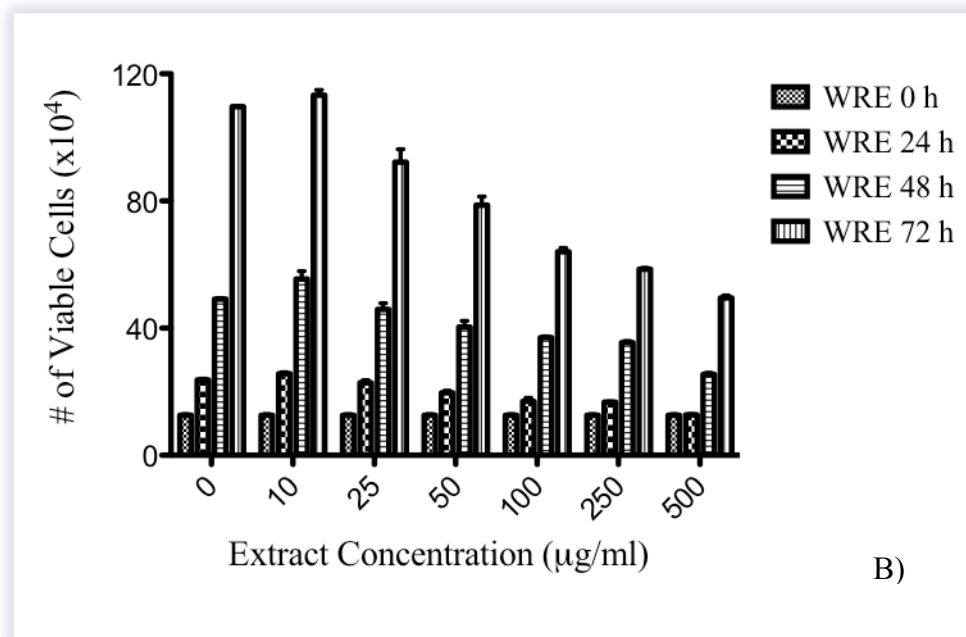
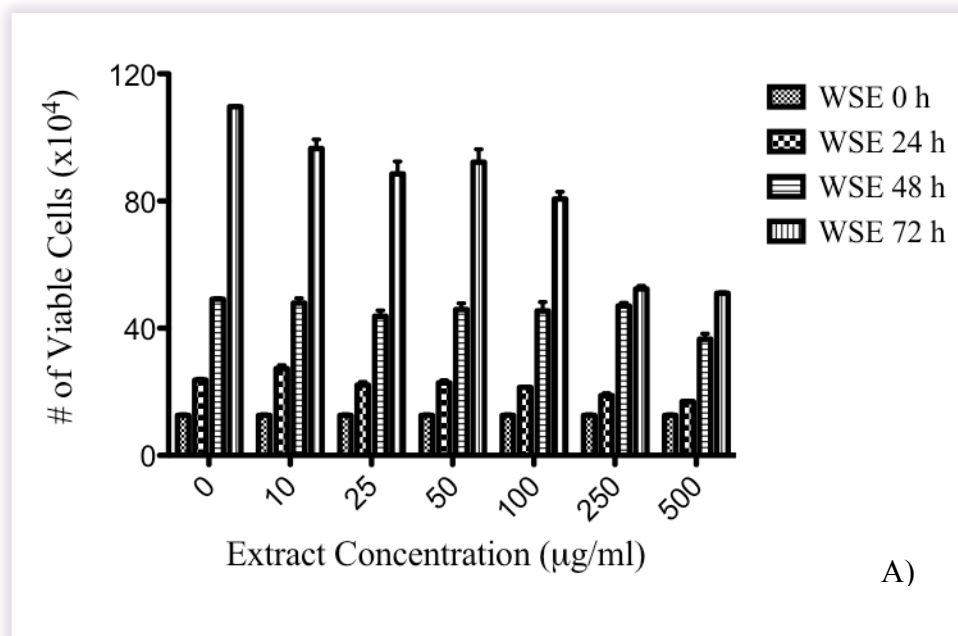


**Figure 3.16** Effects of *Rheum ribes* shoot (A) and root (B) aqueous extract on cell survival in HL-60 cells by the TBE assay. HL-60 cells were precultured in 6-well microplates for overnight and then incubated with 0- 500 µg/ml of *Rheum ribes* shoot (A) and root (B) aqueous extract for 24, 48 and 72 hr.

**Table 3.7** IC<sub>50</sub> values and % Viability in HL-60 cells obtained by counting with trypan blue after treatment of *Rheum ribes* for 24, 48 and 72 h.

Parameter	Incubation time (h)					
	24		48		72	
Extracts	IC50 (µg/mL)	% viability*	IC50 (µg/mL)	% viability*	IC50 (µg/mL)	% viability*
ASE	NA	31	100		76	
ARE	75		56		50	
ESE	NA	40	NA	38	NA	35
ERE	125		100		50	
WSE	NA	80	NA	80	NA	50
WRE	NA	50	NA	56	NA	50

\*% viability was calculated considering the viable cell count at highest extract concentration (500 µg/mL) compared to control viable cell count at every incubation time point

IC<sub>50</sub> values that were the *Rheum ribes* extracts concentrations at which 50% of cells are viable were calculated as 180 µg/ml, 100 µg/ml and 76 µg/ml after ASE treatment for 24,48 and 72 h, respectively. IC<sub>50</sub> values were calculated as 75 µg/ml, 56 µg/ml and 50 µg/ml after ARE treatment for 24,48 and 72 h, respectively. The results showed that the difference between IC<sub>50</sub> of ASE and ARE value was statistically significant, p<0.05. The growth inhibitory effect of ARE was higher than ASE in HL-60 cells for all time points, because the amount of extract concentration required to kill 50% of cells were significantly low. ARE cytotoxicity appeared rapidly so that cell viability dropped dramatically for the first 24 h after then cell viability did not change that much and also IC<sub>50</sub> of ARE for 48 h was not significantly different than IC<sub>50</sub> of ARE for 72 h (p>0.05).

IC<sub>50</sub> values were calculated as 275 µg/ml, 230 µg/ml and 225 µg/ml after ESE treatment and 125 µg/ml, 100 µg/ml and 50 µg/ml after ERE treatment for 24,48 and 72 h, respectively. These results showed that ERE was more effective than ESE to inhibit the HL-60 cell growth. It could be also concluded that ESE did not have any growth inhibition effect at a time dependent manner at these concentrations.

50 % inhibition could not be observed in WSE and WRE treatments because even though 500 µg/ml extracts were applied, more than 50 % cells were remained still alive. Nevertheless, there was a decrease in cell number in a dose and time dependent manner. At this point, 500 µg/ml was the highest concentration to apply, however for flow cytometric analysis higher concentrations were checked to define the exact concentration of aqueous extracts to kill the cells. These will be covered in Section 3.8 part of results.

Also, ARE had the highest potential among all extracts with lower IC<sub>50</sub> for all time points except for 72 h because ERE had the same IC<sub>50</sub> value as ARE for 72 h. The content of ERE showed its effects slower than ARE but at time point 72 h same number of cells were died. In absorption spectra it was concluded that ARE contained different components than ERE, just because of this it might be possible that the contents in the ARE stimulate different death pathways than ERE contents did. For further analysis, cell death pathways should have to be analyzed.

Higher inhibitory effect of rhein and aloe-emodin on HL-60 cells were also reported in literature. The effects of other Rheum species on other cell lines were also investigated. In one of this studies, Kang (2008) have isolated some known anthraquinones from the roots of *Rheum palmatum* and examined for their estrogenic activity. Among them, emodin was found to have highest estrogenic activity. The fraction that contains emodin caused cytotoxicity in MCF-7 and MDA-231 cell lines with the statistically significant IC<sub>50</sub> values of 16.4 and 46.3 µg/ml, respectively, for 48 hours showing that emodin had hormone dependent and also independent effects to cells (Kang, 2008).

### 3.7.3 XTT Assay

Metabolically active HL-60 cells were detected using XTT assay upon treatment with *Rheum ribes* extracts for 24, 48 and 72 hours. Mitochondrial enzymes of the metabolically active cells reduced tetrazolium salt, XTT and orange colored formazan product was measured using ELISA plate reader. Cell viability measurements obtained from XTT assay were converted to percent cell viability by setting control (0.1 % DMSO) results as 100% cell viable. Averages of measurements upon treatment with 0 µg/ml, 25 µg/ml, 50 µg/ml, 100 µg/ml, 200 µg/ml, 300 µg/ml *Rheum ribes* different extracts concentrations for 24, 48 and 72 hours were expressed as percentage of the 0.1% DMSO control measurements and % cell viability for different time points (0, 24, 48 and 72 h) versus 0 µg/ml, 10 µg/ml, 25 µg/ml, 50 µg/ml, 100 µg/ml, 250 µg/ml, 500 µg/ml *Rheum ribes* extracts concentrations 3D column graph were constructed (Figure 3.18,19,20). The IC<sub>50</sub> values were determined using GraphPad Prism version 5 for Mac OS X as shown in Table 3.9.

In the Figure 3.17 96-well microtiter plate prepared for use in the XTT assay was shown at the end of 5 h incubation time at 37 °C. A representative 96-well microtiter plate, indicating concentrations of plant extracts was shown in Appendix D.



**Figure 3.17** 96-well microtiter plate prepared for use in the XTT assay. A representative 96-well microtiter plate, indicating concentrations of plant extracts was shown in Appendix D.

As it was mentioned before, *Rheum ribes* had absorbance values at around 415 nm at which XTT measurements were done and absorbance values increased as the extract concentrations increased. In order to prevent interference by *Rheum ribes* extracts, blank wells that were seen in Appendix D were subtracted from sample wells.

Beside *Rheum ribes*'s spectral interference, there was another important reason of *Rheum ribes* to cause misinterpretation of the results with XTT assay. Botanical extracts and chemicals in them have the ability to reduce tetrazolium salt MTT, and denser color formed because of this additional reduction might be supposed as if there were higher metabolically active cells (Shoemaker et al., 2004). One of the plant species used in the study was *Rheum palmatum* that was in the same genus of *Rheum ribes*. In order to prevent misinterpretations, it is advisable to use *Rheum ribes* blanks and subtract them from samples or it is better to count cells with trypan blue when studying with colorful, botanical chemicals.

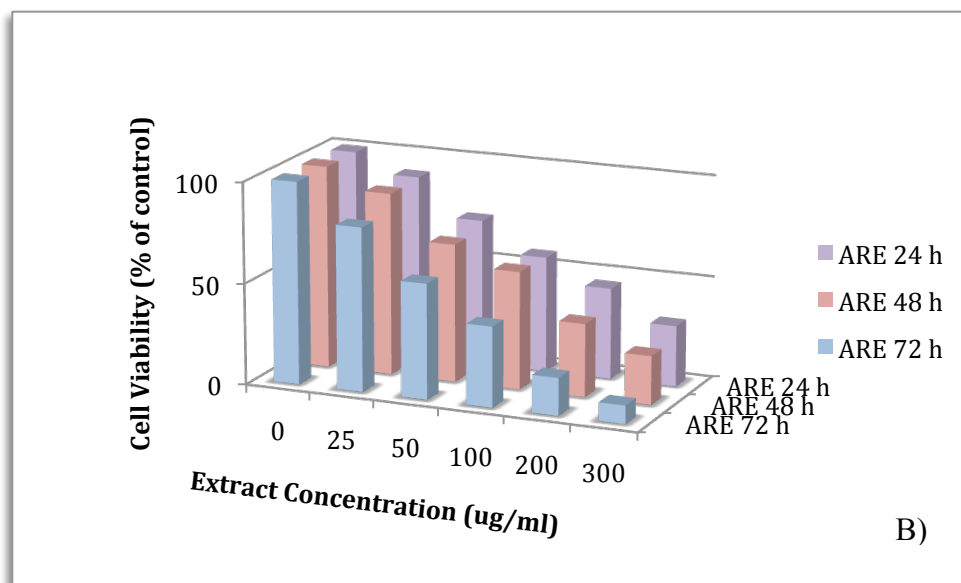
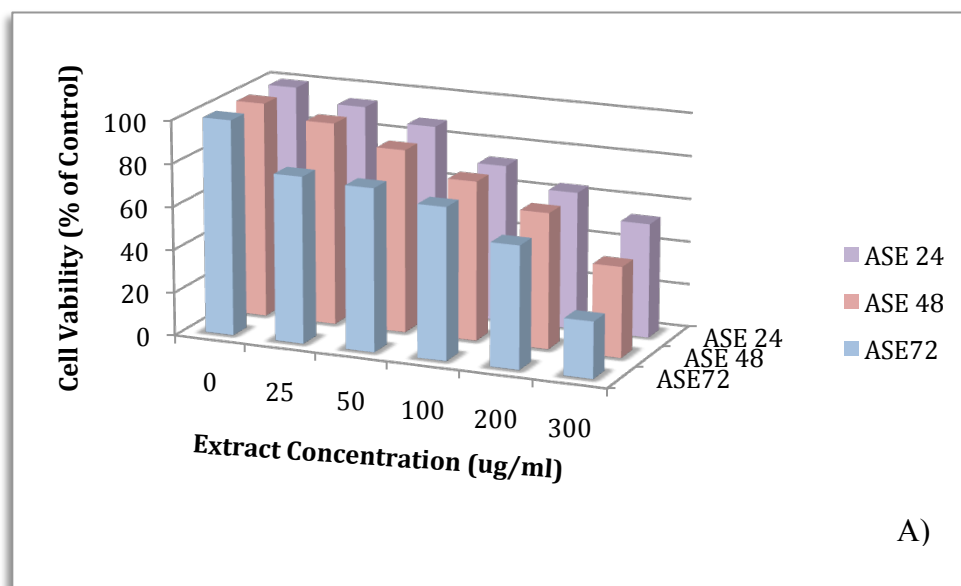


**Figure 3.18** Effects of *Rheum ribes* shoot (A) and root (B) ethyl acetate extract on cell survival in HL-60 cells. Cytotoxicity was measured by the XTT assay. HL-60 cells were precultured in 96-well microplates for overnight and then incubated with 0- 300  $\mu\text{g/ml}$  of *Rheum ribes* shoot (A) and root (B) ethyl acetate extract for 24, 48 and 72 hr. The percentage of cell growth in the control group was designated as 100%.

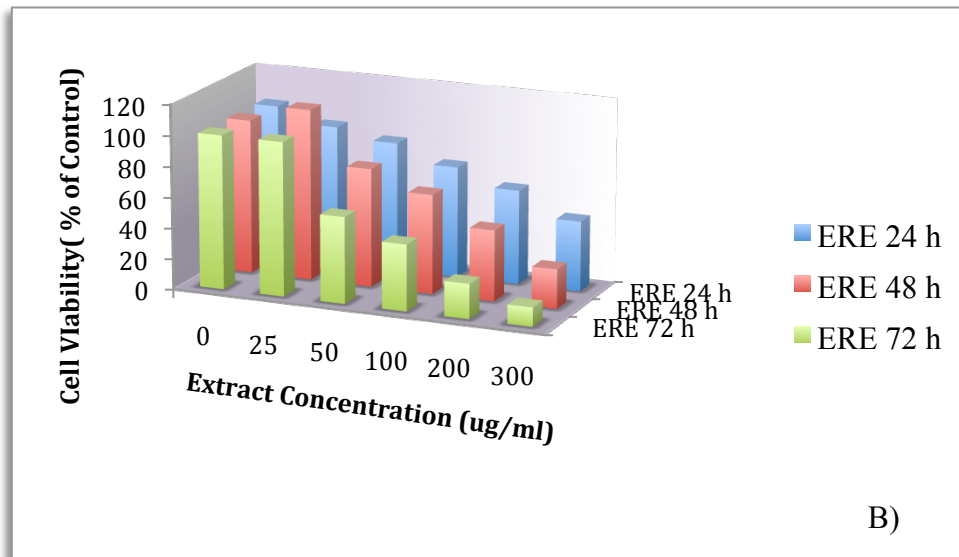
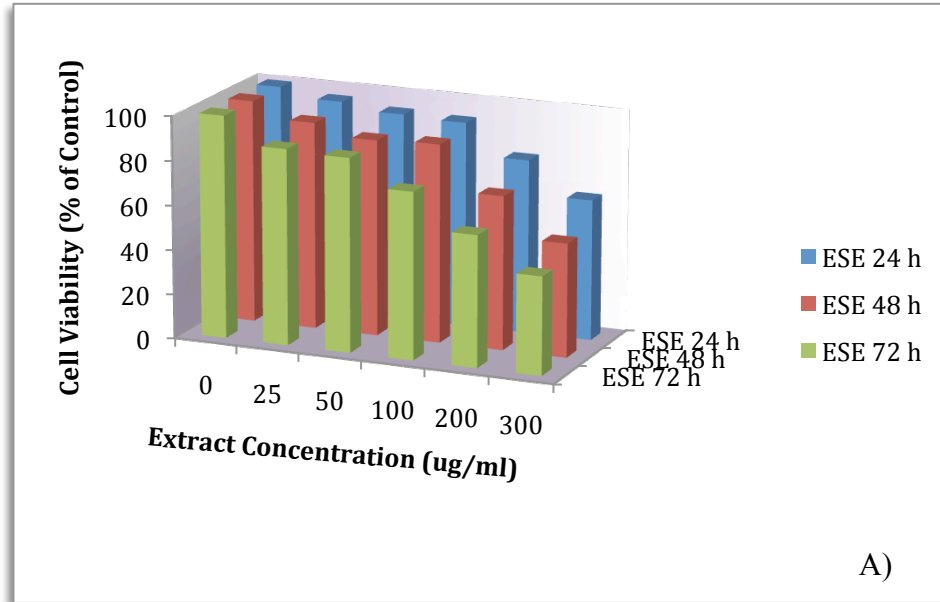


**Figure 3.19** Effects of *Rheum ribes* shoot (A) and root (B) ethanol extract on cell survival in HL-60 cells. Cytotoxicity was measured by the XTT assay. HL-60 cells were precultured in 96-well microplates for overnight and then incubated with 0- 300  $\mu\text{g/ml}$  of *Rheum ribes* shoot (A) and root (B) ethanol extract for 24, 48 and 72 hr. The percentage of cell growth in the control group was designated as 100%.

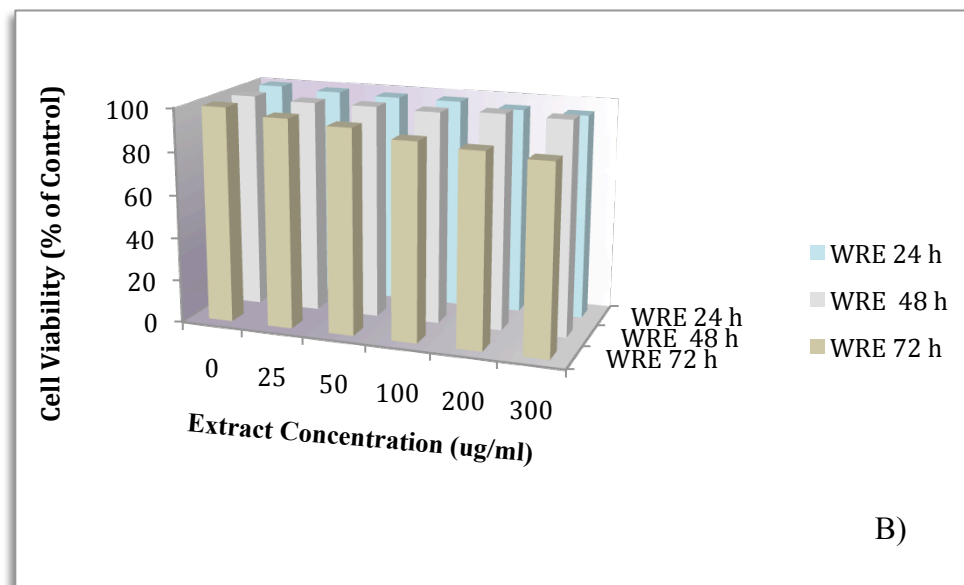
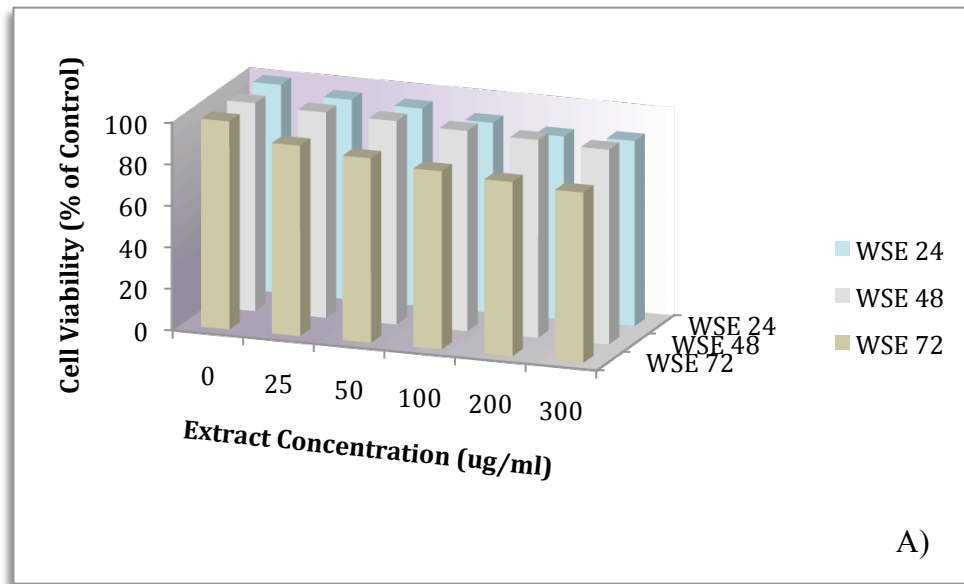


**Figure 3.20** Effects of *Rheum ribes* shoot (A) and root (B) aqueous extract on cell survival in HL-60 cells. Cytotoxicity was measured by the XTT assay. HL-60 cells were precultured in 96-well microplates for overnight and then incubated with 0- 300  $\mu\text{g/ml}$  of *Rheum ribes* shoot (A) and root (B) aqueous extract for 24, 48 and 72 hr. The percentage of cell growth in the control group was designated as 100%.

**Table 3.8** IC<sub>50</sub> values and % Viability in HL-60 cells obtained with XTT Assay after treatment of *Rheum ribes* extracts for 24, 48 and 72 h.

Parameter	Incubation time (h)					
	24		48		72	
Extracts	IC50 (µg/mL)	% viability*	IC50 (µg/mL)	% viability*	IC50 (µg/mL)	% viability*
ASE	NA	53	NA	42	203	
ARE	149		135		74	
ESE	NA	63	NA	51	NA	44
ERE	NA		159		76	
WSE	NA	93	NA	89	NA	81
WRE	NA	95	NA	98	NA	86

IC<sub>50</sub> values that were the *Rheum ribes* extracts concentrations at which 50% of cells are viable were calculated as 288 µg/ml, 252 µg/ml and 192 µg/ml after ASE treatment for 24,48 and 72 h, respectively. The results were not statistically significant for all time points. ASE had growth inhibitory effects, however ASE cytotoxicity was not occurred at a time dependent manner in HL-60 cells.

IC<sub>50</sub> values were calculated as 177 µg/ml, 159 µg/ml and 76 µg/ml after ARE treatment for 24, 48 and 72 h, respectively. The results were not statistically significant for 24 and 48 h, however for 72 cell viability dropped dramatically.

These results showed that the difference between the IC<sub>50</sub> values of ASE and ARE in HL-60 cells was statistically significant, p<0.05 and the growth inhibitory effect of ARE was higher than ASE in HL-60 cells for all time points, because the amount of extract concentration required to inhibit 50% metabolic activity of the cells were significantly low.

IC<sub>50</sub> values were calculated as 417 µg/ml, 310 µg/ml and 253 µg/ml after ESE treatment and 251 µg/ml, 183 µg/ml and 74 µg/ml after ERE treatment for 24, 48 and 72 h, respectively. These results showed that ERE was more effective than ESE to inhibit the HL-60 cell metabolic activity. It could be also concluded that ESE did not have any growth inhibition effect at a time dependent manner at these concentrations, however ERE did.

50 % inhibition could not be observed in WSE and WRE treatments because even though 300 µg/ml extracts applied, more than 50 % cells were remained still metabolically active. However, there was still a decrease in cell number in a dose and time dependent manner that was not statistically significant. At this point, 500 µg/ml was the highest concentration to apply, however for flow cytometric analysis higher concentrations were checked to define the exact concentration of aqueous extracts to inactivate the cells metabolism. These will be covered in Section 3.8 part of results.

Also, ARE had the highest potential among all extracts with lower IC<sub>50</sub> for all time points except for 72 h because ERE had the same IC<sub>50</sub> value as ARE for 72 h.

**Table 3.9** Comparison of IC<sub>50</sub> values in HL-60 cells obtained by TBE and XTT Assay after treatment of *Rheum ribes* for 24, 48 and 72 h.

Parameter	IC <sub>50</sub> (µg/mL) (TBE)			IC <sub>50</sub> (µg/mL) (XTT)		
	Incubation time (h)			Incubation time (h)		
<b>Extracts</b>	24	48	72	24	48	72
<b>ASE</b>	NA	100	76	NA	NA	192
<b>ARE</b>	75	56	50	149	135	74
<b>ESE</b>	NA	NA	NA	NA	NA	NA
<b>ERE</b>	125	100	50	NA	183	76
<b>WSE</b>	NA	NA	NA	NA	NA	NA
<b>WRE</b>	NA	NA	NA	NA	NA	NA

When we compare the IC<sub>50</sub> values obtained from both trypan blue viable cell counting and XTT assay, it was concluded that IC<sub>50</sub> results were higher in XTT assay. This might be because of the indirect implication of values from their metabolic activity.

According to the criteria established by the U.S. National Cancer Institute (NCI), the compounds with IC<sub>50</sub> < 30 µg/mL, 30 µg/mL < IC<sub>50</sub> < 100 µg/mL and IC<sub>50</sub> > 100 µg/mL are judged as active, moderately active and inactive, respectively (Suffness, 1990). Among all extracts, ASE, ARE and ERE exhibited the highest activity and showed moderate cytotoxicity with IC<sub>50</sub> (calculated from TBA assay) < 100 µg/mL that fall within the NCI criteria. Other extracts showed some cytotoxicity, however those were judged as inactive according to NCI criterion for 72 h.

Rhein is an anthraquinone compound existing in Rheum species, have been shown to induce apoptosis in HL-60 cells with an efficacious condition at 100 µM, 6 h.

### **3.8 *Rheum ribes* Shoot and Root Extracts Induces Apoptotic Cell Death**

#### ***3.8.1 Changes in cell size and granularity***

A further method for detection of alteration in cell morphology was flow cytometry analysis of cell size and granularity. Changes in light scatter, i.e. a decrease in forward scatter (FSC) as a sign of lower cell size and an increase in side scatter (SSC) as a sign of granularity compared to control cells, are characteristic for cells dying of apoptosis.

Flow cytometric analyses were performed on aFACScalibur flow cytometer (Becton Dickinson, San Jose, CA, USA) using the CellQuest software for acquisition and analysis. The light-scatter channels were set on linear gains and a minimum of 50,000 cells being analyzed.

Two representative dot plots of untreated, 0.1 % DMSO as control; etoposide and sodium azide as positive control of apoptosis and necrosis, respectively depicted in Figure 3.21.

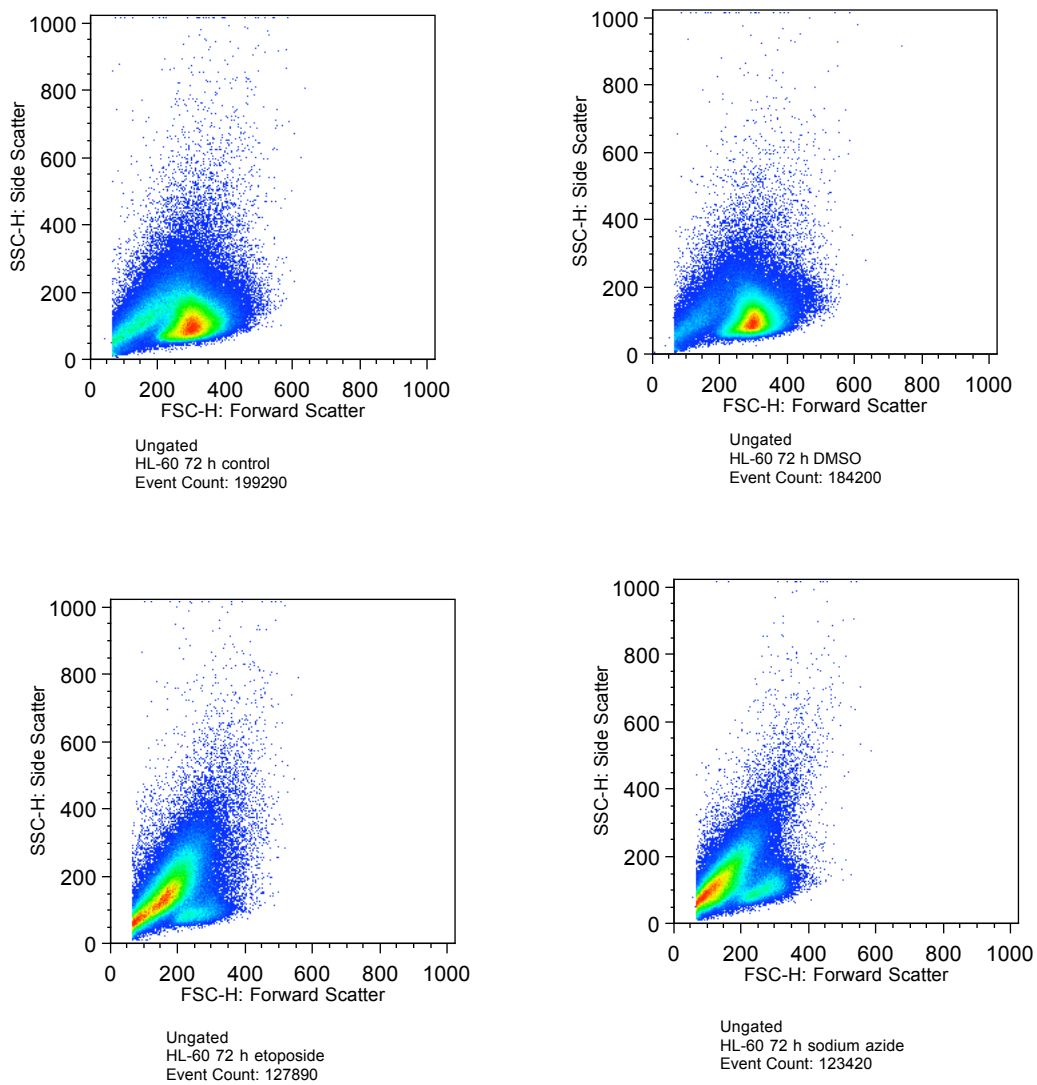


**Figure 3.21** Etoposide and Sodium azide stimulated HL-60 cells exhibit characteristic morphological apoptotic features

Dot plot of untreated and 0.1 % DMSO treated HL-60 cells exhibiting almost uniform cell size and granularity (upper panels); characteristic dot plot of apoptotic cells after *etoposide* and sodium azide treatment (bottom panel): occurrence of a second population of apoptotic cells in the range of lower FSC and similar or higher SSC compared to control cells. Measurement was carried out by flow cytometry as described under “Materials and Methods”

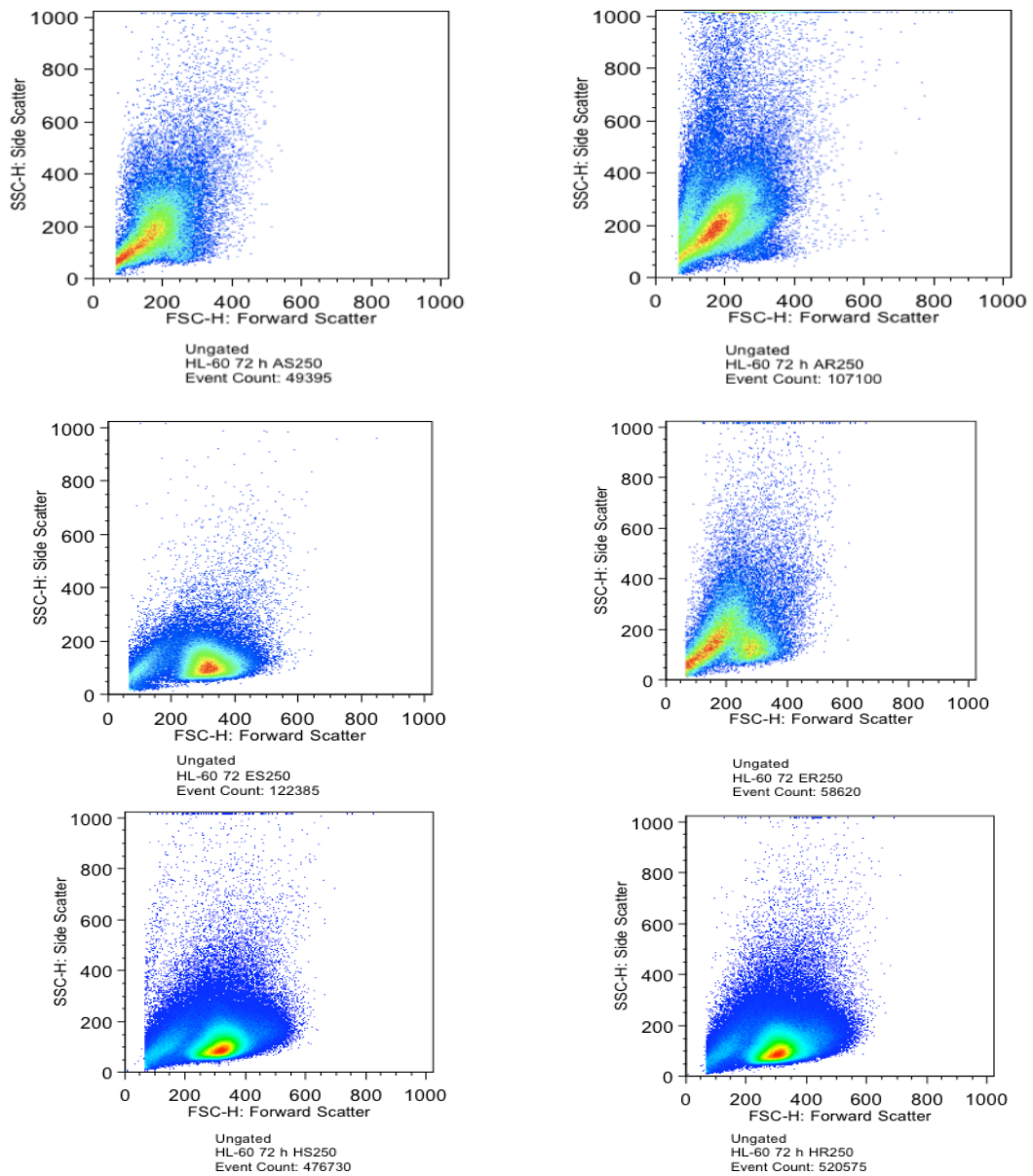


**Figure 3.22** Rheum ribes-treated HL-60 cells exhibit characteristic morphological apoptotic features for 72 h.

As shown in Figures 3.22, flow cytometric analyses revealed significant morphological changes of 250 µg/mL ASE, ARE, ERE in HL-60 cells for 72 h. The decrease in cell size observed in apoptosis led to lower forward scatter values while an increase in granularity was visualized in the dot plot as higher sideward scatter values.

Light microscopy combined with flow cytometry visualized the occurrence of the characteristic cell shrinkage (shift of the cell cloud to the left in FSC) and an augmentation of cellular granularity (shift of the cell cloud towards the top), means formation of apoptotic bodies in response to *Rheum ribes* treatment.

### ***3.8.2 Detection of phosphatidylserine translocated to the cell surface***

Alterations of the cell membrane, namely translocation of phosphatidyl-serine to the outer cell membrane was detectable by flow cytometry using Annexin V-apc. Co-staining with 7AAD allowed to clearly exclude necrotic cell death.

In this study, it was showed that after cells were stimulated by etoposide , sodium azide and *Rheum ribes* extracts, through staining cells with annexin V-apc and 7AAD, it is possible to detect live, nonapoptotic cells (annexin V/7AAD double negative), early apoptotic cells (annexin V single positive), and late apoptotic or necrotic cells (annexin V/7AAD double positive) by flow cytometry.

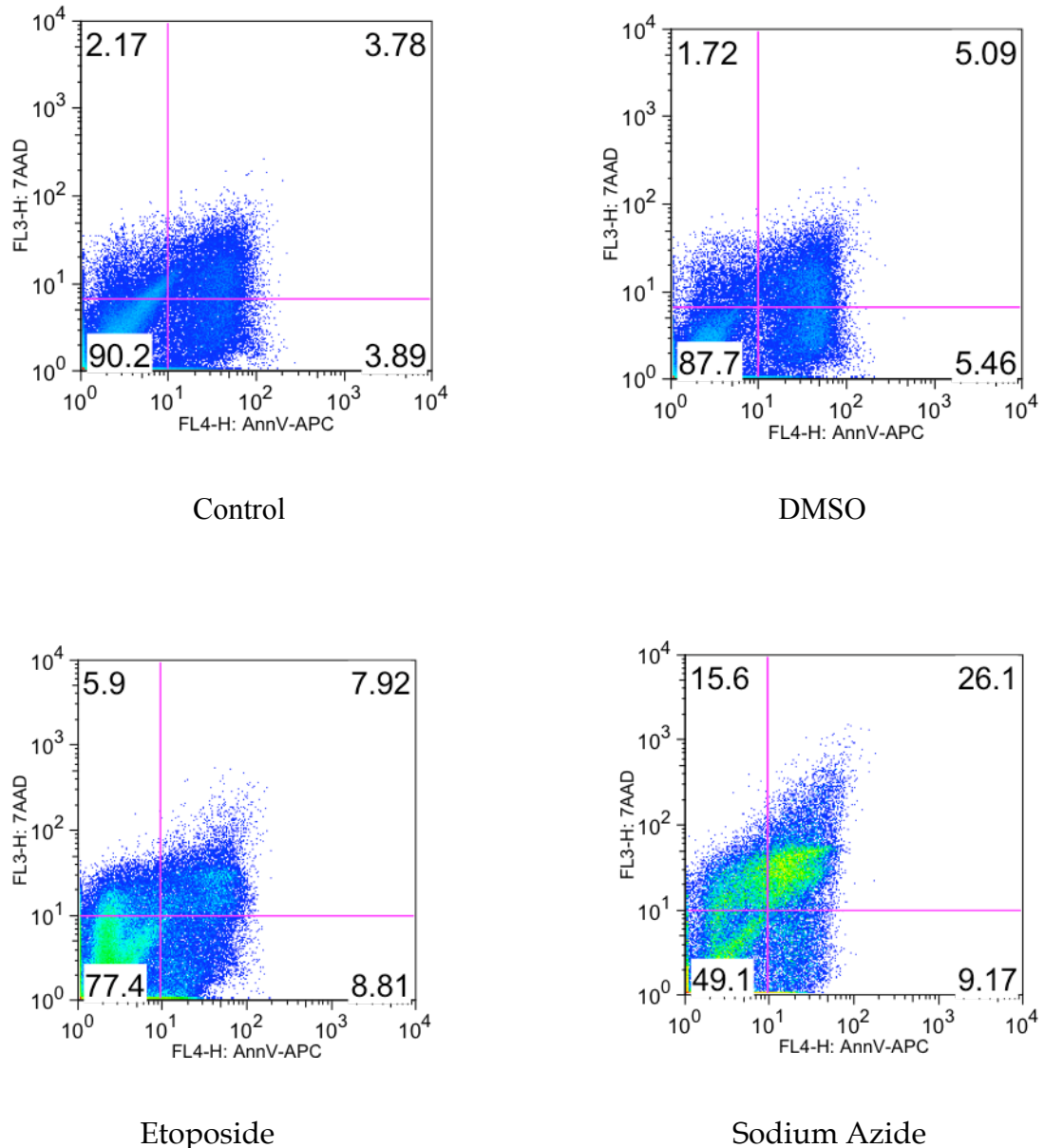


**Figure 3.23** Etoposide and Sodium azide induced translocation of phosphatidylserine to the outer cell membrane in HL-60 cells. FACS analysis of either untreated or 0.1 % DMSO treated for 72 h (upper panel) etoposide (68  $\mu$ M) and sodium azide (0.02% w/v) stimulated cells (18 h; lower panel) after staining with Annexin V-*apc* (FL-4) and 7AAD (FL-3): cells appearing in the lower right quadrant show positive Annexin V-*apc* staining, which indicates phosphatidylserine translocation to the cell surface, and no DNA staining with 7AAD, demonstrating intact cell membranes, both features of early apoptosis. Necrotic or late apoptotic cells would appear in the upper right quadrant: Annexin V-FITC- and 7AAD-positive. The figure shows representative histograms out of three independent experiments.

*Rheum ribes* treatment led to the exposure of phosphatidylserine (PS) on the outside of the plasma membrane, a characteristic event in early stages of apoptosis, detected by Annexin V-apc staining and FACS analysis (Fig 3.23). Co-staining with 7AAD allowed discrimination between apoptotic and necrotic cells.

As shown in Figure 3.24 exposures of HL-60 cells to 250 µg/ml ASE and ARE for 72 h resulted in a shift of 40.2 % and 81.5 %, respectively of the cell population from normal to the early/late apoptotic/necrotic stage.

As shown in Figure 3.24 exposures of HL-60 cells to 250 µg/ml ESE and ERE for 72 h resulted in a shift of 11.6 % and 65.4 %, respectively of the cell population from normal to the early/late apoptotic/necrotic stage.

As shown in Figure 3.24 exposures of HL-60 cells to 1000 µg/ml WSE and WRE for 72 h resulted in a shift of 68 % and 14.6 %, respectively of the cell population from normal to the early/late apoptotic/necrotic stage.

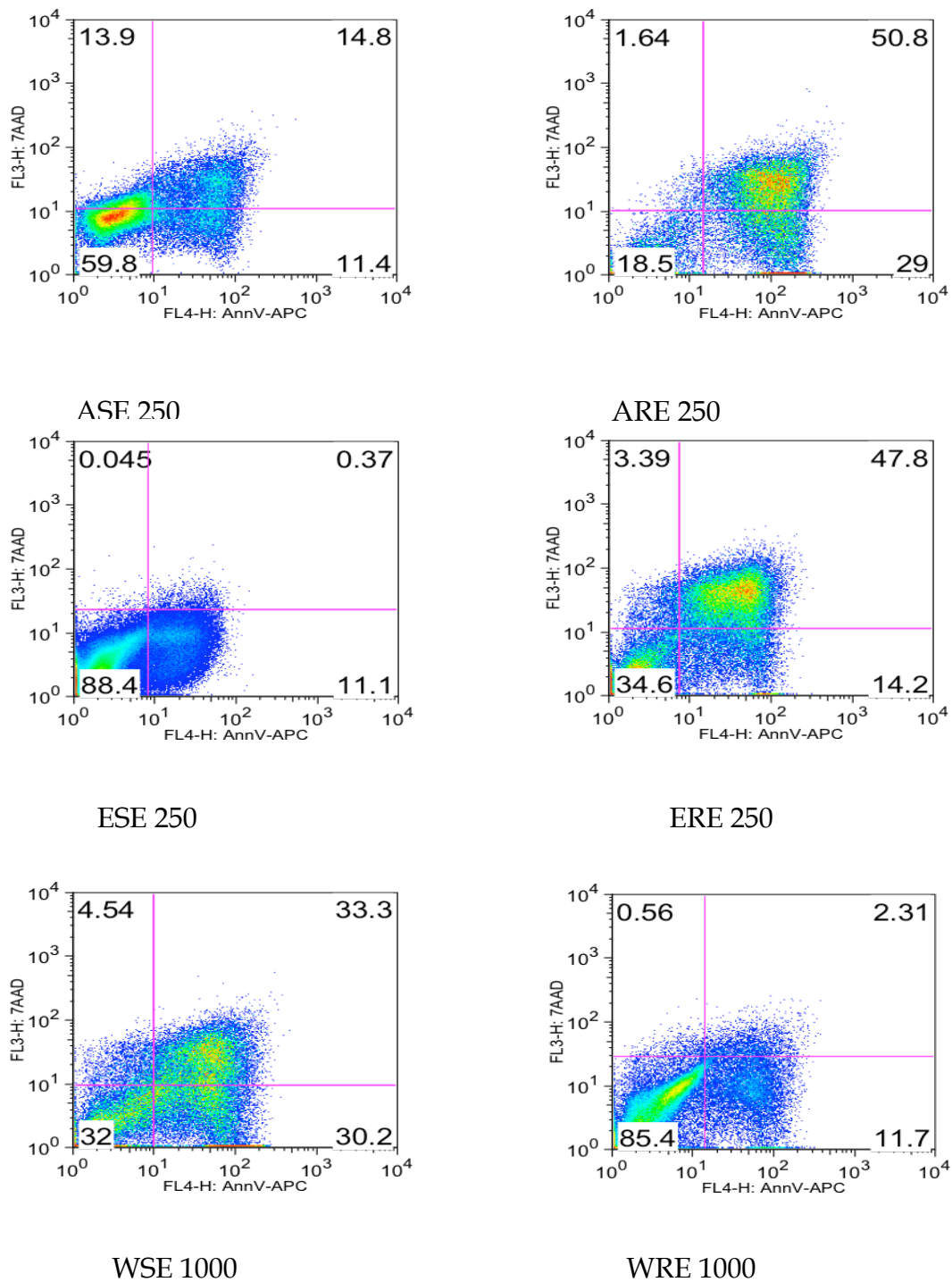


**Figure 3.24** *Rheum ribes* induced translocation of phosphatidylserine to the outer cell membrane in HL-60 cells . FACS analysis of either 250  $\mu\text{g}/\text{mL}$  ASE, ARE, ESE and ERE or 1000  $\mu\text{g}/\text{mL}$  WSE and WRE treated cells (72 h) after staining with Annexin V-apc (FL-4) and 7AAD (FL-3). The figure shows representative histograms out of three independent experiments.

### ***3.8.3 Dose and time kinetics for Rheum ribes induction of apoptosis***

To investigate whether there were differences of induction of apoptosis by different extraction of *Rheum ribes* in dose and time dependent manner, HL-60 cells were treated with 10, 25, 50, 100, 250 and 500 µg/mL of *Rheum ribes* for different time points (24, 48 and 72 h). All conditions were performed in triplicate. The cells were dual-stained with annexin V-apc and 7AAD and analyzed by flow cytometry. Cells treated with 0.1 % DMSO was used as control.

These results demonstrated that there was a time-dependent fashion in annexin V/7AAD double positive cells induced by ASE and ARE as shown in Table 3.11, 12 and Figure 3.25, 26. At 24, 48 and 72 hours, the observed maximal apoptosis for ASE at the maximal concentration, 250 µg/ml, was about 25%, 35 % and 42%, respectively. In contrast, at same time points, the observed maximal apoptosis ARE at their maximal concentration (500µg/ml) was more than 91%. Apoptosis in response to ARE was early, whereas apoptosis in response to ASE was significantly late.

In apoptosis induced by ASE for 72 h, PS externalization occurred as the same time as disruption of membrane integrity whereas for 24 h, PS externalization was an early event. This was a result of presence of early and late apoptotic components in the ASE.

The apoptosis induced by ARE of 10-50 µg/ml for 24, 48 and 72 h was dominantly PS externalization, however for all time point of higher concentration 100-500 µg/ml, dominant cell death was late apoptosis or necrosis which was a result of disruption of membrane integrity. This result showed that the components found in ARE were generally shown characteristics of early apoptotic agents.

**Table 3.10** Percents of Typical Quadrant Analysis of Annexin V-apc/7AAD Flow Cytometry of HL-60 Cells Treated with ASE for 24, 48 and 72 h

<b>Time</b>	<b>Extracts</b>	<b>% Viability</b>	<b>% Early apop</b>	<b>% Late Apop</b>	<b>% death</b>
<b>24 h</b>	<b>DMSO</b>	94.1	4.48	0.94	0.49
	<b>ASE 10</b>	86.8	11.6	1.38	0.31
	<b>ASE 25</b>	85.3	12.3	1.9	0.44
	<b>ASE 50</b>	85.6	12.1	1.97	0.32
	<b>ASE 100</b>	85.3	12.4	1.9	0.34
	<b>ASE 250</b>	84.5	10.9	3.59	1.01
<b>48 h</b>	<b>DMSO</b>	94.5	1.8	0.68	3.07
	<b>ASE 10</b>	95	1.91	0.75	2.33
	<b>ASE 25</b>	95.4	2.22	0.75	1.65
	<b>ASE 50</b>	94.7	2.15	1.06	2.13
	<b>ASE 100</b>	93.8	2.19	1.55	2.49
	<b>ASE 250</b>	74	1.25	4.07	20.07
<b>72</b>	<b>DMSO</b>	94.1	4.48	0.94	0.49
	<b>ASE 10</b>	90.1	7.58	1.99	0.29
	<b>ASE 25</b>	90.7	6.89	2.52	0.37
	<b>ASE 50</b>	90	6.86	2.52	0.62
	<b>ASE 100</b>	85.7	8.91	4.48	0.89
	<b>ASE 250</b>	59.8	11.4	14.8	13.9

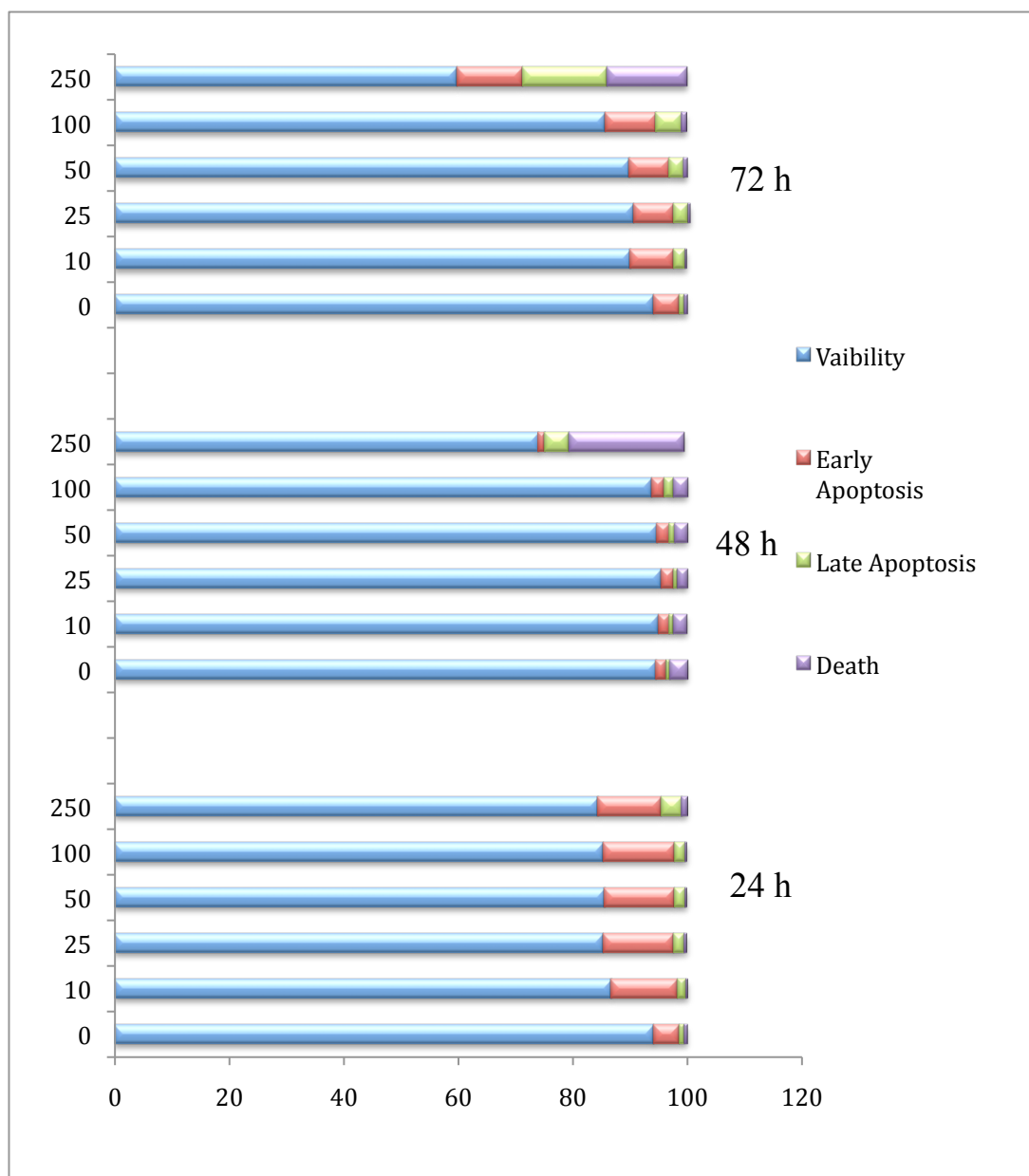


**Figure 3.25** ASE induced apoptosis in a different time and dose fasion. Percents of Typical Quadrant Analysis of Annexin V-apc/7AAD Flow Cytometry of HL-60 Cells Treated with ASE for 24, 48 and 72 h

**Table 3.11** Percents of Typical Quadrant Analysis of Annexin V-apc/7AAD Flow Cytometry of HL-60 Cells Treated with ARE for 24, 48 and 72 h

<b>Time</b>	<b>Extracts</b>	<b>% Viability</b>	<b>% Early apop</b>	<b>% Late Apop</b>	<b>% death</b>
<b>24 h</b>	<b>DMSO</b>	85.6	5.84	2.55	6.05
	<b>ARE 10</b>	83.6	13.2	2.36	0.78
	<b>ARE 25</b>	79.7	15	3.98	1.34
	<b>ARE 50</b>	78.5	14.9	5.05	1.56
	<b>ARE 100</b>	57.7	25.7	13.5	3.1
	<b>ARE 250</b>	58	18.3	20	3.67
	<b>ARE 500</b>	24.1	24	47.7	4.2
<b>48 h</b>	<b>DMSO</b>	91.6	5.23	1.18	1.95
	<b>ARE 10</b>	89.8	6.62	2.13	1.47
	<b>ARE 25</b>	88.5	6.94	2.53	1.99
	<b>ARE 50</b>	87.9	6.57	3.36	2.19
	<b>ARE 100</b>	72.1	7.92	11.5	8.46
	<b>ARE 250</b>	36.9	10.4	29.8	22.8
	<b>ARE 500</b>	28.6	10.8	40.7	19.9
<b>72</b>	<b>DMSO</b>	86.5	10.3	2.7	1.08
	<b>ARE 10</b>	81.6	14.2	4.02	0.18
	<b>ARE 25</b>	81.2	16.2	4.36	0.29
	<b>ARE 50</b>	77.8	16.2	5.7	0.38
	<b>ARE 100</b>	51.9	24.2	22.5	1.36
	<b>ARE 250</b>	18.5	29	50.8	1.64
	<b>ARE 500</b>	9.04	23.1	66.3	1.56

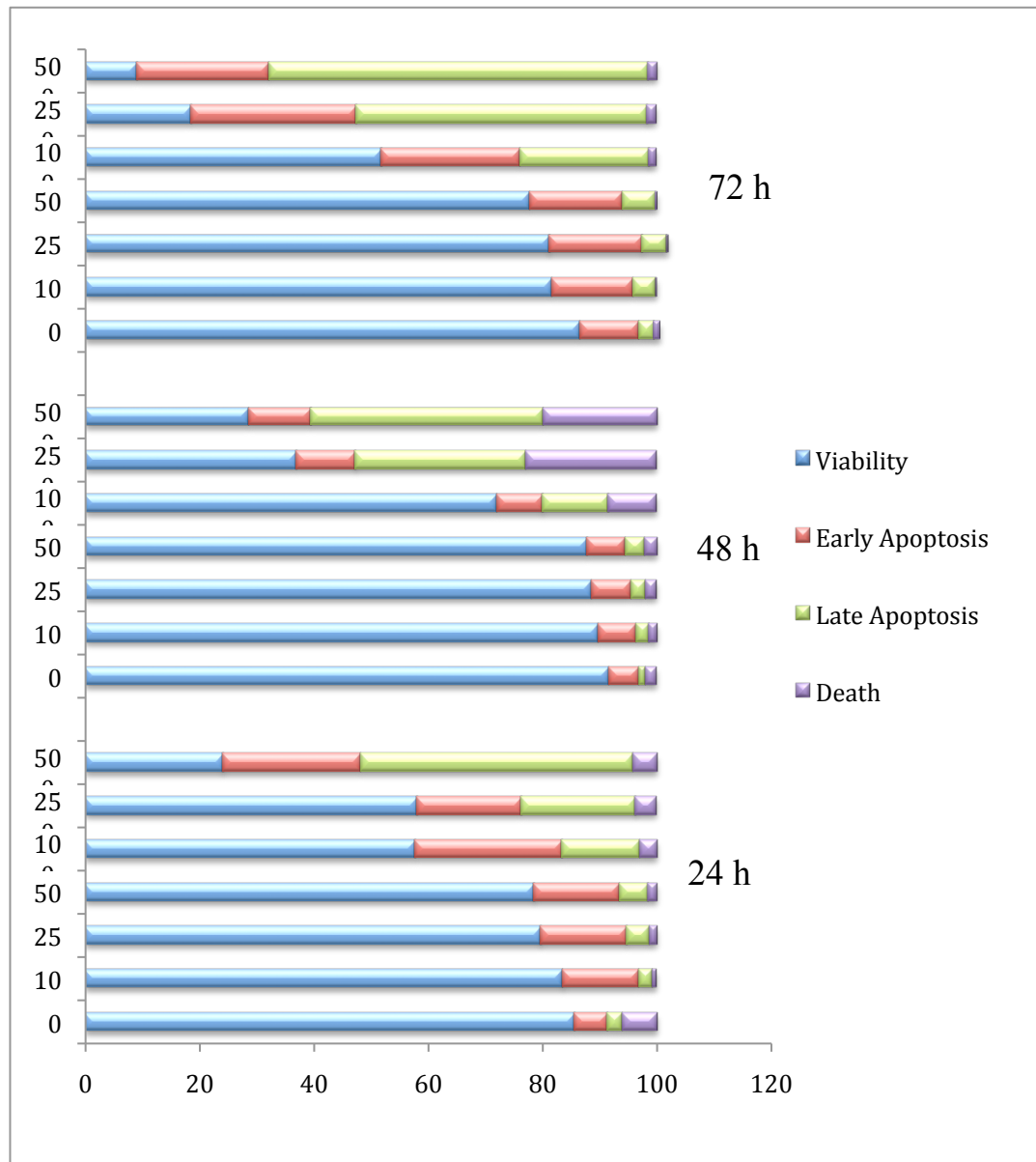


**Figure 3.26** ARE induced apoptosis in a different time and dose fashion. Percents of Typical Quadrant Analysis of Annexin V-apc/7AAD Flow Cytometry of HL-60 Cells Treated with ARE for 24, 48 and 72 h

At 24, 48 and 72 hours, the observed maximal apoptosis for ESE at the maximal concentration, 500 µg/ml, was about about 15 % as shown in Table 3.13 and Figure 3.22. The results showed that there was no significant dose or time dependent cell death upon exposure to ESE.

These results demonstrated that there was a dose and time-dependent fashion in annexin V/7ADD double positive cells induced by ERE as shown in Table 3.14 and Figure 3.23. At 24, 48 and 72 hours, the observed maximal apoptosis for ERE at the maximal concentration, 500 µg/ml, was about 53%, 63 % and 88%, respectively.

In apoptosis induced by ERE for all time points, PS externalization occurred as the same time as disruption of membrane integrity. This was a result of presence of early apoptotic components in the ERE.

The apoptosis induced by ERE of 10-100 µg/ml for 24, 48 and 72 h was dominantly PS externalization, however for all time points of higher concentrations 250 and 500 µg/ml, dominant cell death was late apoptosis or necrosis which was a result of disruption of membrane integrity. This result showed that the components found in ERE were generally shown characteristics of early apoptotic agents.

**Table 3.12** Percents of Typical Quadrant Analysis of Annexin V-apc/7AAD Flow Cytometry of HL-60 Cells Treated with ESE for 24, 48 and 72 h

Hours	Extracts	% Viability	% Early apop	% Late Apop	% death
<b>24 h</b>	<b>DMSO</b>	81.8	14.7	2.98	0.58
	<b>ESE 10</b>	81.7	15.9	2.07	0.35
	<b>ESE 25</b>	83.8	13.9	1.79	0.47
	<b>ESE 50</b>	82.4	14.7	2.4	0.45
	<b>ESE 100</b>	81.6	15.7	2.27	0.41
	<b>ESE 250</b>	83.3	13.6	2.71	0.4
	<b>ESE 500</b>	83.8	12.4	3.41	0.37
<b>48 h</b>	<b>DMSO</b>	94.6	2.56	0.67	2.18
	<b>ESE 10</b>	94	3.71	0.83	1.45
	<b>ESE 25</b>	94.2	3.65	0.81	1.37
	<b>ESE 50</b>	93.5	3.61	0.92	1.94
	<b>ESE 100</b>	93.9	3.5	1.01	1.56
	<b>ESE 250</b>	90.6	3.69	2.09	3.62
	<b>ESE 500</b>	86.5	2.85	3.29	7.31
<b>72</b>	<b>DMSO</b>	85	12.1	2.32	0.57
	<b>ESE 10</b>	89	9.77	1.08	0.1
	<b>ESE 25</b>	89.9	9.11	0.86	0.11
	<b>ESE 50</b>	88	10.7	1.16	0.11
	<b>ESE 100</b>	89.6	9.01	1.22	0.13
	<b>ESE 250</b>	88.9	9.08	1.87	0.17
	<b>ESE 500</b>	88.2	8.72	2.69	0.41

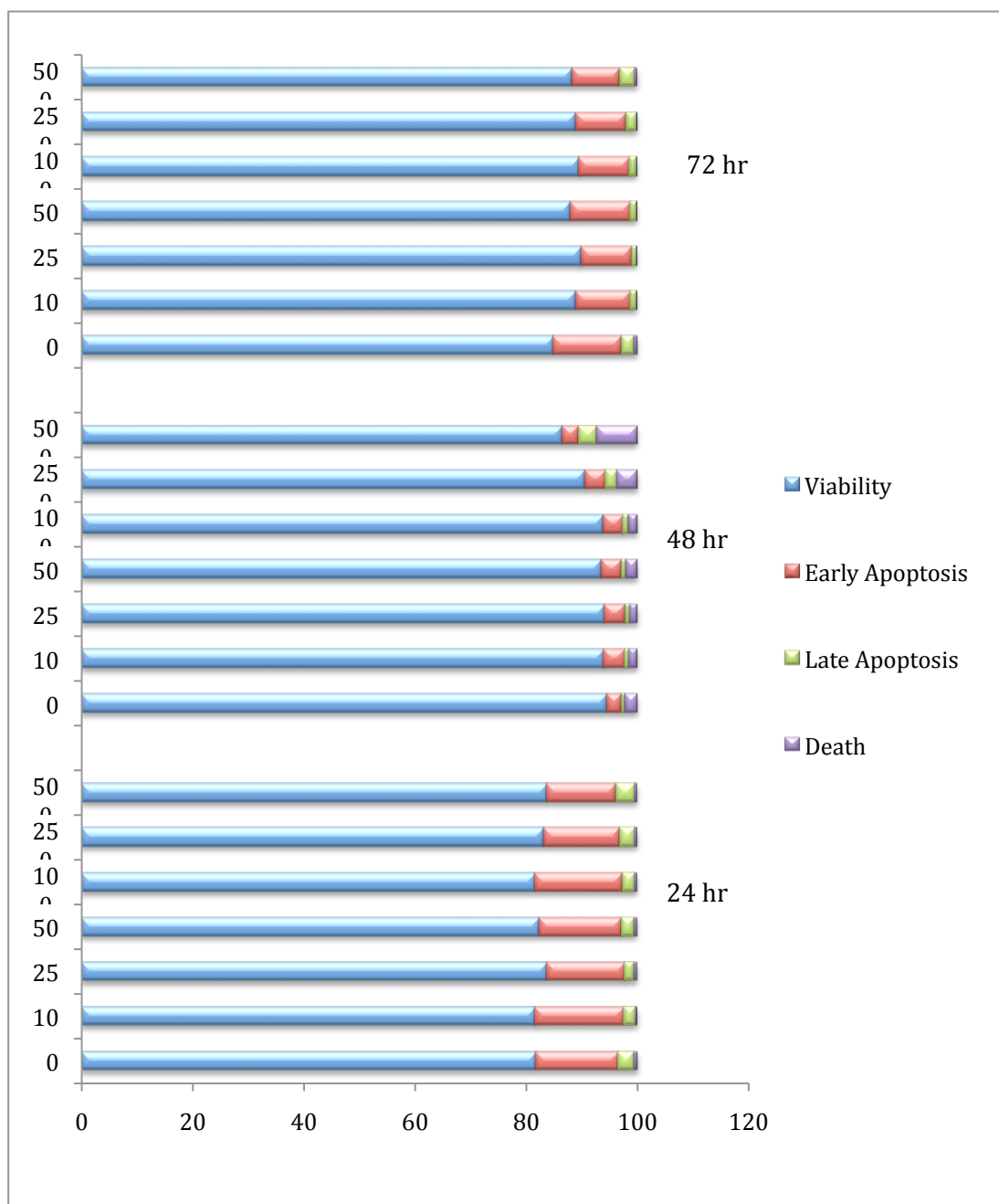


**Figure 3.27** ESE induced apoptosis in a different time and dose fashion. Percents of Typical Quadrant Analysis of Annexin V-apc/7AAD Flow Cytometry of HL-60 Cells Treated with ESE for 24, 48 and 72 h

**Table 3.13** Percents of Typical Quadrant Analysis of Annexin V-apc/7AAD Flow Cytometry of HL-60 Cells Treated with ERE for 24, 48 and 72 h

hours	Extracts	Viability	Early apop	Late Apop	death
<b>24 h</b>	<b>DMSO</b>	80.5	12.5	5.53	1.46
	<b>ERE 10</b>	81.8	10	6.25	1.89
	<b>ERE 25</b>	79.1	10.6	8.07	2.15
	<b>ERE 50</b>	75.1	11.3	10.9	2.7
	<b>ERE 100</b>	70.3	10.3	15.6	3.84
	<b>ERE 250</b>	66.5	8.74	19.3	5.47
	<b>ERE 500</b>	47.8	10.3	35.3	6.63
<b>48 h</b>	<b>DMSO</b>	89.3	9.03	0.88	0.78
	<b>ERE 10</b>	86.3	11.2	1.67	0.8
	<b>ERE 25</b>	85.3	11.2	2.46	1.01
	<b>ERE 50</b>	81.8	11.9	4.47	1.83
	<b>ERE 100</b>	70.6	14.2	9.95	5.28
	<b>ERE 250</b>	49.4	18.9	20.6	11.2
	<b>ERE 500</b>	36.2	21.1	27.5	15.2
<b>72</b>	<b>DMSO</b>	87.7	5.46	5.09	1.72
	<b>ERE 10</b>	80.7	12.5	6.37	0.49
	<b>ERE 25</b>	74.4	14.5	10.2	0.9
	<b>ERE 50</b>	68.7	14.7	15.3	1.34
	<b>ERE 100</b>	51	14.9	31.4	2.67
	<b>ERE 250</b>	34.6	14.2	47.8	3.39
	<b>ERE 500</b>	12.6	15.5	69.6	2.36

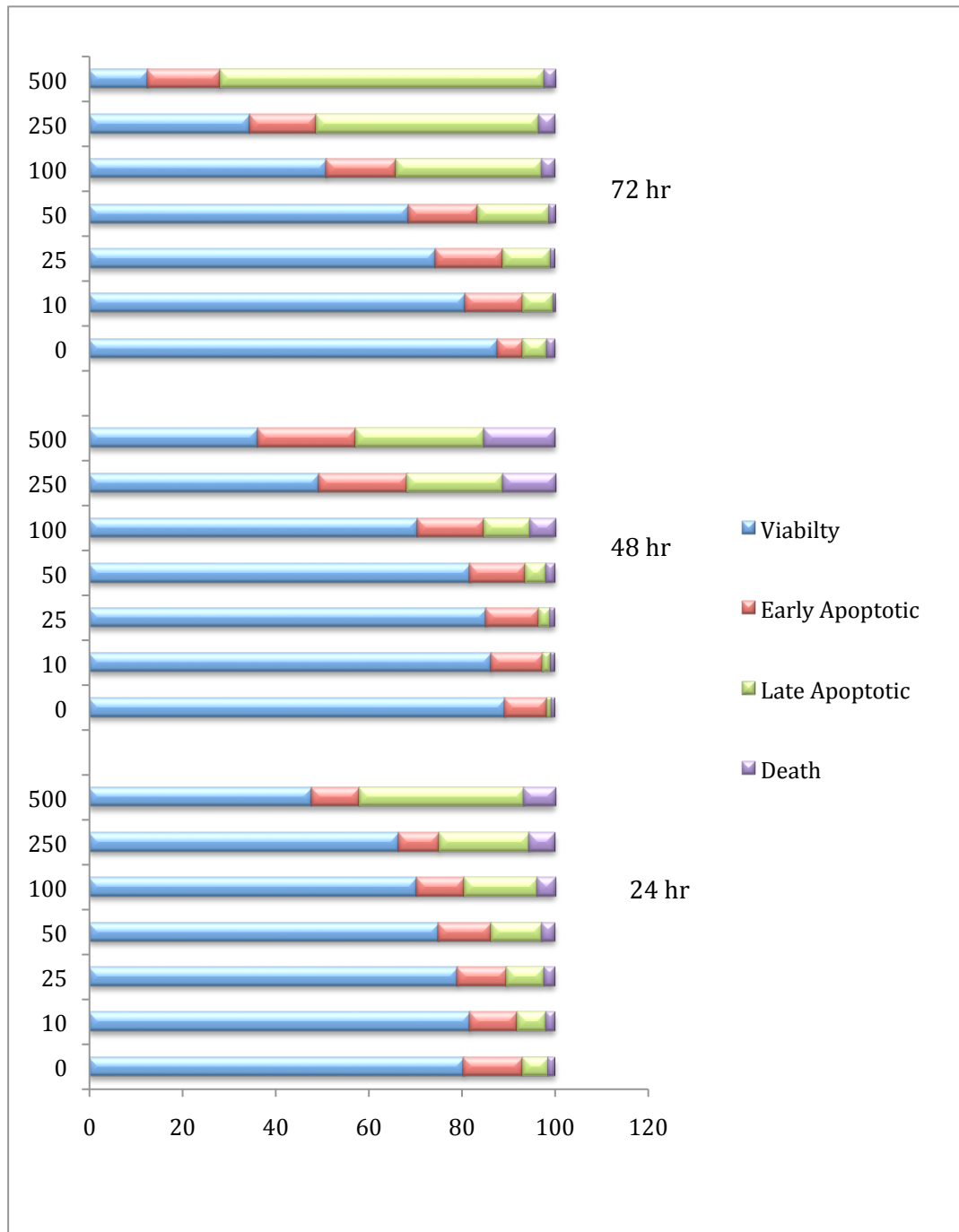


**Figure 3.28** ERE induced apoptosis in a different time and dose fashion. Percents of Typical Quadrant Analysis of Annexin V-apc/7AAD Flow Cytometry of HL-60 Cells Treated with ERE for 24, 48 and 72 h

**Table 3.14** Percents of Typical Quadrant Analysis of Annexin V-apc/7AAD Flow Cytometry of HL-60 Cells Treated with WSE for 72 h

hours	Extracts	Viability	Early apop	Late Apop	death
<b>72</b>	<b>DMSO</b>	87.8	9.23	2.43	0.51
	<b>WSE 100</b>	84	11.4	3.85	0.76
	<b>WSE 500</b>	76.4	13.1	8.34	2.19
	<b>WSE 1000</b>	32	30.2	33.3	4.54
	<b>WSE 2000</b>	40.4	25.7	29.5	4.39
	<b>WSE 5000</b>	15.4	25.8	56.6	2.14

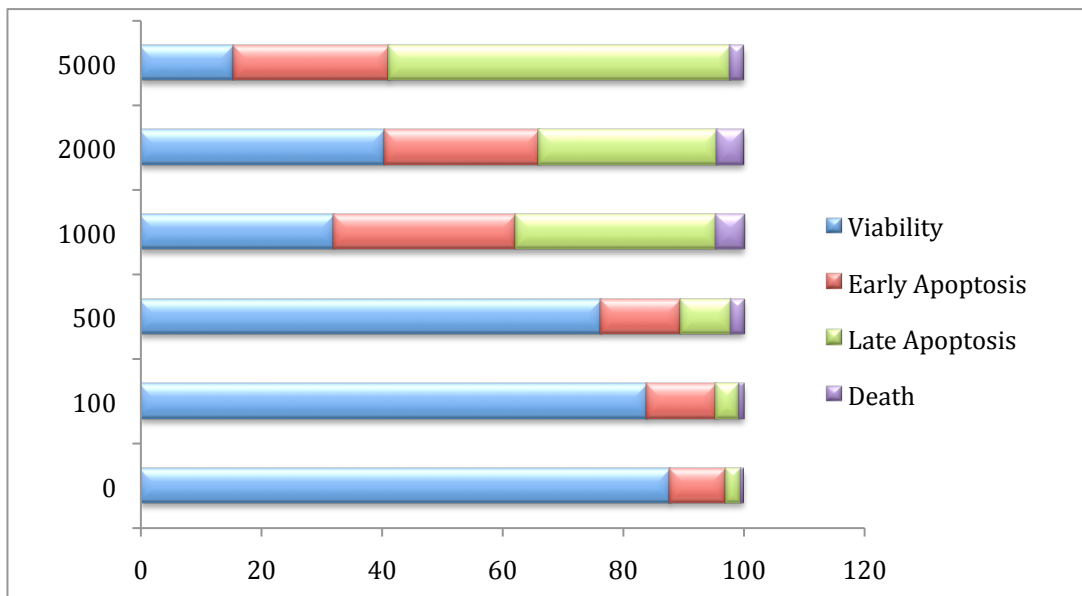


Figure 3.29 WSE induced apoptosis in a different time and dose fashion. Percents of Typical Quadrant Analysis of Annexin V-apc/7AAD Flow Cytometry of HL-60 Cells Treated with WSE for 72 h.

At 72 hours, the observed maximal apoptosis for WSE at the maximal concentration, 5000 µg/ml, was about about 85 % as shown in Table 3.15 and Figure 3.29. The results also showed that there was significant dose dependent cell death upon exposure to WSE, however these concentrations were significantly higher than other solvent extracts.

At 72 hours, the observed maximal apoptosis for WRE at the maximal concentration, 5000 µg/ml, was about about 80 % as shown in Table 3.16 and Figure 3.30. The results also showed that there was significant dose dependent cell death upon exposure to WRE, however these concentrations were significantly higher than other solvent extracts.

Aqueous extracts were the only extracts that shoot extracts were more effective than root extracts. This means water as a more polar solvent extract more apoptotic components of *Rheum ribes* in shoot than in root.

**Table 3.15** Percents of Typical Quadrant Analysis of Annexin V-apc/7AAD Flow Cytometry of HL-60 Cells Treated with WRE for 72 h

hours	Extracts	Viability	Early apop	Late Apop	death
<b>72</b>	<b>DMSO</b>	89	9.2	1.22	0.57
	<b>WRE 100</b>	89.6	8.65	1.4	0.37
	<b>WRE 500</b>	87.2	10.1	2.13	0.57
	<b>WRE 1000</b>	85.4	11.7	2.31	0.56
	<b>WRE 2000</b>	65.7	25.3	8.05	0.56
	<b>WRE 5000</b>	21.9	46.2	29.8	2.16

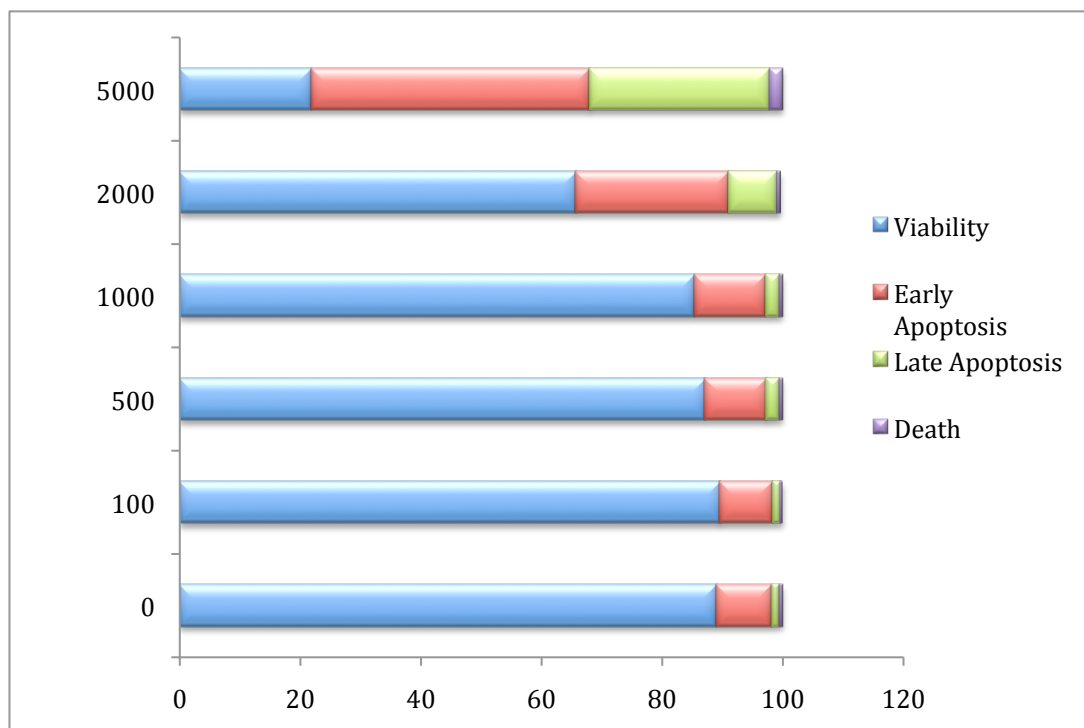


**Figure 3.30** WSE induced apoptosis in a different time and dose fashion. Percents of Typical Quadrant Analysis of Annexin V-apc/7AAD Flow Cytometry of HL-60 Cells Treated with WSE for 72 h.

### **3.9 Terminal deoxynucleotidyl Transferase Biotin-dUTP Nick End Labeling (TUNEL)**

The duration of apoptosis is relatively short and variable depending on cell type, inducer of apoptosis. Each of the methods presented above has its advantages and suffers limitations. So combination of several apoptosis assay can provide a more definite identification of apoptotic cells.

Another apoptosis indicator, DNA fragmentation, was examined with TUNEL method. The fragmented DNAs were observed as bright yellow as in Figure 3.27 and 3.28.



**Figure 3.31** TUNEL image of 0.1 % DMSO treated HL-60 cells, control indicating unfragmented DNA (Olympus CKX 41, 400X)

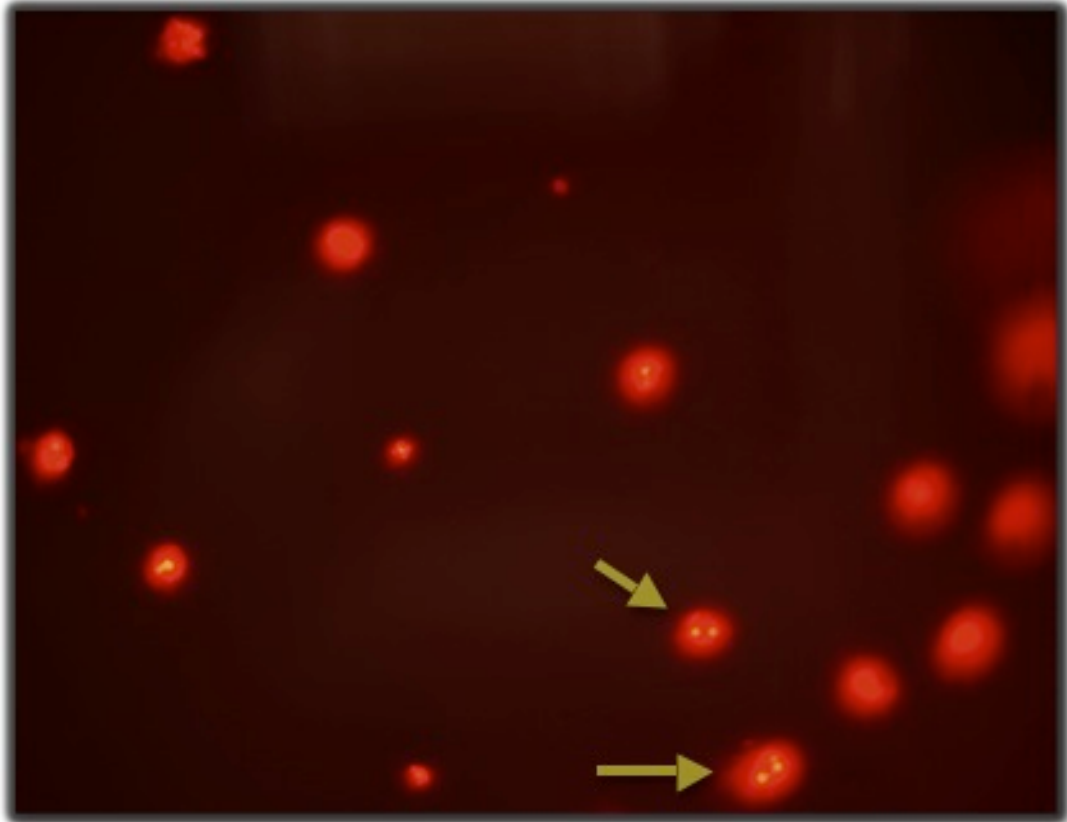


**Figure 3.32** TUNEL image of HL-60 cells treated with 100 µg/ml of ESE. Arrows were indicating DNA fragmented cells observed as bright yellow (Olympus CKX 41, 400X)

Figure 3.32 and 3.33 were showing HL-60 cells treated with 100 µg/ml ESE and ERE for 16 hours, respectively. With these treatment conditions, as it was seen from number of bright yellow dots, ERE caused apoptosis in HL-60 cells more than ESE did but the fluorescence was not so intense. In order not to miss the apoptosis, 16 hours incubation time was selected with the lower ESE and ERE concentration.

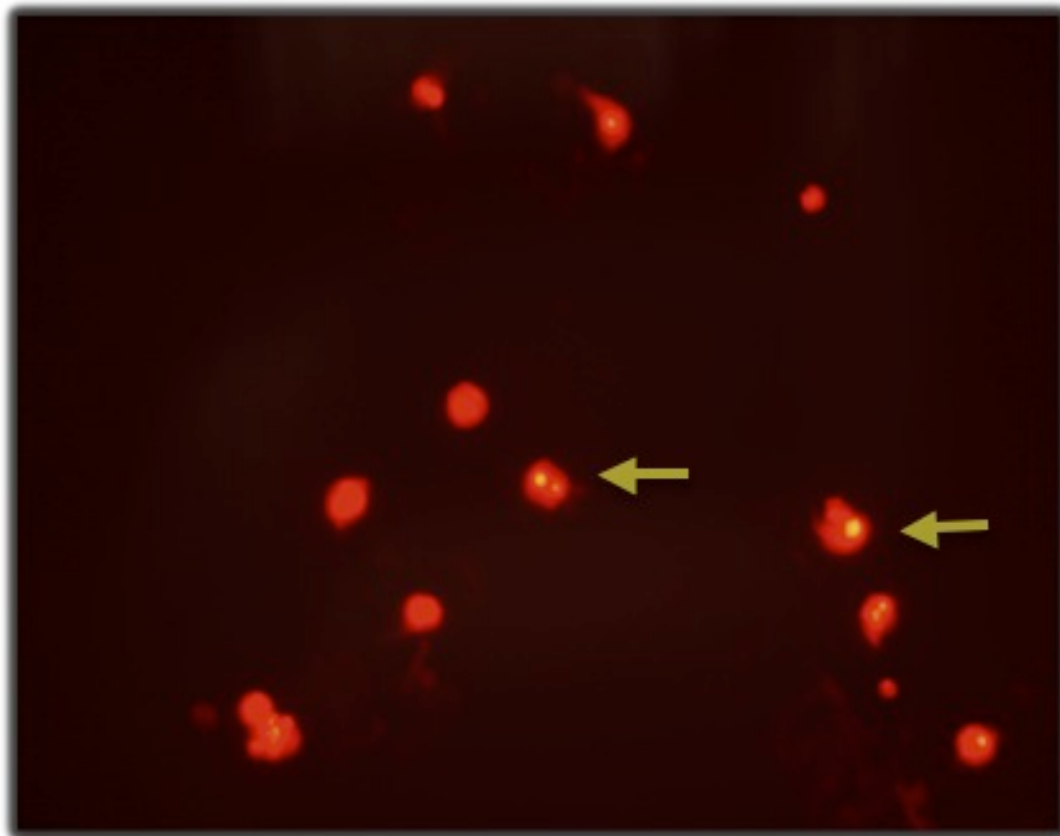


**Figure 3.33** TUNEL image of HL-60 cells treated with 100 µg/ml of ERE. Arrows were indicating DNA fragmented cells observed as bright yellow (Olympus CKX 41, 400X)

There are other reports indicating the effects of Rhenum species on apoptosis in several cell lines. In human cervical Bu 25 TK cancer cells and human lung squamous carcinoma CH 27 cells, emodin induced apoptosis through mitochondrial activation of caspase 3 and 9 and with Bax upregulation (Srinivas et al., 2003; Lee, 2001).

It is known that quinones could react with oxygen and produce reactive oxygen species and exert antiproliferative activities by creating ROS. Emodin being an anthraquinone, has this ability. P450 enzymes metabolize emodin to its genotoxic intermediates, 2-hydroxyemodin and w-hydroxyemodin, which increase the ROS formation (Mueller et al., 1998). Su et al. (2005) demonstrated that emodin caused apoptosis by generating ROS in human lung adenocarcinoma cells, A549, as a result

Bax levels elevated and Bcl-2 levels reduced, mitochondrial membrane potential decreased, cytochrome c was released and subsequently caspase 2, 3, 9 activated, and also survival molecules downregulated. Pretreatment of cells with an antioxidant, ascorbic acid, abolished apoptosis, indicating that apoptosis was generated because of ROS formation (Su et al., 2005). Apoptosis was observed also in human tongue cancer SCC-4 cells (Lin et al., 2009) due to ROS generated by emodin. Furthermore, chemotherapeutic drugs and emodin cotreatment enhanced the therapy.

### 3.10 DNA Fragmentation Induced By *Rheum ribes*

The integrity of DNA was assessed by agarose gel electrophoresis. Incubation of HL-60 cells with 100, 250 and 500  $\mu\text{g}/\text{ml}$  of ESE and ERE and 250, 500 and 1000  $\mu\text{g}/\text{ml}$  of WSE and WRE for 48 h elicited a characteristic ‘ladder’ of DNA fragments representing integer multiples of the internucleosomal DNA length (about 180-200 bp) (Figure 3.34).

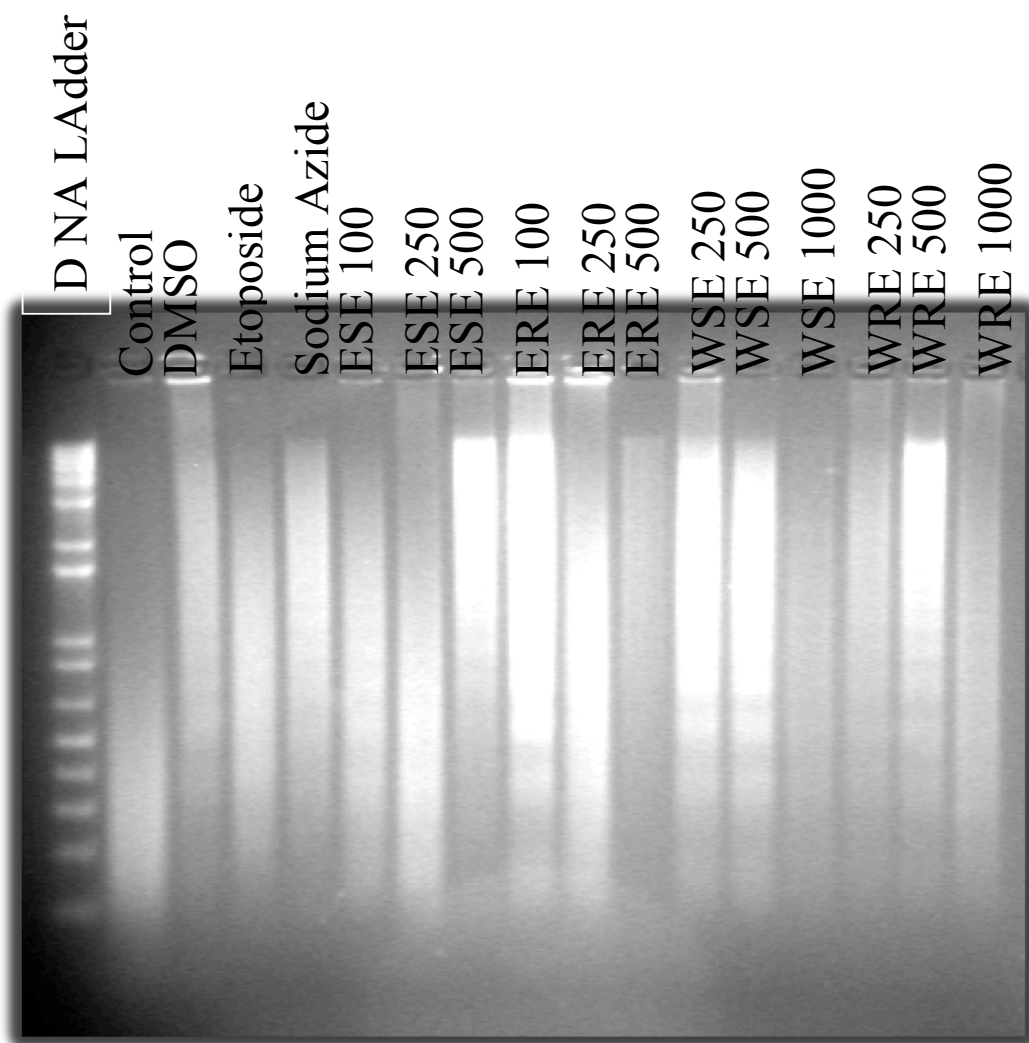


**Figure 3.34** *Rheum ribes* treated HL-60 cells show apoptosis specific DNA ladder. HL-60 cells were treated with 100, 250 and 500  $\mu\text{g}/\text{ml}$  of ESE and ERE and 250, 500 and 1000  $\mu\text{g}/\text{ml}$  of WSE and WRE for 48 h. Fragmented DNA was isolated and subjected to agarose electrophoreses. Bands were visualized with ethidium bromide.

### 3.11 Modulation of the levels of Bcl-2 family members by Rheum ribes in HL-60 cells

#### 3.11.1 Qualification of RNA by Agarose Gel Electrophoresis

After isolation of total RNAs with RNeasy Kit (Qiagen) as described in Materials and Methods with the title “*Isolation of Total RNA from HL-60 cells*”, they were run on denaturing agarose gel electrophoresis in order to check the quality and intactness of purified RNAs. The upper band represents 28S large ribosomal subunit, and second band represents 18S ribosomal small subunit. The band present at the bottom of the gel corresponds to the mixture of tRNAs and 5S ribosomal RNAs (Figure 3.35). If contaminated RNase degraded them during the isolation, we could not see the three bands as shown in figure. It would be a smear instead of intact bands.

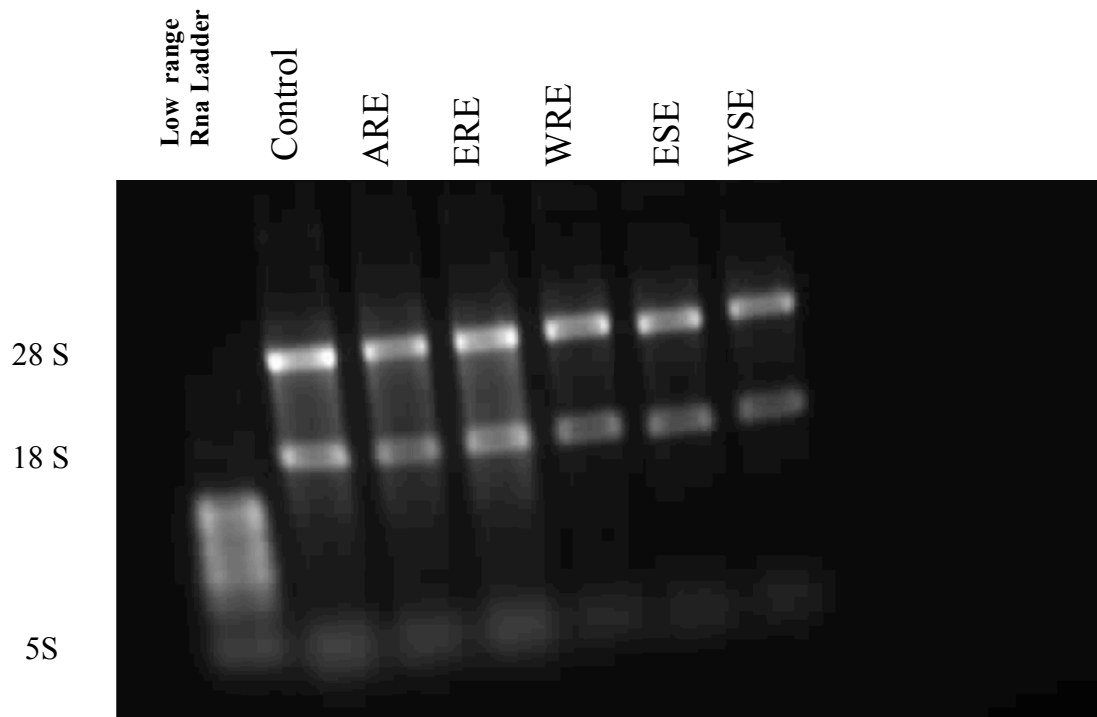


**Figure 3.35** Total RNA isolated from HL-60 cells which were 0.1 % DMSO treated and 100 µg/ml of ARE, ERE, WRE, ESE and WSE for 24 h. Low Range RNA ladder (lane 1) (1% agarose gel)

Typical markers of RNA quality are fairly sharp and intense bands of 18S (~1900bases) and 28S (~4800 bases) rRNA subunits. DNA contamination of the RNA will migrate as high molecular weight ethidium-bromide staining material. Smearing of the ribosomal RNA bands will evidence degradation of the RNA. The 28S rRNA band should be approximately twice as intense as the 18S rRNA band. This 2:1 ratio (28S:18S) is a good indication that the RNA is intact. Partially degraded RNA will have a smeared appearance, will lack the sharp rRNA bands, or will not exhibit a 2:1 ratio.

### ***3.11.2 Qualification of RNA by Bioanalyzer***

The integrity and purity of isolated RNAs were also analyzed by Bioanalyzer (Agilent). The ratio of 28S to 18S is important in this analysis, the more the ratio reaches to 2, the better the integrity, if the ratio is too small, and this indicates RNA is fragmented. Bioanalyzer result of RNA sample was shown in Figure 3.30. The ratio of 28S to 18S was 1.7, 2.1 and 1.8 for control, ESE and ERE, respectively as shown in Figure 3.36. It was seen from bioanalyzer results that quality of RNA was good (Fig 3.37)

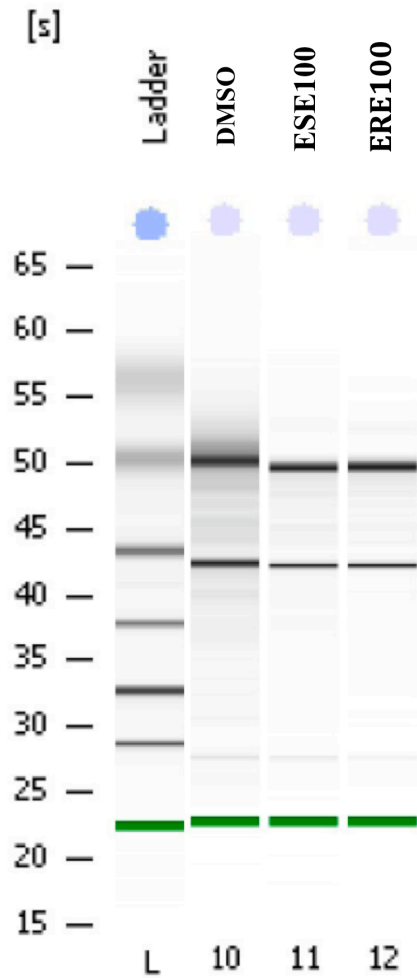


**Figure 3.36** Gel image of Bioanalyzer (Agilent) result of total RNA isolated from HL-60 cells which were 0.1 % DMSO treated and 100 µg/ml of ESE and ERE for 24 h. RNA ladder (lane 1)

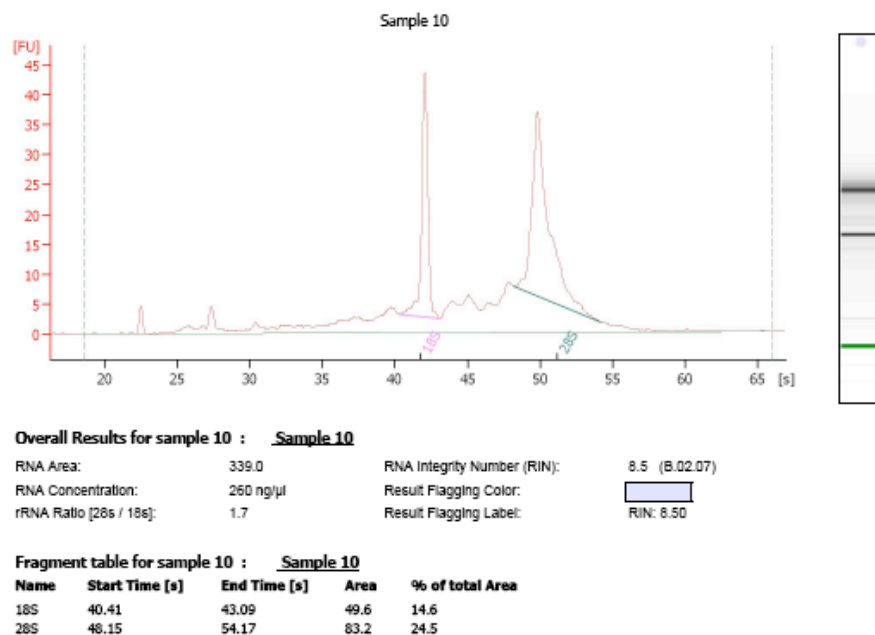


**Figure 3.37** Bioanalyzer (Agilent) result of total RNA isolated from HL-60 cells, which were 0.1 % DMSO treated for 24 h.

In order to standardize the process of RNA integrity interpretation, Agilent Technologies has introduced a new tool for RNA quality assessment. The RNA Integrity Number (RIN) was developed to remove individual interpretation in RNA quality control. It took the entire electrophoretic trace into account. The RIN software algorithm allows for the classification of riboeukaryotic total RNA, based on a numbering system from 1 to 10, with 1 being the most degraded profile and 10 being the most intact. In this way, interpretation of an electropherogram is facilitated, comparison of samples is enabled and repeatability of experiments is ensured.

According to Bioanalyzer results, total RNAs isolated from HL-60 cells, which were treated with 0.1 %DMSO, ESE and ERE for 24 h had RIN as 8.5, 9.3 and 9.6, respectively (Fig 3.38). It was shown that extracted total RNAs were in quality.

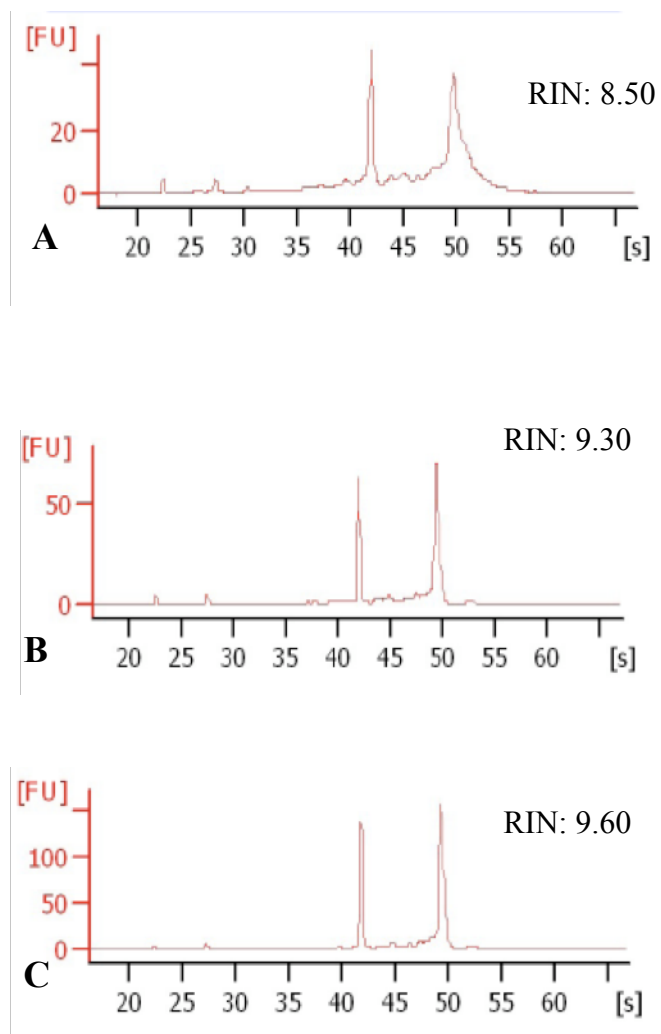


**Figure 3.38** Bioanalyzer (Agilent) result of total RNA isolated from HL-60 cells, which were (A) 0.1 % DMSO and 100  $\mu\text{g}/\text{ml}$  of (B) ESE (C) ERE treated for 24 h.

### 3.11.3 Determination of RNA purity and concentration

After agarose gel electrophoresis, the concentrations of isolated RNAs were determined spectrophotometrically at 260nm. 1 unit of optical density was described as the absorbance of 40ug/ml of RNA in 1cm length quartz cuvette against TE buffer. Furthermore Optical density at 280nm was also determined to check the contaminant proteins in isolated RNA suspensions. The ratio of OD<sub>260</sub>/OD<sub>280</sub> should be in between 1.8-2.0 for better isolation. Lower values mean that there were considerable protein contaminations, which may affect the further RT-PCR reactions (Table 3.17)

**Table 3.16** Spectrophotometric determination of total RNA concentration (*mg/ml*) and OD<sub>260</sub>/OD<sub>280</sub> ratios of all samples

Sample	OD <sub>260</sub>	OD <sub>280</sub>	OD <sub>260</sub> / OD <sub>280</sub>	[RNA] mg/ml
Control	0.0517	0.0262	1.978	0.2069
ARE	0.0533	0.0269	1.984	0.2131
ESE	0.0485	0.0255	1.905	0.1941
ERE	0.0436	0.0223	1.953	0.1745
WSE	0.0469	0.0232	2.023	0.1877
WRE	0.0496	0.0268	1.855	0.1985

### 3.11.4 Expression Analysis of Apoptosis Related Genes Bcl-2 and Bax

One important indicator of apoptosis is the change in the expression levels of Bcl-2 family genes. The expression of apoptotic gene Bax increases whereas the expression of antiapoptotic gene Bcl-2 decreases during apoptosis, resulting in increase of Bax/Bcl-2 ratio (Cory and Adams, 2002). The effects of 100 µg/ml ESE and ERE treatment on apoptosis were investigated by qRT-PCR, measuring gene

expression levels of Bax and Bcl-2 in HL-60 cells. The changes in expression levels of corresponding genes in HL-60 were given in Table 3.14. Fold changes in gene expressions were calculated using  $2^{-\Delta\Delta Ct}$  method. Gene expressions in 1% DMSO treated cells were used as controls.

**Table 3.17** Effects of 100 µg/ml of ESE and ERE treatment on Bax/Bcl-2 ratio in HL-60 cells for 24 hours

<b>Genes</b>	<b>Extracts</b>	ESE 100	ERE 100
Bcl-2		↓2.47 fold	↓5.41 fold
Bax		↑1.41 fold	↑2.49 fold
Bax/Bcl-2		↑3.49	↑13.9

As seen in Table 3.18 and Figure 3.39 Bcl-2 expression decreased with 2.47 and 5.41 fold with 100 µg/ml ESE and ERE for 24 h treatment with respect to 0.1 % DMSO treatment in HL-60 cells, respectively. Bax expression increased 1.41 and 2.49 fold with 100 µg/ml ESE and ERE for 24 h treatment with respect to 0.1 % DMSO treatment in HL-60 cells, respectively.

ERE treatment for 24 hours changed the expression levels of Bax and Bcl-2 genes in HL-60 cells in favor of apoptosis with an 13.9 fold increase in the ratio of Bax/ Bcl-2. This ratio was 3.49-fold increase in ESE treatment. The increase in the ratio of Bax to Bcl-2 was greater for 100 µg/ml ERE than ESE in HL-60 cells, showing ERE showed more apoptotic activity though Bax/Bcl-2 expression system.

ESE and ERE induced apoptosis through distinctly down regulated Bcl-2 gene levels and slightly up regulate expression of Bax gene levels.

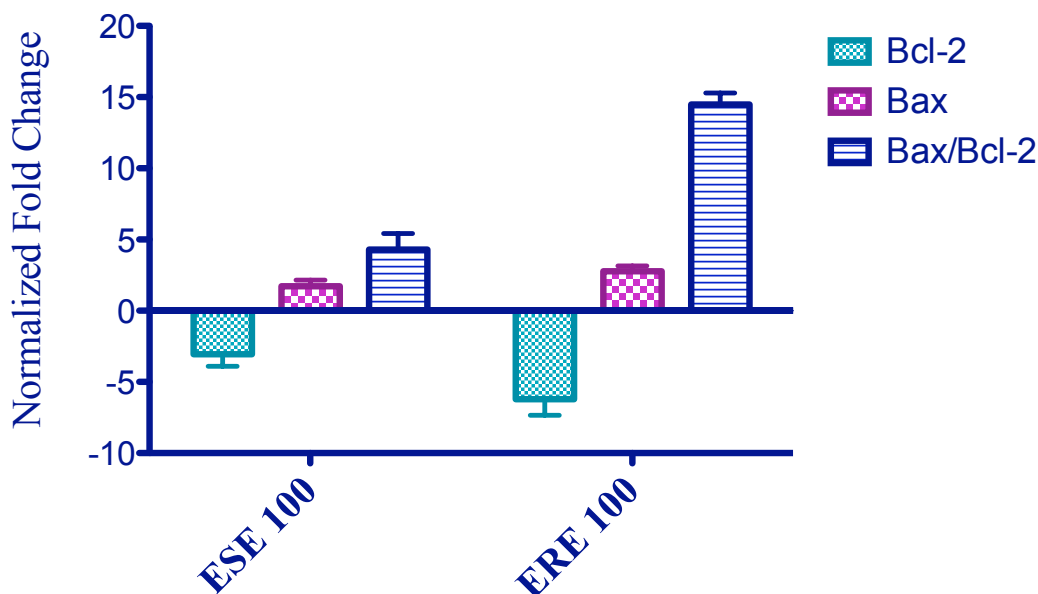


**Figure 3.39** Expression of Bax and Bcl-2 genes in HL-60 cells upon treatment with 100 µg/ml of ESE and ERE for 24 hours. The values are the average of triplicate measurements from two biological replicates. The results were normalized to 0.1% DMSO control.

The effects of 100 µg/ml WSE and WRE treatment on apoptosis were investigated by semi quantitative RT-PCR, measuring gene expression levels of Bax and Bcl-2 in HL-60 cells.

The gel images of RT-PCR product were shown in Figure 3.40. After densitometric analysis with ImageJ, the ratios of the densities of Bcl-2, BAX and GAPDH genes are calculated as in Table 3.19. Gene expressions in 1% DMSO treated cells were used as controls.

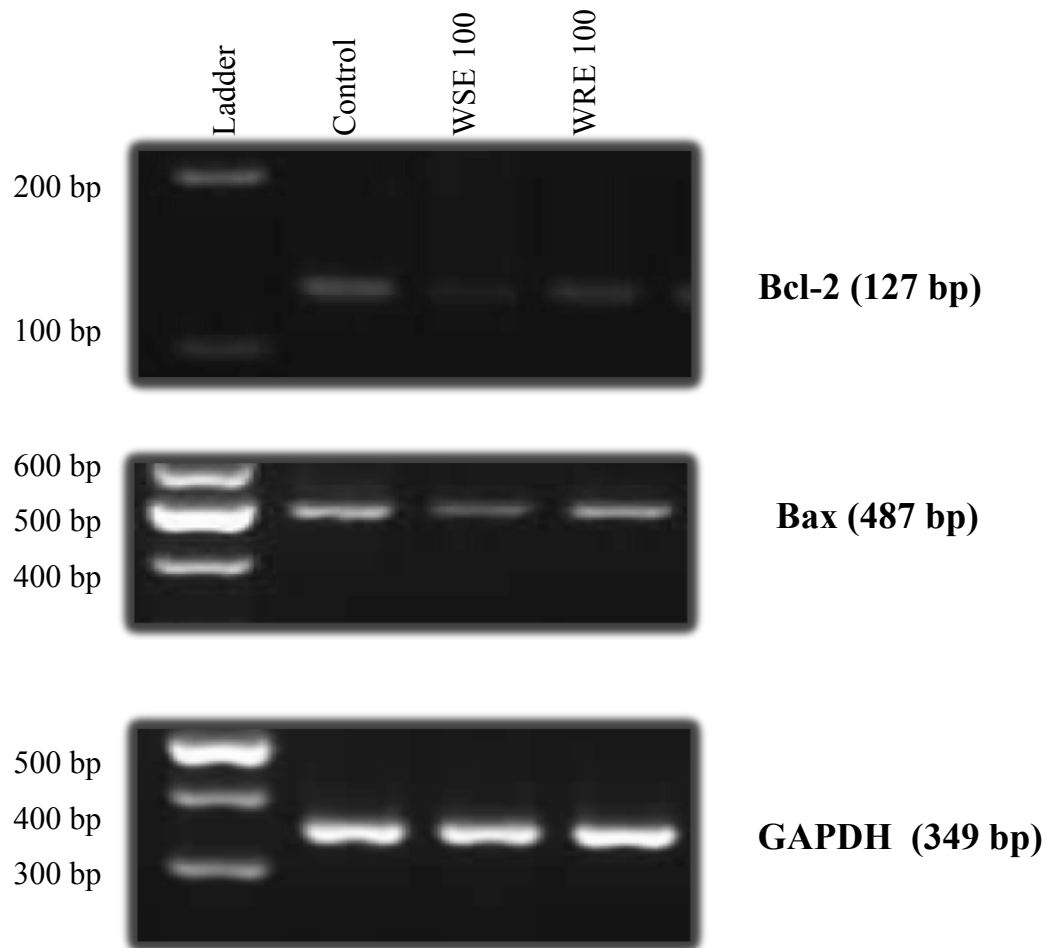


**Figure 3.40** The gel image of RT-PCR product of Bax and Bcl-2 genes in HL-60 cells upon treatment with 100  $\mu\text{g/ml}$  of WSE and WRE for 24 hours. The values are the average of triplicate measurements from two biological replicates.

As seen in Figure 3.41 Bcl-2 expression decreased with 1.91 and 2.51 fold with 100  $\mu\text{g/ml}$  WSE and WRE for 24 h treatment with respect to 0.1 % DMSO treatment in HL-60 cells, respectively. Bax expression was also decreased with 1.28 and 1.81 fold with 100  $\mu\text{g/ml}$  WSE and WRE for 24 h treatment with respect to 0.1 % DMSO treatment in HL-60 cells, respectively.

**Table 3.18** Effects of 100 µg/ml of WSE and WRE treatment on Bax/Bcl-2 ratio in HL-60 cells for 24 hours

Genes	Extracts	WSE 100	WRE 100
	Bcl-2		↓1.91 fold
Bax		↓1.28 fold	↓1.81 fold
Bax/Bcl-2		↑1.5	↑1.3

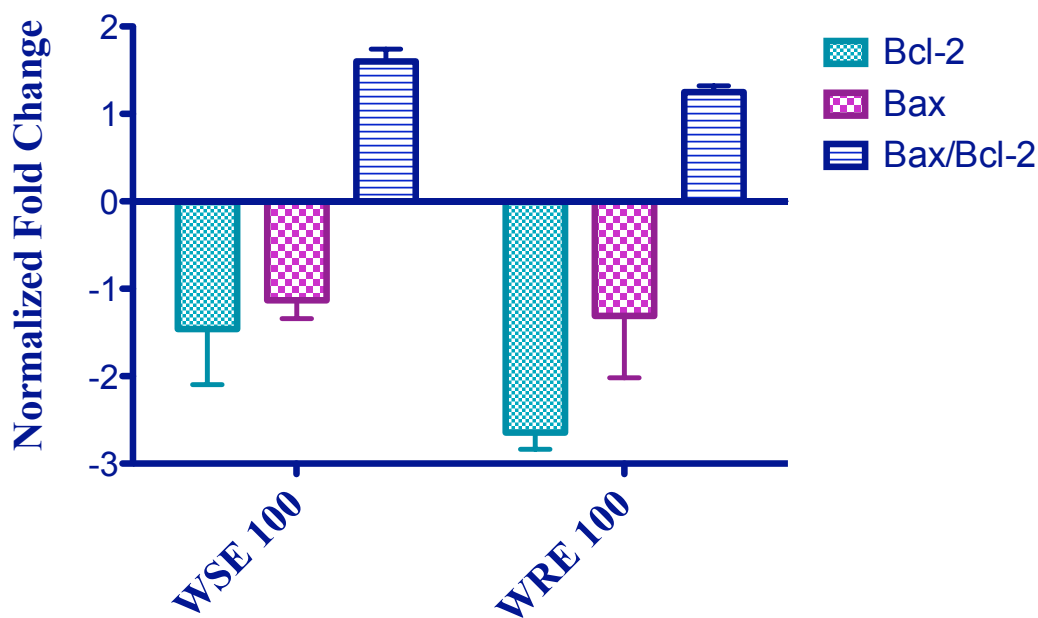


**Figure 3.41** Expression of Bax and Bcl-2 genes in HL-60 cells upon treatment with 100 µg/ml of WSE and WRE for 24 hours. The values are the average of triplicate measurements from two biological replicates.

In HL-60 cells Bax and Bcl-2 expression changes were less than 2 fold. It was also concluded in cytotoxicity studies that, at this indicated concentration WSE and WRE did not change the cell viability significantly for 24 h.

### 3.12 Western Blot Analysis of Apoptosis Related Protein *Bax*

The levels of Bax proteins in HL-60 cells were examined by Western blotting after cells were treated with indicated concentrations of *Rheum ribes* extracts for 72 h.

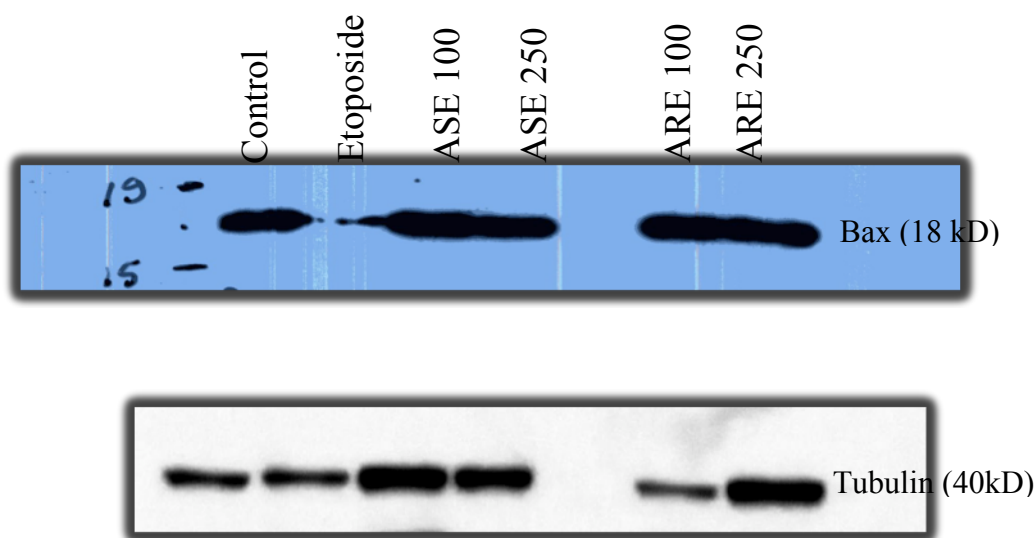


**Figure 3.42** Expression of Bax protein in HL-60 cells upon treatment with 100 and 250  $\mu\text{g}/\text{ml}$  of ASE and ARE for 72 hours. The values are the average of triplicate measurements from two biological replicates.

As shown in Figure 3.42 in Western blot Analysis, Bax protein expression did not significantly changed in both ASE and ARE in HL-60 cells in all the treatment concentrations compared to controls for 72 h.

As shown in Figure 3.43 in Western blot Analysis, Bax protein expression did not significantly changed in both ESE and ERE in HL-60 cells in all the treatment concentrations compared to controls for 72 h.

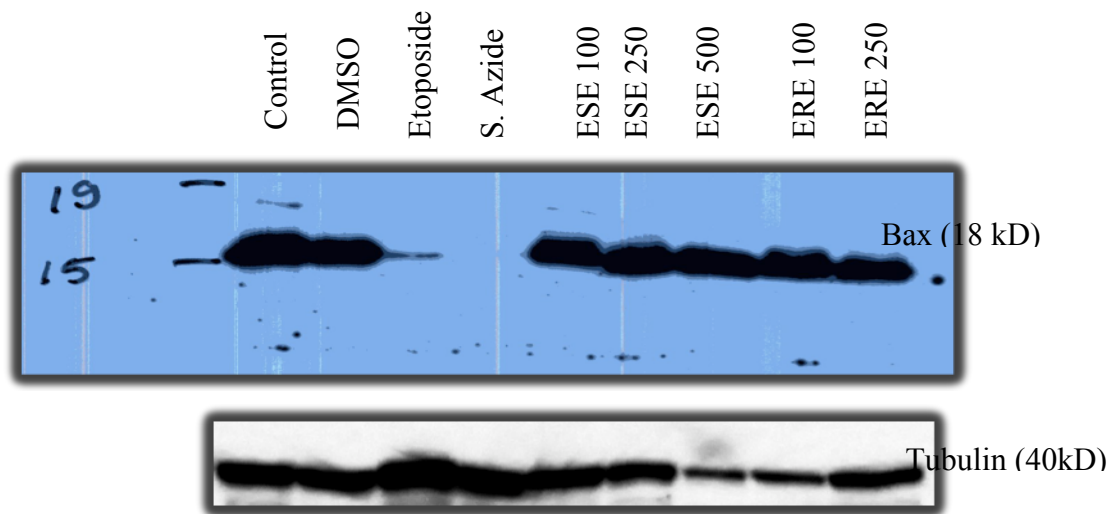


**Figure 3.43** Expression of Bax protein in HL-60 cells upon treatment with 100, 250 and 500  $\mu\text{g/ml}$  of ESE and ERE for 72 hours. The values are the average of triplicate measurements from two biological replicates.

As shown in Figure 3.44 in Western blot Analysis, Bax protein expression did not significantly changed in both WSE and WRE in HL-60 cells in all the treatment concentrations compared to controls for 72 h.

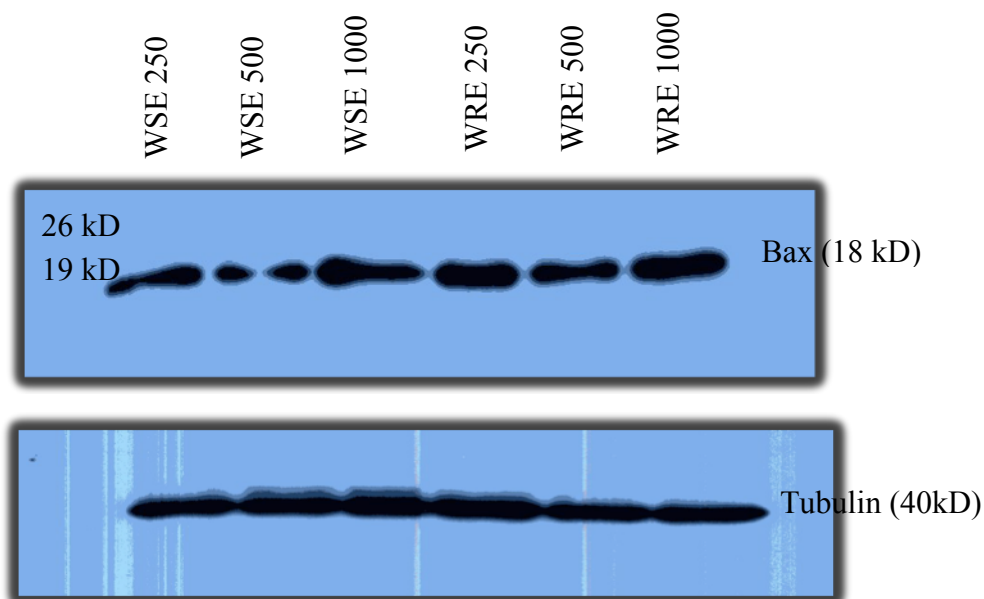


**Figure 3.44** Expression of Bax protein in HL-60 cells upon treatment with 250, 500 and 1000  $\mu\text{g/ml}$  of WSE and WRE for 72 hours. The values are the average of triplicate measurements from two biological replicates.

### 3.13 Detection of cytochrome c release

Recent evidence has demonstrated that mitochondria participate in the execution of apoptosis by release of cytochrome c. Binding of cytochrome c to Apaf-1 results in the cleavage of procaspase-9 or other caspase, which in turn activate caspase-3. To directly examine mitochondrial involvement, release of cytochrome c into the cytoplasm was determined.

After HL-60 cells were treated with *Rheum ribes*, mitochondria fraction was isolated from cytosol. The cytochrome c was detected in mitochondria fraction and cytosol fraction by western blot. Figure 3.45 and 46 showed cytochrome c increase in cytosol; in the same time, cytochrome c decrease in mitochondria. These results suggest ARE and ERE lead to cytochrome c translocation from mitochondria into cytosol.

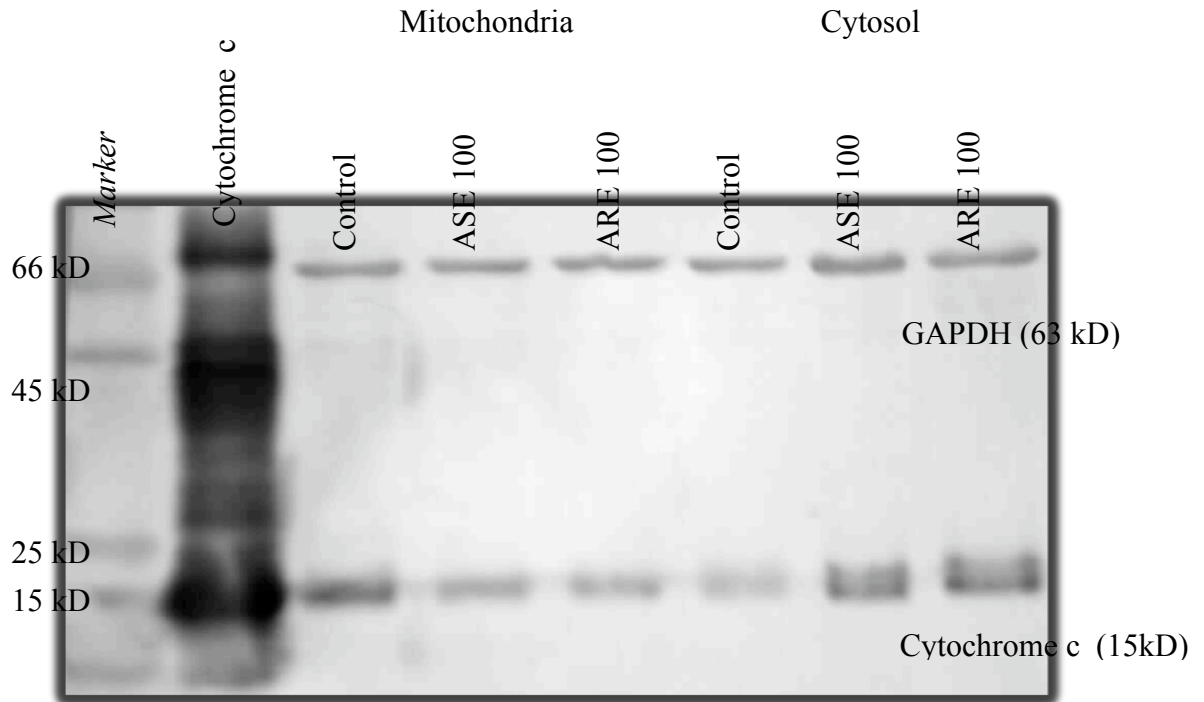


**Figure 3.45** Cytochrome c release from mitochondria into cytosol induced by 100  $\mu\text{g/ml}$  of ASE and ARE for 24 hours. HL-60 cells were cultured in normal growth medium and then either left untreated (0.1 % DMSO, as control) or treated with 100  $\mu\text{g/ml}$  of ASE or ARE for 24 h at 37°C in a CO<sub>2</sub> incubator. Total cellular protein 20  $\mu\text{g}$  per lane was separated by 12% sodium dodecyl sulfate-polyacrylamide gel electrophoresis (SDS-PAGE), transferred to PVDF membrane, and probed with antibodies that recognize mouse anti-cytochrome c monoclonal antibody. Arrows indicate the position of cytochrome c or GAPDH. Equal protein loading was confirmed by reprobing the stripped blots with mouse anti- GAPDH monoclonal antibody. The results shown are representative of at least three independent experiments.

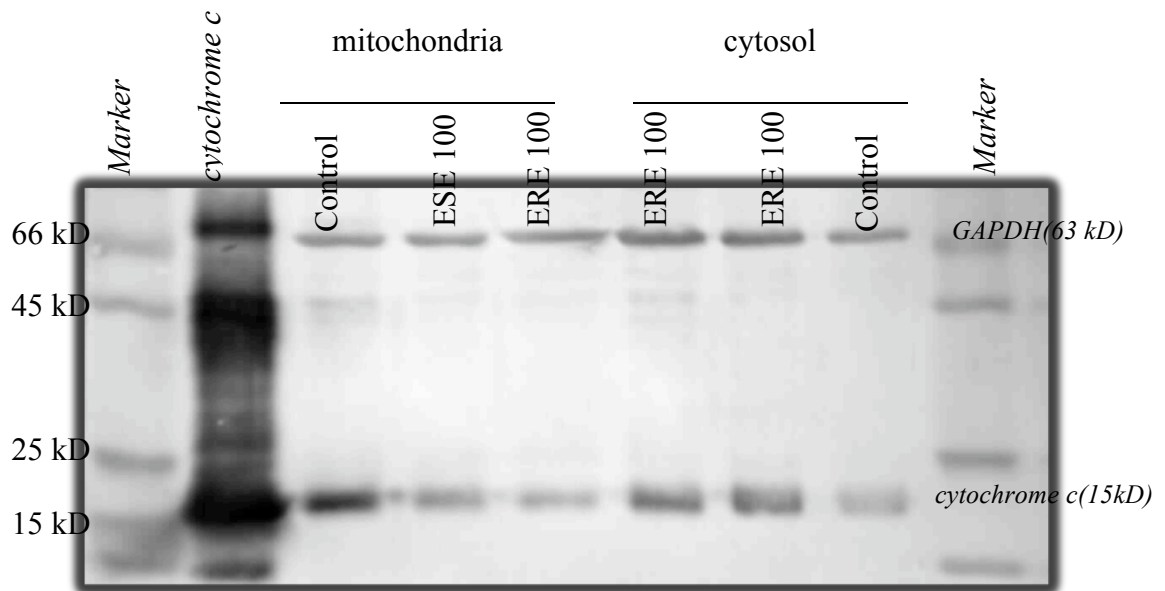


**Figure 3.46** Cytochrome c release from mitochondria into cytosol induced by 100  $\mu\text{g/ml}$  of ESE and ERE for 24 hours. HL-60 cells were cultured in normal growth medium and then either left untreated (0.1 % DMSO, as control) or treated with 100  $\mu\text{g/ml}$  of ESE or ERE for 24 h at 37<sup>0</sup>C in a CO<sub>2</sub> incubator. Total cellular protein 20 $\mu\text{g}$  per lane was separated by 12% sodium dodecyl sulfate-polyacrylamide gel electrophoresis (SDS-PAGE), transferred to nitrocellulose, and probed with antibodies that recognize mouse anti-cytochrome c monoclonal antibody. Arrows indicate the position of cytochrome c or GAPDH. Equal protein loading was confirmed by reprobing the stripped blots with mouse anti- GAPDH monoclonal antibody. The results shown are representative of at least three independent experiments.

### **3.14 The role of Caspase-3 *Rheum ribes* Induced Apoptotic Pathway**

Caspases comprise a family of different cysteine protease that are synthesized as inactive zymogens and converted to an active complex composed of several heterodimeric subunits. These enzymes participate in a cascade that is triggered in response to proapoptotic signals and ends in the cleavage of a variety of proteins, resulting in disassembly of the cell. To investigate differences in caspase activation by different extracts of *Rheum ribes*, we analyzed activation of caspase-3. We monitored the processing of procaspases in immunoblot analyses using antibodies specific to caspase-3 and caspase-3 catalytic activities using its specific colorimetric tetrapeptide substrates Ac-DEVD-AFC.

#### ***3.14.1 Rheum ribes induces activation of caspase-3***

HL-60 cells were either left untreated or treated with ASE and ARE with a concentration of 100 and 250 µg/ml for 24 h. At the indicated time points, cells were collected. Protein extracts were prepared and fractionated by SDS-PAGE.

Treatment of HL-60 cells with *Rheum ribes* resulted in the conversion of the inactive 32-kDa caspase-3 precursors to the proteolytically cleaved p17 subunit, indicating that caspase-3 was activated during *Rheum ribes* -induced apoptosis.

As shown in Figure 3.47 the cleavage pattern of the caspase-3 did not differ between ASE and ARE stimulation. However, corresponding to the different kinetics of apoptosis obtained from flow cytometry analysis, ARE-induced caspase activation was more rapid and efficient than ASE.

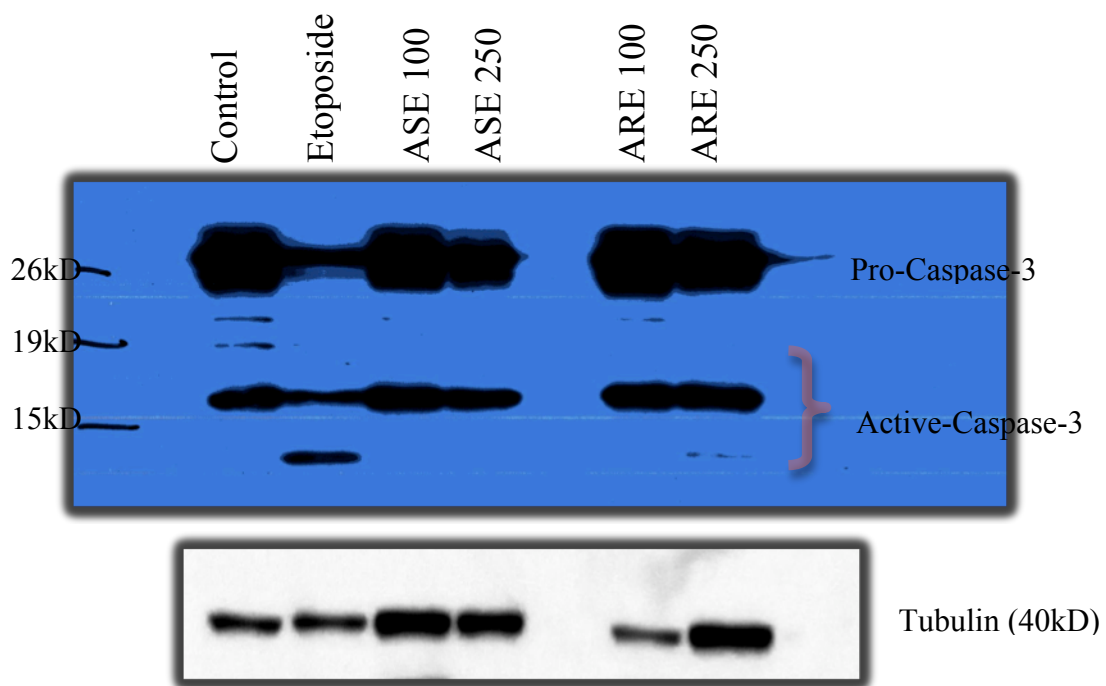


**Figure 3.47** Caspase-3 was cleaved with ASE and ARE. HL-60 cells were cultured in normal growth medium and then either left untreated (M, as control) or treated with etoposide (Eto 68  $\mu\text{g}/\text{ml}$ ), for 24 hours. Total cellular protein 20 $\mu\text{g}$  per lane was separated by 12% SDS-PAGE, transferred to PVDF membrane, and probed with the respective caspase-3 antibody. Arrows indicated the position of full-length caspase-3 and its cleavage fragment p17. Equal protein loading was confirmed by reprobng the stripped blots with mouse anti-tubulin monoclonal antibody.

As shown in Figure 3.48 for etoposide, sodium azide ERE caspase-3 cleavage, the active fragment p17 was clearly presented on blot, but for ESE, although the p32 pro-caspase were clear on the blot, the p17 was not appear on the blot. The reason could be that the time points and indicated concentrations were not appropriate for ESE. Moreover, corresponding to the different kinetics of apoptosis obtained from flow cytometry analysis, ERE-induced caspase activation was more rapid and efficient than ESE.

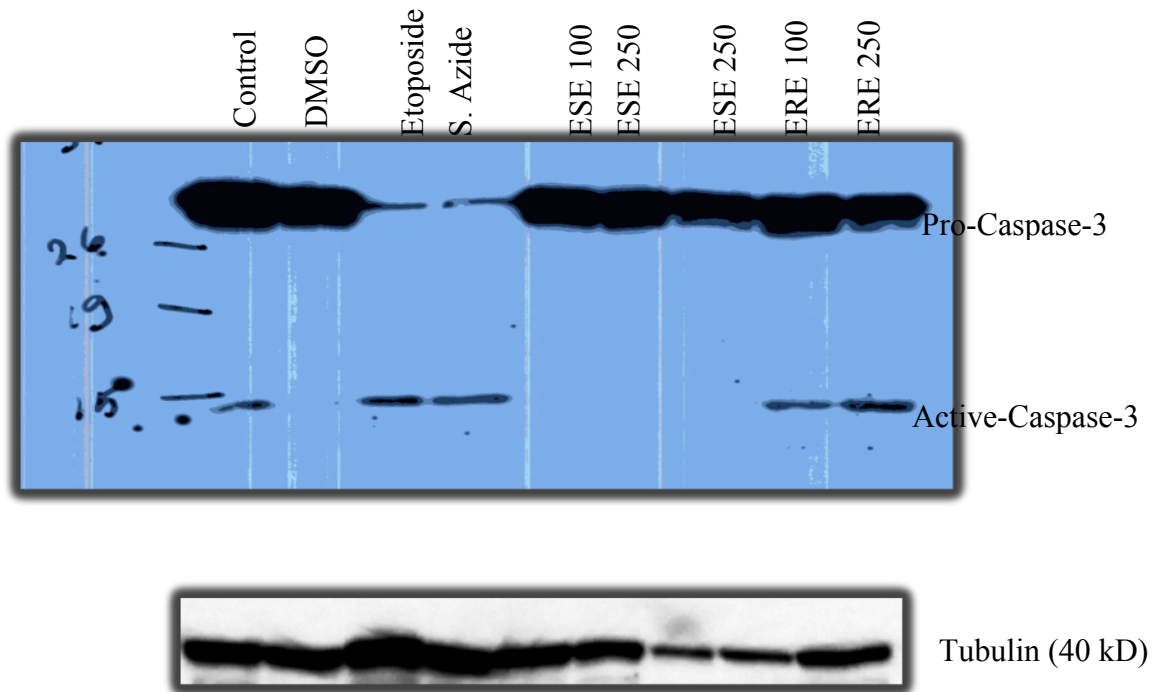


**Figure 3.48** Caspase-3 was cleaved with ESE and ERE. HL-60 cells were cultured in normal growth medium and then either left untreated (M, as control) or treated with etoposide (Eto 68  $\mu\text{g}/\text{ml}$ ), for 24 hours. Total cellular protein 20 $\mu\text{g}$  per lane was separated by 12% SDS-PAGE, transferred to PVDF membrane, and probed with the respective caspase-3 antibody. Arrows indicated the position of full-length caspase-3 and its cleavage fragment p17. Equal protein loading was confirmed by reprobng the stripped blots with mouse anti-tubulin monoclonal antibody.

As shown in Figure 3.49 there were no significantly caspase-3 cleavage in both WSE and WRE in HL-60 cells in all the treatment concentrations compared to controls for 72 h. It was also concluded in flow cytometry analysis that, at this indicated concentrations WRE did not change the cell viability significantly for 72 h, however WSE at 72 hours, the observed maximal apoptosis for WRE at the concentration, 1000  $\mu\text{g}/\text{ml}$ , was about about 68 %. The cell death obtained in WSE might be not mediated though caspase-3 activation.

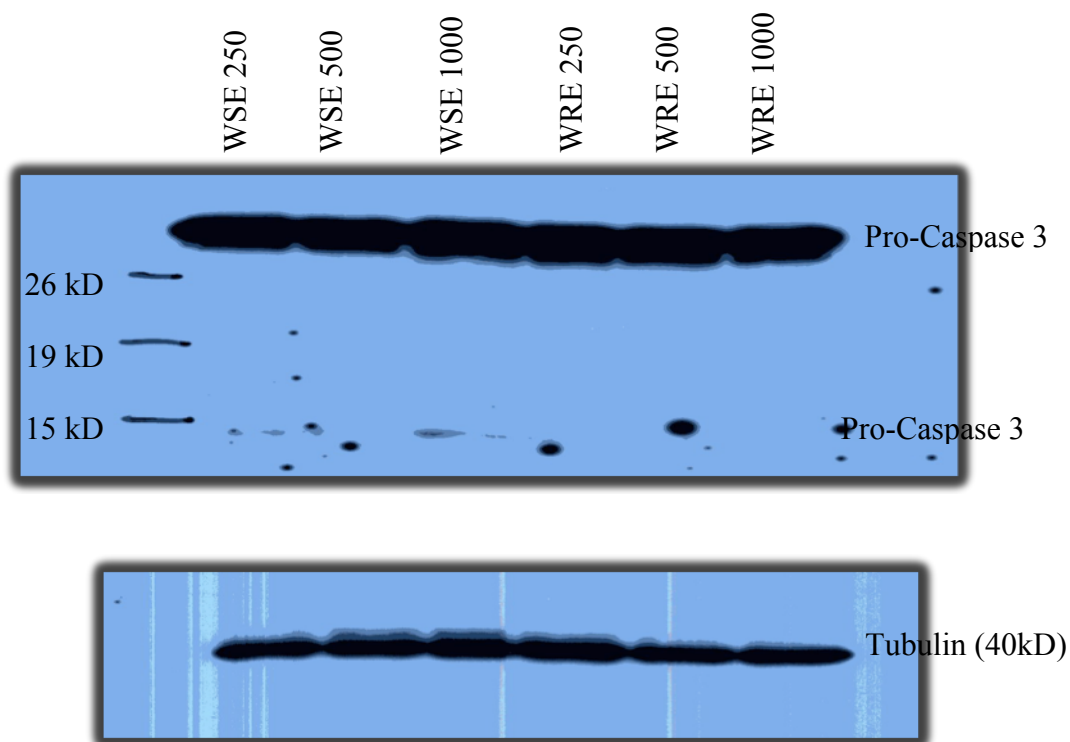


**Figure 3.49** Caspase-3 was cleaved with WSE and WRE. HL-60 cells were cultured in normal growth medium and then either left untreated (M, as control) for 72 hours. Total cellular protein 20 $\mu$ g per lane was separated by 12% SDS-PAGE, transferred to PVDF membrane, and probed with the respective caspase-3 antibody. Arrows indicated the position of full-length caspase-3 and its cleavage fragment p17. Equal protein loading was confirmed by reprobng the stripped blots with mouse anti-tubulin monoclonal antibody.

### 3.14.2 *Rheum ribes* induces catalytic activity of caspase-3

To confirm that the processing of caspase-3 resulted in an active form of the enzyme, the ability to cleave Ac-DEVD-AFC, a fluorogenic tetrapeptide substrate for caspase-3, was evaluated. Treatment of HL-60 cells with concentrations of 250  $\mu\text{g/ml}$  ASE and ARE or greater caused a significant increase in the caspase-3 catalytic activity (Fig. 3.50). ARE at a concentration of 250  $\mu\text{g/ml}$  also induced a dramatic increase of caspase-3 activity as early as 12 h after exposure (Fig. 3.52).

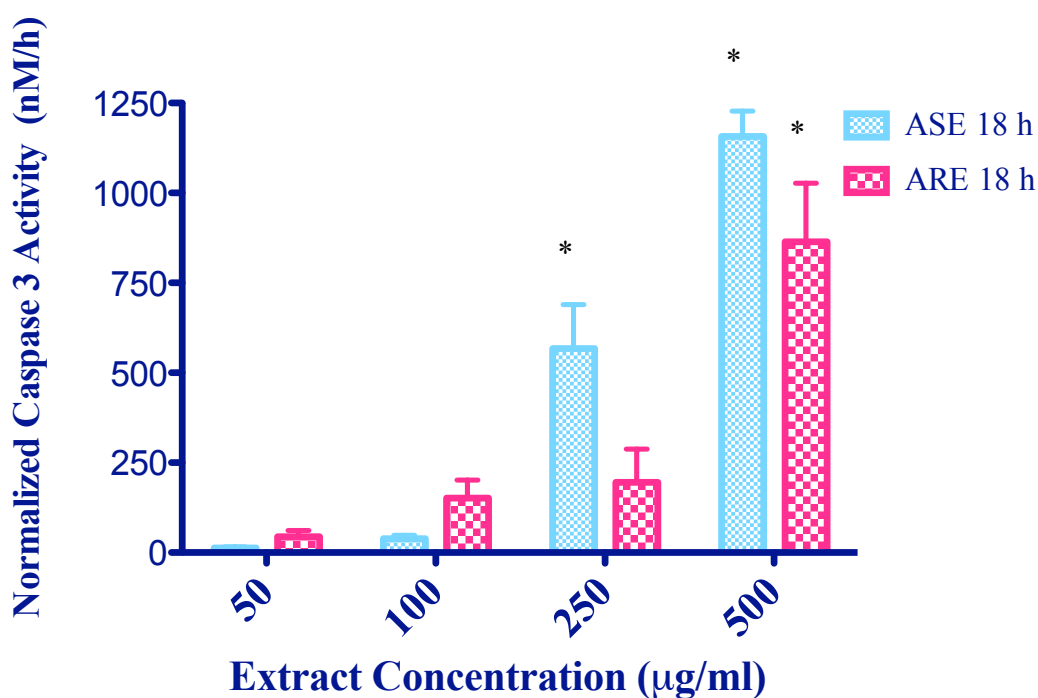


**Figure 3.50** ASE and ARE induced the activation of caspase-3. HL-60 cells were incubated with ASE and ARE at the indicated concentrations for 18 h. Whole cell extracts were analyzed for caspase-3 catalytic activities using its specific colorimetric tetrapeptide substrates Ac-DEVD-AFC. Each data point is given as the means $\pm$ SD. from at least three independent experiments. (\*) Significantly different when compared to vehicle (0.1 % DMSO)-treated groups ( $p < 0.05$ ).

Treatment of HL-60 cells with concentrations of 250  $\mu\text{g/ml}$  ERE and 500  $\mu\text{g/ml}$  ESE or greater caused a significant increase in the caspase-3 catalytic activity (Fig. 3.51). ERE induced caspase-3 activity at a concentration of 250  $\mu\text{g/ml}$  did not change at a time dependent manner between 3 to 24 h after exposure (Fig. 3.52).

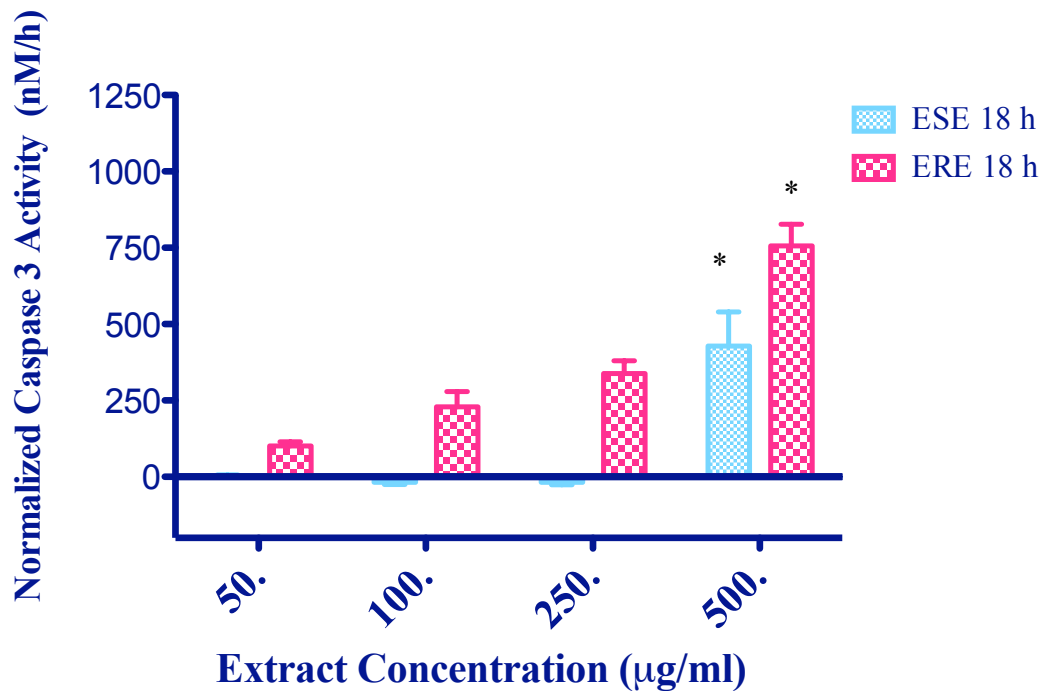


**Figure 3.51** ESE and ERE induced the activation of caspase-3. HL-60 cells were incubated with ESE and ERE at the indicated concentrations for 18 h. Whole cell extracts were analyzed for caspase-3 catalytic activities using its specific colorimetric tetrapeptide substrates Ac-DEVD-AFC. Each data point is given as the means $\pm$ SD. from at least three independent experiments. (\*) Significantly different when compared to vehicle (0.1 % DMSO)-treated groups ( $p < 0.05$ ).

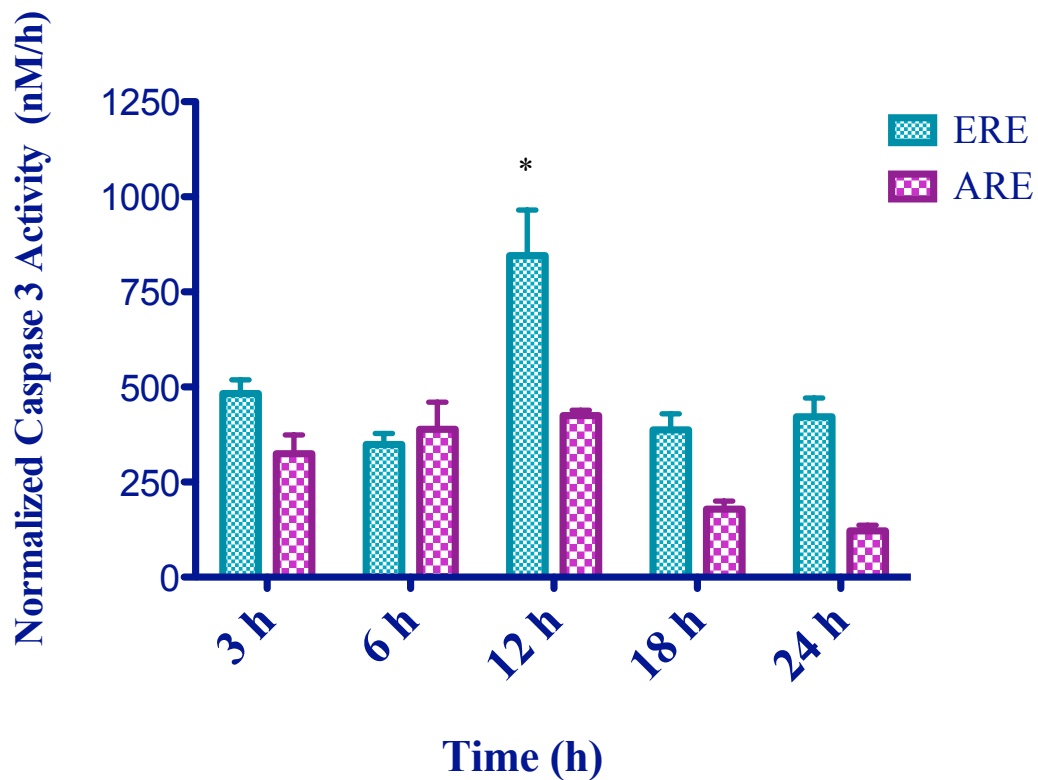


**Figure 3.52** ARE and ERE induced the activation of caspase-3. HL-60 cells were incubated with 250  $\mu\text{g/ml}$  ARE and ERE as indicated time and whole cell extracts were prepared. Whole cell extracts were analyzed for caspase-3 catalytic activities using its specific colorimetric tetrapeptide substrates Ac-DEVD-AFC. Each data point is given as the means $\pm$ SD. from at least three independent experiments. (\*) Significantly different when compared to vehicle (0.1 % DMSO)-treated groups ( $p < 0.05$ ).

### ***3.14.3 Inhibition of the Caspase cascade Did not Suppress the Antiproliferative Effects of Rheum ribes***

To evaluate the contribution of caspase activation to apoptosis induced by *Rheum ribes* the broadspectrum caspase inhibitor zVAD-fmk was applied. Using flow cytometry analysis of phosphatidylserine translocation a complete abrogation of ASE-induced (250 µg/ml) apoptosis after pretreatment with 25µM zVAD-fmk for 1 h was observed (Table 3.20). Unexpectedly zVAD did not block apoptosis, however it increased the cell death due to apoptosis. The results needed further confirmations but in this point it could be concluded that zVAD did not block ASE induced apoptosis which means ASE did not induced apoptosis in HL-60 cells via caspase dependent pathway. ASE induced cell death increased with Necrostatin-1, however cell death dominantly late apoptosis or necrosis. It could be concluded that ASE induced cell death depend on zVAD and Necrostatin-1 related pathway, however, further analysis had to be performed to make a final conclusion.

ESE induced apoptosis did not significantly changed in the presence of zVAD or necrostatin-1. (Table 3.21)

**Table 3.19** Percents of Typical Quadrant Analysis of Annexin V-apc/7AAD Flow Cytometry of HL-60 Cells Treated with ASE for 72 h in the presence of zvad and nec-1

Time	zvad	-				+				-				+			
	nec-1	-				-				+				+			
72 hrs	<i>Extracts</i>	<i>V.</i>	<i>E.A</i>	<i>L.A</i>	<i>D.</i>	<i>V.</i>	<i>E.A.</i>	<i>L.A.</i>	<i>D.</i>	<i>V.</i>	<i>E.A</i>	<i>L.A</i>	<i>D.</i>	<i>V.</i>	<i>E.A</i>	<i>L.</i>	<i>D.</i>
	DMSO	87	9.24	3.23	0.5	77.3	13.9	7.68	1.16	82.1	11.2	5.67	1.04	69.8	15.9	12	2.32
	ASE 250	59.8	11.4	14.8	13.9	48.9	22.4	21.3	7.34	40.7	17.3	31	11	45.5	14.2	24.7	15.6

**Table 3.20** Percents of Typical Quadrant Analysis of Annexin V-apc/7AAD Flow Cytometry of HL-60 Cells Treated with ESE for 72 h in the presence of zvad and nec-1

Time	zvad	-				+				-				+			
	nec-1	-				-				+				+			
72 hrs	<i>Extracts</i>	<i>V.</i>	<i>E.A</i>	<i>L.A</i>	<i>D.</i>	<i>V.</i>	<i>E.A.</i>	<i>L.A.</i>	<i>D.</i>	<i>V.</i>	<i>E.A</i>	<i>L.A</i>	<i>D.</i>	<i>V.</i>	<i>E.A</i>	<i>L.</i>	<i>D.</i>
	<b>DMSO</b>	85	12.1	2.32	0.57	77.1	16.2	5.42	1.32	81.8	13.4	3.84	1.01	71.1	16.9	9.42	2.59
	<b>ESE 250</b>	88.9	9.08	1.87	0.17	86.8	10.1	2.85	0.31	85.3	10.4	3.79	0.49	76.4	16.7	5.97	0.94
	<b>ESE 500</b>	88.2	8.72	2.69	0.41	72.2	18.4	8.6	0.84	72.1	17	9.79	1.07	58	24.6	15.3	2.07

**Table 3.21** Percents of Typical Quadrant Analysis of Annexin V-*apc*/7AAD Flow Cytometry of HL-60 Cells Treated with ARE for 24, 48 and 72 h in the presence of *zvad* and *nec-1*

Time	<i>zvad</i>	-				+				-				+			
	<i>nec-1</i>	-				-				+				+			
	<i>Extracts</i>	<i>V.</i>	<i>E.A</i>	<i>L.A</i>	<i>D.</i>	<i>V.</i>	<i>E.A.</i>	<i>L.A.</i>	<i>D.</i>	<i>V.</i>	<i>E.A</i>	<i>L.A</i>	<i>D.</i>	<i>V.</i>	<i>E.A</i>	<i>L.</i>	<i>D.</i>
24 hrs	DMSO	80.5	12.5	5.53	1.46	81.2	11.0	6.28	1.54	78.9	13.8	5.79	1.51	77	13.7	7.7	1.65
	ARE 100	54.4	31.5	12.9	1.22	69.7	19.1	9.98	1.2	53.7	31.4	13.6	1.23	66.2	20.1	12.4	1.29
	ARE 250	45.5	31.8	21.1	1.5	57.2	21.8	19.2	1.84	33.4	30.6	33.8	2.14	55.6	21.4	20.7	2.4
	ARE 500	23.5	28.2	46.4	1.84	39.1	19.9	37.9	3.15	21.6	29.2	47.8	1.37	35.9	22	39.1	2.97
48 hrs	DMSO	91.6	5.23	1.18	1.95	89.7	5.41	2.04	2.87	87.9	7.52	1.77	2.85	86.6	7.38	2.53	3.45
	ARE 100	72.1	7.92	11.5	8.46	68.5	6.46	16.4	8.57	48.8	7	24.2	19.9	60	5.61	19.8	14.6
	ARE 250	36.9	10.4	29.8	22.8	44.1	6.31	30.9	18.7	27.7	9.93	37.4	25	32.1	4.64	38.7	24.6
	ARE 500	28.6	10.8	40.7	19.9	25.6	4.24	44.3	25.9	24.5	6.7	42	26.8	24.5	6.7	42	26.8
72 hrs	DMSO	86.5	10.3	2.7	0.46	76.7	15.7	6.48	1.08	81.5	12.7	4.79	0.97	70.2	16.8	10.5	2.48
	ARE 100	51.9	24.2	22.5	1.36	59.7	17.4	21.5	1.41	36.4	20.4	40.8	2.38	43.3	16.3	37.5	2.83
	ARE 250	18.5	29	50.8	1.64	18.9	18.7	59.8	2.51	8.39	24.7	65	1.89	10.9	14.7	72.8	1.69
	ARE 500	9.04	23.1	66.3	1.56	13.4	12.7	71.7	2.15	13.1	16.4	68.7	1.86	12.5	10.5	75.1	1.87

**Table 3.22** Percents of Typical Quadrant Analysis of Annexin V-apc/7AAD Flow Cytometry of HL-60 Cells Treated with ERE for 24, 48 and 72 h in the presence of zvad and nec-1

Time	zvad	-				+				-				+			
	nec-1	-				-				+				+			
	<i>Extracts</i>	<i>V.</i>	<i>E.A</i>	<i>L.A</i>	<i>D.</i>	<i>V.</i>	<i>E.A.</i>	<i>L.A.</i>	<i>D.</i>	<i>V.</i>	<i>E.A</i>	<i>L.A</i>	<i>D.</i>	<i>V.</i>	<i>E.A</i>	<i>L.</i>	<i>D.</i>
24 hrs	<b>DMSO</b>	80.5	12.5	5.53	1.46	81.2	11.0	6.28	1.54	78.9	13.8	5.79	1.51	77	13.7	7.7	1.65
	<b>ERE 100</b>	70.3	10.3	15.6	3.84	73.5	7.9	16.1	2.54	68	8.29	19	4.66	69.8	7.07	20.8	2.33
	<b>ERE 250</b>	66.5	8.74	19.3	5.47	63.2	7.54	25.7	3.54	61.9	8.29	23.7	6.11	66.5	6.82	23.3	3.35
	<b>ERE 500</b>	47.8	10.3	35.3	6.63	52.3	7.65	35.1	4.98	46.4	8.19	36.9	8.54	55.6	7.39	32.5	4.47
48 hrs	<b>DMSO</b>	89.3	9.03	0.88	0.78	87.6	8.77	1.95	1.67	85.2	11.8	1.6	1.39	83.8	11.2	2.87	2.16
	<b>ERE 100</b>	70.6	14.2	9.95	5.28	65	12.1	16.2	6.71	60	13.7	15.5	10.8	64.6	11.9	16.1	7.47
	<b>ERE 250</b>	49.4	18.9	20.6	11.2	55.3	13.8	19.2	11.7	43.4	18.1	22.4	16.1	42.6	12.5	28.1	16.8
	<b>ERE 500</b>	36.2	21.2	27.5	15.2	41.8	11.3	30	16.9	30.2	17.8	30.9	21.1	29.3	10.9	38.4	21.4
72 hrs	<b>DMSO</b>	87	3.23	0.5	0.5	77.3	13.9	7.68	1.16	82.1	11.2	5.67	1.04	69.8	15.9	12	2.32
	<b>ERE 100</b>	51	14.9	31.4	2.67	70.9	7.45	20.3	1.37	37.6	14.8	43.5	4.08	61.1	7.7	28.8	2.39
	<b>ERE 250</b>	34.6	14.2	47.8	3.39	25.8	10.1	61	3.14	12.8	15.9	66.5	4.86	10.6	8.97	77.3	3.13
	<b>ERE 500</b>	12.6	15.5	69.6	2.36	17.3	7.64	72.7	2.35	4.12	14.7	78.7	3	6	5.8	86.7	

ARE-induced apoptosis after pretreatment with 25 $\mu$ M zVAD-fmk for 1 h was observed (Table 3.22). 24 h treatment of ARE at a concentration of 100  $\mu$ g/ml or higher induced apoptosis in HL-60 cells, however zVAD revealed apoptotic cell death significantly. At this time point, it could be concluded that ARE induced apoptosis was caspase dependent cell death. However, it could be also concluded that cell death due to ARE did not 100 % depend on caspase cascade because there were still high percentage of apoptotic cell death. The constituents of ARE induced cell death in HL-60 cells in both caspase dependent and independent pathway for 24 h. In later time points ARE induced cell death dominantly late apoptosis or necrosis as being rapid acting feature of ARE. zVAD could not revealed ARE induced cell death at 48 and 72 h significantly. Cell death due to ARE stimulus depend more on caspase independent pathway than caspase-dependent at indicated time points. Necrostatin-1 did not effect ARE induced cell death, which were significantly deferent than ASE induced cell death.

It could be concluded that ARE induced cell death depend on dominantly caspase independent cell death, however there were still some constituted that induced caspase dependent cell death in HL-60 cell death. ARE did not have any constitute that induced apoptosis in HL-60 cells with Necrostatin-1 related pathway. Other apoptotic pathway analysis had to be done to be 100 % sure.

ERE-induced apoptosis after pretreatment with 25 $\mu$ M zVAD-fmk for 1 h was observed (Table 3.23). 24 h treatment of ERE at concentration of 100-500  $\mu$ g/ml although there were apoptotic cell death at lower concentrations zvad did not affect the apoptosis induction, however at concentration of 500  $\mu$ g/ml zvad revealed ERE induced apoptosis in HL-60 cells. ERE did not induce apoptosis via caspase dependent cell death dominantly. Caspase independent cell death did not revealed by Necrostatin-1, contarily nec-1 induced cell death in HL-60 cells in the presence of ERE. These findings also indicated that *Rheum ribes* extracts could change the cell death mechanism of other drugs. Further analysis or isolation of constitutes of *Rheum ribes* could finalize which cell death mechanism was induced with.

### **3.15 Effect of *Rheum ribes* on CYP1A1 and CYP 1B1 mRNA Expressions in HL-60 cells**

Chemopreventive substances show their effects by delaying or reversing the process of carcinogenesis at various points. Such mechanisms may be divided as blocking effects and suppressing effects. The earliest stage is the direct inhibition of free radical mediated DNA damage that leads to mutagenesis (Newmark, 1992). The other way is to enhance the ability of target tissues to metabolize mutagens. At the site of first entry, these mutagens are metabolized in phase I reactions by cytochrome P-450 (CYPs) enzymes and are then conjugated (phase II biotransformation) to make them more water soluble and ready for excretion. The phase I and II enzymes occur in the intestinal mucosa as well as the liver. Some of these enzymes are ubiquitously present in other major organs of the body. The flavonoids have been reported to modulate the activities of these enzymes and needs to be explored (Johnson, 1994).

The effects of 24 h treatment of 100 µg/ml of ESE and ERE on expression levels of CYP 1B1 and CYP1A1 gene in HL-60 cells were investigated. (Table 3.24; 25) It could be concluded ESE and ERE decreased CYP1B1, whereas increased CYP1A1 gene expression. The effects of ERE significantly different and higher than ESE. (Fig 3.53; 54)

The *Rheum ribes* constituted effects on CYP1B1 expression in a time dependent manner, however CYP1A1 induction could not be changed significantly with time.

**Table 3.23** Effects of 100  $\mu\text{g/ml}$  of ESE and ERE treatment on CYP 1B1 gene expression in HL-60 cells for 24 hours

Extracts	Time (h)	
	24	48
ESE 100	↓1.958 fold	↓4.11 fold
ERE 100	↓5.38 fold	↓14.02 fold

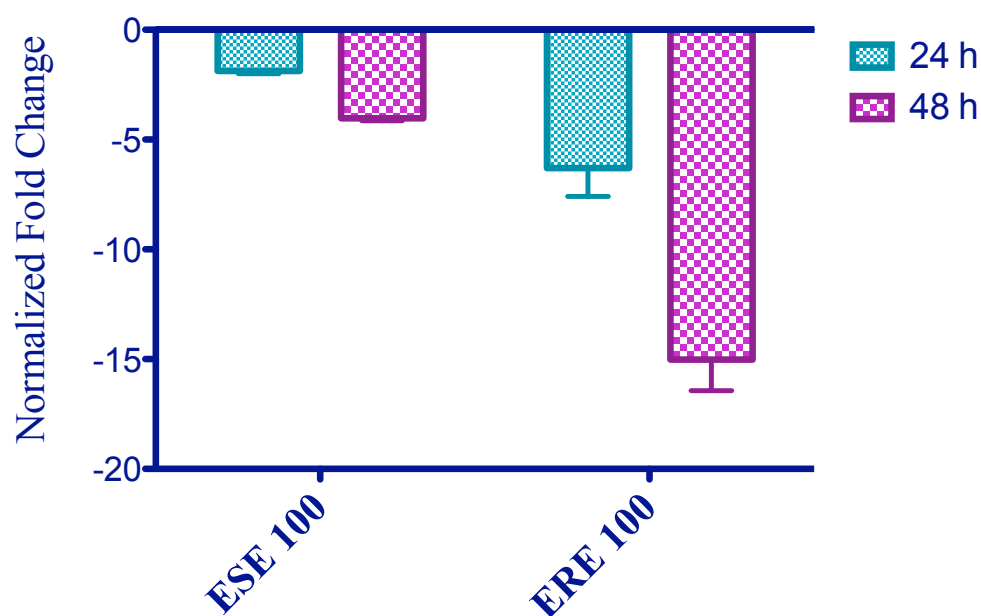


**Figure 3.53** Expression of CYP1B1 genes in HL-60 cells upon treatment with 100  $\mu\text{g/ml}$  of ESE and ERE for 24 and 48 hours. The values are the average of triplicate measurements from two biological replicates.

**Table 3.24** Effects of 100 µg/ml of ESE and ERE treatment on CYP 1A1 gene expression in HL-60 cells for 24 hours

Extracts	Time (h)	
	24	48
ESE 100	↑ 2.47 fold	↑ 2.67 fold
ERE 100	↑ 5.09 fold	↑ 5.39 fold

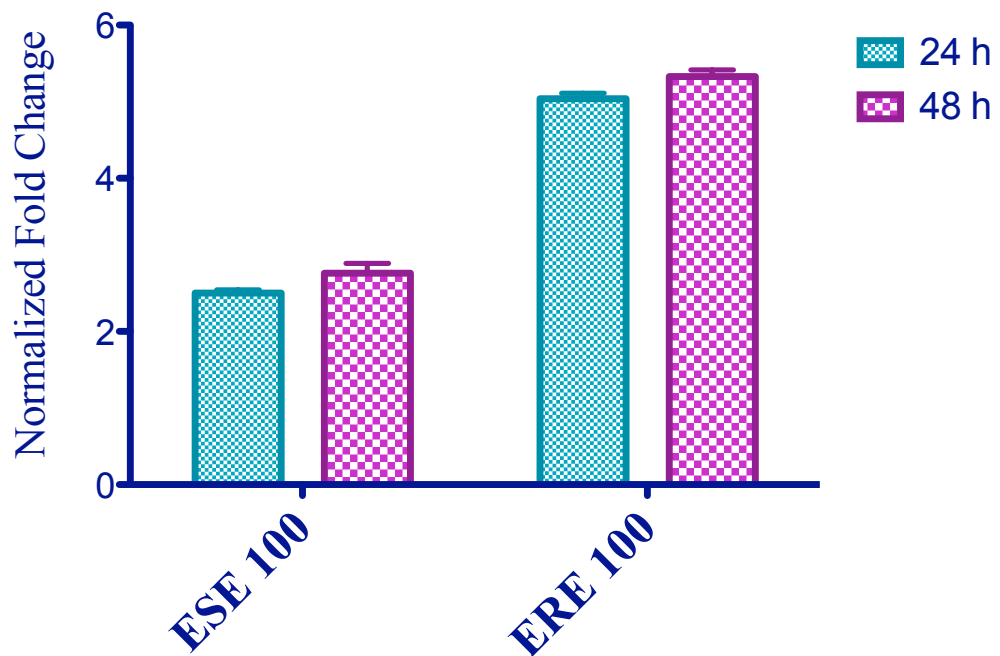


**Figure 3.54** Expression of CYP1A1 genes in HL-60 cells upon treatment with 100 µg/ml of ESE and ERE for 24 and 48 hours. The values are the average of triplicate measurements from two biological replicates

### 3.16 Effect of *Rheum ribes* on GST Enzyme Activity in HL-60 cells

GSTs are the major Phase II detoxifying enzymes and have many other important functions in the cell as well as their role in apoptosis. Therefore, we studied the effect of *Rheum ribes* on GST enzyme activities of HL-60 cells.

GST activity was increased statistically significantly with respect to DMSO control, while it was decreased to control levels at higher ESE concentrations. The increase in GST activity at low ESE concentrations might be the protective response of cells against ROS generation, however, at higher concentrations of ESE, GSH depletion may occur in a short time resulting in drop in GST activity, and the cells began to die as shown in Table 3.26.

**Table 3.25** Effects of ESE treatment on GST Enzyme Activity in HL-60 cells with the indicated concentrations for 24, 48 and 72 hours

<b>Time (hr)</b> <b>ESE (<math>\mu\text{g/ml}</math>)</b>	<b>24</b>	<b>48</b>	<b>72</b>
<b>0</b>	53.65 $\pm$ 3.42	132.44 $\pm$ 19.57	183.19 $\pm$ 15.53
<b>25</b>	55.88 $\pm$ 7.91	183.19 $\pm$ 5.70	123.32 $\pm$ 9.80
<b>50</b>	60.84 $\pm$ 8.61	139.95 $\pm$ 13.21	119.42 $\pm$ 28.58
<b>100</b>	43.69 $\pm$ 16.42	103.05 $\pm$ 10.31	122.37 $\pm$ 3.78
<b>200</b>	27.04 $\pm$ 2.96	68.99 $\pm$ 5.86	140.76 $\pm$ 5.00
<b>300</b>	22.00 $\pm$ 1.54	39.26 $\pm$ 5.86	20.37 $\pm$ 4.40

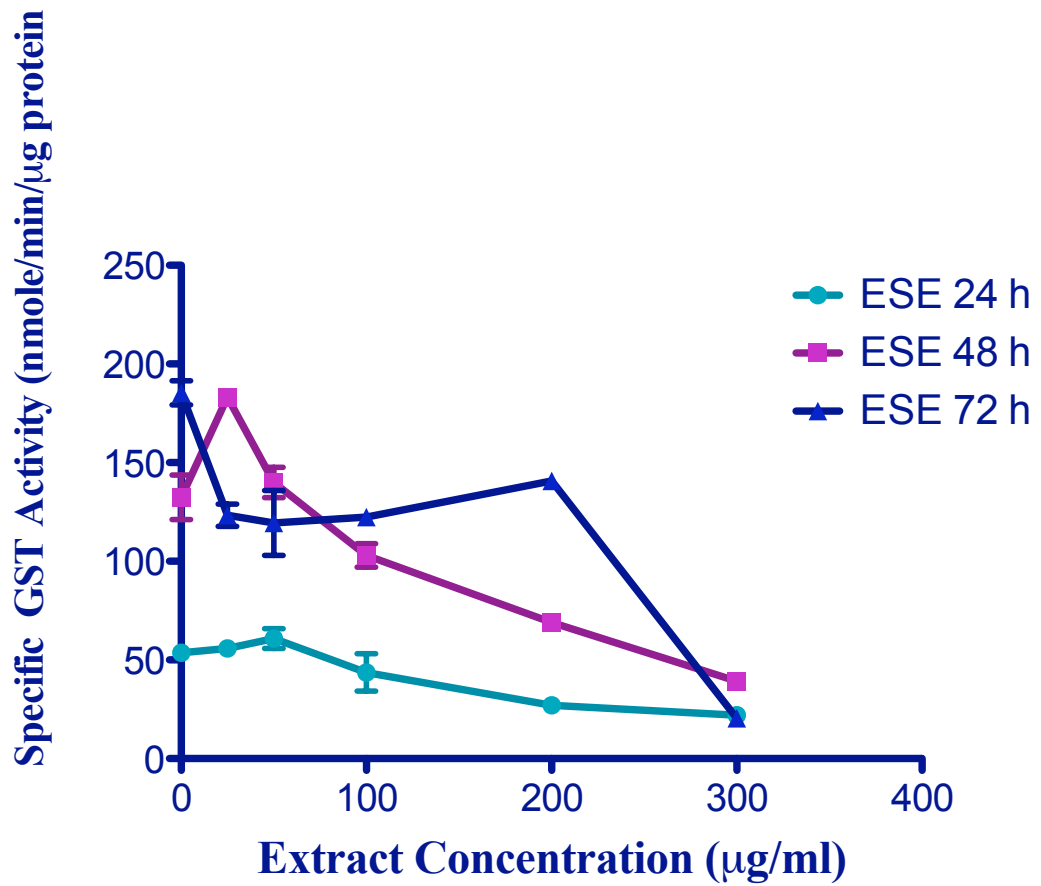


**Figure 3.55** Effects of ESE treatment at the indicated concentrations for 24, 48 and 72 h on GST activity against CDNB in HL-60 cells. Each data point is given as the means±SD. from at least three independent experiments. (\*) Significantly different when compared to vehicle (0.1 % DMSO)-treated groups ( $p < 0.05$ ).

The increase in GST activity at early time point with increasing concentrations of ERE might be the protective response of cells against ROS generation, however, for late time points at higher concentrations of ERE, GSH depletion may occur in a short time resulting in drop in GST activity, and the cells began to die as shown in Table 3.27. Figure 3.56 were showing GST enzyme activity of HL-60 cells at 24, 48 and 72 h. GST activity of DMSO controls were accepted as 100% activity, changes in other samples' activities were calculated with respect to 0.1% DMSO control.

**Table 3.26** Effects of ERE treatment on GST Enzyme Activity in HL-60 cells with the indicated concentrations for 24, 48 and 72 hours

<b>Time (hr)</b>	<b>24</b>	<b>48</b>	<b>72</b>
<b>ERE (<math>\mu\text{g/ml}</math>)</b>			
<b>0</b>	53.65 $\pm$ 3.42	132.44 $\pm$ 19.57	183.19 $\pm$ 15.53
<b>25</b>	216.74 $\pm$ 7.91	492.37 $\pm$ 72.79	474.28 $\pm$ 20.11
<b>50</b>	218.84 $\pm$ 32.35	315.20 $\pm$ 21.60	350.05 $\pm$ 14.84
<b>100</b>	159.97 $\pm$ 12.72	264.20 $\pm$ 18.11	427.39 $\pm$ 55.29
<b>200</b>	132.44 $\pm$ 19.58	66.58 $\pm$ 5.04	67.86 $\pm$ 2.88
<b>300</b>	215.34 $\pm$ 31.83	64.15 $\pm$ 3.73	66.58 $\pm$ 5.04

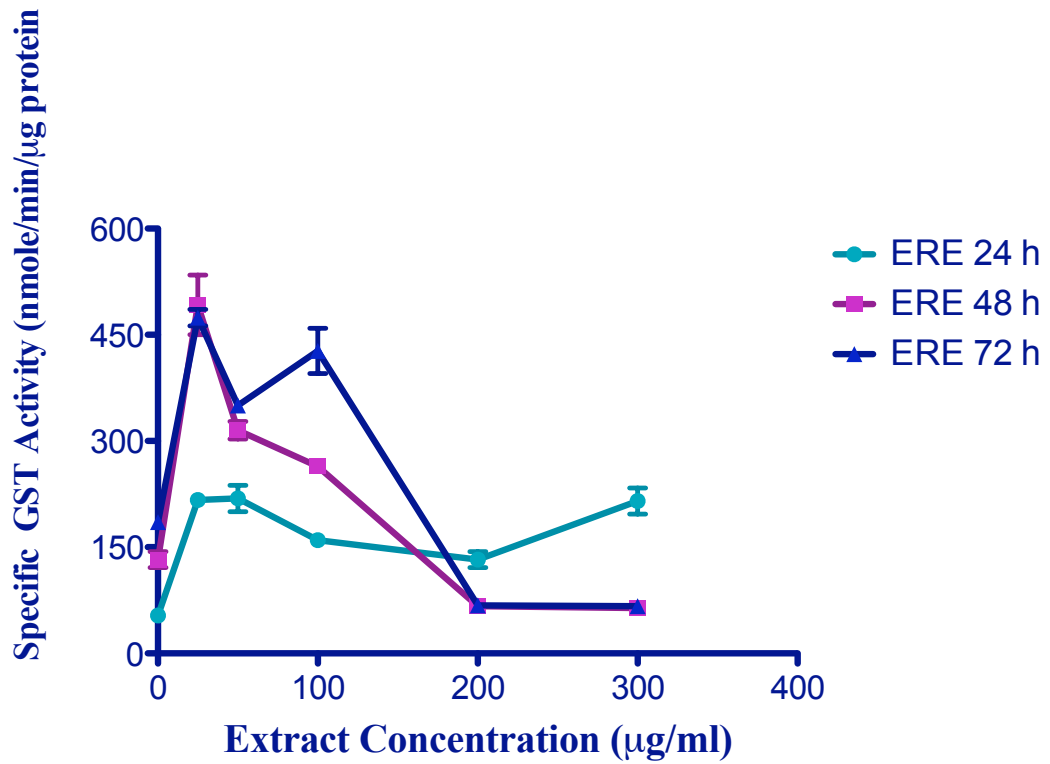


**Figure 3.56** Effects of ERE treatment at the indicated concentrations for 24, 48 and 72 h on GST activity against CDNB in HL-60 cells. Each data point is given as the means±SD. from at least three independent experiments. (\*) Significantly different when compared to vehicle (0.1 % DMSO)-treated groups ( $p < 0.05$ ).

## CHAPTER IV

### 4. CONCLUSION

*Rheum ribes* shoot and root dry powder samples were prepared and extracted with four different solvents namely ethyl acetate, methanol, ethanol and water. Additionally, 70% methanol extracts were fractionated with chloroform and n-butanol in order to gather all the biologically active compounds from the plant by polarity differentiation. The obtained *Rheum ribes* freeze-dried extracts and fractions were characterized by their antioxidant capacity and total polyphenol and flavonoid contents. Different biological activities of the extracts were determined by their cytotoxic and apoptotic properties on HL-60 cell with its mechanism of action in this study.

The major findings were as follows;

The polar solvents achieved the highest yield for extractable substances. The order of the yields from high to low was: Water > Ethanol  $\geq$  Methanol > Ethyl acetate.

All of the extracts and fractions had absorption maxima characteristic of hydroxyanthraquinones and their derivatives and flavonoids, since it was reported as the peaks around 240 nm, 270 nm and 400 nm are the characteristic peaks for phenolic anthraquinones (Rajendran, 2007).

The values of % of antioxidant activity (%RSA) were found to be inversely proportional to EC<sub>50</sub> values. The smaller the EC<sub>50</sub> value the greater the RSA and reducing ability of *Rheum ribes*. The order of % RSA of *Rheum ribes* was ASE < WSE < MSE < WRE < ESE < MRE < ERE < ARE.

The order of  $EC_{50}$   $ARE < ERE < MRE < WRE < WSE < ESE < MSE < ASE$ . All of the extracts and fractions reached over 90 % RSA except ASE at extract concentrations of 0.0026–1.33 mg/ml in 30 min.

Total phenolic compounds of the shoot and root extracts of *Rheum ribes* prepared in ethyl acetate, methanol, ethanol and water were determined as mg equivalents of gallic acid per g of crude extracts. MRE presented the highest total phenolic content, among the others, however the phenolic content of WRE was statistically lower than all. MSE presented the highest total phenolic content; among the other shoot extracts, although it was still not significantly different than ASE, ESE and WSE. Total phenolic content of shoot extracts significantly increased after fractionation, however it was not same for root fractions.

Total flavonoid compounds of the shoot and root extracts of *Rheum ribes* prepared in ethyl acetate, methanol, ethanol and water were determined as mg equivalents of catechin per g of crude extracts. ERE presented the highest total flavonoid content, among the others, however the flavonoid content of WRE was statistically lower than all. WSE presented the highest total phenolic content; among the other shoot extracts, on the other hand the flavonoid content of ASE was statistically lower than all.

From the chemical analysis of *Rheum ribes* extracts; ASE has the least effective extract among all shoot extract. Shoot extract with lowest polarity has least antioxidative activity with least phenolic flavonoid content.

During plant extraction using different polarity solvents change the extraction efficiency. Although yields were almost similar between shoot and root extracts in all solvent systems, the antioxidative properties and total phenolic and flavonoid contents were different in different solvent systems. If we were extracting shoot it would be better to use more polar solvents, whereas root extraction is better when we use less polar solvents.

Biological activity studies were carried out using HL-60 cells. *Rheum ribes* extract prepared in ethyl acetate, ethanol and water were applied at different concentrations for 24, 48 and 72 h to the feeding environment of the cells. As a

conclusion, ARE had the highest potential among all extracts with lower IC<sub>50</sub> for all time points from the obtained results of both trypan blue and XTT assay.

Additionally, flow cytometric analysis of *Rheum ribes* induced exposure of phosphatidylserine (PS) on the outside of the plasma membrane a characteristic event in early stages of apoptosis were detected by Annexin V-apc staining and it was observed that ARE and ERE induced apoptosis in HL-60 cells with a lower effective concentration than other extracts. These results demonstrated that there was a dose and time-dependent fashion in *Rheum ribes* induced apoptosis, which had also shown variations depending on the extract type.

Flow cytometric analysis also indicated that, *Rheum ribes* aqueous extract of both shoots and roots induced apoptosis with a concentration of higher than 1000 µg/ml.

TUNEL method indicated the presence of apoptosis in HL-60 cells at 100 µg/ml ESE and ERE treatment for 16 hours.

As evidenced by DNA fragmentation, it appears that apoptosis is the main mechanism for cell killing in the presence of ESE, ERE, WSE and WRE. The apoptosis-inducing effect of them in HL-60 cells appeared in a concentration-dependent manner. This efficacy was found to be similar to its cytotoxic activity in HL-60 cells.

Apoptosis is also tightly regulated by a series of genes. The Bcl-2 protein family is an important regulator of apoptosis, which consists of anti-apoptotic (such as Bcl-2) and pro-apoptotic members (such as Bax). Bcl-2 has been shown to have the ability to prevent cytochrome c release from the mitochondria, which is an important event during apoptosis mediated by mitochondrial pathways, but overexpression of pro-apoptotic Bax induces the release of cytochrome c from the mitochondria. Whereas, when Bcl-2 heterodimerizes with Bax, it abrogates the ability of Bax and blocks apoptosis in cells. ESE and ERE induced apoptosis through distinctly down regulated Bcl-2 gene levels and slightly up regulate expression of Bax gene levels. However, there were no evidence in the increase of Bax protein levels at the indicated dose and time points.

*Rheum ribes* lead to cytochrome c translocation from mitochondria into cytosol.

*Rheum ribes* induced apoptosis depend more on caspase independent pathway than caspase-dependent.

Chemopreventive effects of *Rheum ribes* were investigated at the gene level of CYP1B1 and CYP1A1, and GST enzyme activity against cDNB. As a conclusion, *Rheum ribes* modulated activities of these enzymes generally at a time dependent level, thus promising for the prevention and therapy of cancer and needs to be further explored.

Considering all the results obtained in the present study, *Rheum ribes* could be considered as a dietary antioxidant and anticancer agent. Our investigations for the pursuit of these interactions may not result in hundred percent prevention or in total cure of cancer, but this was a rational way forward, to catch on to the cutting-edge technologies.

## REFERENCES

- Abu-Irmaileh, B. E., & Afifi, F. U. (2003). Herbal medicine in Jordan with special emphasis on commonly used herbs. *Journal of Ethnopharmacology*, 89, 193–197.
- Alasalvar, C., Grigor, J. M., Zhang, D., Quantick, P. C., & Shahidi, F. (2001). Comparison of volatiles, phenolics, sugars, antioxidant vitamins, and sensory quality of different colored carrot varieties. *Journal of Agricultural Food Chemistry*, 49, 1410–1416.
- Amr, A., & Al-Tamimi, E. (2007). Stability of the crude extracts of *Ranunculus acris* anthocyanins and their use as food colourants. *Journal of Food Science and Technology*, 42, 985–991.
- Arends, M.J., Morris, R.G., Wyllie, A.H., (1990). "Apoptosis: The role of the endonuclease", *Am. J. Pathol.*, March 136, Vol 3, pp.593-608.
- Arends, M.J., Wylie, A.H., (1991). "Apoptosis: Mechanisms and roles in pathology", *Int. Rev. Exp. Pathol.*, Vol 32, pp.223-254.
- Awika, J. M., Rooney, L. W., & Waniska, R. D. (2005). Anthocyanins from black sorghum and their antioxidant properties. *Food Chemistry*, 90, 293–301.
- Balasundram, N., Sundram, K., & Samman, S. (2006). Phenolic compounds in plants and agri-industrial by-products: Antioxidant activity, occurrence, and potential uses. *Food Chemistry*, 99, 191–203.
- Barlow, S.N. (1990) Toxicological aspects of antioxidants used as food additives. *Food antioxidants*, Elsevier , pp. 253–307.
- Başağa H., Poli., Tekkaya C., Aras İ., (1997). Free radical scavenging and oxidative properties of silybin complexes on microsomal lipid peroxidation. *Cell. Biochem. Func.* 15, 1:27-33.

Batist, G., Tulpule, A., Sinha, B.K., Katki, A.G., Myers, C.C. and Cowan, K.H., (1986). "Overexpression of a Novel Anionic Glutathione S- Transferase in Multidrug Resistant Human Breast Cancer Cells", *J. Biol. Chem.*, Vol 261, pp.1544-1549.

Baydar, N. G., Ozkan, G., & Sagdic, O. (2004). Total phenolic contents and antibacterial activities of grape (*Vitis vinifera* L.) extracts. *Food Chemistry*, 15, 335–339.

Baytop, T. (1999). *Rheum ribes* L. In T. Baytop (Ed.). *Therapy with medicinal plants in Turkey* , *Nobel Tip Publication Press*, 1, pp. 319–320).

Bazzas, B. S. F., Khajehkaramadin, M., & Shokoheizadeh, H. R. (2005). In vitro antimicrobial activity of *Rheum ribes* extract obtained from various plant parts against clinical isolates of gram-negative pathogens. *Iranian Journal of Pharmaceutical Research*, 2, 87–91.

Beckman, C.H., (2000). *Physiol. Mol. Plant Pathol.* 57 101.

Bleve, M., Ciurlia, L., Erroi, E., Lionetto, G., Longoc, L., Rescioa, L., (2008). An innovative method for the purification of anthocyanins from grape skin extracts by using liquid and sub-critical carbon dioxide. *Separation and Purification Technology*, 64, 192 197.

Blois, M.S., (1958). Antioxidant determinations by use of a stable free radical. *Nature*, 181, 1199-1200

Bonjar, G. H. S. (2004a). Evaluation of antibacterial properties of Iranian medicinal-plants against *Micrococcus luteus*, *Serratia marcescens*, *Klebsiella pneumoniae* and *Bordetella bronchoseptica*. *Asian journal of Plant Science*, 3, 82–86.

Boyland, E. and Chasseaud, L.F., (1969). "The role of glutathione and glutathione S-transferases in mercapturic acid biosynthesis", *Adv. Enzymol. Rel. Areas Mol. Biol.*, Vol 32, pp.173-219.

Bravo, L. (1998). Polyphenols: Chemistry, dietary sources, metabolism, and nutritional significance. *Nutrition Reviews*, 56317, 333.

Bucic'-Kojic', A., Planinic', M., Tomas, S., Bilic', M., & Velic, D. (2007). Study of solid- liquid extraction kinetics of total polyphenols from grape seeds. *Journal of Food Engineering*, 81, 236-242.

Cai, Y., Sun, M., Xing, J., & Corke, H. (2004). Antioxidant phenolic constituents in roots of *Rheum officinale* and *Rubia cordifolia*: structure-radical scavenging activity relationships. *Journal of Agricultural Food Chemistry*, 52, 7884-7890.

Castañeda-Ovando, A., de Lourdes Pacheco-Hernández, Ma, Elena, Ma, Páez-Hernández, J. A., RodríguezGalán-Vidal, J. A., & Galán-Vidal, C. A. (2009). Chemical studies of anthocyanins: A review. *Food Chemistry*, 113, 859-871.

Caridi, D., Trenerry, V. C., Rochfort, S., Duong, S., Laughler, D., & Jones, R. (2007). Profiling and quantifying quercetin glucosides in onion (*Allium cepa* L.) varieties using capillary zone electrophoresis and high performance liquid chromatography. *Food Chemistry*, 105, 691-699.

Chabner, B., (1982). "Pharmacological Principle of Cancer Treatment", WB Saunders, Co., *Philadelphia*, pp.276-313

Chasseaud, L.F., (1979). "The role of glutathione and glutathione S-transferases in the metabolism of chemical carcinogens and other electrophilic agents", *Adv. Cancer. Res.*, Vol 29, pp.175-274.

Collins, S.J., (1987). "The HL-60 promyelocytic leukemia cell line: proliferation, differentiation, and cellular oncogene expression", *Blood*, Vol 70, pp.1233-1244.

Cook, A.R., (1996). "Leukemia In: The new cancer sourcebook", Omnigraphics, Inc., Detroit, pp.593-627

Corrales, M., Fernández García, A., Butz, P., & Tauscher, B. (2009). Extraction of anthocyanins from grape skins assisted by high hydrostatic pressure. *Journal of Food Engineering*, 90, 415-421.

Cullen, J. (1966). *Rheum* L. In PH. Davis (Ed.). *Flora of Turkey and the East Aegean Islands*. Edinburgh: Edinburgh University Press, 2, pp. 268-269.

Dalton, W.T., Jr Ahearn, M.J., McCredie, K.B., Freireich, E.J., Stass, S.A. and Trujillo, J.M., (1988). "HL-60 cell line was derived from a patient with FAB-M2 and not FAB-M3", *Blood*, January, Vol 71 (1), pp.242-247.

D'Archivio, M., Filesi, C., Di Benedetto, R., Gargiulo, R., Giovannini, C., & Masella, R.(2007). Polyphenols, dietary sources and bioavailability. *Annali dell'Istituto Superiore di Sanità*, 43(4), 348–361.

Darzynkiewicz, Z., Juan, G., Li, X., Gorczyca, W., Murakami, T. And Traganos, F., (1997), "Cytometry in cell necrobiology: analysis of apoptosis and accidental cell death (necrosis)", *Cytometry*, Vol 27, pp.1-20.

Datta, S.R., Dudek, H., Tao, X., Masters, S., Fu, H., Gotoh, Y. and Greenberg, M.E., (1997). "Akt phosphorylation of BAD couples survival signals to the cell- intrinsic death machinery", *Cell*, Vol 91, pp.231-241

Desagher, S., Osen-Sand, A., Nichols, A., Eskes, R., Montessuit, S., Lauper, S., Maundrell, K., Antonsson, B. and Martinou, J.C., (1999). "Bid-induced conformational change of Bax is responsible for mitochondrial cytochrome c release during apoptosis", *Jornal of Cell Biology*, Vol 144, pp.891-901.

Deveraux, Q.L., Takahashi, R., Salvesen, G. and Reed J., (1997). "X-linked IAP is a direct inhibitor of cell-death proteases", *Nature*, Vol 388, pp.300-304.

Escarpa, A., Morales, M. D., & Gonzalez, M. C. (2002). Analytical performance of commercially available and unavailable phenolic compounds using real samples by high-performance liquid chromatography-diode array detection. *Analytica Chimica Acta*, 460, 61–72.

Fadok, V. A., Voelker, D.R., Campbell, P.A., Cohen, J.J., Bratton, D.L., Henson, P.M., (1992). "Exposure of phosphatidylserine on the surface of apoptotic lymphocytes triggers specific recognition and removal by macrophages", *Journal of Immunology*, 148, pp.2207-2216.

Fernandez Garcia, A., Butz, P., & Tauscher, B. (2001). Effects of high pressure processing on carotenoid extractability, antioxidant activity, glucose diffusion and water binding of tomato puree (*Lycopersicum Sculentum* Mill). *Journal of Food Science*, 66, 1033–1038.

Fredj, D., Francois, D. (1990), Purification of colored substances, especially anthocyanosides, from berries. Patent No. FR 2641283.

Freshney, R. I., (2005). "Culture of Animal Cell: A manual of Basic Technique", (5<sup>th</sup> Edition).

Gallagher, R., Collins, S., Trujillo, J., McCredie, K., Ahearn, M., Tsai, S., Metzgar, R., Aulakh, G., Ting, R., Ruscetti, F. and Gallo, R., 1979. "Characterization of the continuous, differentiating myeloid cell line (HL-60) from a patient with acute promyelocytic leukemia", *Blood*, Vol 54, pp.713-733.

Giusti, M. M., & Wrolstad, R. E. (2003). Acylated anthocyanins from edible sources and their applications in food systems. *Biochemical Engineering Journal*, 14, 217–225.

Goping, I.S., Gross, A., Lavoie, J.N., Nguyen, M., Jemmerson, R., Roth, K., Korsmeyer, S.J. and Shore, G.C., (1998). "Regulated targeting of BAX to mitochondria", *Journal of Cell Biology*, Vol 143, pp.207-215.

Gordon, M. H. (1996). Dietary antioxidants in disease prevention. *Natural Products Reports*, 265, 273.

Grice, H. P. (1988). Enhanced tumour development by butylated hydroxyanisole (BHA) from the prospective of effect on forestomach and oesophageal squamous epithelium. *Food and Chemical Toxicology*, 26, 717–723.

Gulcin, I., Oktay, M., Kirecci, E., & Kurevioglu, O. \_I. (2003). Screening of antioxidant and antimicrobial activities of anise (*Pimpinella anisum* L.) seed extracts. *Food Chemistry*, 83, 371–382.

Guner A, Ozhatay N, Ekim T, Baser KHC (Eds.) (2000). Flora of Turkey and the East Aegean Islands. Vol. 11 (Supplement 2), Edinburgh University Press, Edinburgh.

Halliwell, B., & Gutteridge, J. M. (1984). Oxygen toxicology, oxygen radicals, transition metals and disease. *Biochemical Journal*, 219, 1–4.

Halliwell, B., Gutteridge, J.M.C., (1990). Free Radicals in Biology and Medicine. *Clarendon Press*, Oxford, 2nd Eds.

Halliwell, B., Murcia, A., Chiricio, S., Aruoma, O.L., (1995). Free radicals and antioxidant in food and in vivo : What they do and how they work?, *Critical Reviews in Food Science and Nutrition*, Vol.35, 7-20.

Harborne, J.B., (1982). Introduction to Ecological Biochemistry, second ed., Academic Press, New York, NY.

Harborne, J.B., Turner, B.L., (1984). Plant Chemosystematics, Academic Press, London, UK.

Harman D, (1969). Prolongation of life: Role of free radical reaction in aging. *Journal of the American Geriatrics Society*, 17, 721-732.

Hayouni, E. A., Abedrabba, M., Bouix, M., & Hamdi, M. (2007). The effects of solvents and extraction method on the phenolic contents and biological activities in vitro of Tunisian *Quercus coccifera* L. and *Juniperus phoenicea* L. fruit extracts. *Food Chemistry*, 105, 1126–1134.

Havsteen, (2002) B.H. Havsteen, The biochemistry and medical significance of the flavonoids, *Pharmacol. Therapeutics* 96, pp. 67–202

Hollman, P. C. H., & Katan, M. B. (1999). Dietary flavonoids: Intake, health effects and bioavailability. *Food and Chemical Toxicology*, 37, 937–942.

Hui, L., Bo, C., & Shouzhuo, Y. (2005). Application of ultrasonic technique for extracting chlorogenic acid from *Eucommia ulmoides* Oliv. (*E. ulmoides*). *Ultrasonics Sonochemistry*, 12, 295–300.

Jing, W., Baoguo, S., Yanping, C., Yuan, T., & Xuehong, L. (2008). Optimisation of ultrasound-assisted extraction of phenolic compounds from wheat bran. *Food Chemistry*, 106, 804–810.

Kane, D. J., Sarafian, T. A., Anton, R., Gralla, E. B., Valentine, J. S., Ord, T. and Bredesen, D.E., (1993). “Bcl-2 inhibition of neural death: decreased generation of reactive oxygen species”; *Science*, Vol 262, pp.1274-1277.

Kapasakalidis, P. G., Rastall, R. A., & Gordon, M. H. (2006). Extraction of polyphenols from processed black currant (*Ribes nigrum* L.) residues. *Journal of Agricultural and Food Chemistry*, 54, 4016–4021.

Kashiwada, Y., Nonaka, G., Nishioka, I., & Yamagishi, T. (1988). Galloyl and hydroxycinnamoyl glucoses from Rhubarb. *Phytochemistry*, 27, 1473–1477.

Kharbanda, S., Pandey, P., Schofield, L., Israels, S., Roncinske, R., Yoshida, K., Bharti, A., Yuan, Z.M., Saxena, S., Weichselbaum, R., Nalin, C. and Kufe, D., 1997. “Role for Bcl-XL as an inhibitor of cytosolic cytochrome C accumulation in DNA damage-induced apoptosis”, *Proc. Natl. Acad. Sci. USA*, Vol 94, pp.6939–6942.

King, R.J.B., (2000). *Cancer Biology* (2nd Edition), Chapter 7, Chemical Carcinogenesis, pp.81-94.

Kluck, R. M., Bossy-Wetzel, E., Green, D. R. and Newmeyer, D. D., (1997). “The release of cytochrome c from mitochondria: a primary site for Bcl-2 regulation of apoptosis”, *Science*, Vol 275, pp.1132-1136.

Kogure, K., Yamauchi, I., Tokumura, A., Kondou, K., Tanaka, N., Takaishi, Y., et al. (2004). Novel antioxidants isolated from plants of the genera *Ferula*, *Inula*, *Prangos* and *Rheum* collected in Uzbekistan. *Phytomedicine*, 11, 645–651.

Krenn, L., Presse, A., Prodhon, R., Bahr, B., Paper, D. H., Mayer, K. K., et al. (2003). Sulfemodin 8-O-b-D glucoside, a new sulfated anthraquinone glycoside, and antioxidant phenolic compounds from *Rheum emodi*. *Journal of Natural Products*, 66, 1107–1109.

Kroemer, G., Dallaporta, B. and Resche-Rigon M., (1998). “The Mitochondrial Death/Life Regulation in Apoptosis and Necrosis”, *Annual Review of Physiology*, March Vol 60, pp.619-642.

Lapornik, B., Prosek, M., & Golc, Wondra. A. (2005). Comparison of extracts prepared from plant by-products using different solvents and extraction time. *Journal of Food Engineering*, 71, 214–222.

Leonard, S. S., Keil, D., Mehlman, T., Proper, S., Shi, X., & Harris, G. K. (2006). Essiac tea: scavenging of reactive oxygen species and effects on DNA damage. *Journal of Ethnopharmacology*, 103, 288–296.

Li, J, Kim, J.M., Liston, P., Li, M., Miyazaki, T., Mackenzie, A.E., Korneluk, R.G., Tsang, B.K., 1998 “Expression of inhibitor of apoptosis proteins (IAPs) in rat granulosa cells during ovarian follicular development and atresia”, *Endocrinology*, March, Vol 139 (3), pp.1321-8.

Li, P., Nijhawan, D., Budihardjo, I., Srinivasula, S.M., Ahmad, M., Alnemri, E.S. and Wang, X., 1997. “Cytochrome c and dATP-dependent formation of Apaf-1/caspase-9 complex initiates an apoptotic protease cascade”, *Cell*, Vol 91, pp.479–489.

Liu, Q., Cai, W., & Shao, X. (2008). Determination of seven polyphenols in water by high performance liquid chromatography combined with preconcentration. *Talanta*, 77, 679–683.

Lowry, O.H., Rosebrough, N.J., Farr, A.L. and Randal R.J., 1951. “Protein Measurement with the Folin Phenol Reagent”, *Journal of Biological Chemistry*, Vol 248, pp.265-275.

Luthria, D. L., & Pastor-Corrales, M. A. (2006). Phenolic acids content of 15 dry edible bean (*Phaseolus vulgaris* L.) varieties. *Journal of Food Composition and Analysis*, 19, 205–211.

Mattila, P., & Kumpulainen, J. J. (2002). Determination of free and total phenolic acids in plant derived foods by HPLC and diode array detection. *Journal of Agricultural and Food Chemistry*, 48, 3660–3667.

Matsuda, H., Morikawa, T., Toguchida, I., Park, J. Y., Harima, S., & Yoshikawa, M. (2001). Antioxidant constituents from Rhubarb: Structural requirements of stilbenes for the activity and structures of two new anthraquinone glucosides. *Bioorganic and Medicinal Chemistry*, 9, 41–50.

Merikli, A. H., & Tuzlacı, E. (1990). Constituents of *Rheum ribes*. *Fitoterapia*, 61, 375.

Müller, E., Berger, R., Blass E., Sluyts, D., & Pfennig, A. (2008). Ullmann’s encyclopedia of industrial chemistry, Liquid–Liquid Extraction.

Naczk, M., & Shahidi, F. (2006). Phenolics in cereals, fruits and vegetables: Occurrence, extraction and analysis. *Journal of Pharmaceutical and Biomedical Analysis*, 41, 1523–1542.

Nahar, L., & Sarker, S. D. (2005). Supercritical fluid extraction. *Natural Products Isolation*, 20, 47–76.

Namiki, M. (1990). Antioxidants/antimutagens in food. *Critical Reviews in Food Science and Nutrition*, 29, 273–300.

Nardini, M., Cirilo, E., Natella, F., Mencarelli, D., Comisso, A., & Scaccini, C. (2002). Detection of bound phenolic acids: Prevention by ascorbic acid and ethylenediaminetetraacetic acid. *Food Chemistry*, 79, 119–124.

Özbek, H., Ceylan, E., Kara, M., Özgökce, F., & Koyuncu, M. (2004). Hypoglycemic effect of *Rheum ribes* roots in alloxan induced diabetic and normal mice. *Scandinavian Journal of Laboratory Animal Science*, 31, 113–115.

Ozgekce F, Ozcelik H (2004). Ethnobotanical aspects of some taxa in East Anatolia (Turkey), *Econ. Bot.* 58: 697-704.

Ozturk M., F. Aydogmus-Ozturk, M.E. Duru and G. Topcu, Antioxidant activity of stem and root extracts of *Rhubarb* (*Rheum ribes*) An edible medicinal plant, *Food Chem* 103 (2007), pp. 623–630

Palma, M., & Taylor, L. T. (1999). Extraction of polyphenolic compounds from grape seeds with near critical carbon dioxide. *Journal of Chromatography A*, 849, 117–124

Penzes, I., Boross, M., Gergely, I., 1984. Causes of aging and biochemical possibilities for retardation of aging process. pp. 18-38 Academic Press New York.

Pickett, C.B., and Lu, A.Y.H., 1989. "Glutathione-S-Transferase: Gene Structure, Regulation and Biological Functions", *Ann. R. Biochem.*, Vol 60 (11), pp.1327-1332.

Pinelo, M., Rubilar, M., Sineiro, J., & Nunez, M. J. (2004). Extraction of antioxidant phenolics from almond hulls (*Prunus amygdalus*) and pine sawdust (*Pinus pinaster*). *Food Chemistry*, 85, 267–273.

Pinelo, M., Del Fabbro, P., Manzocco, L., Nunez, M. J., & Nicoli, M. C. (2005). Optimization of continuous phenol extraction from *Vitis vinifera* byproducts. *Food Chemistry*, 92, 109–117.

Popa, V. I., Agache, C., Beleca, C., & Popa, M. (2002). Polyphenols from spruce bark as plant growth regulator. *Crop Research*, 24, 398–406.

Popa, V. I., Dumitru, M., Volf, I., & Anghel, N. (2008). Lignin and polyphenols as allelochemicals. *Industrial Crops and Products*, 27, 144–149.

Popa, V.I., Danaila, M., Volf, I., Popa, M.I. (2007). Natural antioxidants from agroindustrial wastes sources, separation and practical implications. In: *Proceedings of the 8th ILI Forum* (pp. 67–70), Rome, 10–12.

Pridham, J.B., 1960. *Phenolics in Plants in Health and Disease*, Pergamon Press, New York, NY.

Punchard, N.A., and Kelly, F.G., 1996. *Free Radicals. A Pratical Approach*, pp. 149-221, Acedemic press, London.

Reed, D.J. and Fariss, M.W., 1984. "Glutathione depletion and susceptibility", *Pharmacol. Rev.*, Vol 36, pp.25-33.

Reed, D. C., 1997. "Cytochrome c: can't live with it--can't live without it", *Cell*, Vol 91, pp.559-562.

Ross, K. A., Beta, T., & Arntfield, S. D. (2009). A comparative study on the phenolic acids identified and quantified in dry beans using HPLC as affected by different extraction and hydrolysis methods. *Food Chemistry*, 113, 336–344.

Rothe, M., Pan, M. G., Henzel, W. J., Ayres, T. M. and Goeddel, D. V., 1995. "TNFR2-TRAF signaling complex contains two novel proteins related to baculoviral inhibitor of apoptosis proteins", *Cell*, Vol 83, pp.1243.

Rubilar, M., Pinelo, M., Franco, D., Sineiro, J., & Nunez, M. J. (2003). Residuos agroindustriales como fuente de antioxidants. *Afinidad*, 60, 153–160.

Russell, W. R., Scobbie L., Labat, A., Duncan, G. J. Duthie, G. G., (2008). Phenolic acid content of fruits commonly consumed and locally produced in Scotland. *Food Chemistry*. doi: 10.1016/j.foodchem.2008.11.086.

Salvesen, G.S. and Dixit, V.M., 1997. "Caspases: intracellular signaling by proteolysis", *Cell*, Vol 91, pp.443-446.

Scaffidi, C., Schmitz, I., Krammer, P. H. and Peter M. E., 1999. "The role of c-FLIP in modulation of CD95-induced apoptosis", *Journal of Biological Chemistry*, Vol 274, pp.1541–1548.

Enayat, S., Banerjee., S., 2009. Comparative antioxidant activity of extracts from leaves, bark and catkins of *Salix aegyptiaca* sp. *Food Chemistry*, Vol 116, pp 23-28

Shahidi, F., 2000. *Nahrung* 44, 158.

Shahidi, F., Naczk, M., 2004. *Phenolics in Food and Nutraceuticals: Sources, Applications and Health Effects*, CRC Press, Boca Raton, FL.

Shokravi, A., & Agha Nasiri, K. (1997). Synthesis of 1,2,3,4,5,6,7,8- Octahydro-9-ethoxy-10-hydroxy-1-anthracenone (OEHA). *Iranian Journal of Chemistry and Chemical Engineering*, 16, 10–15.

Singleton, R. Orthofer and R.M. Lamuela-Raventos, Analysis of total phenols and other oxidation substrates and antioxidants by means of Folin–Ciocalteu reagent, *Oxidants and Antioxidants*

Tabata, M., Sezik, E., Honda, G., Yesilada, E., Fuki, H., Goto, K., et al. (1994). Traditional medicine in Turkey III. Folk Medicine in East Anatolica, Van and Bitlis provinces. *International Journal of Pharmacognosy*, 32, 3–12.

Thornberry, N.A. and Lazebnik, Y., 1998. "Caspases: enemies within", *Science*, Aug 28, Vol 281 (5381), pp.1312-1316.

Tosun, F., & Akyuz-Kızılay, C. (2003). Anthraquinones and flavonoids from *Rheum ribes*. *Journal of Faculty of Pharmacy Ankara*, 32, 31–35.

Tsao, R., & Yang, R. (2003). Optimization of a new mobile phase to know the complex and real polyphenolic composition: Towards a total phenolic index using high-performance liquid chromatography. *Journal of Chromatography A*, 1018, 29–40.

Tuzlaci, E., & Mericli, A. H. (1992). Some studies on *Is kın* (*Rheum ribes*) and its distribution in Turkey. *Proceedings of the 9th symposium on plant drugs* (Pub No. 641, pp. 336–341). Eskişehir, Turkey: Anatolia University Press.

Valenzuela, A., Nieto, S., Cassels, B. K., & Speisky, H. (1992). Inhibitory effect of boldine on fish oil oxidation. *Journal of American Oil Chemists Society*, 68(9), 937.

Wang, S., & Huang, K. (2004). Determination of flavonoids by high performance liquid chromatography and capillary electrophoresis. *Journal of Chromatography A*, 1032, 273–279.

Wang, L., & Weller, C. L. (2006). Recent advances in extraction of nutraceuticals from plants. *Trends in Food Science and Technology*, 17, 300–312.

Wang, Z.-H., Hsu, C.-C., & Yin, M.-C. (2009). Antioxidative characteristics of aqueous and ethanol extracts of glossy privet fruit. *Food Chemistry*, 112, 914–918.

Wichi, H. C. (1986). Safety evaluation of butylated hydroxytoluene (BHT) in the liver, lung and gastrointestinal tract. *Food and Chemical Toxicology*, 24, 1127–1130.

Yang, E., Zang, J., Jockel, J., Boise, L.H., Thompson, C. B. and Korsmeyer, S. J., 1995. “Bad: a heterodimeric partner for Bcl-x and Bcl-2 displaces Bax and promotes cell death”, *Cell*, Jan 27, Vol 80 (2), pp.285-91.

Yesilada E, Sezik E, Honda G, Takaishi Y, Takeda Y, Tanaka T (1999). Traditional medicine in Turkey IX. Folk medicine in north-west Anatolia. *J. Ethnopharmacol.* 64: 195-210.

Zadernowski, R., Czaplicki, S., & Naczek, M. (2009). Phenolic acid profiles of mangosteen fruits (*Garcinia mangostana*). *Food Chemistry*, 112, 685–689.

Zha, J., Harada, H., Yang, E., Jockel, J. and Korsmeyer, S. J., 1996. “Serine phosphorylation of death agonist BAD in response to survival factor results in binding to 14-3-3 not BCL-XL”, *Cell*, Vol 87, pp.619-628.

Zhishen, T. Mengcheng and W. Jianming, The determination of flavonoid contents in mulberry and their scavenging effects on superoxide radicals, *Food Chemistry* 64 (4) (1999), pp. 555–559.

## Appendix A

### DPPH Assay Plate Design

	1	2	3	4	5	6	7	8	9	10	11	12
A	DPPH	DPPH +	2.60 +	5.21 +	10.42 +	20.83 +	41.67 +	83.33 +	166.67 +	333.33 +	666.67 +	1333.33 +
		MetOH	MetOH	MetOH	MetOH	MetOH	MetOH	MetOH	MetOH	MetOH	MetOH	MetOH
B	//	//	//	//	//	//	//	//	//	//	//	//
C	//	//	//	//	//	//	//	//	//	//	//	//
D	//	//	//	//	//	//	//	//	//	//	//	//
E	DPPH	DPPH+ MetOH	2.60 +	5.21 +	10.42 +	20.83 +	41.67 +	83.33 +	166.67 +	333.33 +	666.67 +	1333.33 +
		DPPH	DPPH	DPPH	DPPH	DPPH	DPPH	DPPH	DPPH	DPPH	DPPH	DPPH
F	//	//	//	//	//	//	//	//	//	//	//	//
G	//	//	//	//	//	//	//	//	//	//	//	//
H	//	//	//	//	//	//	//	//	//	//	//	//

**Figure A.1** Representative 96-well microtiter plate, indicating final concentrations of plant extracts

1st column: DPPH control, 2nd column: Methanol Control, 3rd-12th column contain equal amount of Methanol in the rows A-D, but each column contained extracts as horizontally increasing concentrations, 3rd-12th column contain equal amount of DPPH in the rows E-H, but each column contained extracts as horizontally increasing concentrations.

## Appendix B

### Standard Curve for Total Phenol Quantification

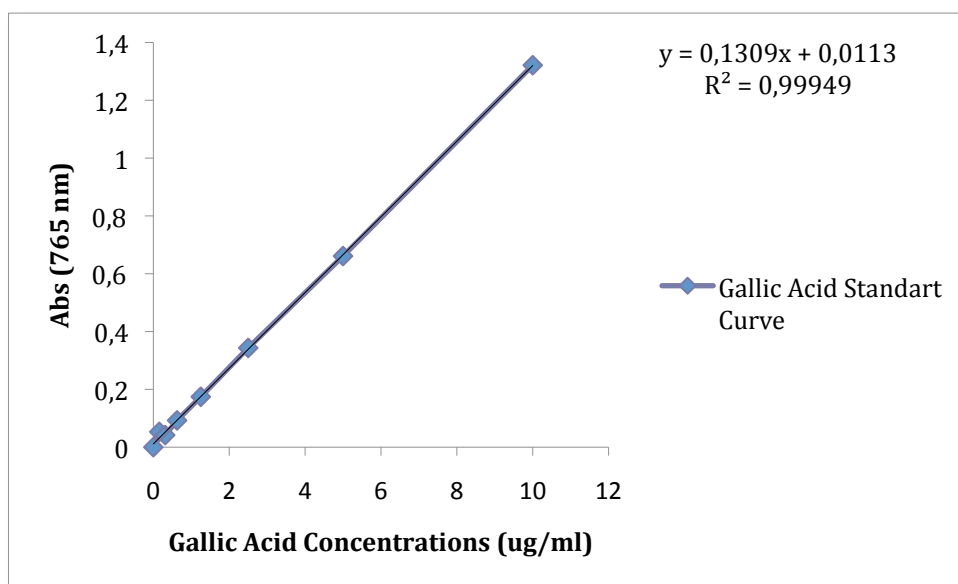


**Figure B.1** Gallic Acid Standart Curve obtained in Folin Ciocalteu Micro Method

## Appendix C

### Standard Curve for Total Flavanol Quantification

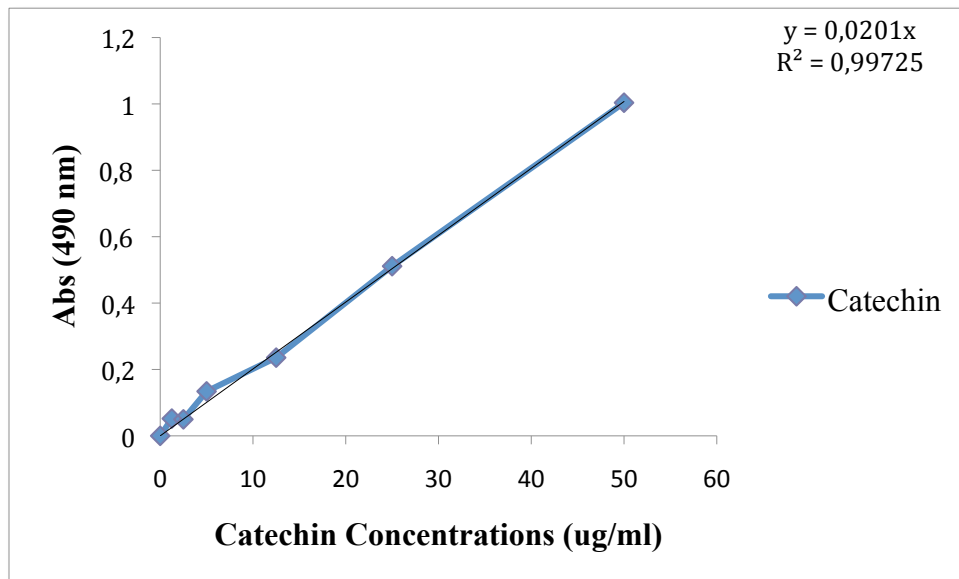


**Figure C.1** Catechin Standart Curve obtained in Aluminium Micro Method

## Appendix D

### XTT Assay Plate Design

	media	media	25	25	50	50	100	100	250	250	500	500
B	media	media	25	25	50	50	100	100	250	250	500	500
C	media	media	25	25	50	50	100	100	250	250	500	500
D	media	media	25	25	50	50	100	100	250	250	500	500
E	Dms0	dms0	25	25	50	50	100	100	250	250	500	500
F	dms0	dms0	25	25	50	50	100	100	250	250	500	500
G	Dms0	dms0	25	25	50	50	100	100	250	250	500	500
H	dms0	dms0	25	25	50	50	100	100	250	250	500	500

**Figure D.1** Representative 96-well microtiter plate, indicating concentrations of plant extracts where,

A-B 3-12: represents control wells, plant extract 1 no cells

C-D 3-12: represents plant extract 1 with cells

E-F 3-12: represents control wells, plant extract 2 no cells

G-H 3-12: represents plant extract 2 with cells

A-B 1-2: represents control wells, media no cells

C-D 1-2: represents control wells, media with cells

E-F 1-2: represents control wells, DMSO no cells

G-H 1-2: represents control wells, DMSO with cells

## Appendix E

### Buffers and Solutions

1. Homogenization Buffer:

- 1.15% (w/v) KCl, 25mM  $K_2HPO_4$ , 5mM EDTA, 0.2mM PMSF, 2mM DTT, pH 7.4

2. Trichloro Acetic Acid (TCA):

- 30% (w/v)

3. Butylated Hydroxy Toluene (BHT):

- 0.04M in ethanol

4. Thiobarbituric Acid (TBA):

- 1% (w/v) in 0.05N NaOH

5. Phosphate Buffered Saline (PBS):

- 18mM NaCl, 18mM  $Na_2HPO_4$ , pH 7.4

6. 2,4-Dinitrophenylhydrazine (DNPH):

- 10 mM in 2M HCl

7. Guanidine hydrochloride (GndHCl):

- 6 M in 20mM phosphate buffer, pH 2.5

8. Solution D (GTC solution).
  - 4M Guanidine isothiocyanide,
  - 25mM Sodium Citrate(pH:7.0)
  - 0.5% (w/v) L-Lauryl Sarcosine
  - 0.1 M 2-mercaptoethanol
  
9. Formaldehyde gel-loading buffer
  - 50% glycerol (diluted in DEPC-treated H<sub>2</sub>O)
  - 10mM EDTA(pH8.0)
  - 0.25% (w/v) bromophenol blue
  - 0.25% (w/v) xylene cyanol FF
  
10. 10x MOPS electrophoresis buffer
  - 200mM MOPS (pH7.0)
  - 50 mM sodium acetate
  - 10mM EDTA
  
11. 10X PCR buffer
  - 100 mM Tris pH 9.0 at 25<sup>0</sup>C, 500 mM KCl, 1% Triton X-100
  
12. Stock Separating Gel Buffer:
  - (1.5 M Tris-HCl, pH 8.8)
  
13. Stock Stacking Gel Buffer :
  - (0.5 M Tris-HCl, pH 6.8)
  
14. 10 % (w/v) SDS Solution
  - 10 mg per 100 mL dH<sub>2</sub>O
  
15. Stock Gel Solution: (Acrylamide-BIS, 30 % A, 2.67 % C)
  - 60.0 gm acrylamide were dissolved in about 175 ml distilled water and then 1.6 gm BIS (Bis-acrylamide) were added and

solution was completed to 200 ml with distilled water. Finally, the solution was filtered through coarse filter paper.

16. Catalyst:

- (10 % w/v Ammonium Persulfate “APS” freshly prepared)

17. Tracking Dye:

- (0.05 % w/v Bromophenol Blue)

18. 5X Electrode (Running) Buffer:

- (25 mM Tris, 192 mM Glycine, pH 8.3 )

This buffer was diluted 1:5 and 1 gr solid SDS was added to 1 liter of buffer before use.

19. 4 X Sample Dilution Buffer: (SDS Reducing Buffer)

- 0.25 M Tris-HCl buffer, pH 6.8 containing 8 % SDS, 40 % glycerol, 20 % 2-mercaptoethanol, 0.004 % bromophenol blue. It was prepared mixing the following volumes of given solutions:

2.5 ml 1M Tris-HCl, pH 6.8 + 4.0 ml Glycerol + 2.0 ml 2-mercaptoethanol + 0.4 ml Tracking Dye+ 0.8 gm SDS + Distilled water to 10.0 ml

20. Towbin Transfer Buffer

- (25 mM Tris, 192 mM glycine and 20% methanol)

21. TBST Buffer

- (500mM NaCl, 20mM Tris pH:7.4, 0.05% Tween20)

## 22. BCIP/NBT Substrate Solution

- Solution A) mix the solutions given below

<b>Stock Solutions</b>	<b>Volume to be taken</b>
1.5 M Tris-HCl pH:8.8	2.67 mL
1 M NaCl	4.0 mL
Diethanolamine	0.096 mL
100mM MgCl <sub>2</sub>	0.820 mL
100mM ZnCl <sub>2</sub>	0.040 mL
Nitroblue tetrazolium	12 mg
dH <sub>2</sub> O	up to 40 mL

After adjusting pH of this solution to 9.55, final volume of solution A is completed to 40 mL with dH<sub>2</sub>O.

- Solution B) 2.0 mg/mL Phenazine methosulfate
- Solution C) 5.44 mg Bromochloroindoylphosphate in 0.136 mL  
N<sup>7</sup>-N dimethyl formamide

BCIP/NBT Solution is prepared by mixing 40 mL of Solution A, 0.268mL Solution B, and 0.136mL Solution C.

## 23. 10X TBE (pH 8.3)

- 0.89 M Tris base
- 0.89 M Boric acid
- 20 mM EDTA

## 24. Lysis buffer Buffer B

- 100 mM HEPES, pH 7.2

- 100 mM NaCl
- 10 mM DTT
- 20 % Glycerol
- 0.1 % CHAPS
- 1 mM EDTA

25. Substrate solution (prepare immediately before experiment)

- Buffer B 9 ml
- 10 mM DEVD-AFC in DMSO 45  $\mu$ l
- 16 % DTT 100  $\mu$ l

## Appendix F

### Standard Curve for Lowry Assay

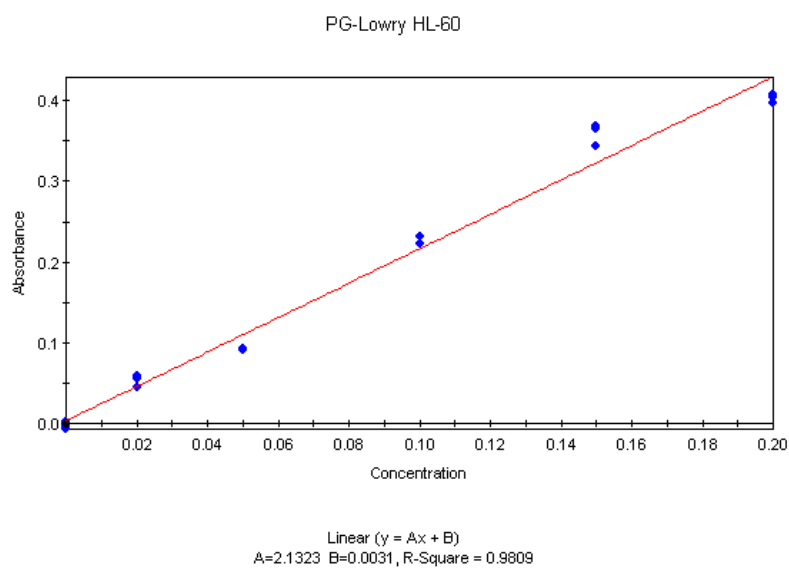


**Figure F.1** Standard curve for the determination of protein amount by micro

## Appendix G

### Flow Cytometry Analysis

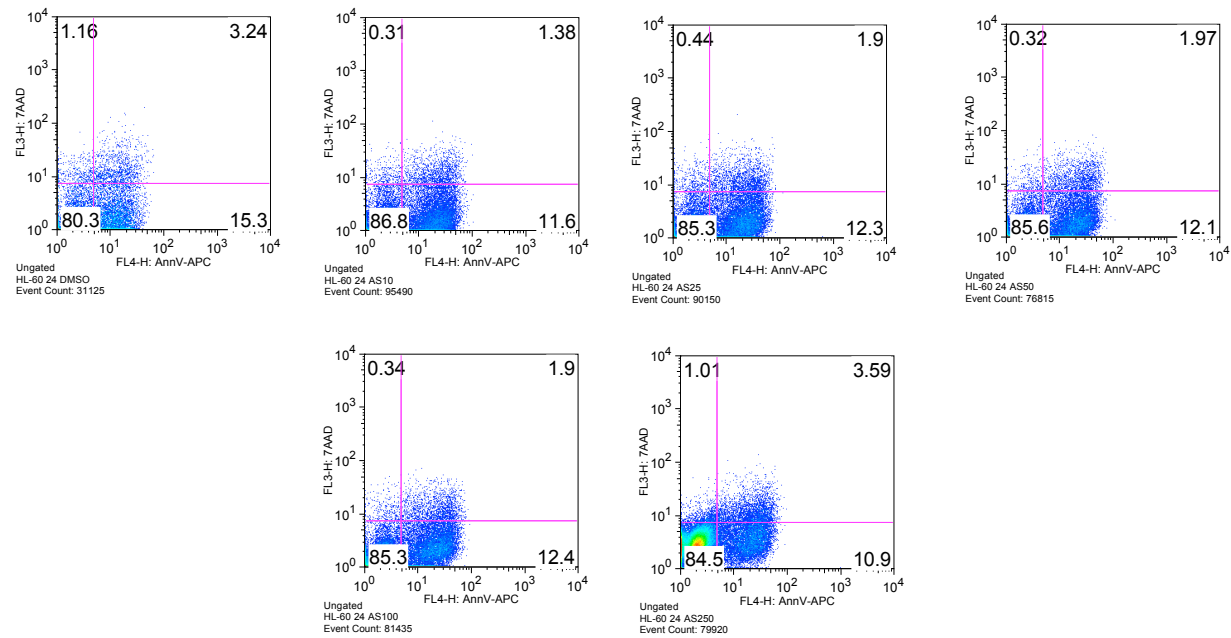


**Figure G.1** Cell apoptosis, percentage of HL-60 cells after treatment with ASE by flow cytometric analysis for 24 h. Cells were treated with ASE at various concentrations (10, 25, 50, 100 and 250  $\mu\text{g/mL}$ ) for 24 h. After treatment, cells were stained with annexin V/7AAD and analyzed by flow cytometry.

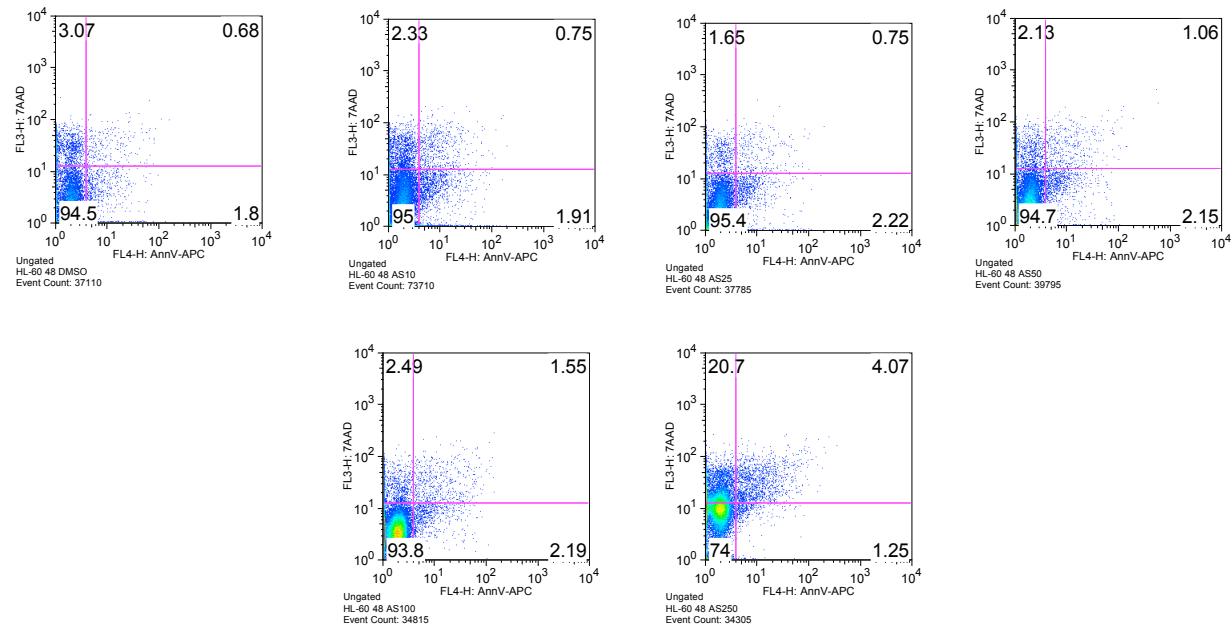


**Figure G.2** Cell apoptosis, percentage of HL-60 cells after treatment with ASE by flow cytometric analysis for 48 h. Cells were treated with ASE at various concentrations (10, 25, 50, 100 and 250  $\mu\text{g}/\text{mL}$ ) for 48 h. After treatment, cells were stained with annexin V/7AAD and analyzed by flow cytometry.

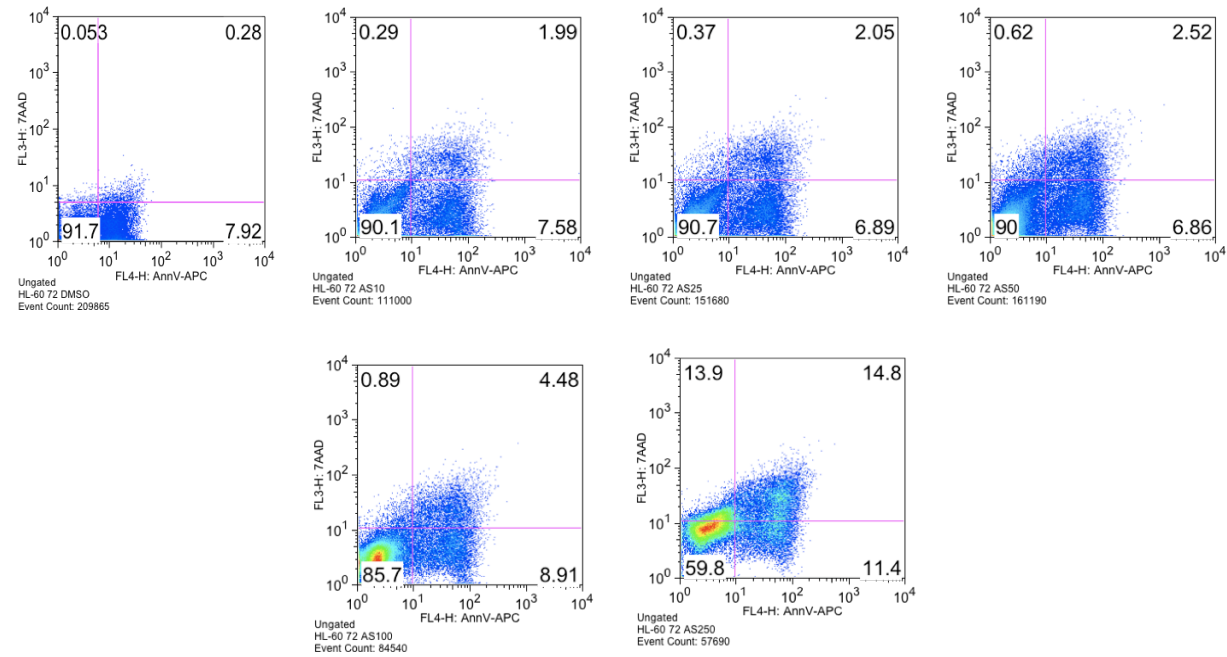


**Figure G.3** Cell apoptosis, percentage of HL-60 cells after treatment with ASE by flow cytometric analysis for 72 h. Cells were treated with ASE at various concentrations (10, 25, 50, 100 and 250  $\mu\text{g}/\text{mL}$ ) for 72 h. After treatment, cells were stained with annexin V/ 7AAD and analyzed by flow cytometry.

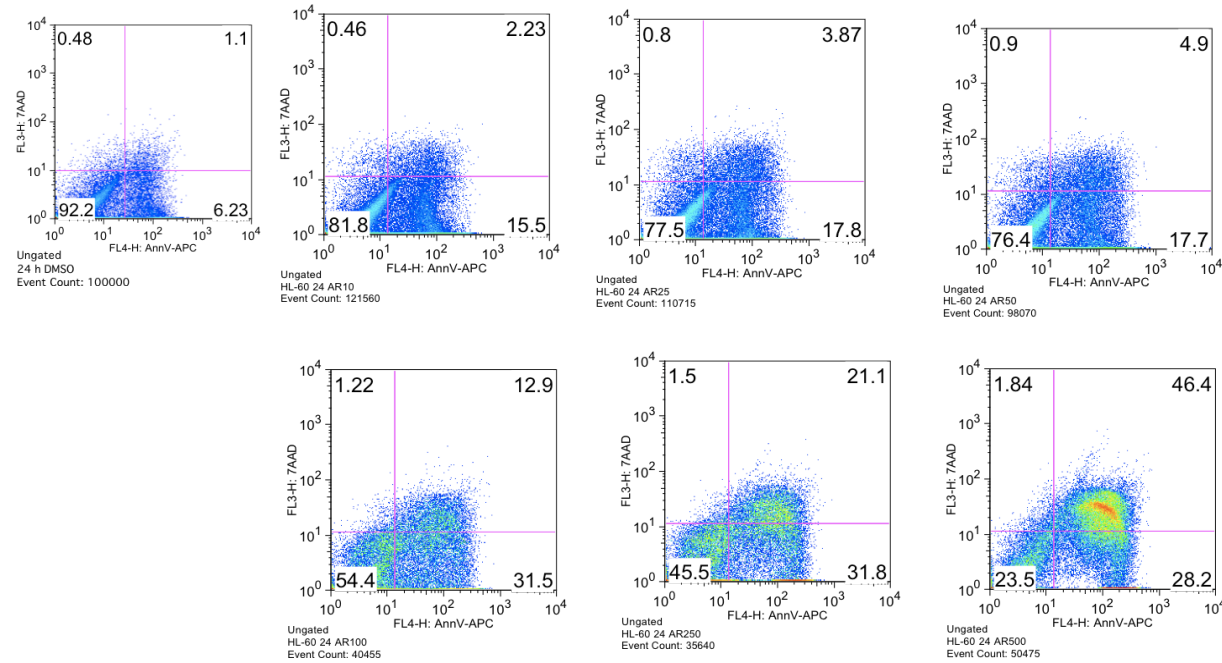


**Figure G.4** Cell apoptosis, percentage of HL-60 cells after treatment with ARE by flow cytometric analysis for 24 h. Cells were treated with ARE at various concentrations (10, 25, 50, 100, 250 and 500 µg/mL) for 24 h. After treatment, cells were stained with annexin V/7AAD and analyzed by flow cytometry.

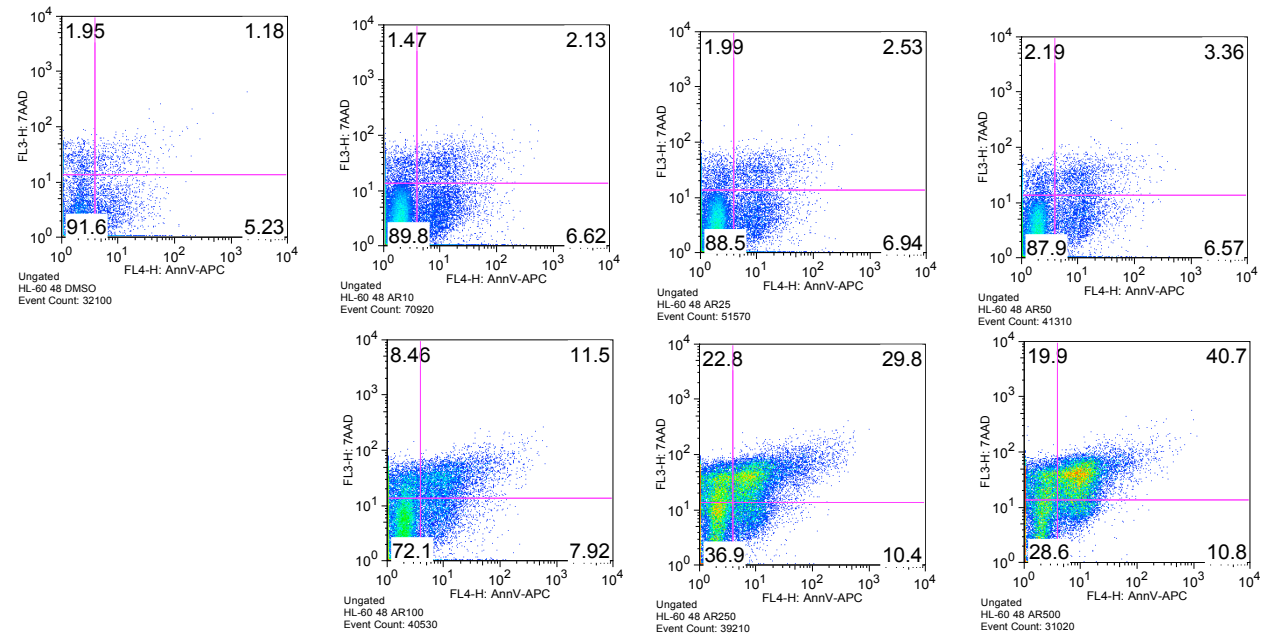


**Figure G.5** Cell apoptosis, percentage of HL-60 cells after treatment with ARE by flow cytometric analysis for 48 h. Cells were treated with ARE at various concentrations (10, 25, 50, 100, 250 and 500 µg/mL) for 48 h. After treatment, cells were stained with annexin V/7AAD and analyzed by flow cytometry.

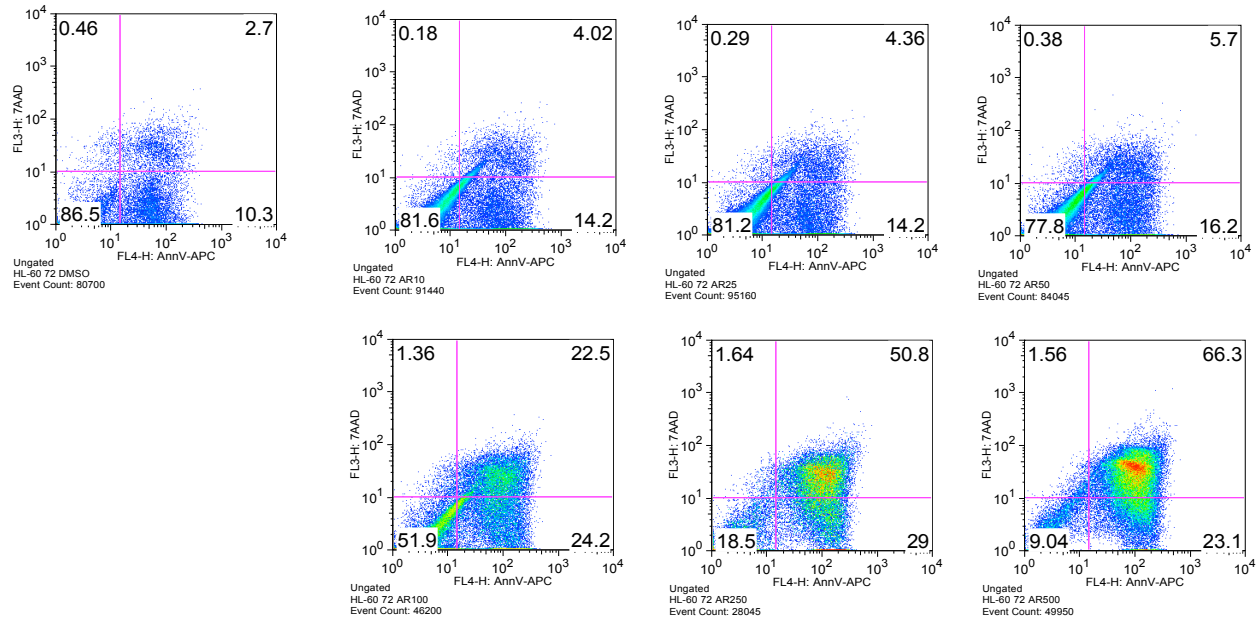


**Figure G.6** Cell apoptosis, percentage of HL-60 cells after treatment with ARE by flow cytometric analysis for 72 h. Cells were treated with ARE at various concentrations (10, 25, 50, 100, 250 and 500  $\mu\text{g/mL}$ ) for 72 h. After treatment, cells were stained with annexin V/7AAD and analyzed by flow cytometry.

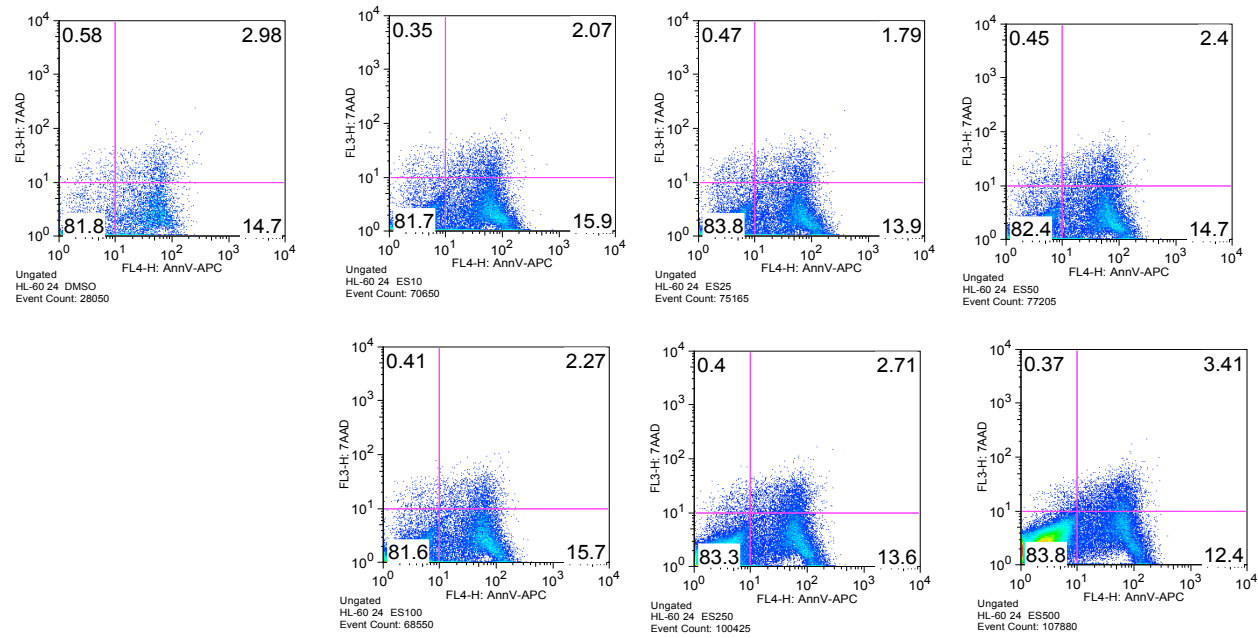


**Figure G.7** Cell apoptosis, percentage of HL-60 cells after treatment with ESE by flow cytometric analysis for 24 h. Cells were treated with ESE at various concentrations (10, 25, 50, 100, 250 and 500  $\mu\text{g/mL}$ ) for 24 h. After treatment, cells were stained with annexin V/7AAD and analyzed by flow cytometry.

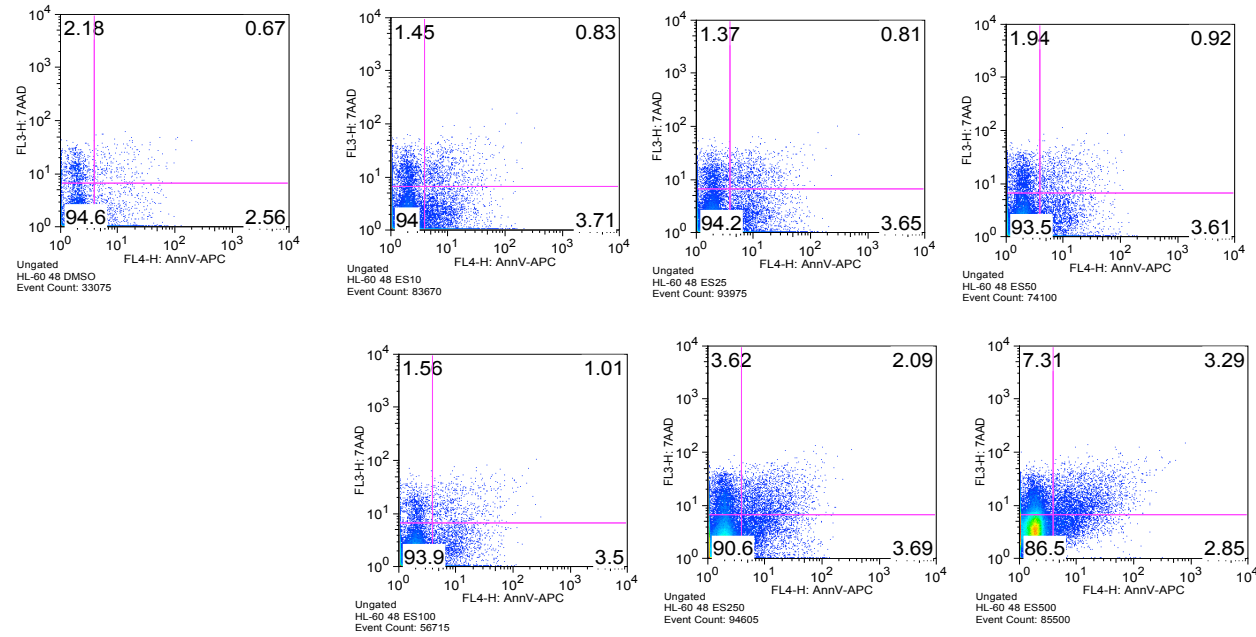


**Figure G.8** Cell apoptosis, percentage of HL-60 cells after treatment with ESE by flow cytometric analysis for 48 h. Cells were treated with ESE at various concentrations (10, 25, 50, 100, 250 and 500  $\mu\text{g}/\text{mL}$ ) for 48 h. After treatment, cells were stained with annexin V/7AAD and analyzed by flow cytometry.

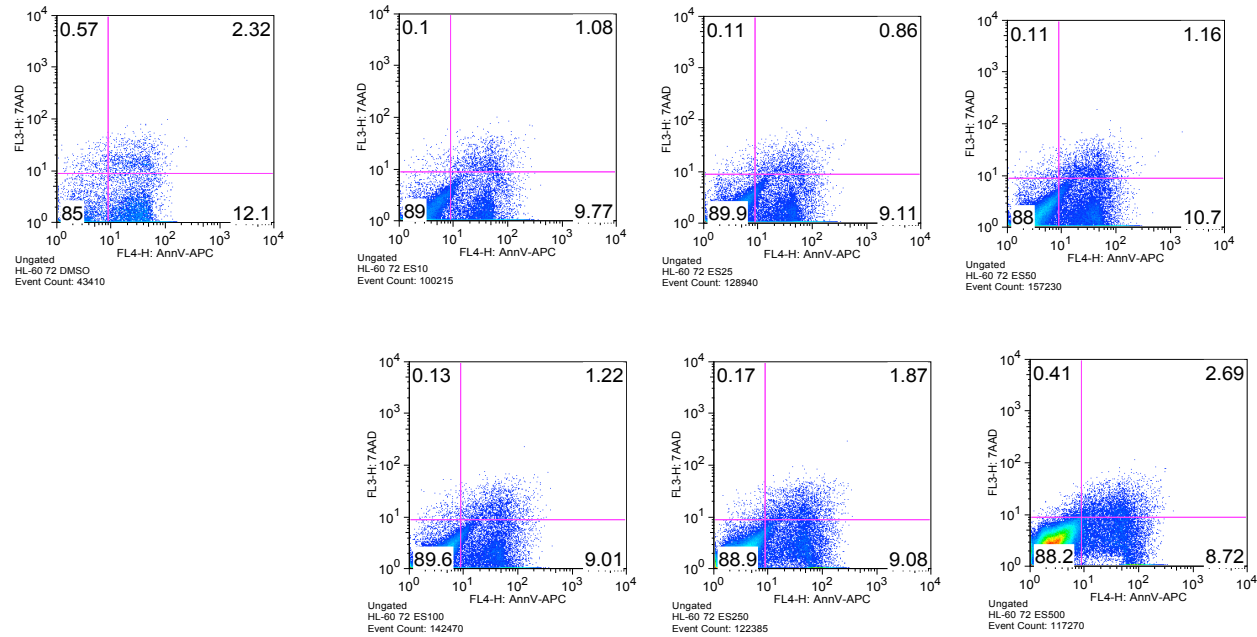


**Figure G.9** Cell apoptosis, percentage of HL-60 cells after treatment with ESE by flow cytometric analysis for 72 h. Cells were treated with ESE at various concentrations (10, 25, 50, 100, 250 and 500 µg/mL) for 72 h. After treatment, cells were stained with annexin V/7AAD and analyzed by flow cytometry.

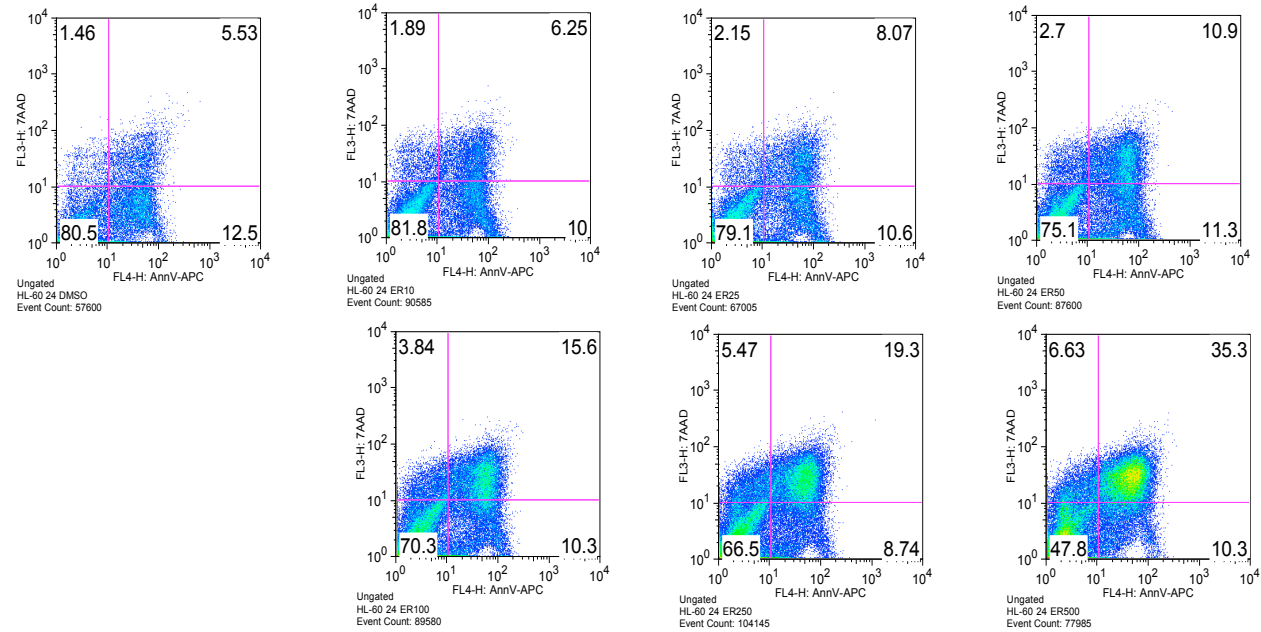


**Figure G.10** Cell apoptosis, percentage of HL-60 cells after treatment with ERE by flow cytometric analysis for 24 h. Cells were treated with ERE at various concentrations (10, 25, 50, 100, 250 and 500  $\mu\text{g/mL}$ ) for 24 h. After treatment, cells were stained with annexin V/7AAD and analyzed by flow cytometry.

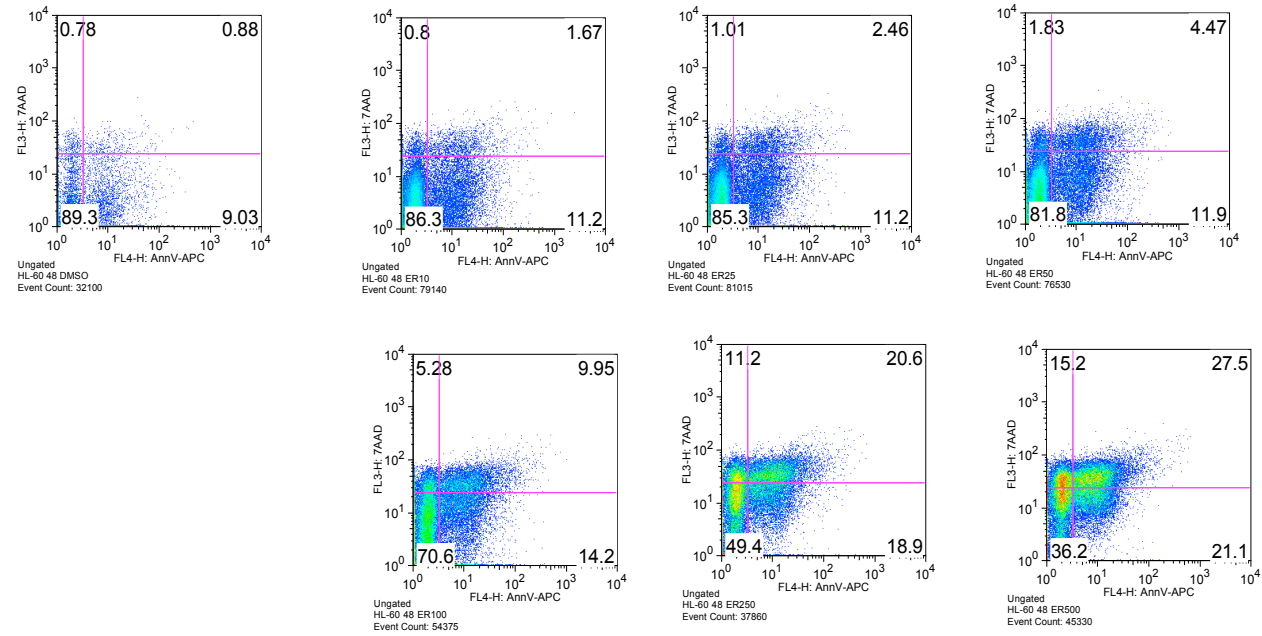


**Figure G.11** Cell apoptosis, percentage of HL-60 cells after treatment with ERE by flow cytometric analysis for 48 h. Cells were treated with ERE at various concentrations (10, 25, 50, 100, 250 and 500  $\mu\text{g}/\text{mL}$ ) for 48 h. After treatment, cells were stained with annexin V/7AAD and analyzed by flow cytometry.

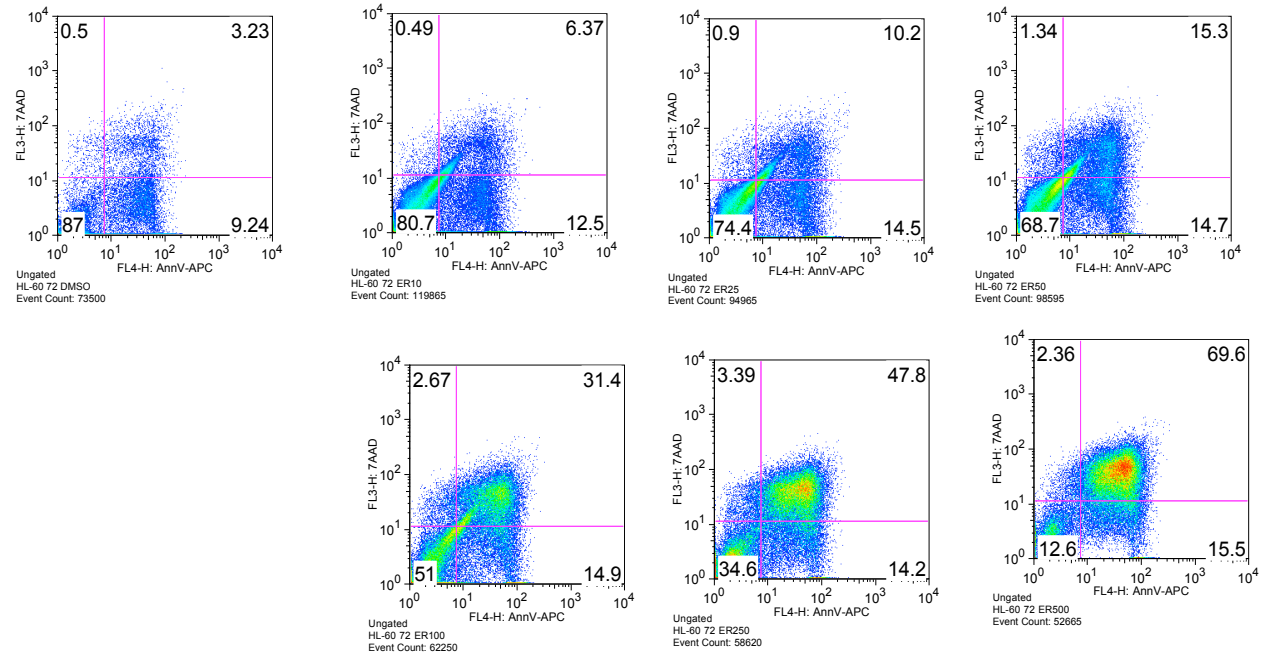


**Figure G.12** Cell apoptosis, percentage of HL-60 cells after treatment with ERE by flow cytometric analysis for 72 h. Cells were treated with ERE at various concentrations (10, 25, 50, 100, 250 and 500 µg/mL) for 72 h. After treatment, cells were stained with annexin V/7AAD and analyzed by flow cytometry.

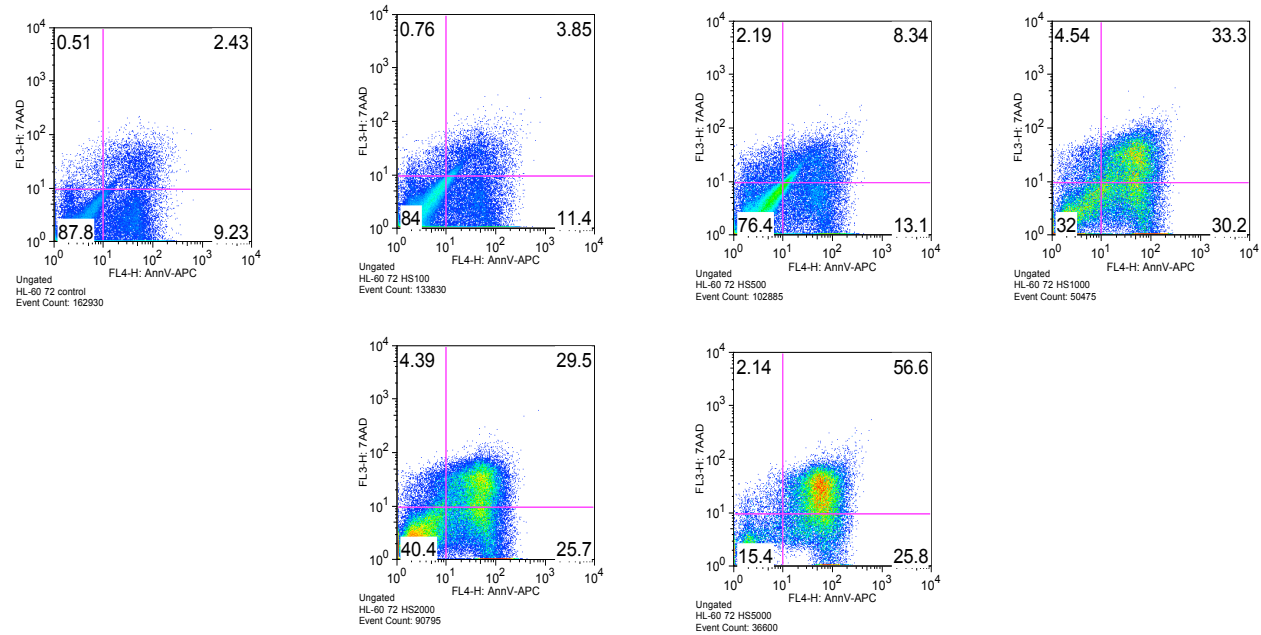


**Figure G.13** Cell apoptosis, percentage of HL-60 cells after treatment with WSE by flow cytometric analysis for 72 h. Cells were treated with WSE at various concentrations (100, 500, 1000, 2000 and 5000 µg/mL) for 72 h. After treatment, cells were stained with annexin V/7AAD and analyzed by flow cytometry.

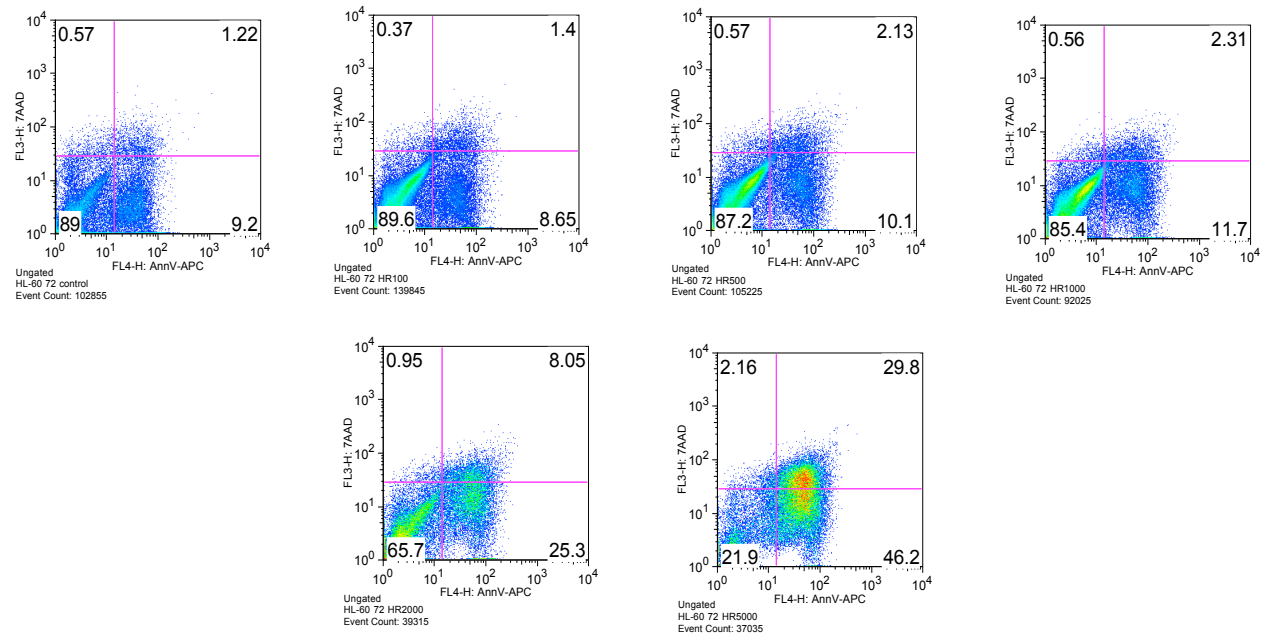


**Figure G.14** Cell apoptosis, percentage of HL-60 cells after treatment with WRE by flow cytometric analysis for 72 h. Cells were treated with WRE at various concentrations (100, 500, 1000, 2000 and 5000 µg/mL) for 72 h. After treatment, cells were stained with annexin V/7AAD and analyzed by flow cytometry.

## Appendix H

### qRT-PCR Melting and Standard Curve

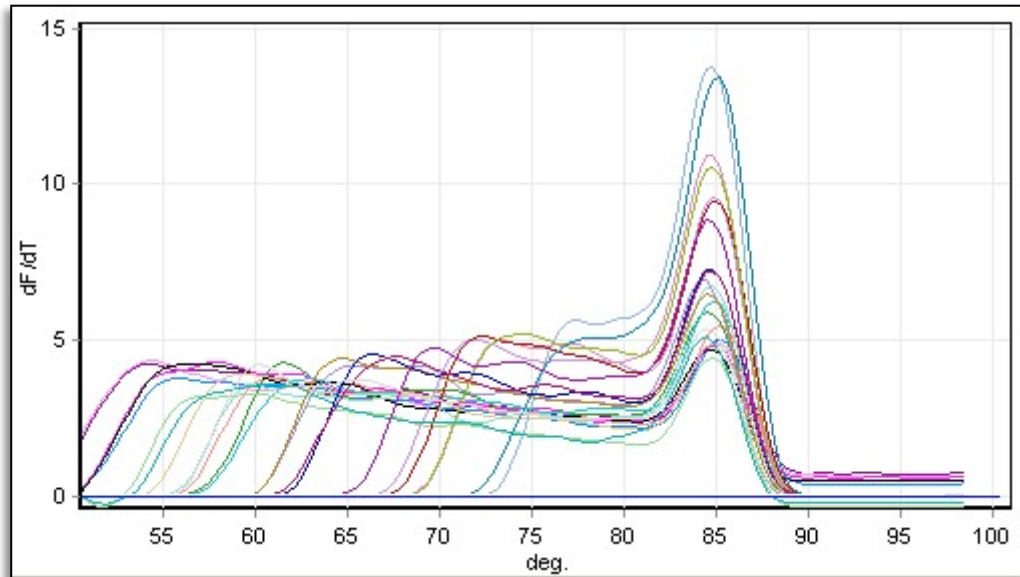


Figure H.1 Melting curve showing the fluorescence of SYBR Green I dye versus the temperature. One peak in melting analysis confirms that a single PCR product was detected.

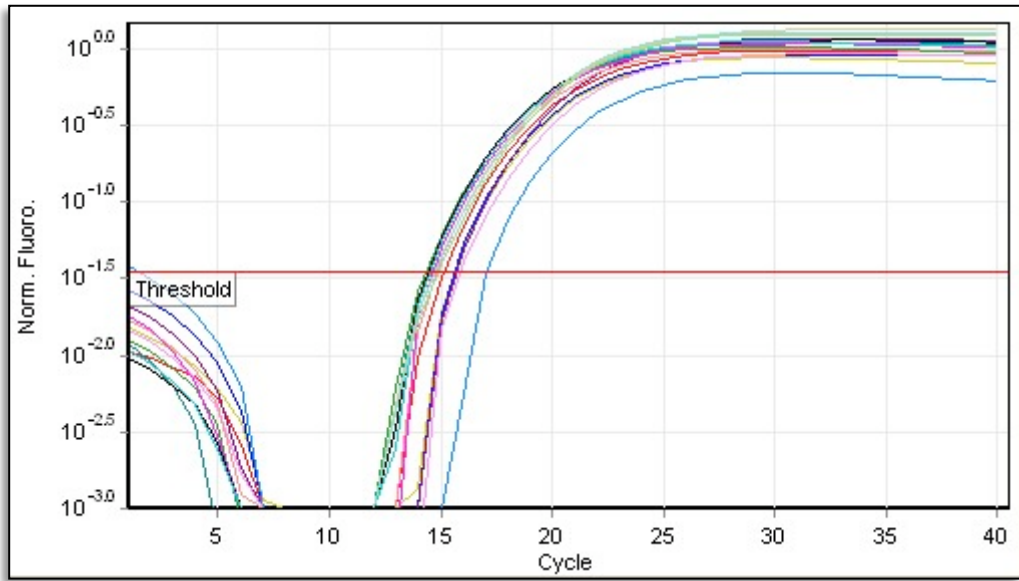


Figure H.2 Quantitation data for Cycling A.Green

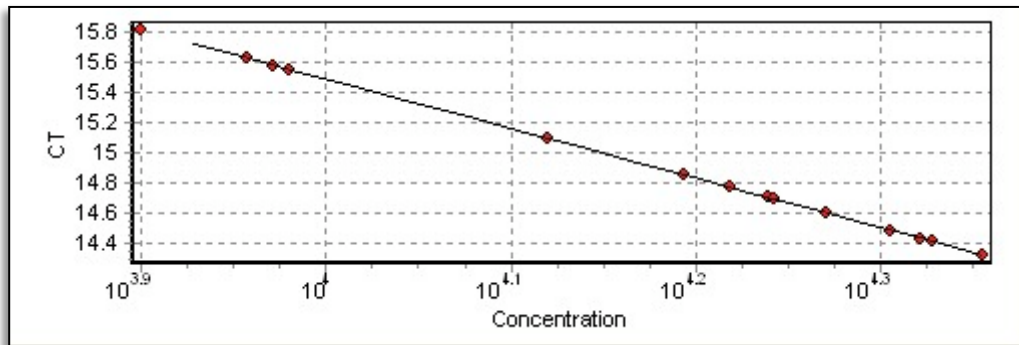


Figure H.3 qRT-PCR Standard Curve

## CURRICULUM VITAE

### PERSONAL INFORMATION

Surname, Name: Uyar, Pembegül  
Nationality: Turkish (TC)  
Date and Place of Birth: 26 October 1977 , Konya  
Marital Status: Single  
Phone: +90 533 349 15 35  
Fax: +90 312 210 79 76  
email: [pembeguluyar@gmail.com](mailto:pembeguluyar@gmail.com)

### EDUCATION

Degree	Institution	Year of Graduation
PhD	METU Biotechnology	2011
BS (Honors)	METU Biology	2001
High School	Bursa A.O.S. Fen Lisesi	1995

### WORK EXPERIENCE

Year	Place	Enrollment
January 2002-	METU Biotechnology	Teaching-Research Assistant
2000 (July-September)	Eczacibasi Baxter	Intern researcher
December 2008-2009	UCI, USA	Visiting Scholar

### TEACHING EXPERIENCE

Year and Enrollment	Courses
2002-2011, Teaching Assistant	Physiology (Bio-252)
	Animal Cell Culture Techniques (Gene-405)
	Experimental Tech. in Molecular Biology (Gene-475)

## FOREIGN LANGUAGES

Advanced English, Beginner German

## PUBLICATIONS

### Abstracts Published in Conferences

1. **P. Uyar**, F. Özgökçe, N. Çoruh, and M. İşcan, "Antioxidant and antiproliferative effects of Turkish *Rheum ribes* ethanolic extract", 20th IUBMB International Congress of Biochemistry and Molecular Biology and 11th FAOBMB Congress, June 18-23, 2006, Kyoto, Abstrs, p. 717,2006.
2. **P. Uyar**, F. Özgökçe, N. Çoruh, and M. İşcan, "Antioxidative and antiproliferative effects of Turkish *Rheum ribes* aqueous extract", FEBS Journal, 273(Suppl.1), pp. 353, 2006.
3. **P. Uyar**, F. Özgökçe, N. Çoruh, and M. İşcan, "Cytotoxic and antioxidant activities of Turkish *Rheum Ribes*", XI<sup>th</sup> International Congress of Toxicology, Montréal, Canada , 2007
4. **P. Uyar**, F. Özgökçe, N. Çoruh, and M. İşcan "Antiproliferation and induction of apoptosis by *Rheum ribes* on HL-60 human acute promyeloblastic leukemia cell line" Semi-international Multidisciplinary Cancer Research Symposium in Bursa, Turkey, 2008 (ORAL)
5. **P. Uyar**, F.R.Sahinkaya, F. Özgökçe, N. Çoruh, and M. İşcan "Role of CYP 1B1 in modulation of antiproliferation properties of *Rheum ribes* in HL-60 cells" Semi-international Multidisciplinary Cancer Research Symposium in Bursa, Turkey , 2008

6. **Pembegül Uyar** , *Esra Uzun Demir* , *Gülây Kansu*, *Mesude Iscan* “The Effect of Hypoallergenic Denture Base Materials on Cytotoxicity and Apoptosis in Fibroblasts” The 14<sup>th</sup> Biomedical Science and Technology Symposium in Muğla,Turkey, 2008
7. **P. Uyar**, F. Özgökçe, N. Çoruh, and M. İşcan, “Effects of *Rheum ribes* ethanolic extracts on cytochromes p450 1B1 (CYP1B1) gene expression and glutathione-S-transferase (GST) activity in HL-60 cells”, ISSX 10th European Regional Meeting, Vienna, Austria, 2008
8. **P. Uyar**, F. Özgökçe, N. Çoruh, and M. İşcan, “Effects of *Rheum ribes* Shoot and Root Ethanol Extracts on Proliferation and Apoptosis in HL-60 Cells” The IX<sup>th</sup> Word Conference on Clinical Pharmacology and Therapeutics, July 27-August 1, 2008, Quebec, Canada
9. **P. Uyar**, F. Özgökçe, N. Çoruh, and M. İşcan, “*Rheum ribes* Ekstrelerinin HL-60 Üzerinde Antiproliferatif ve Apoptotik Etkileri” XX. Ulusal Biyokimya Kongresi , (29 Ekim-1 Kasım 2008) , Kapadokya , Türkiye (ORAL)
10. **P. Uyar**, E. Sakallı, F. Özgökçe, N. Çoruh, and M. İşcan, “*Rheum ribes* Ekstrelerinin MCF-7 Hücrelerinde Büyüme Önleyici ve Apoptozis İndükleyici Etkisi” XX. Ulusal Biyokimya Kongresi , Oct 29-Nov 1 2008, Kapadokya, Türkiye
11. E. Sakallı, **P. Uyar** and M. İşcan “Cytotoxicity of Emodin and Comparative Effects on GST activity in MCF-7 and MDA-231 cell line” 21. Ulusal Biyokimya Kongresi , Oct 28-31 2009, İstanbul, Turkey
12. E. Sakallı, **P. Uyar** and M. İşcan “Emodin MCF-7 ve MDA-231 Hücrelerinde Sitotoksitesitesi ve Apoptozis Gen İfadeleri Üzerindeki Karşılaştırılmalı Etkileri” 22. Ulusal Biyokimya Kongresi , Oct 27-30 2010, Eskişehir, Turkey

## **IN SERVICE TRAINING**

1. 2nd National HPLC and Other Separation Techniques (October 7-9, 2004, GATA, Ankara, Turkey)
2. Principles in Cell Culture Technology and Artificial Organs (Hücre Kültürü Teknolojisinde Temel Prensipler ve Yapay Organlar). November 24-26, 2004, Ege University Applied Science-Technology Research Institute
3. Uygulamalı Moleküler Tanı Teknikleri Oct 29-Nov.1 2008, Kapadokya, Turkey
4. 2nd Microarray Training and Data Analysis Course, METU Central Laboratory, Molecular Biology and Biotechnology R&D Center (November 24-25 2008, Ankara, Turkey)
5. UCI Animal Care and Use Training, UCI USA (ULART) September 2009 Irvine, USA
6. Certificate Program of Animal Use for Testing in Scientific Program (80 hrs; Sept. 20- Oct 1 2010 ; Kobay D.H.L. A.Ş. Local Ethics Committee, Ankara, Turkey)
7. Prokaryotik ve Ökaryotik Hücrelere Gen Aktarımı Çalıştay1, October 27, 2010 Eskişehir, Turkey

## **AWARDS AND HONORS**

1. Turkish Biochemical Society Young Scientist Grant, FEBS 2006, İstanbul, Turkey
2. Travel Grant, CPT 2008, Quebec, Canada
3. Turkish Biochemical Society Young Scientist Grant, UBK 2008, Kapadokya, Turkey

## **PROJECTS INVOLVED**

1. Investigation of Antioxidative and Apoptotic Characteristics of Turkish Medicinal Plants (YUUP)
2. Identification and Characterization of Phenolics and Flavonoids from -Turkish Medicinal Plants with HPLC.
3. Investigation of the Biological Effects of Hypo-allergenic Denture Base Materials using molecular techniques.
4. Automatic Cell Counting By Image Processing
5. Study the role of death-receptor induced apoptosis in T cells (UCI)
6. Microarray Expression Profiles in Breast Cancer MCF-7 and MDA-231 Cells Following Exposure to Emodin

## **MEMBERSHIPS**

1. Turkish Biochemical Society, Turkey
2. International Society for the Study of Xenobiotics (ISSX), USA
3. The Society for In Vitro Biology (SIVB), USA